ISSN 1007-9327 (print)
ISSN 2219-2840 (online)

# World Journal of *Gastroenterology*

*World J Gastroenterol* 2018 February 21; 24(7): 767-876

Published by Baishideng Publishing Group Inc

World Journal of Gastroenterology

Contents

Weekly Volume 24 Number 7 February 21, 2018


## MINIREVIEWS

767 Epidemiology, determinants, and management of AIDS cholangiopathy: A review

*Naseer M, Dailey FE, Juboori AA, Samiullah S, Tahan V*

## ORIGINAL ARTICLE

### Basic Study

775 Glucose transporter expression in the human colon

*Merigo F, Brandolese A, Facchin S, Missaggia S, Bernardi P, Boschi F, D'Incà R, Savarino EV, Sbarbati A, Sturniolo GC*

794 Translational pancreatic cancer research: A comparative study on patient-derived xenograft models

*Rubio-Manzanares Dorado M, Marín Gómez LM, Aparicio Sánchez D, Pereira Arenas S, Praena-Fernández JM, Borrero Martín JJ, Farfán López F, Gómez Bravo MÁ, Muntané Relat J, Padillo Ruiz J*

810 Cryopreservation for delayed circulating tumor cell isolation is a valid strategy for prognostic association of circulating tumor cells in gastroesophageal cancer

*Brungs D, Lynch D, Luk AW, Minaei E, Ranson M, Aghmesheh M, Vine KL, Carolan M, Jaber M, de Souza P, Becker TM*

819 Metformin attenuates motility, contraction, and fibrogenic response of hepatic stellate cells *in vivo* and *in vitro* by activating AMP-activated protein kinase

*Li Z, Ding Q, Ling LP, Wu Y, Meng DX, Li X, Zhang CQ*

833 Fish oil alleviates liver injury induced by intestinal ischemia/reperfusion *via* AMPK/SIRT-1/autophagy pathway

*Jing HR, Luo FW, Liu XM, Tian XF, Zhou Y*

### Retrospective Cohort Study

844 Elderly patients had more severe postoperative complications after pancreatic resection: A retrospective analysis of 727 patients

*Chen YT, Ma FH, Wang CF, Zhao DB, Zhang YW, Tian YT*

### Retrospective Study

852 Predictors of functional benefit of hepatitis C therapy in a 'real-life' cohort

*Steinebrunner N, Stein K, Sandig C, Bruckner T, Stremmel W, Pathil A*

862 Predictors of post-treatment stenosis in cervical esophageal cancer undergoing high-dose radiotherapy

*Kim JW, Kim TH, Kim JH, Lee IJ*

## CASE REPORT

870 Esophageal metastasis of stem cell-subtype hepatocholangiocarcinoma: Rare presentation of a rare tumor

*Salimon M, Chapelle N, Matysiak-Budnik T, Mosnier JF, Frampas E, Touchefeu Y*

## CORRECTION

876 Correction for "Evaluation of a multiplex PCR assay for detection of cytomegalovirus in stool samples from patients with ulcerative colitis" (*World J Gastroenterol* 2015; 21: 12667-12675)

*Hokama A*

## ABOUT COVER

Editorial board member of *World Journal of Gastroenterology*, Serdar Topaloglu, MD, Associate Professor, Department of Surgery, School of Medicine, Karadeniz Technical University, Trabzon 61080, Turkey

## AIMS AND SCOPE

*World Journal of Gastroenterology* (*World J Gastroenterol*, *WJG*, print ISSN 1007-9327, online ISSN 2219-2840, DOI: 10.3748) is a peer-reviewed open access journal. *WJG* was established on October 1, 1995. It is published weekly on the 7th, 14th, 21st, and 28th each month. The *WJG* Editorial Board consists of 642 experts in gastroenterology and hepatology from 59 countries.

The primary task of *WJG* is to rapidly publish high-quality original articles, reviews, and commentaries in the fields of gastroenterology, hepatology, gastrointestinal endoscopy, gastrointestinal surgery, hepatobiliary surgery, gastrointestinal oncology, gastrointestinal radiation oncology, gastrointestinal imaging, gastrointestinal interventional therapy, gastrointestinal infectious diseases, gastrointestinal pharmacology, gastrointestinal pathophysiology, gastrointestinal pathology, evidence-based medicine in gastroenterology, pancreatology, gastrointestinal laboratory medicine, gastrointestinal molecular biology, gastrointestinal immunology, gastrointestinal microbiology, gastrointestinal genetics, gastrointestinal translational medicine, gastrointestinal diagnostics, and gastrointestinal therapeutics. *WJG* is dedicated to become an influential and prestigious journal in gastroenterology and hepatology, to promote the development of above disciplines, and to improve the diagnostic and therapeutic skill and expertise of clinicians.

## INDEXING/ABSTRACTING

*World Journal of Gastroenterology* (*WJG*) is now indexed in Current Contents®/Clinical Medicine, Science Citation Index Expanded (also known as SciSearch®), Journal Citation Reports®, Index Medicus, MEDLINE, PubMed, PubMed Central and Directory of Open Access Journals. The 2017 edition of Journal Citation Reports® cites the 2016 impact factor for *WJG* as 3.365 (5-year impact factor: 3.176), ranking *WJG* as 29th among 79 journals in gastroenterology and hepatology (quartile in category Q2).



NAME OF JOURNAL
*World Journal of Gastroenterology*

ISSN
ISSN 1007-9327 (print)
ISSN 2219-2840 (online)

LAUNCH DATE
October 1, 1995

FREQUENCY
Weekly



EDITORIAL OFFICE
Ze-Mao Gong, Director
*World Journal of Gastroenterology*
Baishideng Publishing Group Inc
7901 Stoneridge Drive, Suite 501,
Pleasanton, CA 94588, USA
Telephone: +1-925-2238242
Fax: +1-925-2238243
E-mail: editorialoffice@wjgnet.com
Help Desk: http://www.f6publishing.com/helpdesk
http://www.wjgnet.com

PUBLISHER
Baishideng Publishing Group Inc
7901 Stoneridge Drive, Suite 501,
Pleasanton, CA 94588, USA
Telephone: +1-925-2238242
Fax: +1-925-2238243
E-mail: bpgoffice@wjgnet.com
Help Desk: http://www.f6publishing.com/helpdesk
http://www.wjgnet.com

PUBLICATION DATE
February 21, 2018



INSTRUCTIONS TO AUTHORS
Full instructions are available online at http://www.wjgnet.com/bpg/gerinfo/204

ONLINE SUBMISSION
http://www.f6publishing.com

World Journal of Gastroenterology

Submit a Manuscript: http://www.f6publishing.com

*World J Gastroenterol* 2018 February 21; 24(7): 767-774

DOI: 10.3748/wjg.v24.i7.767

ISSN 1007-9327 (print) ISSN 2219-2840 (online)

MINIREVIEWS

# Epidemiology, determinants, and management of AIDS cholangiopathy: A review

Maliha Naseer, Francis E Dailey, Alhareth Al Juboori, Sami Samiullah, Veysel Tahan

Maliha Naseer, Francis E Dailey, Alhareth Al Juboori, Sami Samiullah, Veysel Tahan, Division of Gastroenterology and Hepatology, Department of Internal Medicine, University of Missouri, Columbia, MO 65212, United States

ORCID number: Maliha Naseer (0000-0001-6891-1378); Francis E Dailey (0000-0001-8353-0709); Alhareth Al Juboori (0000-0002-2641-9892); Sami Samiullah (0000-0002-1498-0527); Veysel Tahan (0000-0001-6796-9359).

Author contributions: All authors equally contributed to this paper with conception and design of the study, literature review and analysis, drafting and critical revision and editing, and final approval of the final version.

Conflict-of-interest statement: No potential conflicts of interest.



Manuscript source: Invited manuscript

Correspondence to: Veysel Tahan, MD, FACP, FACG, FESBGH, Assistant Professor of Clinical Medicine, Division of Gastroenterology and Hepatology, Department of Internal Medicine, University of Missouri, 1 Hospital Drive, Columbia, MO 65212, United States. tahanv@health.missouri.edu
Telephone: +1-573-8846044
Fax: +1-573-8844595

Received: December 25, 2017
Peer-review started: December 25, 2017
First decision: January 4, 2018
Revised: January 24, 2018
Accepted: February 1, 2018
Article in press: February 1, 2018
Published online: February 21, 2018

## Abstract

Diseases of the liver and biliary tree have been described with significant frequency among patients with human immunodeficiency virus (HIV), and its advanced state, acquired immunodeficiency syndrome (AIDS). Through a variety of mechanisms, HIV/AIDS has been shown to affect the hepatic parenchyma and biliary tree, leading to liver inflammation and biliary strictures. One of the potential hepatobiliary complications of this viral infection is AIDS cholangiopathy, a syndrome of biliary obstruction and liver damage due to infection-related strictures of the biliary tract. AIDS cholangiopathy is highly associated with opportunistic infections and advanced immunosuppression in AIDS patients, and due to the increased availability of highly active antiretroviral therapy, is now primarily seen in instances of poor access to antiretroviral therapy and medication non-compliance. While current published literature describes well the clinical, biochemical, and endoscopic management of AIDS-related cholangiopathy, information on its epidemiology, natural history, and pathology are not as well defined. The objective of this review is to summarize the available literature on AIDS cholangiopathy, emphasizing its epidemiology, course of disease, and determinants, while also revealing an updated approach for its evaluation and management.

**Key words:** Prognosis; Human immunodeficiency virus complications; Epidemiology; Human immunodeficiency virus cholangiopathy; Acquired immunodeficiency syndrome; Mortality

**Core tip:** Though a declining phenomenon in the Western world, acquired immunodeficiency syndrome (AIDS)-related cholangiopathy has been shown to cause significant burden and remains an important etiology of hepatobiliary pathology in those affected with human immunodeficiency virus (HIV). While it is linked to advanced immunosuppression in AIDS patients, particularly in those with extremely low CD4 counts and opportunistic infections, as well as those with drug-resistant HIV infection, it is also seen in developing countries due to less available anti-retroviral therapy, decreased awareness, and medication non-compliance.

Naseer M, Dailey FE, Juboori AA, Samiullah S, Tahan V. Epidemiology, determinants, and management of AIDS cholangiopathy: A review. *World J Gastroenterol* 2018; 24(7): 767-774 Available from: URL: http://www.wjgnet.com/1007-9327/full/v24/i7/767.htm DOI: http://dx.doi.org/10.3748/wjg.v24.i7.767

## INTRODUCTION

Human immunodeficiency virus (HIV) is a global pandemic and it has been estimated that 37 million people are infected with it worldwide. Acquired immunodeficiency syndrome (AIDS) is associated with high morbidity and mortality due to increased risk of opportunistic infections and malignancy[1]. However, there has been significant decline in morbidity and mortality associated with HIV/AIDS with the advent of highly active antiretroviral therapy (HAART)[2]. In December of 2013, UNAIDS (Joint United Nations Programme on HIV/AIDS) proposed new targets for HIV treatment scale-up *i.e.*, by 2020, 90% of all people living with HIV will know their HIV status, 90% of all people with diagnosed HIV infection will receive sustained antiretroviral therapy and 90% of all people receiving antiretroviral therapy will have viral suppression for effective control of HIV[3].

HIV affects the hepatic parenchyma and biliary tree, leading to liver inflammation and biliary strictures. According to observational cohort studies published by the D.A.D. study group (Data collection on Adverse Events of Anti-HIV drugs) and Palella *et al*[4], deaths in HIV infection due to liver disease are on the rise; approximately 14%-18% of deaths among HIV/AIDS patients were attributed to liver diseases in these studies[5].

Hepatobiliary dysfunction is common in HIV/AIDS. It has been well established that HIV directly affects hepatocytes, Kupffer cells, and endothelial cells[6]. Abnormalities in liver chemistries are common among HIV-infected persons, even in the absence of hepatitis B and C infections. Mechanisms by which HIV exerts its effect on hepatocytes include but are not limited to: oxidative stress secondary to mitochondrial injury, lipotoxicity, immune-mediated cell damage, accumulation of toxic metabolites within hepatocytes, and translocation of gut microbiota causing systemic inflammation, senescence, and nodular regenerative hyperplasia[7].

Liver diseases in HIV are generally classified into three main categories. The first group consists of diseases associated with immunosuppression, including AIDS cholangiopathy, acalculous cholecystitis, AIDS-related neoplasms (non-Hodgkin lymphoma and Kaposi sarcoma), and vanishing bile duct syndrome. The next set relates to drug-induced hepatotoxicity secondary to HAART. The last category involves worsening of co-infection with hepatitis B and C viruses, encompassing accelerated liver damage and progression of fibrosis. In addition, patient with HIV/AIDS are at increased risk of non-alcoholic fatty liver disease and nodular regenerative hyperplasia[8].

AIDS cholangiopathy is a well-documented biliary syndrome in severely immunocompromised AIDS patients[9]. It occurs when strictures in the biliary tract develop due to opportunistic infections, leading to biliary obstruction and cholestatic liver damage[10]. The condition was first recognized in 1983 by Pitlik *et al*[11] and Guarda *et al*[12] among immunocompromised humans. Following these reports, investigations of right upper quadrant pain and elevated liver enzymes in severely immunocompromised AIDS patients revealed several opportunistic pathogens, implicating the pathogenesis of AIDS cholangiopathy[13]. Furthermore, Schneiderman *et al*[14] published a case series in 1987 highlighting the endoscopic appearance of papillary stenosis involving the intrahepatic and extrahepatic biliary tree and associated with sclerosing cholangitis. In 1989, Cello identified four patterns of cholangiographic features resembling primary sclerosing cholangitis (PSC), including papillary stenosis, long extrahepatic strictures, acalculous cholecystitis, and intrahepatic and extrahepatic sclerosing lesions[15].

Several case series and reviews are published highlighting the clinical, biochemical, and endoscopic management of AIDS-related cholangiopathy. Still, little is known about its epidemiology and natural history, as well as the determinants of its pathology in developed and developing countries. In this review article, we will focus on the epidemiology, determinants, and management of AIDS related cholangiopathy.

## EPIDEMIOLOGY

Actual data on the incidence and prevalence of AIDS-related cholangiopathy is largely lacking, especially from developing countries. In the pre-HAART era, the estimated prevalence of this entity was 26%-46%[16]. To date, approximately 250 cases are reported in the

literature-mostly before the introduction of HAART. Although rarely reported in developed countries, AIDS-related cholangiopathy remains an important differential of cholestatic liver disease in HIV-infected patients, attributable to resistance to the first line antiretroviral medications[17]. Meanwhile, it is still a problem in developing countries due to poor access to HAART, decreased awareness about the disease, and medication non-compliance[18].

## DETERMINANTS

Although exact knowledge about the natural history of AIDS cholangiopathy and its determinants is not available from currently published literature, the disease is found to be associated with advanced immunosuppression (CD4 count < 100/mm$^3$). Approximately 82% of patients with this disease have opportunistic infections at the time of diagnosis[19]. At the time of diagnosis of cholangitis in AIDS patients, approximately 27% have been found to also have Pneumocystis carinii pneumonia, 100% with candidiasis, 20% with HSV infection, and 26% with cutaneous Kaposi sarcoma[20]. AIDS-related cholangitis is most commonly reported in young men who have sex with men with a mean age of 37 years[21]. Conversely, it is more common in heterosexual men in developing counties and rarely associated with Kaposi sarcoma[22].

## ETIOLOGY AND PATHOGENESIS

Opportunistic infections of the biliary tract associated with advanced immunosuppression in AIDS has been well documented in the literature. *Cryptosporidium parvum* (*C. parvum*) is the most common pathogen associated with AIDS cholangiopathy and has been has been isolated in 20%-57% of patients[23]. Sources of samples for diagnosis include: bile duct epithelium by ampullary biopsy, bile samples, and stool samples. Epidemiological studies show that *C. parvum*-associated diarrhea is common in developed and developing countries and can be seen in both immunocompetent and immunocompromised hosts[24]. However, cholangiopathy is only reported in the immunocompromised state associated with AIDS. The incidence of *C. parvum* infection in AIDS patients is reported to be 3%-4% in developed countries and approximately 50% in patients in the developing world prior to the advent of HAART[25]. This pathogen is still the most common infectious cause of AIDS cholangiopathy in patients who either do not have access to medications or have documented resistance to first-line HAART.

It has been proposed that HIV and *C. parvum* acts synergistically in the biliary system. The mechanism by which *C. parvum* causes AIDS cholangiopathy is not entirely clear. Results of the *in vitro* study published by O'Hara and associates in 2007 suggests that *C. parvum* induces apoptotic cell death in the infected cholangiocytes through Fas/Fas ligand (FasL) system which is further potentiated by the synergistic effects of the HIV-1 trans-activator of transcription (Tat) protein (Figure 1). FasL protein expression in the cytoplasm of the cultured hepatocyte and its translocation is enhanced by the HIV-1 Tat protein. In addition, the HIV-1 Tat protein causes release of full-length FasL in infected cells; consequently, apoptotic cell death in uninfected cholangiocytes leads to damage of the biliary epithelia, which occurs almost exclusively in patients infected with HIV[26,27]. Another proposed mechanism of pathology is autonomic nerve damage in the intestine caused by *C. parvum*, resulting in sphincter of Oddi dysfunction and papillary stenosis, which is in turn linked to disordered motility in the biliary tract[28].

The next-most common pathogen implicated in the pathogenesis of AIDS cholangiopathy is cytomegalovirus (CMV). It is estimated that 10%-20% of AIDS cholangitis is caused by CMV. Here, the damage is usually found in the arterioles close to the biliary canals, rather than within biliary epithelial cells. It has been postulated that CMV causes vascular injury leading to ischemic damage[15].

Microsporidia is another opportunistic pathogen that has been found to be associated with AIDS cholangiopathy in immunocompromised hosts. The estimated prevalence of AIDS cholangiopathy caused by microsporidia is around 10%, and *Enterocytozoon bieneusi* (*E. bieneusi*) is involved in 80%-90% of these cases. A series of 20 cases reported by some researchers showed that *E. bieneusi* was the only causative organism in those HIV-infected patients with diarrhea. Another study published by Pol *et al*[29] found this pathogen in the biliary samples of all 8 patient studies[30].

There are several other pathogens implicated in AIDS cholangiopathy, but are less well-described. Isospora is a well-known opportunistic pathogen in AIDS patients associated with chronic diarrhea; however, its association with AIDS cholangiopathy is relatively underestimated[31]. Recently, Histoplasma capsulatum was also reported in HIV infections, causing structural changes suggestive of AIDS cholangiopathy. In some cases, multiple pathogens are involved in the pathogenesis[32]. Clearly, there are several opportunistic infections associated with the development of cholangiopathy in AIDS, with the most common being *C. parvum*, CMV, and *E. bieneusi*.

## DIAGNOSIS

Clinical, biochemical and imaging studies necessary for the diagnosis of AIDS related cholangiopathy are as follows:

### *Symptoms and signs*

The clinical presentation of AIDS cholangiopathy

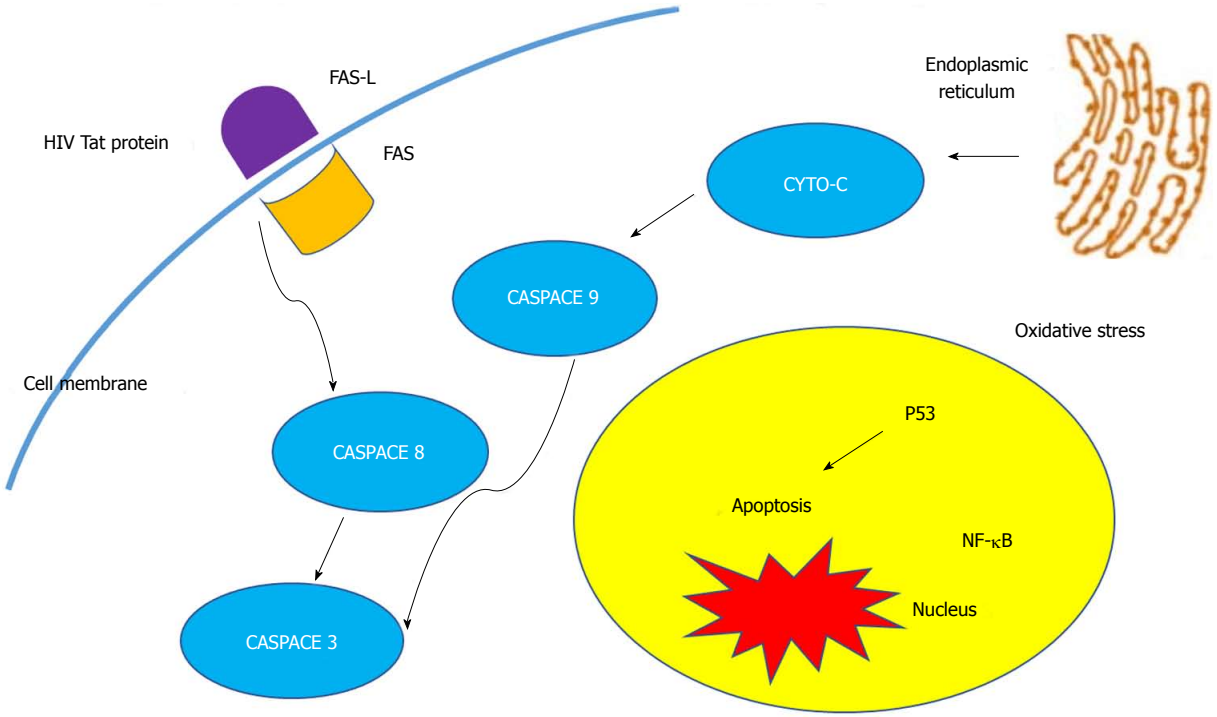


**Figure 1 Molecular mechanism of human immunodeficiency virus cholangiopathy induced by *Cryptosporidium parvum*.**

is variable, ranging from asymptomatic disease to severe right upper quadrant pain associated with nausea, vomiting, and diarrhea. Presence of papillary stenosis is the primary determinant of abdominal pain severity. Less common presenting features include fever and jaundice, usually seen with complete bile duct obstruction. When present, fevers are usually low-grade, but spiking high-grade fevers can be seen with superimposed bacterial cholangitis. Substantial weight loss is also seen commonly, while pruritus is uncommon. On physical examination, abdominal tenderness and hepatomegaly are reported in some case reports[21,33,34].

### *Laboratory criteria*

Elevated liver enzymes, especially markedly elevated alkaline phosphatase and gamma-glutamyl transferase (GGT), is the most common biochemical abnormality associated with AIDS cholangiopathy. It is especially seen in AIDS cholangiopathy associated with disseminated mycobacterium avium complex (MAC). Obstruction of the smaller branches of the biliary tree due to granulomatous infiltration from disseminated MAC is the possible underlying explanation. Only mild to moderate elevation has been observed in other liver chemistries such as alanine aminotransferase and aspartate aminotransferase. Serum bilirubin may remain normal or elevated, depending on the severity of papillary duct stenosis. In approximately one-fourth of patients, the presentation of AIDS cholangiopathy is subtle and not associated with any biochemical abnormalities despite the evidence of cholangiographic abnormalities on imaging studies[35,36].

### *Liver biopsy*

Microscopically, the changes of AIDS cholangiopathy are usually consistent with sclerosing cholangitis[37].

### *Imaging studies*

**Ultrasound:** Being cost-effective, sonography is an ideal screening imaging modality in an HIV-infected patient suspected to have hepatobiliary pathology. The most common abnormalities associated with AIDS cholangiopathy include the dilatation of intrahepatic and extrahepatic ducts, followed by a prominent/dilated common bile duct (CBD), and in some patients, a beaded appearance can also be noted. According to a study published by Daly and associates, ultrasound is 98% accurate in predicting normal or abnormal endoscopic retrograde cholangiopancreatography (ERCP) in AIDS cholangiopathy-it is 97% sensitive and 100% specific in predicting ERCP abnormalities in this clinical setting. Another commonly seen abnormality is the presence of hyperechoic echogenic nodules at the distal end of the CBD, which represents edema of the papilla of Vater noted on ERCP[38,39].

**Contrast-enhanced multidetector computed tomography:** Computed tomography (CT) scans are used widely to evaluate causes of acute and chronic abdominal pain, such as acute pancreatitis in HIV-infected patients. Abdominal CT scans with contrast provide detailed information about hepatic and pancreatic parenchyma and vasculature. In HIV cholangitis, findings of intrahepatic and extrahepatic biliary ductal dilatation in the absence of external compression from malignant

masses are seen commonly[40].

**Cholangiography:** Magnetic resonance cholangiopancreatography (MRCP) is noninvasive and has similar sensitivity to ERCP in diagnosing the characteristic findings of AIDS cholangiopathy. In addition, the risk of complications seen more in ERCP such as iatrogenic pancreatitis, duodenal perforation, hemorrhage, and ascending cholangitis are rare. Currently, MRCP is preferred over ERCP unless there is need for diagnostic and therapeutic procedures, such as brushing, sphincterotomy, or placement of stents due to biliary strictures.

According to the published literature, the most common cholangiographic finding in AIDS cholangiopathy is papillary stenosis, which is a smoothly tapered stricture at the distal end of the CBD at the level of the hepatopancreatic ampulla. In two-thirds of cases, papillary stenosis is present either alone or in combination with intrahepatic ductal dilatation and multifocal intrahepatic biliary strictures with alternating normal segments, or saccular dilatations. The characteristic "beaded" appearance of intrahepatic sclerosing cholangitis-like pattern without intrahepatic and extrahepatic bile duct abnormalities is observed in 20% of patients. The fourth cholangiographic pattern seen in 6%-15% of patients corresponds to a 1-3 cm segmental extrahepatic biliary stricture with or without intrahepatic involvement[41-43].

### *Management*

Symptomatic treatment with opioids such as morphine and CT-guided celiac plexus block has been effective in alleviating abdominal pain[44]. Treatment of opportunistic infections is surprisingly ineffective in halting the progression of sclerosing cholangitis and papillary stenosis. Cryptosporidium, by far the most common pathogen implicated in the pathogenesis of AIDS cholangitis, has no effective eradication therapy[45]. In a few studies, paromomycin, azithromycin, and more recently nitazoxanide have been used without promising results[46,47]. Intravenous gancyclovir and foscarnet are also not beneficial for treatment of CMV-related cholangitis[48]. Though albendazole has been used with some success in disseminated Enterocytozoon intestinalis infection including cholangitis, the therapeutic effect seems to be transient[49]. Trimethoprim-sulfamethoxazole for cyclopora has been used with little success[50]. Treatment is recommended with oral trimethoprim-sulfamethoxazole in addition to ivermectin for isospora[51].

Use of ursodeoxycholic acid (URSO) in AIDS cholangiopathy is associated with symptomatic improvement in abdominal pain and normalization of liver chemistries after sphincterotomy for papillary stenosis[52]. According to the pilot study published by Castiella *et al*[53] in 1997, which included four patients with AIDS cholangiopathy treated with URSO, 100% reported resolution in abdominal pain after 2-4 mo on treatment, and 50% showed improvement in alkaline phosphatase. The mechanism for improvement in pain and liver chemistries with URSO treatment in AIDS cholangiopathy is not yet clear.

To date, the best treatment of opportunistic pathogens causing AIDS-related cholangiopathy is restoration of immune function using HAART or switching to second-line HAART if there is evidence of resistance. The data regarding improvement in clinical symptoms and radiological findings after HAART initiation is conflicting. While most case series studies show improvement in abdominal pain, normalization of liver chemistries, and decrease in the progression of intrahepatic and extrahepatic biliary involvement, a case described by Imai *et al*[54] showed that intrahepatic biliary duct stenosis progressed even after the timely initiation of HAART[55].

Endoscopic sphincterotomy usually provides symptomatic relief of abdominal pain in cholangitis associated with papillary stenosis by decompressing the bile ducts and improving drainage in the biliary tree. The value of endoscopic sphincterotomy has been evaluated in multiple case series. Endpoints of follow-up evaluation were improvement in pain score and cholestasis, decrease in the biliary dilatation, and decreased progression of sclerosing cholangitis. According to the prospective study published by Cello *et al*[56], ERCP sphincterotomy was associated with significant improvement in pain scores up to at least 9 mo of follow-up. However, there was no significant improvement in the level of alkaline phosphatase, and progression of intrahepatic sclerosing cholangitis was observed. These findings are supported by several other studies as well. Though experience is limited, there have been reports of successful biliary stent use in patients with both long and proximal strictures[57].

## PROGNOSIS

The survival of patient with AIDS cholangiopathy is generally poor because of disease association with advanced stages of immunosuppression and the presence of multiple opportunistic infections. In the pre-HAART era, 1-year survival was reported to be 14%-41% with a mean survival of 7-12 mo[58,59]. Remarkable improvement was reported in the median survival of the patients with AIDS cholangiopathy during the last decade, including reports of up to 34 mo median survival. This is thought to be due to earlier diagnosis and management of HIV/AIDS, and improved access to HAART. According to the prospective study published by Ko[60], the factors associated with poor prognosis in AIDS cholangiopathy include history or presence of opportunistic infections, and elevation in the level of alkaline phosphatase eight times above the upper limit of normal. CD4 count, severity of cholangiopathy, and sphincterotomy for decompression of the biliary tract each have no effect

on mortality. In the same study, factors associated with improved survival of the patient but became insignificant after adjusting for confounding factors were older age (30 years or older), the absence of opportunistic infection, diagnosis of AIDS after 1993, and AIDS cholangiopathy after 1996.

## COMPLICATIONS

So far, the primary complications reported to be caused by AIDS-related cholangiopathy are development of cholangiocarcinoma and progression of sclerosing cholangitis despite appropriate treatment. Chronic biliary infection from opportunistic pathogens seen in AIDS cholangiopathy initiate the dysplastic process in the biliary epithelium, leading to development of cholangiocarcinoma. These complications can occur even after restoration of immune function with HAART and improvement in CD4 count, pointing to the fact that the biliary dysplasia associated with AIDS cholangiopathy is irreversible and refractory to HAART-induced immune restoration[61-63].

## CONCLUSION

Clearly, there is still much to be learned regarding AIDS cholangiopathy, particularly with its epidemiology, natural history, and determinants of pathology. While proper diagnosis of this disease has been well described and refined over the years, efficacious treatment methods for improving both symptomatic and pathologic processes, as well as preventing grave complications, still leave much to be desired. Hopefully, increased awareness of AIDS cholangiopathy through review articles such as this, will lead to further studies and better treatment options for afflicted patients, across both developed and developing countries, in the near future.

## REFERENCES


1 **Fettig J**, Swaminathan M, Murrill CS, Kaplan JE. Global epidemiology of HIV. *Infect Dis Clin North Am* 2014; **28**: 323-337 [PMID: 25151559 DOI: 10.1016/j.idc.2014.05.001]

2 **GBD 2015 Mortality and Causes of Death Collaborators**. Global, regional, and national life expectancy, all-cause mortality, and cause-specific mortality for 249 causes of death, 1980-2015: a systematic analysis for the Global Burden of Disease Study 2015. *Lancet* 2016; **388**: 1459-1544 [PMID: 27733281 DOI: 10.1016/S0140-6736(16)31012-1]

3 **Bain LE**, Nkoke C, Noubiap JJN. UNAIDS 90-90-90 targets to end the AIDS epidemic by 2020 are not realistic: comment on "Can the UNAIDS 90-90-90 target be achieved? A systematic analysis of national HIV treatment cascades". *BMJ Glob Health* 2017; **2**: e000227 [PMID: 28589026 DOI: 10.1136/bmjgh-2016-000227]

4 **Palella FJ Jr**, Delaney KM, Moorman AC, Loveless MO, Fuhrer J, Satten GA, Aschman DJ, Holmberg SD. Declining morbidity and mortality among patients with advanced human immunodeficiency virus infection. HIV Outpatient Study Investigators. *N Engl J Med* 1998; **338**: 853-860 [PMID: 9516219]

5 **Smith CJ**, Ryom L, Weber R, Morlat P, Pradier C, Reiss P, Kowalska JD, de Wit S, Law M, el Sadr W, Kirk O, Friis-Moller N, Monforte Ad, Phillips AN, Sabin CA, Lundgren JD; D:A:D Study Group. Trends in underlying causes of death in people with HIV from 1999 to 2011 (D:A:D): a multicohort collaboration. *Lancet* 2014; **384**: 241-248 [PMID: 25042234 DOI: 10.1016/S0140-6736(14)60604-8]

6 **Puri P**, Kumar S. Liver involvement in human immunodeficiency virus infection. *Indian J Gastroenterol* 2016; **35**: 260-273 [PMID: 27256434 DOI: 10.1007/s12664-016-0666-8]

7 **Kaspar MB**, Sterling RK. Mechanisms of liver disease in patients infected with HIV. *BMJ Open Gastroenterol* 2017; **4**: e000166 [PMID: 29119002 DOI: 10.1136/bmjgast-2017-000166]

8 **Hessamfar-Bonarek M**, Morlat P, Salmon D, Cacoub P, May T, Bonnet F, Rosenthal E, Costagliola D, Lewden C, Chêne G; Mortalité 2000 & 2005 Study Groups. Causes of death in HIV-infected women: persistent role of AIDS. The 'Mortalité 2000 & 2005' Surveys (ANRS EN19). *Int J Epidemiol* 2010; **39**: 135-146 [PMID: 19805489 DOI: 10.1093/ije/dyp300]

9 **Housset C**, Lamas E, Courgnaud V, Boucher O, Girard PM, Marche C, Brechot C. Presence of HIV-1 in human parenchymal and non-parenchymal liver cells in vivo. *J Hepatol* 1993; **19**: 252-258 [PMID: 8301058]

10 **Abdalian R**, Heathcote EJ. Sclerosing cholangitis: a focus on secondary causes. *Hepatology* 2006; **44**: 1063-1074 [PMID: 17058222]

11 **Pitlik SD**, Fainstein V, Garza D, Guarda L, Bolivar R, Rios A, Hopfer RL, Mansell PA. Human cryptosporidiosis: spectrum of disease. Report of six cases and review of the literature. *Arch Intern Med* 1983; **143**: 2269-2275 [PMID: 6651420]

12 **Guarda LA**, Stein SA, Cleary KA, Ordóñez NG. Human cryptosporidiosis in the acquired immune deficiency syndrome. *Arch Pathol Lab Med* 1983; **107**: 562-566 [PMID: 6688714]

13 **Margulis SJ**, Honig CL, Soave R, Govoni AF, Mouradian JA, Jacobson IM. Biliary tract obstruction in the acquired immunodeficiency syndrome. *Ann Intern Med* 1986; **105**: 207-210 [PMID: 3014940]

14 **Schneiderman DJ**. Hepatobiliary abnormalities of AIDS. *Gastroenterol Clin North Am* 1988; **17**: 615-630 [PMID: 3049366]

15 **Cello JP**. Acquired immunodeficiency syndrome cholangiopathy: spectrum of disease. *Am J Med* 1989; **86**: 539-546 [PMID: 2712061]

16 **Enns R**. AIDS cholangiopathy: "an endangered disease". *Am J Gastroenterol* 2003; **98**: 2111-2112 [PMID: 14572552]

17 **Braitstein P**, Brinkhof MW, Dabis F, Schechter M, Boulle A, Miotti P, Wood R, Laurent C, Sprinz E, Seyler C, Bangsberg DR, Balestre E, Sterne JA, May M, Egger M; Antiretroviral Therapy in Lower Income Countries (ART-LINC) Collaboration; ART Cohort Collaboration (ART-CC) groups. Mortality of HIV-1-infected patients in the first year of antiretroviral therapy: comparison between low-income and high-income countries. *Lancet* 2006; **367**: 817-824 [PMID: 16530575]

18 **Fleming AF**. Opportunistic infections in AIDS in developed and developing countries. *Trans R Soc Trop Med Hyg* 1990; **84** Suppl 1: 1-6 [PMID: 2201107]

19 **Glasgow BJ**, Anders K, Layfield LJ, Steinsapir KD, Gitnick GL, Lewin KJ. Clinical and pathologic findings of the liver in the acquired immune deficiency syndrome (AIDS). *Am J Clin Pathol* 1985; **83**: 582-588 [PMID: 2986450]

20 **Cello JP.** Gastrointestinal tract manifestations of AIDS. In: Sande MA, volberding PA. The medical management of AIDS. 5th ed. Philadelphia: W.B. Saunders Company; 1997: 181-195

21 **De Angelis C**, Mangone M, Bianchi M, Saracco G, Repici A, Rizzetto M, Pellicano R. An update on AIDS-related cholangiopathy. *Minerva Gastroenterol Dietol* 2009; **55**: 79-82 [PMID: 19212310]

22 **Gao Y**, Chin K, Mishriki YY. AIDS Cholangiopathy in an Asymptomatic, Previously Undiagnosed Late-Stage HIV-Positive Patient from Kenya. *Int J Hepatol* 2011; **2011**: 465895 [PMID: 21994858 DOI: 10.4061/2011/465895]

23 **Wilcox CM**, Mönkemüller KE. Hepatobiliary diseases in patients with AIDS: focus on AIDS cholangiopathy and gallbladder disease.

*Dig Dis* 1998; **16**: 205-213 [PMID: 9732180]
24 **Squire SA**, Ryan U. Cryptosporidium and Giardia in Africa: current and future challenges. *Parasit Vectors* 2017; **10**: 195 [PMID: 28427454 DOI: 10.1186/s13071-017-2111-y]
25 **Hunter PR**, Nichols G. Epidemiology and clinical features of Cryptosporidium infection in immunocompromised patients. *Clin Microbiol Rev* 2002; **15**: 145-154 [PMID: 11781272]
26 **Chen XM**, LaRusso NF. Mechanisms of attachment and internalization of Cryptosporidium parvum to biliary and intestinal epithelial cells. *Gastroenterology* 2000; **118**: 368-379 [PMID: 10648465]
27 **O'Hara SP**, Small AJ, Gajdos GB, Badley AD, Chen XM, Larusso NF. HIV-1 Tat protein suppresses cholangiocyte toll-like receptor 4 expression and defense against Cryptosporidium parvum. *J Infect Dis* 2009; **199**: 1195-1204 [PMID: 19265483 DOI: 10.1086/597387]
28 **Yusuf TE**, Baron TH. AIDS Cholangiopathy. *Curr Treat Options Gastroenterol* 2004; **7**: 111-117 [PMID: 15010025]
29 **Pol S**, Romana CA, Richard S, Amouyal P, Desportes-Livage I, Carnot F, Pays JF, Berthelot P. Microsporidia infection in patients with the human immunodeficiency virus and unexplained cholangitis. *N Engl J Med* 1993; **328**: 95-99 [PMID: 8416439]
30 **Sheikh RA**, Prindiville TP, Yenamandra S, Munn RJ, Ruebner BH. Microsporidial AIDS cholangiopathy due to Encephalitozoon intestinalis: case report and review. *Am J Gastroenterol* 2000; **95**: 2364-2371 [PMID: 11007244]
31 **Walther Z**, Topazian MD. Isospora cholangiopathy: case study with histologic characterization and molecular confirmation. *Hum Pathol* 2009; **40**: 1342-1346 [PMID: 19447468 DOI: 10.1016/j.humpath.2009.01.020]
32 **Kapelusznik L**, Arumugam V, Caplivski D, Bottone EJ. Disseminated histoplasmosis presenting as AIDS cholangiopathy. *Mycoses* 2011; **54**: 262-264 [PMID: 19821907 DOI: 10.1111/j.1439-0507.2009.01791.x]
33 **Keaveny AP**, Karasik MS. Hepatobiliary and pancreatic infections in AIDS: Part II. *AIDS Patient Care STDS* 1998; **12**: 451-456 [PMID: 11361992]
34 **Devarbhavi H**, Sebastian T, Seetharamu SM, Karanth D. HIV/AIDS cholangiopathy: clinical spectrum, cholangiographic features and outcome in 30 patients. *J Gastroenterol Hepatol* 2010; **25**: 1656-1660 [PMID: 20880175 DOI: 10.1111/j.1440-1746.2010.06336.x]
35 **Das CJ**, Sharma R. Hepatobiliary and pancreatic: AIDS cholangiopathy. *J Gastroenterol Hepatol* 2006; **21**: 774 [PMID: 16729390]
36 **Benhamou Y**, Caumes E, Gerosa Y, Cadranel JF, Dohin E, Katlama C, Amouyal P, Canard JM, Azar N, Hoang C. AIDS-related cholangiopathy. Critical analysis of a prospective series of 26 patients. *Dig Dis Sci* 1993; **38**: 1113-1118 [PMID: 8389687]
37 **Forbes A**, Blanshard C, Gazzard B. Natural history of AIDS related sclerosing cholangitis: a study of 20 cases. *Gut* 1993; **34**: 116-121 [PMID: 8381757]
38 **Daly CA**, Padley SP. Sonographic prediction of a normal or abnormal ERCP in suspected AIDS related sclerosing cholangitis. *Clin Radiol* 1996; **51**: 618-621 [PMID: 8810689]
39 **Da Silva F**, Boudghene F, Lecomte I, Delage Y, Grange JD, Bigot JM. Sonography in AIDS-related cholangitis: prevalence and cause of an echogenic nodule in the distal end of the common bile duct. *AJR Am J Roentgenol* 1993; **160**: 1205-1207 [PMID: 8498216]
40 **Carucci LR**, Halvorsen RA. Abdominal and pelvic CT in the HIV-positive population. *Abdom Imaging* 2004; **29**: 631-642 [PMID: 15520901]
41 **Bouche H**, Housset C, Dumont JL, Carnot F, Menu Y, Aveline B, Belghiti J, Boboc B, Erlinger S, Berthelot P. AIDS-related cholangitis: diagnostic features and course in 15 patients. *J Hepatol* 1993; **17**: 34-39 [PMID: 8445217]
42 **Bilgin M**, Balci NC, Erdogan A, Momtahen AJ, Alkaade S, Rau WS. Hepatobiliary and pancreatic MRI and MRCP findings in patients with HIV infection. *AJR Am J Roentgenol* 2008; **191**: 228-232 [PMID: 18562750 DOI: 10.2214/AJR.07.3197]
43 **Tonolini M**, Bianco R. HIV-related/AIDS cholangiopathy: pictorial review with emphasis on MRCP findings and differential diagnosis. *Clin Imaging* 2013; **37**: 219-226 [PMID: 23465971 DOI: 10.1016/j.clinimag.2012.03.008]
44 **Collazos J**, Mayo J, Martínez E, Callejo A, Blanco I. Celiac plexus block as treatment for refractory pain related to sclerosing cholangitis in AIDS patients. *J Clin Gastroenterol* 1996; **23**: 47-49 [PMID: 8835900]
45 **Hoepelman AI**. Current therapeutic approaches to cryptosporidiosis in immunocompromised patients. *J Antimicrob Chemother* 1996; **37**: 871-880 [PMID: 8737137]
46 **White AC Jr**, Chappell CL, Hayat CS, Kimball KT, Flanigan TP, Goodgame RW. Paromomycin for cryptosporidiosis in AIDS: a prospective, double-blind trial. *J Infect Dis* 1994; **170**: 419-424 [PMID: 8035029]
47 **Rossignol JF**, Ayoub A, Ayers MS. Treatment of diarrhea caused by Cryptosporidium parvum: a prospective randomized, double-blind, placebo-controlled study of Nitazoxanide. *J Infect Dis* 2001; **184**: 103-106 [PMID: 11398117]
48 **Oku T**, Maeda M, Waga E, Wada Y, Nagamachi Y, Fujita M, Suzuki Y, Nagashima K, Niitsu Y. Cytomegalovirus cholangitis and pancreatitis in an immunocompetent patient. *J Gastroenterol* 2005; **40**: 987-992 [PMID: 16261436]
49 **Molina JM**, Oksenhendler E, Beauvais B, Sarfati C, Jaccard A, Derouin F, Modaï J. Disseminated microsporidiosis due to Septata intestinalis in patients with AIDS: clinical features and response to albendazole therapy. *J Infect Dis* 1995; **171**: 245-249 [PMID: 7798674]
50 **Deodhar L**, Maniar JK, Saple DG. Cyclospora infection in acquired immunodeficiency syndrome. *J Assoc Physicians India* 2000; **48**: 404-406 [PMID: 11273176]
51 **Lagrange-Xélot M**, Porcher R, Sarfati C, de Castro N, Carel O, Magnier JD, Delcey V, Molina JM. Isosporiasis in patients with HIV infection in the highly active antiretroviral therapy era in France. *HIV Med* 2008; **9**: 126-130 [PMID: 18257775 DOI: 10.1111/j.1468-1293.2007.00530.x]
52 **Chan MF,** Koch J, Cello JP. Ursodeoxycholic acid for symptomatic AIDS associated cholangiopathy. *Gastrointest Endosc* 1994; **40**: 103
53 **Castiella A**, Iribarren JA, López P, Arrizabalaga J, Rodríguez F, von Wichmann MA, Arenas JI. Ursodeoxycholic acid in the treatment of AIDS-associated cholangiopathy. *Am J Med* 1997; **103**: 170-171 [PMID: 9274905]
54 **Imai K**, Misawa K, Matsumura T, Fujikura Y, Mikita K, Tokoro M, Maeda T, Kawana A. Progressive HIV-associated Cholangiopathy in an HIV Patient Treated with Combination Antiretroviral Therapy. *Intern Med* 2016; **55**: 2881-2884 [PMID: 27725553]
55 **Mahajani RV**, Uzer MF. Cholangiopathy in HIV-infected patients. *Clin Liver Dis* 1999; **3**: 669-684, x [PMID: 11291244]
56 **Cello JP**, Chan MF. Long-term follow-up of endoscopic retrograde cholangiopancreatography sphincterotomy for patients with acquired immune deficiency syndrome papillary stenosis. *Am J Med* 1995; **99**: 600-603 [PMID: 7503081]
57 **Cordero E**, López-Cortés LF, Belda O, Villanueva JL, Rodríguez-Hernández MJ, Pachón J. Acquired immunodeficiency syndrome-related cryptosporidial cholangitis: resolution with endobiliary prosthesis insertion. *Gastrointest Endosc* 2001; **53**: 534-535 [PMID: 11275908]
58 **Hessol NA**, Koblin BA, van Griensven GJ, Bacchetti P, Liu JY, Stevens CE, Coutinho RA, Buchbinder SP, Katz MH. Progression of human immunodeficiency virus type 1 (HIV-1) infection among homosexual men in hepatitis B vaccine trial cohorts in Amsterdam, New York City, and San Francisco, 1978-1991. *Am J Epidemiol* 1994; **139**: 1077-1087 [PMID: 8192140]
59 **Ducreux M**, Buffet C, Lamy P, Beaugerie L, Fritsch J, Choury A, Liguory C, Longuet P, Gendre JP, Vachon F. Diagnosis and prognosis of AIDS-related cholangitis. *AIDS* 1995; **9**: 875-880 [PMID: 7576321]
60 **Ko WF**, Cello JP, Rogers SJ, Lecours A. Prognostic factors for the survival of patients with AIDS cholangiopathy. *Am J Gastroenterol* 2003; **98**: 2176-2181 [PMID: 14572564]

61 **Datta J**, Shafi BM, Drebin JA. Extrahepatic cholangiocarcinoma developing in the setting of AIDS cholangiopathy. *Am Surg* 2013; **79**: 321-322 [PMID: 23461961]
62 **Charlier C**, Lecuit M, Furco A, Estavoyer JM, Lafeuillade A, Dupont B, Lortholary O, Viard JP. Cholangiocarcinoma in HIV-Infected patients with a history of Cholangitis. *J Acquir Immune Defic Syndr* 2005; **39**: 253-255 [PMID: 15905745]
63 **Mangeya N**, Mafukidze AT, Pascoe M, Mbuwayesango B, Madziva D, Ndlovu N, Corbett EL, Miller RF, Ferrand RA. Cholangiocarcinoma presenting in an adolescent with vertically acquired HIV infection. *Int J STD AIDS* 2008; **19**: 717-718 [PMID: 18824629 DOI: 10.1258/ijsa.2008.008078]

**P- Reviewer**: Akbulut S, Waheed Y **S- Editor**: Ma YJ **L- Editor**: A
**E- Editor**: Huang Y

World Journal of Gastroenterology

Submit a Manuscript: http://www.f6publishing.com

*World J Gastroenterol* 2018 February 21; 24(7): 775-793

DOI: 10.3748/wjg.v24.i7.775

ISSN 1007-9327 (print) ISSN 2219-2840 (online)

ORIGINAL ARTICLE

Basic Study

# Glucose transporter expression in the human colon

Flavia Merigo, Alessandro Brandolese, Sonia Facchin, Silvia Missaggia, Paolo Bernardi, Federico Boschi, Renata D'Incà, Edoardo Vincenzo Savarino, Andrea Sbarbati, Giacomo Carlo Sturniolo

Flavia Merigo, Silvia Missaggia, Paolo Bernardi, Andrea Sbarbati, Department of Neuroscience, Biomedicine and Movement, Human Anatomy and Histology Section, University of Verona, Verona I-37134, Italy

Alessandro Brandolese, Department of Medicine, Gastroenterology Section, University of Verona, Verona I-37134, Italy

Sonia Facchin, Renata D'Incà, Edoardo Vincenzo Savarino, Giacomo Carlo Sturniolo, Department of Surgery, Oncology and Gastroenterology, Gastroenterology Section, University Hospital of Padua, Padua I-35128, Italy

Federico Boschi, Department of Computer Science, University of Verona, Verona I-37134, Italy

ORCID number: Flavia Merigo (0000-0002-6919-7169); Alessandro Brandolese (0000-0003-2977-992X); Sonia Facchin (0000-0002-6774-590X); Silvia Missaggia (0000-0002-8437-379X); Paolo Bernardi (0000-0002-1225-9525); Federico Boschi (0000-0001-9623-6859); Renata D'Incà(0000-0003-1169-1890); Edoardo Vincenzo Savarino (0000-0002-3187-2894); Andrea Sbarbati (0000-0002-0954-2119); Giacomo Carlo Sturniolo (0000-0002-2398-110X).

Author contributions: Merigo F was involved in experimental design, immunohistochemistry, data analyses, and manuscript writing; Brandolese A contributed to clinical sample documentation, presentation of the results, and manuscript writing; Facchin S, D'Incà R and Savarino EV contributed to clinical sample collection and documentation; Missaggia S contributed to immunohistochemistry analysis; Bernardi P performed SEM analysis; Boschi F analyzed the data; Sbarbati A and Sturniolo GC were involved in experimental design, final critical reading of the manuscript before submission; all authors contributed to the final manuscript.

Institutional review board statement: The study was reviewed and approved by the Ethics Committee of Padua University Hospital (study n° 2813P) Institutional Review Board.

Conflict-of-interest statement: All authors declare no conflicts of interest.

Data sharing statement: Technical appendix and data set are available from the corresponding author at flavia.merigo@univr.it. Participants gave informed consent for data sharing. The present data are anonymized and the risk of identification is low.



Manuscript source: Unsolicited manuscript

Correspondence to: Flavia Merigo, BSc, Human Anatomy and Histology Section, Department of Neuroscience, Biomedicine and Movement, University of Verona, Strada Le Grazie 8, Verona I-37134, Italy. flavia.merigo@univr.it
Telephone: +39-45-8027155
Fax: +39-45-8027163

Received: December 6, 2017
Peer-review started: December 6, 2017
First decision: December 12, 2017
Revised: December 13, 2017
Accepted: December 19, 2017
Article in press: December 19, 2017
Published online: February 21, 2018

## Abstract

### *AIM*

To investigate by immunostaining glucose transporter expression in human colorectal mucosa in controls and patients with inflammatory bowel disease (IBD).

### *METHODS*

Colorectal samples were obtained from patients undergoing lower endoscopic colonoscopy or recto-sigmoidoscopy. Patients diagnosed with ulcerative

colitis ($n$ = 18) or Crohn's disease ($n$ = 10) and scheduled for diagnostic colonoscopy were enrolled. Patients who underwent colonoscopy for prevention screening of colorectal cancer or were followed-up after polypectomy or had a history of lower gastrointestinal symptoms were designated as the control group (CTRL, $n$ = 16). Inflammatory status of the mucosa at the sampling site was evaluated histologically and/or endoscopically. A total of 147 biopsies of colorectal mucosa were collected and processed for immunohistochemistry analysis. The expression of GLUT2, SGLT1, and GLUT5 glucose transporters was investigated using immunoperoxidase labeling. To compare immunoreactivity of GLUT5 and LYVE-1, which is a marker for lymphatic vessel endothelium, double-labeled confocal microscopy was used.

***RESULTS***

Immunohistochemical analysis revealed that GLUT2, SGLT1, and GLUT5 were expressed only in short epithelial portions of the large intestinal mucosa. No important differences were observed in glucose transporter expression between the samples obtained from the different portions of the colorectal tract and between the different patient groups. Unexpectedly, GLUT5 expression was also identified in vessels, mainly concentrated in specific areas where the vessels were clustered. Immunostaining with LYVE-1 and GLUT5 antibodies revealed that GLUT5-immunoreactive (-IR) clusters of vessels were concentrated in areas internal to those that were LYVE-1 positive. GLUT5 and LYVE-1 did not appear to be colocalized but rather showed a close topographical relationship on the endothelium. Based on their LYVE-1 expression, GLUT5-IR vessels were identified as lymphatic. Both inflamed and non-inflamed mucosal colorectal tissue biopsies from the IBD and CTRL patients showed GLUT5-IR clusters of lymphatic vessels.

***CONCLUSION***

Glucose transporter immunoreactivity is present in colorectal mucosa in controls and IBD patients. GLUT5 expression is also associated with lymphatic vessels. This novel finding aids in the characterization of lymphatic vasculature in IBD patients.

**Key words:** Ulcerative colitis; Colon; Crohn's disease; Glucose transporter; LYVE-1, Immunohistochemistry



**Core tip:** Our study demonstrates that GLUT2, SGLT1, and GLUT5 glucose transporters are expressed in the colorectal mucosa in controls and patients with inflammatory bowel disease (IBD). In addition, it provides first evidence that GLUT5 expression is associated with lymphatic vessels in controls and IBD patients. GLUT5-immunoreactive vessels were isolated or clustered in specific areas. We interpreted the presence of clusters as a pattern related to proliferative zones. As GLUT5 is the main fructose transporter, fructose may have a role in the atypical aggregation of lymphatic vessels. This novel finding yields further insight into the characterization of lymphatic vasculature, whose dysfunction is a long-recognized feature in humans with IBD.

Merigo F, Brandolese A, Facchin S, Missaggia S, Bernardi P, Boschi F, D'Incà R, Savarino EV, Sbarbati A, Sturniolo GC. Glucose transporter expression in the human colon. *World J Gastroenterol* 2018; 24(7): 775-793 Available from: URL: http://www.wjgnet.com/1007-9327/full/v24/i7/775.htm DOI: http://dx.doi.org/10.3748/wjg.v24.i7.775

## INTRODUCTION

Facilitative monosaccharide transport across the cell membrane is mediated by the GLUT family of membrane proteins encoded by the solute carrier transporter 2 (*SLC2*) gene. The GLUT protein family comprises 14 isoforms that differ by expression pattern and by affinity for sugars, polyols, and other carbon compounds[1]. The GLUT5 and GLUT2 (also known as SLC2A5 and SLC2A2, respectively) isoforms are predominantly but not exclusively distributed in the intestine.

GLUT5 is a sugar transporter that facilitates fructose uptake. In mice, GLUT5 mRNA is abundantly detected by in situ hybridization and PCR in the small intestine but not in the large intestine. It is expressed in the small intestine and other organs such as the brain, testes, skeletal muscle, adipocytes, and kidneys[2,3]. In enterocytes, it is located on the apical membrane. In the small intestine of rats, GLUT5 expression may be increased by exposure to fructose (or its metabolites), steroids, and thyroid hormones depending on age and weaning stage[4-7]. GLUT5 expression differs according to insulin-resistance in adipocytes and duodenal enterocytes[8,9]. It is also implicated in the development of metabolic diseases such as fructose-induced hypertension and non-alcoholic fatty liver disease[10].

GLUT2 expression is widely present throughout the digestive system[11], greatest in the small intestine and least in the terminal ileum. Molecular biology studies indicate that it is not expressed in the large intestine in mice[12]. In humans, GLUT2 expression has been observed in enterocytes and enteroendocrine L-cells. In enterocytes, it is mainly located in the basolateral membrane where it facilitates the passage of glucose towards the interstitial space and bloodstream. In mice, it has been observed in the apical region of enterocytes after a sugar-rich meal or when insulin-resistance develops[13-16]. GLUT2 is also expressed in enteroendocrine L-cells of the distal small intestine and large intestine in humans, and it is responsible for the secretion of glucagon-like peptide 1 (GLP-1)[17-19].

Because of the gradient of glucose concentration between the cytosol and the intestinal lumen, glucose uptake by enterocytes depends mostly on SGLT1, which is a $Na^+$/glucose co-transporter of the human family SLC5[20]. SGLT1 is located on the apical membrane of enterocytes[21]. In mice, SGLT1 expression was found to be intensely present from the duodenum to the end of the ileum where its levels tend to decrease, as demonstrated by in situ hybridization and PCR techniques. In the large intestine, SGLT1 expression remains controversial because SGLT1 mRNA in the proximal colon has been detected by in situ hybridization but not by PCR[12]. SGLT1 is also known to be implicated in glucose-mediated GLP1 exocytosis through depolarization of the L-cell membrane[22].

Further implications of these transporters other than sugar uptake and metabolism have been proposed for inflammation, malignancy, and gut microbiota regulation. Research has shown that GLUT5 activity and expression are regulated under normal conditions but they are altered in pathological conditions[7]. GLUT5 is over-expressed in malignant but not in normal human tissues, including colonic and hepatic tissues, and it can be considered an important diagnostic or therapeutic target in tumors relying on fructose for proliferation such as breast cancer and pancreatic cancer[23-25]. GLUT5 mRNA levels in non-inflamed small intestine of rats with iodacetamide-induced colitis were observed to be lower than in controls, suggesting a possible link between this fructose transporter and inflammatory cytokines. On the other hand, fructose absorption in rabbit was found to be inversely proportional to TNF-alpha expression and bacterial lipopolysaccharide (LPS) exposure[26,27]. In mice models, GLUT5 deficiency has been reported to be associated with severe malabsorption due to dilation of the cecum and colon[28].

GLUT2 has a high affinity for glucosamine, an amino-monosaccharide with anti-inflammatory activity against sodium dextran sulfate-induced colitis, which is a model for inflammatory bowel disease (IBD) in rats[29]. Moreover, it has also been reported to have a role in modulating gut microbiota: after intestinal-specific deletion of GLUT2 in mice, an increase in commensal bacteria was observed in association with an improvement in inflammatory status[19].

SGLT1 (like GLUT2) mRNA and protein levels were found to be significantly increased in intestinal biopsies of diabetic human subjects[9]. Some mechanisms of cellular survival linked to SGLT1 have been demonstrated in Caco-2 cells models when exposed to bacterial LPS[30]. Furthermore, SGLT1 expression in these models was found to be inversely proportional to TNF-alpha expression, implicating its potential involvement in colonic inflammatory diseases[31]. In addition, in vivo studies on mice have shown that oral glucose and 3-O-methyl-d-glucose (a non-metabolizable glucose analogue ) administration promotes survival in endotoxic shock induced by LPS[32]. These studies suggest a protective role for SGLT1 in inflammatory processes or sepsis, possibly by maintaining intestinal barrier integrity. SGLT1 acts through the inhibition of intestinal epithelial cell activation mediated by phosphorylation of the signaling molecule Nf-KB, a protein complex involved in the gene regulation of several cellular responses, which is a known mechanism in the epithelium of patients with Crohn's disease (CD) and ulcerative colitis (UC)[33-35].

These findings raise expectations for future discoveries; however, most studies to date on sugar transporters in the gastrointestinal tract have been performed using molecular biology in murine or in vitro models. Since topographical variations in glucose transporters have been detected mainly by biochemical rather than standard immunohistochemical analysis also in humans, the localization and distribution of glucose transporters in the large intestinal mucosa of the colon have not yet been clarified.

For this reason, the aim of this study was to investigate by immunostaining at light and confocal microscopy the expression of the major intestinal glucose transporters (GLUT5, GLUT2, SGLT1) in human colonic mucosa in control subjects and subjects with IBD.

## MATERIALS AND METHODS

The study protocol was approved by the Ethics Committee of Padua University Hospital (study No. 2813P). Written, informed consent was obtained from all participants prior to inclusion in the study. The study was prospectively conducted from December 2013 to November 2015.

### *Patients*

Patients diagnosed with UC or CD and scheduled for diagnostic colonoscopy were enrolled. Patients who underwent colonoscopy for prevention screening of colorectal cancer or were followed-up after polypectomy or lower gastrointestinal symptoms were designated as the control group (CTRL). Inclusion criteria are presented in Table 1.

The UC patient group ($n$ = 18) included 8 men and 10 women (mean age 47 years, range 30-66; average body-mass index (BMI, weight in kg divided by height in m squared) 24 kg/m$^2$, range 18-32.9 kg/m$^2$.

The CD patient group ($n$ = 10) included 5 men and 5 women (mean age 37 years, range 19-53; average BMI 23.6 kg/m$^2$, range19.6-26.1 kg/m$^2$.

The CTRL patient group ($n$ = 16) included 6 men and 10 women (mean age 56 years, range 27-72, average BMI 24.85 kg/m$^2$, range 18.1-31.1 kg/m$^2$. All CTRL patients were evaluated based on histological and/or endoscopic examination of intestinal biopsies; none was affected by UC or CD.

Patients were classified by their BMI into one of three groups: normal weight for BMI < 24.9 kg/m$^2$,

**Table 1 Criteria of inclusion for patients in each group**

| Patient group | Periodic Follow-up (*n*) | New stadiation of IBD (*n*) | Abdominal pain (*n*) | Chronic diarrhea (*n*) | Colorectal cancer screening (*n*) | Stipsis (*n*) | Hemorrhoids (*n*) |
|---|---|---|---|---|---|---|---|
| UC | 16 | 2 | - | - | - | - | - |
| CD | 2 | 8 | - | - | - | - | - |
| CTRL | 3[1] | - | 5 | 4 | 2 | 1 | 1 |

[1]Follow up after polypectomy. CD: Crohn's disease; UC: Ulcerative colitis; CTRL: Controls; IBD: Inflammatory bowel disease.

**Table 2 Number of biopsies analyzed by immunohistochemistry in each tract of large intestine**

| Patient group | Biopsy status | Large Intestine | | | | | |
|---|---|---|---|---|---|---|---|
| | | Proximal Tract | | | Distal Tract | | |
| | | Cecum colon (*n*) | Ascending colon (*n*) | Transverse colon (*n*) | Descending colon (*n*) | Sigmoid colon (*n*) | Rectum (*n*) |
| UC | Inflamed | 2 | 6 | 4 | 6 | 7 | 7 |
| | Non-Inflamed | 7 | 9 | 5 | 6 | 3 | 3 |
| CD | Inflamed | 0 | 4 | 3 | 4 | 4 | 4 |
| | Non-Inflamed | 1 | 1 | 0 | 1 | 2 | 1 |
| CTRL | Inflamed | 2 | 4 | 3 | 2 | 4 | 4 |
| | Non-Inflamed | 7 | 5 | 6 | 6 | 7 | 7 |

CD: Crohn's disease; UC: Ulcerative colitis; CTRL: Controls.

overweight for 25.0-29.9, and obese for > 30 kg/m$^2$.

### *Colorectal samples*

Colorectal samples were obtained from patients undergoing lower endoscopic colonoscopy or recto-sigmoidoscopy (2 in the CTRL group). Biopsies of portions of the colonic tract were taken for diagnostic purposes according to the endoscopist's judgment, and for immunohistochemistry (IHC). The biopsies were collected from adjacent sites to compare the level of inflammation in independent samples. In 14 of the 44 patients who underwent a complete colonoscopy, biopsies were obtained of all 6 portions of the colon-rectum (cecum, ascending colon, transverse, descending, sigmoid colon, rectum). In the remaining 30 patients, biopsies were obtained only from the endoscopically examined portions.

A total of 147 biopsies of colonic mucosa were collected for IHC analysis. Inflammatory status of the mucosa at the sampling site was evaluated endoscopically in all biopsies and histologically in 127 out of 147 biopsies by an experienced pathologist who evaluated the mononuclear and polymorphonuclear cell infiltration of the mucosal layer. For the endoscopic findings, inflammatory status was graded according to the Mayo endoscopic score in the UC patients (Mayo score of 0 indicates normal colonic mucosa, > 0 evidence of macroscopic active inflammation), and according to the Rutgeerts score in previously resected CD (3 out of 10) patients (Rutgeerts score of 0-1 indicates normal ileocolic anastomosis, and > 1 macroscopic relapse of CD). For the non-resected CD and CTRL patients, inflammatory mucosal status was graded as documented in the endoscopic report. Based on histological and endoscopic grading, their status towards inflammation and classification as inflamed or non-inflamed was determined. When the endoscopic grade differed from the histological grade, the final biopsy status was decided on the basis of the pathologist's assessment. The complete list of all biopsies analyzed by IHC, classified according to inflammation status, is shown in Table 2.

### *Tissue preparation*

After sampling, specimens were fixed in 40 g/L formaldehyde and processed by embedding in paraffin using standard methods. Sections were cut to 7 μm thickness, mounted on polylysine-coated microscope slides, and processed for immunoperoxidase and double immunofluorescence labeling. Primary and secondary antibodies are listed in Table 3.

### *Peroxidase-immunohistochemistry*

Sections were deparaffinized in xylene, rehydrated through passages in alcohol with decreasing concentrations to water, and then microwaved at 800 W for three five-minute cycles in 0.01 mol/L citrate buffer (pH 6) to optimize antigen retrieval. Endogenous peroxidase activity was blocked by incubating the slides in 30 mL/L $H_2O_2$ in methanol for 30 min. After rinsing in PBS, the slides were first incubated with blocking solution (3 mL/L Triton X-100, 10 g/L bovine serum albumin, and 10 mL/L normal swine or rabbit serum); the solution was used to dilute the antibodies. Subsequently, the sections were incubated with primary antibodies overnight at 4 ℃ and then reacted with biotinylated secondary antibody for 1 h at room temperature. The immunoreaction was detected using a Vectastain Elite ABC kit (Vector Laboratories, Burlingame, CA, United States) and then visualized with 3.3'-diaminobenzidine tetrahydrocloride (Dako, Milan, Italy) for 5-10 min. Finally, the sections were mounted in Entellan (Merck,

**Table 3 Primary and secondary antibodies for immunohistochemical analysis**

| Antibody | Host | Dilution | Source |
|---|---|---|---|
| Anti-GLUT2 | Goat | 1:200 | cat#ab111117, abcam, Cambridge, United Kingdom |
| Anti-GLUT5 | Rabbit | 1:400 | cat#ab36057, abcam |
| Anti-SGLT1 | Rabbit | 1:200 | cat#ab14686, abcam |
| Anti-LYVE-1 | Rabbit | 1:500 | cat#Bs-1311R, Bioss,Woburn, MA, United States |
| Anti-VEGF | Rabbit | 1:200 | cat#RB-222, Thermo Scientific, Fremont, CA, United States |
| Polyclonal anti-rabbit IgG/biotinylated | Swine | 1:400 | cat#E0353, Dako, Milan, Italy |
| Polyclonal anti-goat IgG/biotinylated | Rabbit | 1:400 | cat#E0466, Dako |
| Cy™3-Fab fragment anti-rabbit IgG | Goat | 1:100 | cat#111-167, Jackson Lab., Baltimore, MD, United States |
| FITC-fab fragment anti-rabbit IgG | Goat | 1:100 | cat#111-097, Jackson Lab. |
| Unconjugated fab fragment anti-rabbit IgG | Goat | 1:30 | cat#111-007, Jackson Lab. |

Milan, Italy).

Sections processed as above, but without the primary antibody, were used as negative control. Control sections for SGLT1 were also prepared by preabsorbing the primary antibodies with the corresponding peptide (5 μg/mL of antibody; SGLT1 peptide, cat#ab99447, abcam). Sections of human small intestine were used as positive controls.

### *Light microscopy*

Sections were examined with an Olympus BX51 microscope (Olympus, Tokyo, Japan) equipped with a digital camera (DKY-F58 CCD JVC, Yokohama, Japan). Digital images were analyzed and processed with Image-ProPlus 7.0 software (Media Cybernetics, Silver Spring, MD, United States). Images were composed with Adobe Photoshop software ver. 6.0 (Adobe Systems, Mountain View, CA, United States) to regulate contrast and brightness.

### *Immunofluorescence microscopy*

Double immunofluorescent staining was used to compare immunolabeling of GLUT5 with that of lymphatic vessel endothelial hyaluronan receptor 1 (LYVE-1), a marker for lymphatic vessel endothelium in humans and rodents, and with that vascular endothelial growth factor (VEGF), a marker of vascular endothelial cells.

The double-label assay was carried out sequentially using a method that relied on the use of secondary monovalent Fab fragments because all primary antibodies are raised in the same species[36,37]. Paraffin sections (processed as described above) were used for double staining, which was performed as described in Merigo *et al*[38]. After completing the staining protocol, the sections were immersed 1 g/L Sudan Black B (Merck) in 70% ethanol for 20 min at room temperature to reduce tissue autofluorescence. After rinsing, the sections were mounted with fluorescent mounting medium (DAKO) and observed with a Zeiss LSM 510 confocal microscope equipped with argon (488 nm) and helium/neon (543 nm) excitation beams. Sequential acquisition, *i.e.*, one color at a time, was utilized on double-labeled tissues to avoid side-band excitation of the inappropriate fluorophore. All images for publication were composed using Adobe Photoshop software, adjusting only brightness and contrast.

Control sections were prepared using one of the following methods: (1) replacing the second primary antibody with normal rabbit serum; or (2) exchanging the fluorophores of the secondary antibodies; or (3) omitting the primary antibody; or (4) changing the sequence of secondary antibody application.

### *Scanning electron microscopy*

Sections of colonic mucosa, previously immunostained for GLUT5 antibody, were reused for scanning electron microscopy (SEM) analysis. After removal of the coverslip, the samples were brought to absolute alcohol, processed by critical point drying (CPD 030, Balzers, Vaduz, Liechtenstein), mounted on stubs with colloidal silver, sputtered with gold by means of an MED 010 coater (Balzers), and examined under an FEI XL30 scanning electron-microscope (FEI Company, Eindhoven, NL).

## RESULTS

The results of immunohistochemical analysis of samples from the cecum, ascending and transverse colon were grouped together as data of the proximal tract; the results of samples from the descending, sigmoid colon, and rectum were grouped as data of the distal portion of the large intestine.

### *Immunohistochemical analysis of GLUT2, SGLT1, and GLUT5 expression in large intestine*

Immunostaining for GLUT2 was detected on the apical cell pole and/or basolateral membrane of epithelial intestinal cells. Only small portions of the epithelium were positive for GLUT2 (Figure 1A-D). A few samples in each group of patients were immunostained for GLUT2 in both the proximal and the distal tract (Table 4).

Immunoreactivity for SGLT1 was concentrated mainly on the apical pole of epithelial cells, which were often observed in small clusters of 2 or 3 (Figure 1E and F). SGLT1 expression was observed in the samples from the distal tract; no substantial differences between the three patient groups were noted (Table 4).

Two distinct expression patterns of GLUT5 immunoreactivity were observed throughout the portions of the large intestine. GLUT5 expression was found on

**Table 4 Percentage of samples with GLUT2, SGLT1 and GLUT5 expression in epithelial cells of large intestine biopsies**

| Patient group | Large | | | | Intestine | | | |
|---|---|---|---|---|---|---|---|---|
| | Biopsy status | Proximal | Tract | | Biopsy status | Distal | Tract | |
| | | GLUT2, % | SGLT1, % | GLUT5, % | | GLUT2, % | SGLT1, % | GLUT5, % |
| UC | Inflamed ($n$ = 12) | 8 | 9 | 17 | Inflamed ($n$ = 20) | 0 | 15 | 15 |
| | Non-inflamed ($n$ = 21) | 5 | 5 | 33 | Non-inflamed ($n$ = 12) | 8 | 8 | 17 |
| CD | Inflamed ($n$ = 7) | 0 | 0 | 0 | Inflamed ($n$ = 12) | 8 | 8 | 0 |
| | Non-inflamed ($n$ = 2) | 0 | 0 | 0 | Non-inflamed ($n$ = 4) | 0 | 0 | 0 |
| CTRL | Inflamed ($n$ = 9) | 11 | 0 | 33 | Inflamed ($n$ = 10) | 30 | 10 | 0 |
| | Non-inflamed ($n$ = 18) | 17 | 0 | 17 | Non-inflamed ($n$ = 20) | 20 | 1 | 15 |

CD: Crohn's disease; UC: Ulcerative colitis; CTRL: Controls.

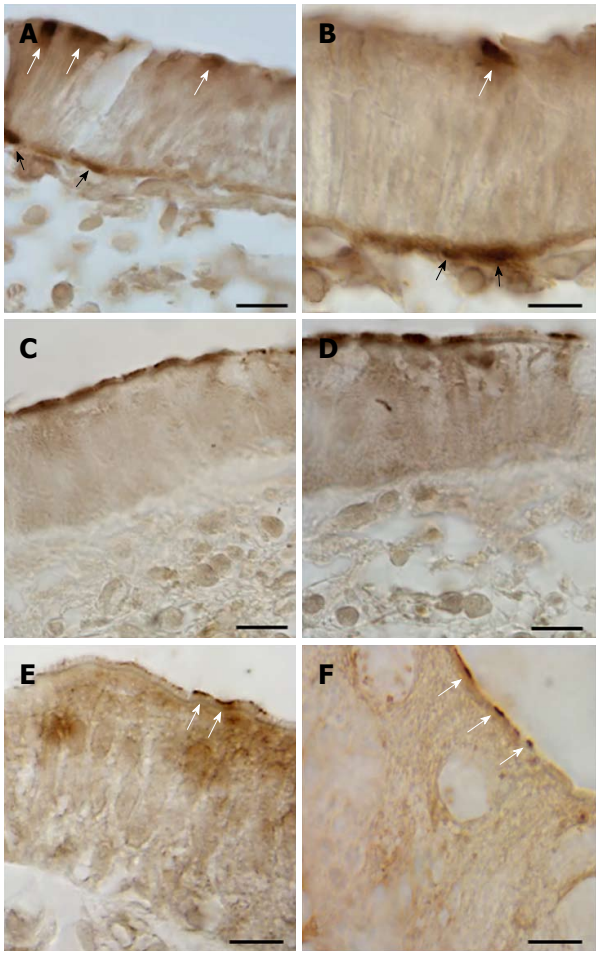


**Figure 1 Immunoperoxidase staining showing GLUT2 (A-D) and SGLT1 (E and F) immunoreactivity in epithelial cells of the cecum (A and B), descending (C and D), and sigmoid (E and F) colon of human intestine.** White arrows indicate staining on the apical pole, black arrows on the basolateral membrane of epithelial intestinal cells. Scale bar: (A, C, D) 50 μm; (B, E, F) 5 μm.

the apical membrane of epithelial cells, most likely representing labeling of the brush border membrane (Figure 2A-L). Only short portions of the epithelium showed positive epithelial cells. This staining was observed from the cecum to the rectum in both the UC and CTRL groups, but without significant differences between them (Table 4).

GLUT5 staining was also seen in vascular structures, where it displayed a heterogeneous pattern of expression and distribution. GLUT5 immunoreactivity was observed in the endothelial cells of small vessels, with well-defined endothelium, and slit-like or rounded luminal spaces. The vessels were scattered separately just below the epithelium or around the glands in the intestinal mucosa (Figure 3A-C). This pattern was defined as normal GLUT5 expression in vessels because no samples lacking this characteristic were observed.

In some samples, however, this immunoreactivity pattern was detected in small, numerous vessels which, though remaining individually distinct, tended to aggregate. They were mainly concentrated below the epithelium or around the glands (Figure 3D-I).

No specific labeling was seen in the control sections when IHC was performed without the primary antibody (Figure 3J).

Aggregation of GLUT5-immunoreactive (-IR) vessels was much more evident in other samples, where GLUT5 immunostaining was observed to be mainly concentrated in specific areas formed by clusters of GLUT5-IR vessels scattered throughout the intestinal tract (Figure 4A-F). The clusters varied in number (number ranged from 1 to 12 *per* section) and size (min area 262 $\mu m^2$; max area 10695 $\mu m^2$) and were predominantly localized beneath the epithelium (Figure 5A and B) or around the glands (Figure 5C and D). They consisted of many non-rounded vessels which appeared to be strongly dilated, with only short portions lining the lumen covered by endothelial cells. The flat endothelial cells were stained for GLUT5 (Figure 5B). The epithelium overlying these aggregates often appeared damaged by the presence of vacuolar structures (Figure 5E and F). The epithelium was missing in some cases.

### *GLUT5-IR clusters in samples from UC, CD, and CTRL patients*

GLUT5-IR clusters were observed throughout the entire tract of the large intestine in the samples of both inflamed and non-inflamed mucosal tissue from the UC, CD, and CTRL patients. The percentage of samples with GLUT5-IR clusters is shown in Table 5.

In the UC patients, the expression of GLUT5-IR clusters was higher in the samples from the distal than from the proximal tract, especially in the samples of non-inflamed tissue (83.3% *vs* 47.6%). The

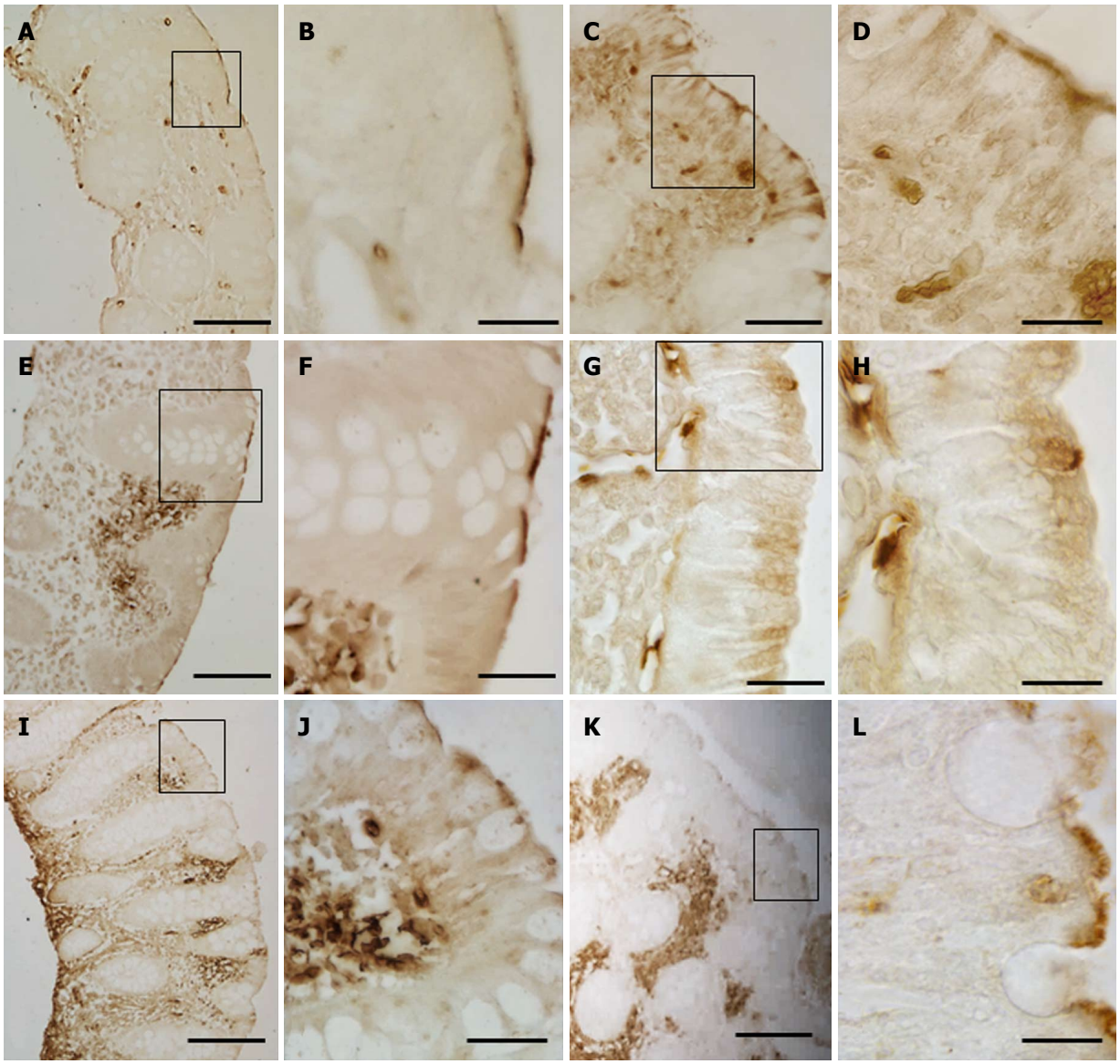


**Figure 2 Immunoperoxidase staining showing GLUT5 immunoreactivity in the brush border membrane of epithelial cells in lumen of cecum (A and B), ascending (C and D), transverse (E and F), descending (G and H), sigmoid (I and J) colon, and rectum (K and L).** The boxed area in (A, C, E, G, I, K) is shown at higher magnification in (B, D, F, H, J, L, respectively). Scale bar: (A, E, G, I) 50 μm; (C, K) 25 μm; (D, F) 10 μm; (B, H, J, L) 5 μm.

percentage of inflamed and non-inflamed samples was similar in the proximal tract (50% *vs* 47.6%), whereas in the distal tract the percentage of non-inflamed samples was higher (83.3% *vs* 55%).

In the CD patients, the percentage of GLUT5-IR clusters was higher in inflamed samples obtained from the distal than from the proximal tract (83% *vs* 71%), whereas the percentage was higher in non-inflamed samples from the proximal tract than from the distal tract (50% *vs* 25%). However, it was always higher in the inflamed than in the non-inflamed samples from both the proximal (70% *vs* 50%) and the distal tract (83% *vs* 25%).

In the CTRL group, the percentage of GLUT5-IR clusters in both the inflamed (60% *vs* 55.5%) and non-inflamed tissue samples (85% *vs* 44.4%) was higher in those obtained from the distal tract than from the proximal tract. The percentage was similar for the inflamed samples and non-inflamed samples from the proximal tract (55.5% *vs* 44.4%) and higher in the non-inflamed as compared to the inflamed tissue samples from the distal tract (85% *vs* 60%). Figure 6 reports the percentages of samples with GLUT5-IR clusters as bar graphs, for both the proximal (Panel A) and the distal (Panel B) tract.

The expression of GLUT5-IR clusters was also evaluated in a sample group obtained by classifying the patients according to their BMI (Table 6). In the UC and CTRL patients, the expression of GLUT5-IR clusters was higher in the inflamed samples of patients with normal weight as compared with non-inflamed samples from the proximal tract; whereas in the distal tract the percentage of GLUT5-IR clusters was always higher in the non-inflamed samples as compared

**Table 5 Percentage of samples with GLUT5 expression in clusters of lymphatic vessels in large intestine biopsies**

| Patient group | Large Intestine | | | |
|---|---|---|---|---|
| | Proximal Tract | | Distal Tract | |
| | Biopsy status | GLUT5, % | Biopsy status | GLUT5, % |
| UC | Inflamed ($n$ = 12) | 50.0 | Inflamed ($n$ = 20) | 55.0 |
| | Non-Inflamed ($n$ = 21) | 47.6 | Non-Inflamed ($n$ = 12) | 83.3 |
| CD | Inflamed ($n$ = 7) | 71.0 | Inflamed ($n$ = 12) | 83.0 |
| | Non-Inflamed ($n$ = 2) | 50.0 | Non-Inflamed ($n$ = 4) | 25.0 |
| CTRL | Inflamed ($n$ = 9) | 55.5 | Inflamed ($n$ = 10) | 60.0 |
| | Non-Inflamed ($n$ = 18) | 44.4 | Non-Inflamed ($n$ = 20) | 85.0 |

CD: Crohn's disease; UC: Ulcerative colitis; CTRL: Controls.

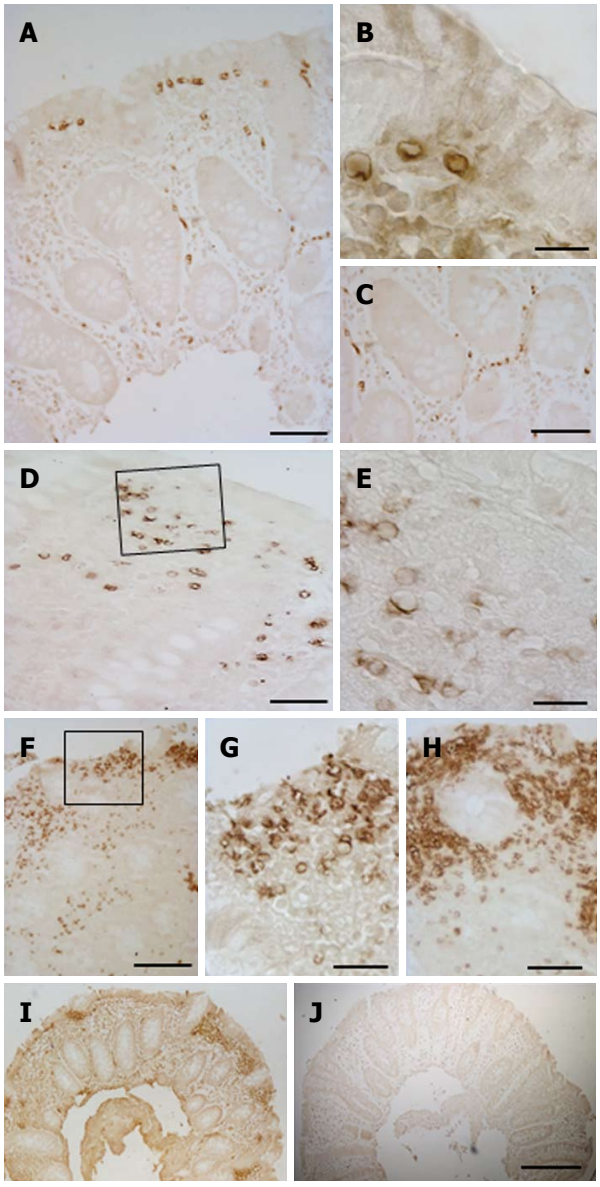


**Figure 3 Immunoperoxidase staining showing GLUT5 immunoreactivity in small, rounded vessels in cecum (A and C), ascending (B and I), transverse (D and E), and sigmoid (F-H) colon of human intestine. No specific staining is observed in adjacent sections (I and J) when GLUT5 antibody was omitted (J).** The boxed area in (D and F) is shown at higher magnification in (E and G, respectively). Scale bar: (I and J) 125 μm; (A, C, D, F) 50 μm; (B, E, G, H) 10 μm.

to the inflamed samples from all three groups. The percentage was higher in the inflamed than in the non-inflamed tissue samples from both the proximal and distal tract in the normal weight and overweight CD patients.

### *SEM analysis of GLUT5 immunoreactivity*

The GLUT5 positive sections were also observed at SEM for a more detailed evaluation of the labeled areas. Comparison between the SEM (Figure 7A and C) and the light microscope (Figure 7B and D) images showed that the area with GLUT5 immunoreactivity (Figure 8A-E) was characterized by large spaces and numerous dilated vessels, probably lymphatic because of the absence of red blood cells inside the lumen (Figure 8G and H). The vessels had a non-continuous endothelium, as observed at light microscopy. In the non-labeled areas, there were vessels containing cells inside the lumen that, judging by their rounded appearance, were probably lymphocytes or plasma cells (Figure 8F).

### *Comparison of GLUT5 immunoreactivity with LYVE-1 and VEGF expression in large intestine*

GLUT5 expression was compared with expression of LYVE-1 and VEGF by light immunohistochemistry in contiguous sections and by laser-scanning confocal microscopy in double staining. Light immunohistochemistry revealed the presence of GLUT5 immunoreactivity in areas that were also LYVE-1 positive (Figure 9A, B, G and H). GLUT5 positivity was limited to areas usually located under the epithelium (Figure 9C and I), whereas LYVE-1 staining was distributed in large areas of the lamina propria (Figure 9D and J). The GLUT5 expression pattern was generally much more marked than LYVE-1 labeling, which was formed by short spots (Figure 9E and F). However, some corresponding areas in contiguous sections showed GLUT5 immunoreactivity (Figure 9G and K) but lacked LYVE-1 staining (Figure 9H and L).

Double immunofluorescence microscopy was consistent with light-microscopic evaluation. GLUT5-IR clusters were found distributed inside LYVE-1 positive

**Table 6 Percentage of samples with GLUT5-immunoreactive clusters of vessels in biopsy groups subdivided by patient body mass index**

| Patient group | Biopsy status | Large | | | Intestine | | |
|---|---|---|---|---|---|---|---|
| | | Proximal | Tract | | Distal | Tract | |
| | | Patient | BMI | | Patient | BMI | |
| | | Normal weight, % | Over-weight, % | Obese, % | Normal weight, % | Over-weight, % | Obese, % |
| UC | Inflamed | 71 | 20 | 0 | 70 | 43 | 33 |
| | Non-inflamed | 57 | 25 | 50 | 87 | 100 | 0 |
| CD | Inflamed | 80 | 50 | 0 | 87 | 75 | 0 |
| | Non-inflamed | 100 | 0 | 0 | 50 | 0 | 0 |
| CTRL | Inflamed | 80 | 25 | 0 | 67 | 50 | 0 |
| | Non-inflamed | 22 | 50 | 100 | 82 | 80 | 100 |

BMI: Body mass index; CD: Crohn's disease; UC: Ulcerative colitis; CTRL: Controls.

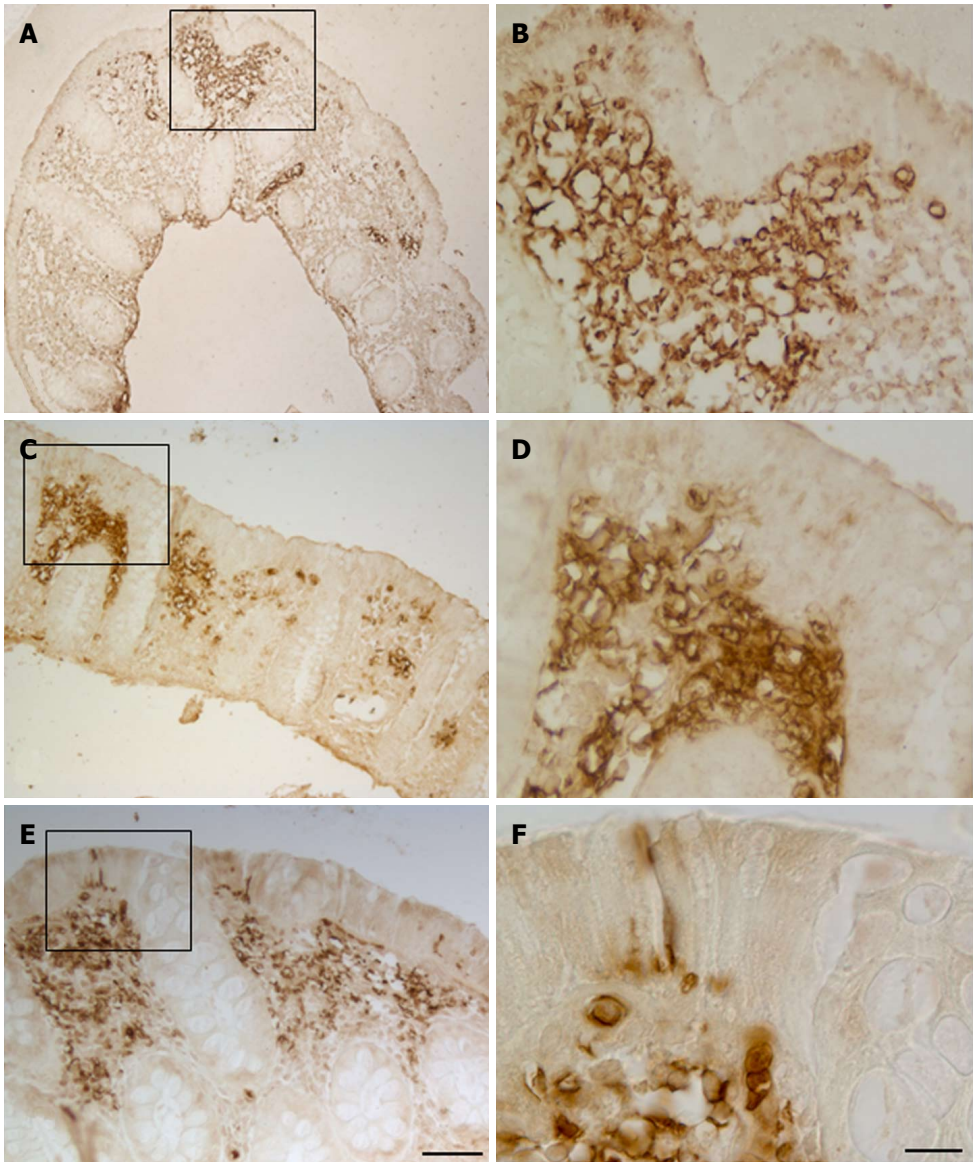


**Figure 4 Immunoperoxidase staining showing GLUT5 immunoreactivity in vessel clusters in ascending (A and B), descending (C and D) colon, and rectum (E and F).** The boxed area in (A, C, E) is shown at higher magnification in (B and D, F respectively). Scale bar: (A, C, E) 125 μm; (B, D, F) 25 μm.

areas and formed by numerous vessels, most of which were irregularly shaped and with ill-defined *lumina* (Figure 10A-F and J-L). GLUT5 and LYVE-1 expression were never colocalized on the morphologically undefined wall but rather were expressed in close proximity to some areas of the endothelium (Figure 10M-O). Some

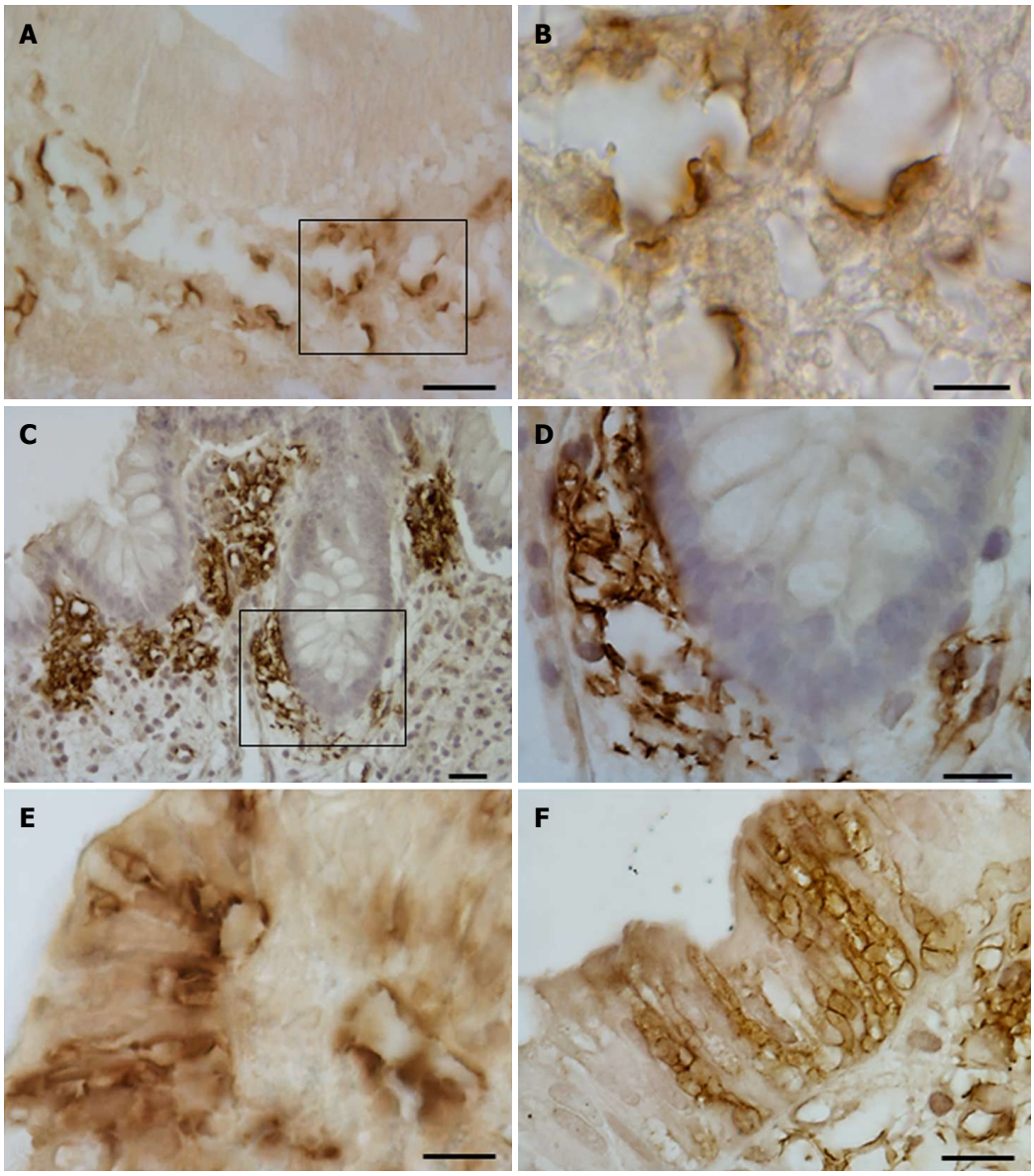


**Figure 5 GLUT5 immunoreactivity is shown in vessel clusters localized beneath the epithelium (A and B) or around the glands (C and D), and in vacuolar structures in the epithelium (E and F).** The boxed area in (A and C) is shown at higher magnification in (B, D, respectively). Scale bar: (A, C, E and F) 25 μm; (D) 10 μm; (B) 5 μm.

vessels showed only GLUT5 expression (Figure 10G-I).

In addition to staining the lymphatic vessels, LYVE-1 also labeled the brush border membrane of some epithelial cells which was observed in both immunohistochemistry (Figure 9D) and double-immunofluorescent experiments, in the latter also seen colocalized with GLUT5 expression (Figure 10P-R).

To further discriminate between lymphatic vessels and blood vessels, expression of GLUT5 and VEGF antibodies was compared in contiguous sections using light immunohistochemistry and immunofluorescence. Both analyses revealed that VEGF expression was absent in GLUT5-IR clusters, confirming that GLUT5-immunoreactivity is selective for lymphatic vessels (data not shown).

In control sections, no specific double-labeling was seen when the second antibody was replaced with normal rabbit serum.

## DISCUSSION

Here we show that GLUT2, SGLT1, and GLUT5 glucose transporters are expressed in the epithelial cells of tissue samples of the large intestine, and that they are mainly located in the brush border membrane from IBD and control patients. Also in the colonic mucosa their location reflects the canonical expression of the small intestine and confirms the tissue-specific expression of GLUT isoforms also in humans. However, unlike the small intestine, their expression is present only in short epithelial portions, involving a limited number of cells. We observed no important differences in glucose transporter expression between the samples obtained from the proximal and distal tracts and

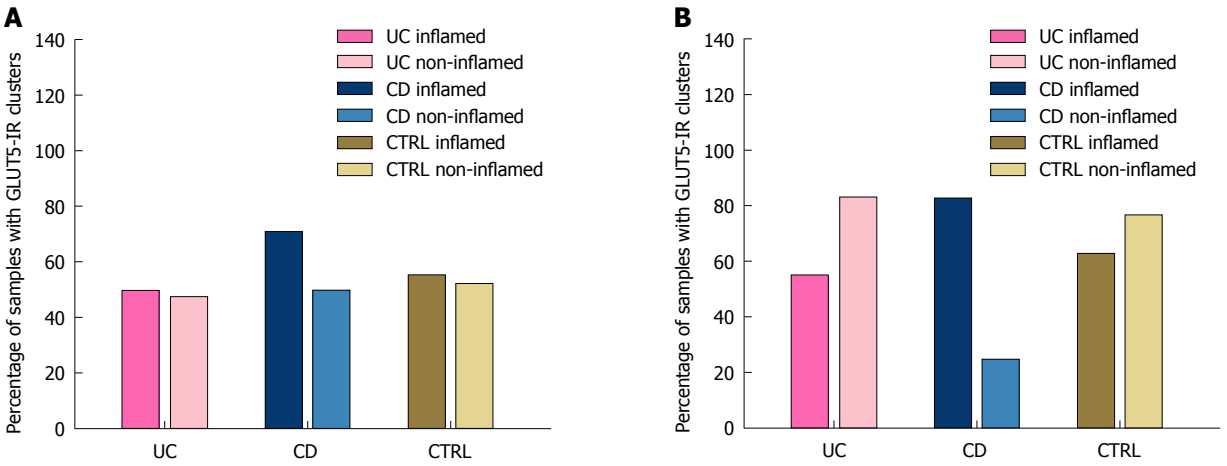


**Figure 6 Bar graphs of the percentage of samples with GLUT5-immunoreactive clusters of lymphatic vessels in the proximal tract (Panel A) and distal tract (Panel B) of large intestine of patients with ulcerative colitis, Crohn's disease, and controls. Inflamed and non-inflamed mucosa can be distinguished for each patient group.** In the UC and CTRL groups, the percentage is similar for inflamed and non-inflamed mucosa in the proximal tract, and higher for non-inflamed than inflamed mucosa in the distal tract. In the CD group, the percentage is higher for inflamed than non-inflamed mucosa in both the proximal and the distal tract. UC: Ulcerative colitis; CD: Crohn's disease; CTRL: Controls.

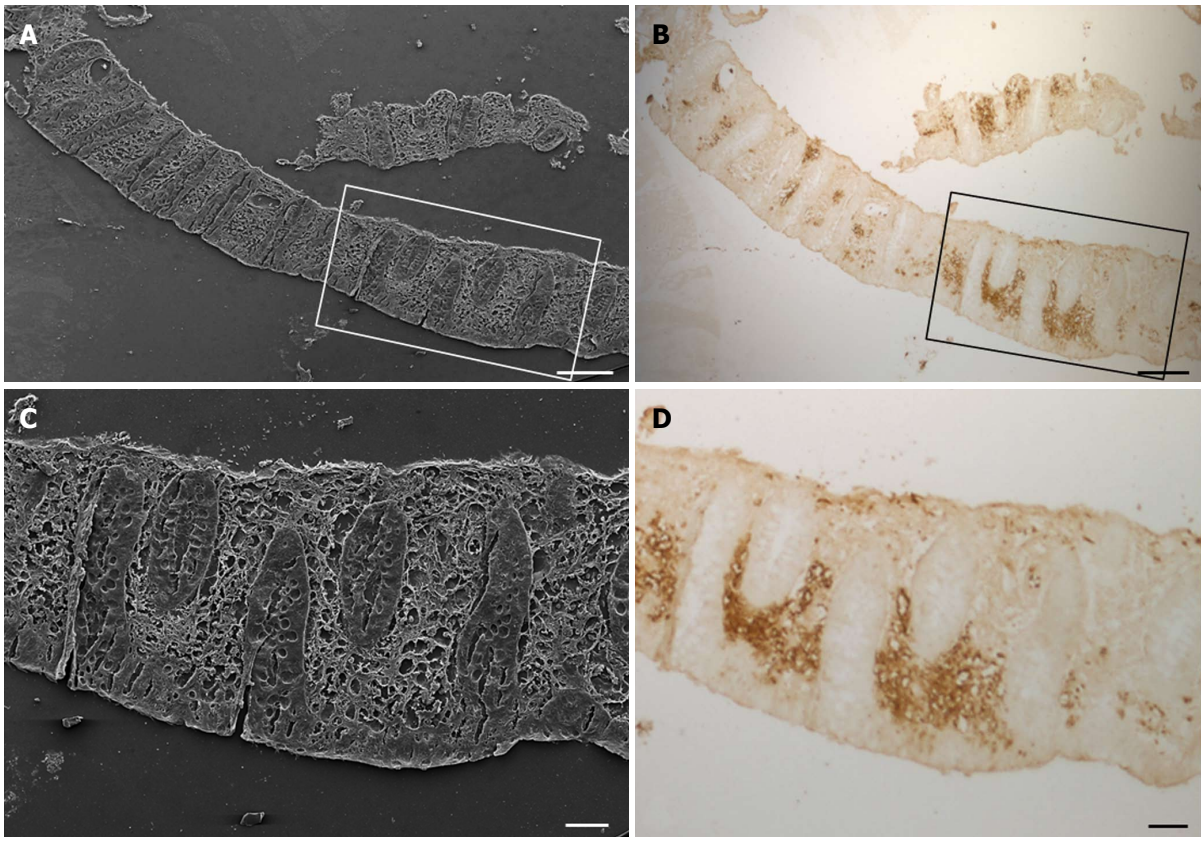


**Figure 7 Scanning electron (A and C) and light (B and D) microscopy images of a sample of descending colon with non-inflamed mucosa after immunoperoxidase GLUT5 staining from a ulcerative colitis patient.** Scale bar: (A and B) 250 μm; (C and D) 100 μm.

between the different patient groups. Nevertheless, we consider this finding important as it provides the first evidence for the distribution of glucose transporter immunoreactivity throughout the epithelial tract of the human large intestine. Because of the limited expression of the glucose transporters, we were unable to compare their expression across the three patient groups. However, we believe that our data support previous findings. In humans, GLUT5 expression has been observed in normal colonic cells; expression of both GLUT2 and GLUT5 has been reported in colon carcinoma and expression of GLUT5 with higher levels of staining than in normal colon cells[23]. GLUT2 and GLUT5 have been found to be overexpressed in many other types of tumors. Since both transporters are involved in fructose uptake, it was suggested that

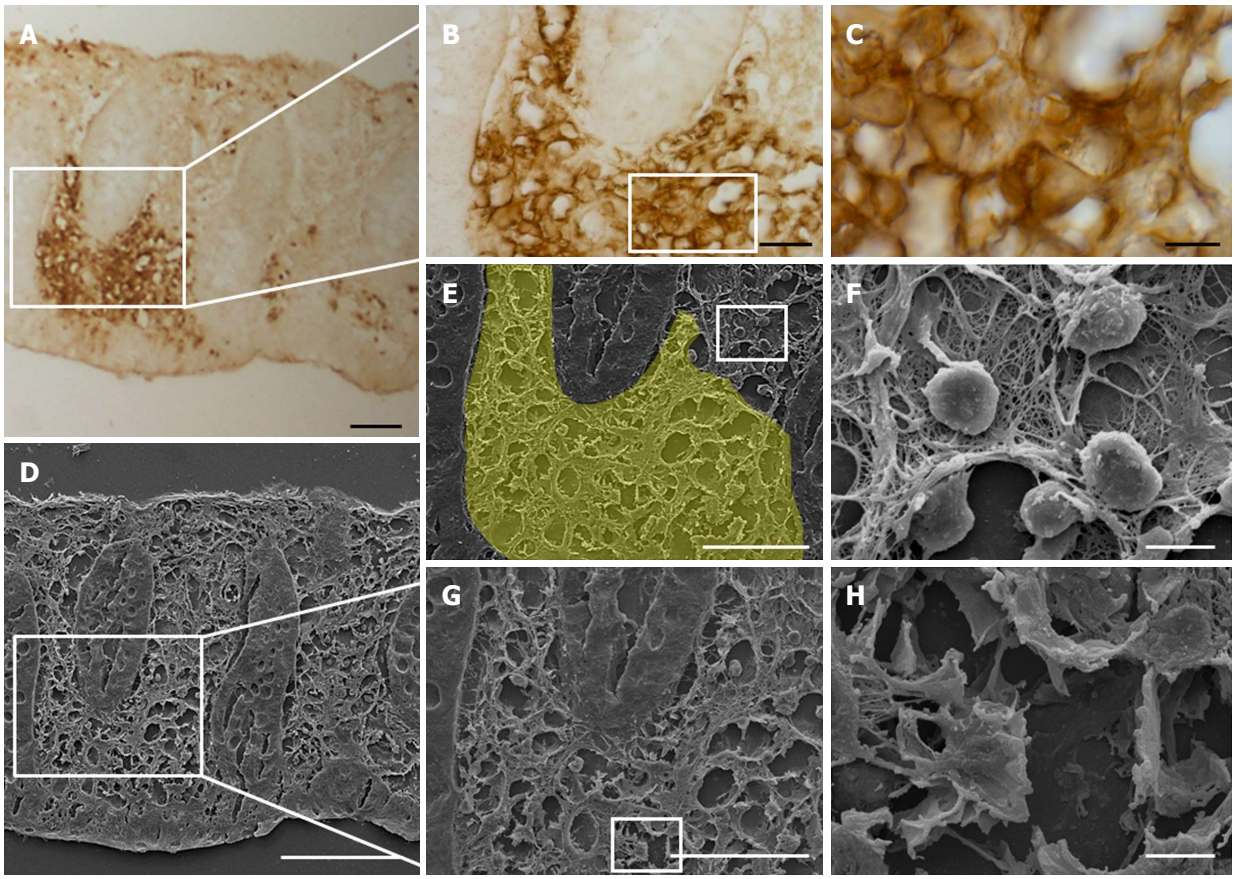


**Figure 8 Light (A-C) and scanning electron (D-H) microscopy images of a sample of descending colon with non-inflamed mucosa after immunoperoxidase GLUT5 staining from a UC patient.** The boxed areas in (A) and (D) are corresponding areas and are shown enlarged in (B) and (G), respectively. The yellow area in (E) represents the immunostaining area shown in (B). The boxed area in (B, E, G) is shown at higher magnification in (C, F, H, respectively). Scale bar: (D) 100 μm ; (A, E, G) 50 μm; (B) 25 μm; (C, F, H) 5 μm.

tumor cells utilize fructose as an energy substrate[23].

On the other hand, while excessive, chronic consumption of the GLUT5 and GLUT2 substrate fructose has been associated with numerous diseases and syndromes, including hypertension, obesity, diabetes, hyperinsulinemia, and non-alcoholic fatty liver disease, the role of fructose transporters in causing or contributing to the diseases is still unclear[10].

In addition, we also identified GLUT5 expression in vessels, mainly concentrated in specific areas where the vessels were clustered. This staining was detected in the samples from IBD and control patients. Furthermore, immunohistochemical and SEM evaluation revealed that the vessels in the GLUT5-IR clusters had a reticular architecture, indistinct and dilated lumen, and were labeled on the endothelium that appeared to be fragmented. Large spaces between the vessels were present. Immunostaining with LYVE-1, a specific marker of lymphatic endothelium, and GLUT5 antibodies in contiguous sections revealed that GLUT5-IR clusters of vessels were concentrated in areas that were well-circumscribed but internal to those that were LYVE-1 positive. This finding was also confirmed in double staining studies. GLUT5 and LYVE-1 did not appear to be colocalized but rather showed a close topographical relationship on the endothelium lining the lumen. Based on their LYVE-1 expression, GLUT5-IR vessels were unambiguously identified as lymphatic. We interpreted the presence of clusters as an impaired pattern of lymphatic capillary networks, probably related to proliferative zones, and consisting of vessels with morphological characteristics resembling those of immature lymphatics. They differed markedly from the vessels that we classified as "normal", which were characterized by a well-defined lumen lined by endothelial cells, a rounded appearance, and a non-aggregated distribution.

To the best of our knowledge, this is the first study to provide evidence that GLUT5 expression is associated with lymphatic vessels in controls and UC and CD patients. This novel finding yields further insight into the characterization of lymphatic vasculature, whose dysfunction is a long-recognized feature in humans with IBD.

There is considerable evidence for the proliferative expansion of lymphatic vessels during the course of inflammatory disease[39-41]. Alteration and remodeling of the lymphatic system, besides blood vessel angiogenesis, are implicated in IBD[42-44]. Increased lymphatic vessels density is a well-established feature in biopsy

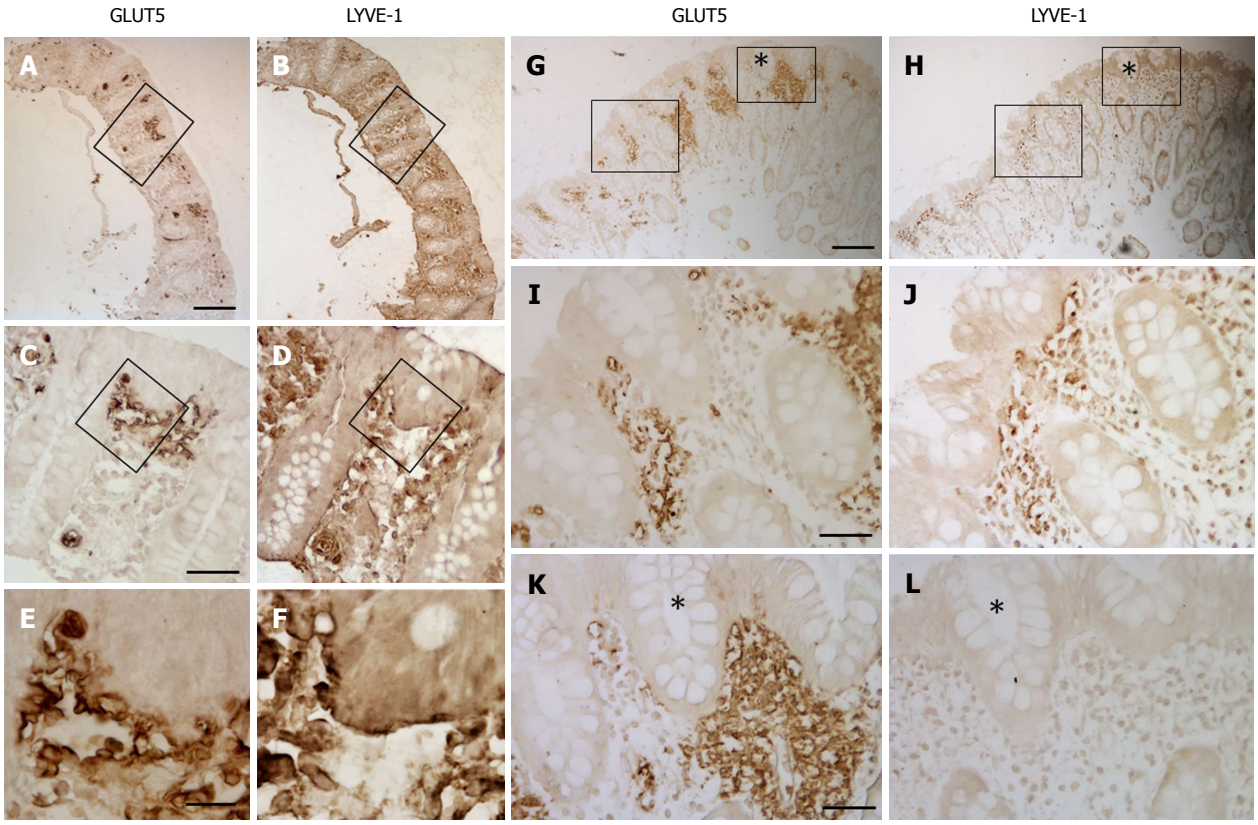


**Figure 9 Immunoperoxidase staining showing GLUT5 and LYVE-1 immunoreactivity in samples of the distal tract of large intestine from UC (A-F) and CD (G-L) patients. In both samples, the mucosa was non- inflamed.** The boxed area in (A and B) is enlarged in (C and D, respectively), the area in (C and D) is enlarged in (E and F, respectively), the area without an asterisk in (G and H) is enlarged in (I and J, respectively), the area with an asterisk in (G and H) is enlarged in (K and L, respectively). Scale bar: (A, B, G, H) 100 μm; (C, D, I-L) 25 μm; (E and F) 10 μm.

samples from CD and UC patients and is correlated with disease severity[42,44-47]. Similarly, a reduced density of lymphatic vessels was demonstrated to be associated with CD recurrence[46].

Moreover, studies have reported that lymphatic vessel dysfunction contributes to perpetuating intestinal inflammation in both UC and CD patients and that the intestinal lymphatic system can profoundly influence gut immune homeostasis[48,49]. However, it is still unclear whether expansion of the lymphatic network in IBD is a defensive mechanism or contributes to worsening the condition. It can be interpreted as a protective/adaptive, local response linked to the necessity to reduce fluid accumulation and to remove infiltrated immune cells, thus limiting further tissue injury**.** But lymphatic vessels also undergo morphological and functional changes in inflammatory conditions that impair their ability to drain fluid[50].

Lymphangiectasia is typically observed in the colonic mucosa of CD and UC patients[44,45], and impaired intestinal lymphatic transport function was found to play a role in the early-stages and development of IBD[51,52]. The relevance of the lymphatic transport function in IBD was also demonstrated in an experimental murine model that showed that acute colitis was aggravated by compromised lymphatic function; in contrast, immune cell clearance, fluid transport, and course of the disease were improved by induction of lymphangiogenesis[53,54].

While it is beyond doubt that increased lymphatic vessel density is closely linked to inflammatory disease, whether this process in IBD is an event that precedes inflammation or is its direct consequence remains to be elucidated.

Here we demonstrated a relevant presence of GLUT5-IR clusters of lymphatic vessels in both inflamed and non-inflamed tissue samples of large intestine from IBD and CTRL patients. The intestinal distal tract was, by far, the area most affected by their presence, especially in the UC and CTRL groups. This finding is consistent with the abundance of lymphatic tissue in the most distal regions of the intestine[50].

To our surprise, we found more non-inflamed than inflamed tissue samples expressing GLUT5-IR clusters in the distal tract of the UC patients and controls: these percentages were similar across all three patient groups when classified by BMI. Differently, in the CD patients, similar results were found for the proximal and the distal intestinal tract, and the number of inflamed samples with GLUT5-IR clusters was higher than non-inflamed tissue samples, also in relation to the BMI of patients. Our data indicate that GLUT5-IR clusters are present in both UC patients and controls, and that their presence does not appear to be conditioned by the level of inflammation of the mucosal area where the

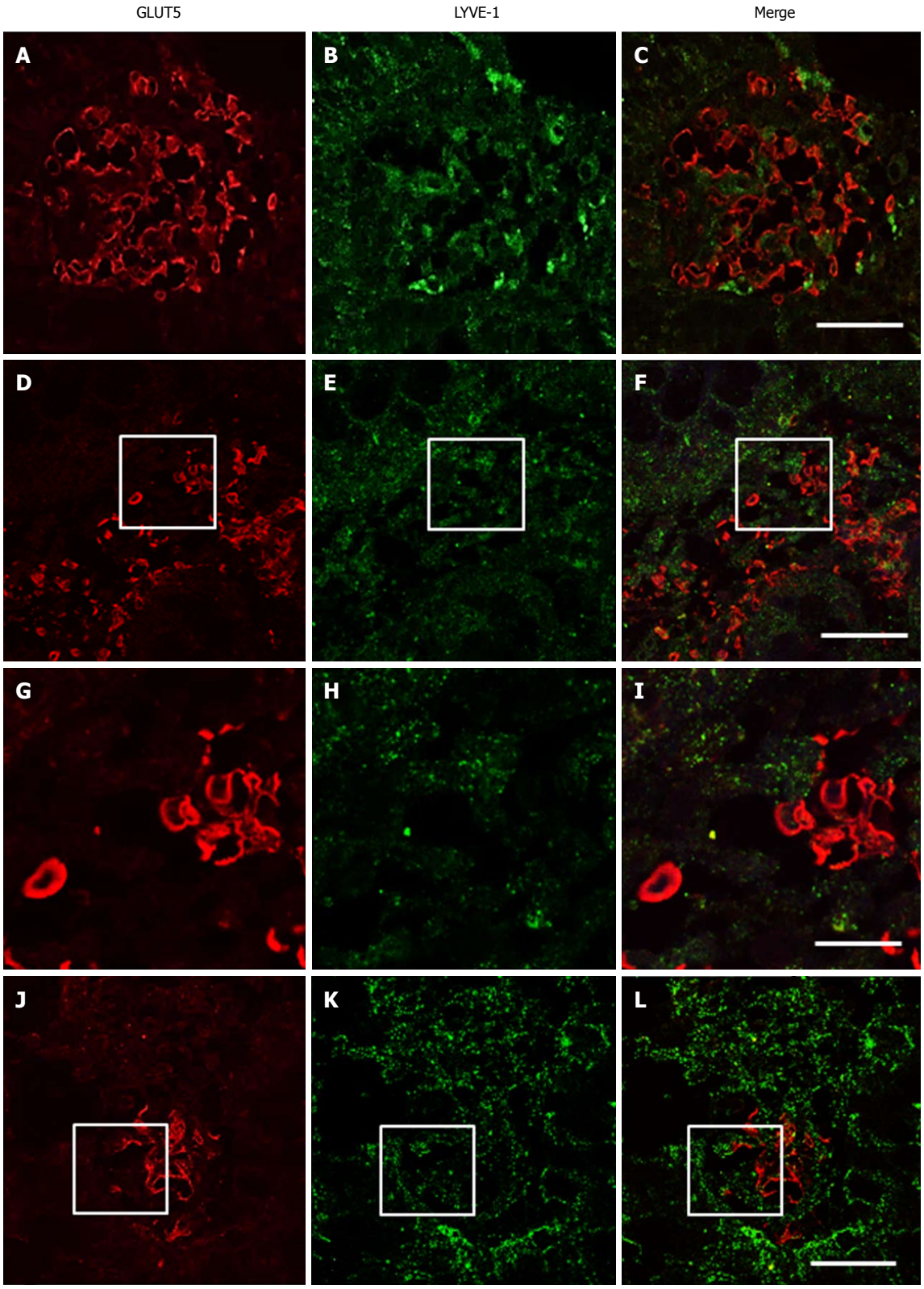
GLUT5
LYVE-1
Merge
A
B
C
D
E
F
G
H
I
J
K
L

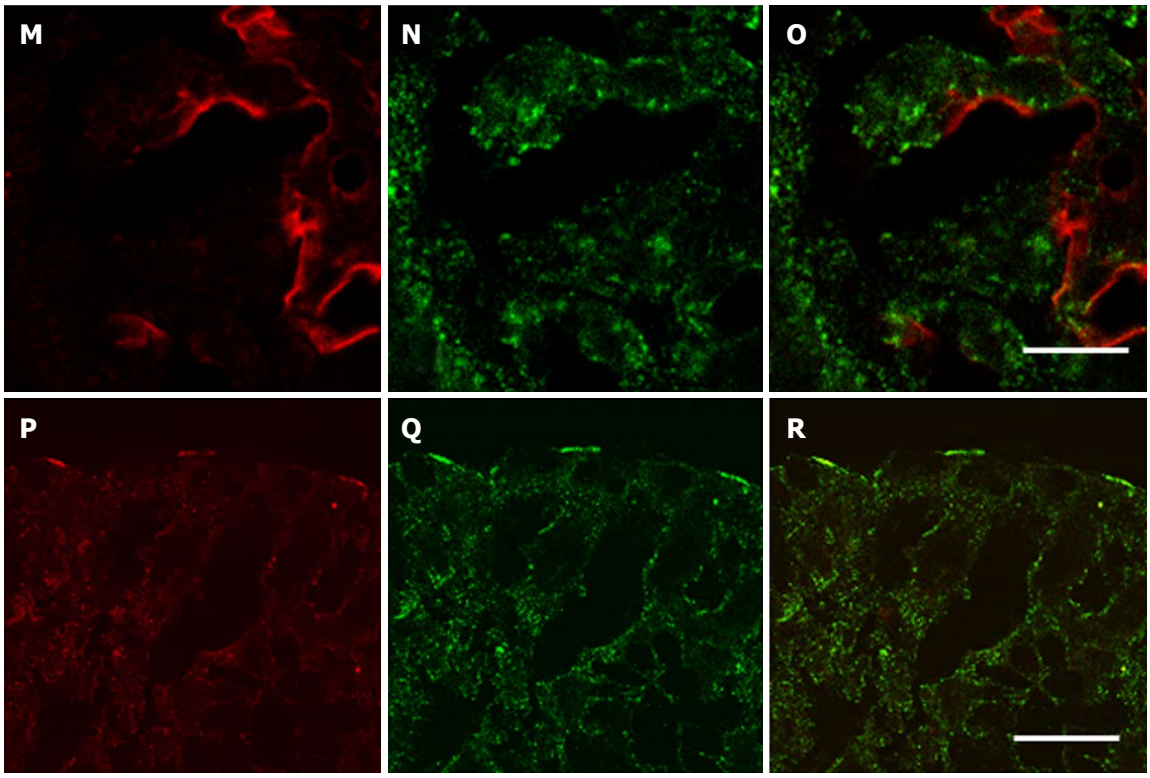


**Figure 10 Double-immunofluorescent confocal microscopy showing expression of GLUT5 (red) with LYVE-1 (green) in samples of descending colon from UC (A-C, J-R) and CD (D-I) patients.** The mucosa was inflamed in the UC sample and non-inflamed in the CD sample. The boxed area in (D-F) is shown at higher magnification in (G-I, respectively); the boxed area in (J-L) is shown at higher magnification in (M-O, respectively). Scale bar: (C, F, L, R) 20 μm; (I, O) 10 μm.

clusters are found. The opposite finding in the CD group may indicate a particular aspect of this condition. Since the amount of tissue analyzed in the CD patients was limited, it may not be completely representative of the whole group, however.

The few studies that have investigated the relationship between lymphoproliferation and inflammation of the area where it occurs have shown that lymphatic proliferation and inflammation do not occur in close association. Several explanations for this have been proposed. Increased lymphatic vessel density has been documented as a persistent feature in samples from IBD patients, in which it was also observed in fibrotic specimens from end-stage disease characterized by low inflammation[42]. Similarly, the increased lymphatic vessel density detected in both the inflamed and non-inflamed tissue samples from the UC and CD patients has been interpreted as a process that occurs before the disease becomes clinically active, and therefore can manifest itself independent of inflammation[46]. No obvious correlation between increased lymphatic vessel density and inflammation was demonstrated in the colonic mucosa of the UC patients, where it has been predicted that structural changes in the mucosa, including "*muscularis* mucosa expansion, infiltration by muscle fibers, and filiform epithelial changes" are an essential prerequisite to justify lymphatic proliferation[45].

Both these interpretations may also be consistent with our data: the first is especially valid for the controls where the presence of vessel clusters can be a subclinical aspect, at times not necessarily related to a particular pathology. The second can be valid for IBD: we sometimes observed vacuolar structures in the epithelium over the areas where lymphatic vessel clusters were present and altered epithelial cell integrity. Recent studies have shown that epithelial barrier dysfunction in IBD can contribute to disease progression by activating immunoregulatory processes, probably following increased exposure of the mucosa to the luminal microbiota or their products[55-58]. Although the underlying mechanism is unclear, defects in intestinal barrier function are now attributed a direct or indirect role in the onset or progression of IBD. We observed morphological epithelial damage limited to certain areas of the epithelium in some samples and only at the light microscope, in which the real damage may be underestimated.

Other mechanisms/factors have been investigated to explain the stimulation of lymphatic vessels in IBD, given that it may occur via different processes in UC and CD. Lymphatic system expansion during inflammation in peripheral tissues progresses through the expansion and proliferation of an existing vascular network or sprouting of new vessels (lymphangiogenesis)[40,59]. However, the expression of lymphangiogenic factors (*e.g.*, VEGF-C, VEGF-D) and cytokines (*e.g.*, TNF and IL-1b), which have been found to be increased in inflammatory conditions**,** were decreased in the

inflamed and non-inflamed colonic tissues of the IBD patients[46,60].

LYVE-1 has also been demonstrated to be selectively expressed in inflammation. In cultured primary lymphatic endothelial cells, LYVE-1 uptake and degradation and inhibition of its gene expression were seen to occur under the stimulus of pro-inflammatory cytokines, leading to a subsequent reversible loss of the surface expression of LYVE-1[61]. Subsequently, quantification of LYVE-1 by RT-PCR in human colonic mucosa revealed a lower mRNA level in both the non-inflamed and inflamed samples from the UC patients than in the controls, but no differences in LYVE-1 mRNA levels were seen in the CD patients[46]. In the UC patients, the reduction was more evident in the non-inflamed than the inflamed samples.

In this study, double-immunofluorescence staining revealed that GLUT5-IR clusters were present in zones with LYVE -1 positivity, however, the appearance of the vessels inside the clusters was very heterogeneous, as was their phenotypic expression: GLUT5-positive but LYVE-1 negative or GLUT5-negative but LYVE-1 positive vessels were often identified, whereas the simultaneous expression of LYVE-1 and GLUT5 was limited to restricted endothelial areas of some clustered vessels. In the cases where LYVE-1 was missing, we saw the expression of GLUT5, which appeared in close continuity with LYVE-1, without ever being colocalized with it. These data strongly suggest a reduced expression of LYVE-1, which may depend on the different degrees of vessel differentiation within the clusters. There is considerable evidence that immature vessels lack LYVE-1 expression, particularly intratumoral lymphatic vessels, that differ morphologically from lymphatic vessels found within normal tissue[62,63]. The reason for this difference is unclear; however, it has been also demonstrated that altered expression of lymphatic endothelial markers such as LYVE-1 may compromise lymphatic transport function[50].

Collectively, our results regarding GLUT5 expression in IBD patients are consistent with previous data obtained for lymphatic proliferation in IBD. The presence of GLUT5 alone does not imply that it is involved in lymphatic proliferation because it was found to be expressed in both normal and clustered lymphatic vessels. However, its expression indicates that GLUT5 may play a role in controlling the formation of lymphatic vessels. It is plausible that aberrant lymphatic growth in clusters may result from the effect of GLUT5 on cellular mechanisms underlying the differentiation of new lymphatic vessels. It may also be that fructose, GLUT5 being its main transporter, may be the energy substrate that endothelial cells use for lymphatic expansion.

In this regard, we speculate that fructose present in the lumen may have some effect on the proliferation of these vessels. We found that a percentage of samples expressed GLUT5 in the brush border membrane of epithelial cells from both the UC and CTRL patients. This finding merits further investigation because it could be a clear example of crosstalk between the cells projecting into the intestinal lumen and underlying environments.

In conclusion, our study provides evidence that GLUT2, SGLT1, and GLUT5 glucose transporters are expressed in the epithelial cells of the mucosa of the large intestine of IBD and control patients. Furthermore, both inflamed and non-inflamed mucosal colorectal tissue biopsies from the IBD and control patients showed GLUT5-IR lymphatic vessel clusters. This finding aids in the characterization of lymphatic vessels in IBD. As GLUT5 is the main fructose transporter in the human intestine, it is conceivable that fructose is a metabolic substrate that has a role in the atypical aggregation of lymphatic vessels.

Quantification of lymphatic vessel density in the gastrointestinal tract, particularly in cancer and chronic inflammatory disease, holds interest because it can be predictive of the early stages of disease. In this regard, GLUT5 expression on endothelial lymphovascular cells may have implications for routine use in the histopathological evaluation of lymphangiogenesis, also in combination with LYVE-1, a marker of lymphatic endothelium that can be down-modulated under inflammatory conditions.

A future area of focus is the precise function of GLUT5 expression in lymphatic vessels and the factors that interfere with the development or maintenance of IBD.

## ARTICLE HIGHLIGHTS

### *Research background*

Glucose transporter expression is present throughout the digestive system, greatest in the small intestine and least in the terminal ileum. Most studies to date on glucose transporters in the gastrointestinal tract have been performed using biochemical rather than standard immunohistochemical analysis also in humans.

### *Research motivation*

The localization and distribution of glucose transporters in the intestinal mucosa of the human colon has not yet been clarified despite evidences that support the role of glucose transporters in broad areas of pure glucose absorption and metabolism, such as inflammation, malignancy, and gut microbiota regulation.

### *Research objectives*

The aim of this study was to investigate by immunostaining at light and confocal microscopy the expression of the major intestinal glucose transporters (GLUT2, SGLT1, GLUT5) in human colonic mucosa in control subjects and subjects with IBD.

### *Research methods*

Patients diagnosed with ulcerative colitis or Crohn's disease and scheduled for diagnostic colonoscopy were enrolled. Patients who underwent colonoscopy for prevention screening of colorectal cancer or were followed-up after polypectomy or lower gastrointestinal symptoms were designated as the control group. Colorectal samples were obtained from patients undergoing lower endoscopic colonoscopy or recto-sigmoidoscopy. Biopsies of portions of the colonic tract (cecum, ascending colon, transverse, descending, sigmoid colon, rectum) were taken for diagnostic purposes according to the endoscopist's judgment and for

immunohistochemistry. Inflammatory status of the mucosa at the sampling site was evaluated endoscopically and histologically.

Samples were fixed in formaldehyde and embedded in paraffin. The expression of GLUT2, SGLT1, and GLUT5 glucose transporters was investigated using immunoperoxidase labeling. Immunoreactivity of GLUT5 was compared with that of LYVE-1, which is a marker for lymphatic vessel endothelium, using double-labeled confocal microscopy.

### Research results

GLUT2, SGLT1, and GLUT5 glucose transporter immunostaining was found in short epithelial portions of the large intestine from IBD and control patients. No difference in glucose transporter expression was observed between the samples obtained from the proximal and distal tracts and between the different patient groups. GLUT5 immunostaining was also detected in vessels, which were mainly concentrated in specific areas. In double fluorescent-labeled sections with GLUT5 and LYVE-1, GLUT5-immunoreactive clusters of vessels were concentrated in areas internal to those that were LYVE-1 positive. The GLUT5 and LYVE-1 labeling patterns were never colocalized but rather showed a close topographical relationship on the endothelium lining the lumen. Based on their LYVE-1 expression, GLUT5 immunoreactive vessels were identified as lymphatic and observed both in inflamed and non-inflamed mucosal colorectal tissue biopsies from the IBD and CTRL patients. This novel finding yields further insight into the characterization of lymphatic vasculature, whose dysfunction is a long-recognized feature in humans with IBD.

### Research conclusions

This study provides evidence that GLUT2, SGLT1, and GLUT5 glucose transporters are expressed in the colorectal mucosa in controls and IBD patients. Furthermore, it provides first evidence that GLUT5 expression is associated with lymphatic vessels in controls and IBD patients. Its expression indicates that GLUT5 may play a role in controlling the formation of lymphatic vessels. GLUT5 expression on endothelial lymphovascular cells may have implications for routine use in the histopathological evaluation of lymphangiogenesis, also in combination with LYVE-1, a marker of lymphatic endothelium that can be down-modulated under inflammatory conditions.

### Research perspectives

A future area of focus is the precise function of GLUT5 expression in lymphatic vessels and the factors that interfere with the development or maintenance of IBD.

## REFERENCES


1 **Mueckler M**, Caruso C, Baldwin SA, Panico M, Blench I, Morris HR, Allard WJ, Lienhard GE, Lodish HF. Sequence and structure of a human glucose transporter. *Science* 1985; **229**: 941-945 [PMID: 3839598 DOI: 10.1126/science.3839598]

2 **Kayano T**, Burant CF, Fukumoto H, Gould GW, Fan YS, Eddy RL, Byers MG, Shows TB, Seino S, Bell GI. Human facilitative glucose transporters. Isolation, functional characterization, and gene localization of cDNAs encoding an isoform (GLUT5) expressed in small intestine, kidney, muscle, and adipose tissue and an unusual glucose transporter pseudogene-like sequence (GLUT6). *J Biol Chem* 1990; **265**: 13276-13282 [PMID: 1695905]

3 **Blakemore SJ**, Aledo JC, James J, Campbell FC, Lucocq JM, Hundal HS. The GLUT5 hexose transporter is also localized to the basolateral membrane of the human jejunum. *Biochem J* 1995; **309** (Pt 1): 7-12 [PMID: 7619085]

4 **Douard V**, Cui XL, Soteropoulos P, Ferraris RP. Dexamethasone sensitizes the neonatal intestine to fructose induction of intestinal fructose transporter (Slc2A5) function. *Endocrinology* 2008; **149**: 409-423 [PMID: 17947353 DOI: 10.1210/en.2007-0906]

5 **Matosin-Matekalo M**, Mesonero JE, Laroche TJ, Lacasa M, Brot-Laroche E. Glucose and thyroid hormone co-regulate the expression of the intestinal fructose transporter GLUT5. *Biochem J* 1999; **339** (Pt 2): 233-239 [PMID: 10191252]

6 **David ES**, Cingari DS, Ferraris RP. Dietary induction of intestinal fructose absorption in weaning rats. *Pediatr Res* 1995; **37**: 777-782 [PMID: 7651763 DOI: 10.1203/00006450-199506000-00017]

7 **Douard V**, Ferraris RP. Regulation of the fructose transporter GLUT5 in health and disease. *Am J Physiol Endocrinol Metab* 2008; **295**: E227-E237 [PMID: 18398011 DOI: 10.1152/ajpendo.90245.2008]

8 **Litherland GJ**, Hajduch E, Gould GW, Hundal HS. Fructose transport and metabolism in adipose tissue of Zucker rats: diminished GLUT5 activity during obesity and insulin resistance. *Mol Cell Biochem* 2004; **261**: 23-33 [PMID: 15362482]

9 **Dyer J**, Wood IS, Palejwala A, Ellis A, Shirazi-Beechey SP. Expression of monosaccharide transporters in intestine of diabetic humans. *Am J Physiol Gastrointest Liver Physiol* 2002; **282**: G241-G248 [PMID: 11804845 DOI: 10.1152/ajpgi.00310.2001]

10 **Douard V**, Ferraris RP. The role of fructose transporters in diseases linked to excessive fructose intake. *J Physiol* 2013; **591**: 401-414 [PMID: 23129794 DOI: 10.1113/jphysiol.2011.215731]

11 **Thorens B**, Cheng ZQ, Brown D, Lodish HF. Liver glucose transporter: a basolateral protein in hepatocytes and intestine and kidney cells. *Am J Physiol* 1990; **259**: C279-C285 [PMID: 1701966]

12 **Yoshikawa T**, Inoue R, Matsumoto M, Yajima T, Ushida K, Iwanaga T. Comparative expression of hexose transporters (SGLT1, GLUT1, GLUT2 and GLUT5) throughout the mouse gastrointestinal tract. *Histochem Cell Biol* 2011; **135**: 183-194 [PMID: 21274556 DOI: 10.1007/s00418-011-0779-1]

13 **Kellett GL**, Brot-Laroche E, Mace OJ, Leturque A. Sugar absorption in the intestine: the role of GLUT2. *Annu Rev Nutr* 2008; **28**: 35-54 [PMID: 18393659 DOI: 10.1146/annurev.nutr.28.061807.155518]

14 **Gouyon F**, Caillaud L, Carriere V, Klein C, Dalet V, Citadelle D, Kellett GL, Thorens B, Leturque A, Brot-Laroche E. Simple-sugar meals target GLUT2 at enterocyte apical membranes to improve sugar absorption: a study in GLUT2-null mice. *J Physiol* 2003; **552**: 823-832 [PMID: 12937289 DOI: 10.1113/jphysiol.2003.049247]

15 **Kellett GL**, Helliwell PA. The diffusive component of intestinal glucose absorption is mediated by the glucose-induced recruitment of GLUT2 to the brush-border membrane. *Biochem J* 2000; **350** Pt 1: 155-162 [PMID: 10926839 DOI: 10.1042/0264-6021:3500155]

16 **Ait-Omar A**, Monteiro-Sepulveda M, Poitou C, Le Gall M, Cotillard A, Gilet J, Garbin K, Houllier A, Château D, Lacombe A, Veyrie N, Hugol D, Tordjman J, Magnan C, Serradas P, Clément K, Leturque A, Brot-Laroche E. GLUT2 accumulation in enterocyte apical and intracellular membranes: a study in morbidly obese human subjects and ob/ob and high fat-fed mice. *Diabetes* 2011; **60**: 2598-2607 [PMID: 21852673 DOI: 10.2337/db10-1740]

17 **Reimann F**, Habib AM, Tolhurst G, Parker HE, Rogers GJ, Gribble FM. Glucose sensing in L cells: a primary cell study. *Cell Metab* 2008; **8**: 532-539 [PMID: 19041768 DOI: 10.1016/j.cmet.2008.11.002]

18 **Depoortere I**. Taste receptors in the gut tune the release of peptides in response to nutrients. *Peptides* 2015; **66**: 9-12 [PMID: 25683908 DOI: 10.1016/j.peptides.2015.01.013]

19 **Schmitt CC**, Aranias T, Viel T, Chateau D, Le Gall M, Waligora-Dupriet AJ, Melchior C, Rouxel O, Kapel N, Gourcerol G, Tavitian B, Lehuen A, Brot-Laroche E, Leturque A, Serradas P, Grosfeld A. Intestinal invalidation of the glucose transporter GLUT2 delays tissue distribution of glucose and reveals an unexpected role in gut homeostasis. *Mol Metab* 2016; **6**: 61-72 [PMID: 28123938 DOI: 10.1016/j.molmet.2016.10.008]

20 **Wright EM**, Turk E. The sodium/glucose cotransport family SLC5. *Pflugers Arch* 2004; **447**: 510-518 [PMID: 12748858 DOI: 10.1007/s00424-003-1063-6]

21 **Hediger MA**, Coady MJ, Ikeda TS, Wright EM. Expression cloning and cDNA sequencing of the Na+/glucose co-transporter. *Nature* 1987; **330**: 379-381 [PMID: 2446136 DOI: 10.1038/330379a0]

22 **Gorboulev V**, Schürmann A, Vallon V, Kipp H, Jaschke A, Klessen D, Friedrich A, Scherneck S, Rieg T, Cunard R, Veyhl-Wichmann M, Srinivasan A, Balen D, Breljak D, Rexhepaj R, Parker HE, Gribble FM, Reimann F, Lang F, Wiese S, Sabolic I, Sendtner M, Koepsell H. Na(+)-D-glucose cotransporter SGLT1

is pivotal for intestinal glucose absorption and glucose-dependent incretin secretion. *Diabetes* 2012; **61**: 187-196 [PMID: 22124465 DOI: 10.2337/db11-1029]

23 **Godoy A**, Ulloa V, Rodríguez F, Reinicke K, Yañez AJ, García Mde L, Medina RA, Carrasco M, Barberis S, Castro T, Martínez F, Koch X, Vera JC, Poblete MT, Figueroa CD, Peruzzo B, Pérez F, Nualart F. Differential subcellular distribution of glucose transporters GLUT1-6 and GLUT9 in human cancer: ultrastructural localization of GLUT1 and GLUT5 in breast tumor tissues. *J Cell Physiol* 2006; **207**: 614-627 [PMID: 16523487 DOI: 10.1002/jcp.20606]

24 **Wuest M**, Trayner BJ, Grant TN, Jans HS, Mercer JR, Murray D, West FG, McEwan AJ, Wuest F, Cheeseman CI. Radiopharmacological evaluation of 6-deoxy-6-[18F]fluoro-D-fructose as a radiotracer for PET imaging of GLUT5 in breast cancer. *Nucl Med Biol* 2011; **38**: 461-475 [PMID: 21531283 DOI: 10.1016/j.nucmedbio.2010.11.004]

25 **Liu H**, Huang D, McArthur DL, Boros LG, Nissen N, Heaney AP. Fructose induces transketolase flux to promote pancreatic cancer growth. *Cancer Res* 2010; **70**: 6368-6376 [PMID: 20647326 DOI: 10.1158/0008-5472.CAN-09-4615]

26 **García-Herrera J**, Marca MC, Brot-Laroche E, Guillén N, Acin S, Navarro MA, Osada J, Rodríguez-Yoldi MJ. Protein kinases, TNF-{alpha}, and proteasome contribute in the inhibition of fructose intestinal transport by sepsis in vivo. *Am J Physiol Gastrointest Liver Physiol* 2008; **294**: G155-G164 [PMID: 17962360 DOI: 10.1152/ajpgi.00139.2007]

27 **García-Herrera J**, Abad B, Rodríguez-Yoldi MJ. Effect of lipopolysaccharide on D-fructose transport across rabbit jejunum. *Inflamm Res* 2003; **52**: 177-184 [PMID: 12755384]

28 **Barone S**, Fussell SL, Singh AK, Lucas F, Xu J, Kim C, Wu X, Yu Y, Amlal H, Seidler U, Zuo J, Soleimani M. Slc2a5 (Glut5) is essential for the absorption of fructose in the intestine and generation of fructose-induced hypertension. *J Biol Chem* 2009; **284**: 5056-5066 [PMID: 19091748 DOI: 10.1074/jbc.M808128200]

29 **Uldry M**, Ibberson M, Hosokawa M, Thorens B. GLUT2 is a high affinity glucosamine transporter. *FEBS Lett* 2002; **524**: 199-203 [PMID: 12135767 DOI: 10.1016/S0014-5793(02)03058-2]

30 **Yu LC**, Flynn AN, Turner JR, Buret AG. SGLT-1-mediated glucose uptake protects intestinal epithelial cells against LPS-induced apoptosis and barrier defects: a novel cellular rescue mechanism? *FASEB J* 2005; **19**: 1822-1835 [PMID: 16260652 DOI: 10.1096/fj.05-4226com]

31 **Barrenetxe J**, Sánchez O, Barber A, Gascón S, Rodríguez-Yoldi MJ, Lostao MP. TNFα regulates sugar transporters in the human intestinal epithelial cell line Caco-2. *Cytokine* 2013; **64**: 181-187 [PMID: 23910014 DOI: 10.1016/j.cyto.2013.07.004]

32 **Palazzo M**, Gariboldi S, Zanobbio L, Selleri S, Dusio GF, Mauro V, Rossini A, Balsari A, Rumio C. Sodium-dependent glucose transporter-1 as a novel immunological player in the intestinal mucosa. *J Immunol* 2008; **181**: 3126-3136 [PMID: 18713983 DOI: 10.4049/jimmunol.181.5.3126]

33 **Yomogida S**, Kojima Y, Tsutsumi-Ishii Y, Hua J, Sakamoto K, Nagaoka I. Glucosamine, a naturally occurring amino monosaccharide, suppresses dextran sulfate sodium-induced colitis in rats. *Int J Mol Med* 2008; **22**: 317-323 [PMID: 18698490 DOI: 10.3892/ijmm_00000025]

34 **Reed KL**, Fruin AB, Gower AC, Gonzales KD, Stucchi AF, Andry CD, O'Brien M, Becker JM. NF-kappaB activation precedes increases in mRNA encoding neurokinin-1 receptor, proinflammatory cytokines, and adhesion molecules in dextran sulfate sodium-induced colitis in rats. *Dig Dis Sci* 2005; **50**: 2366-2378 [PMID: 16416193 DOI: 10.1007/s10620-005-3066-y]

35 **Visekruna A**, Joeris T, Seidel D, Kroesen A, Loddenkemper C, Zeitz M, Kaufmann SH, Schmidt-Ullrich R, Steinhoff U. Proteasome-mediated degradation of IkappaBalpha and processing of p105 in Crohn disease and ulcerative colitis. *J Clin Invest* 2006; **116**: 3195-3203 [PMID: 17124531 DOI: 10.1172/JCI28804]

36 **Lewis Carl SA**, Gillete-Ferguson I, Ferguson DG. An indirect immunofluorescence procedure for staining the same cryosection with two mouse monoclonal primary antibodies. *J Histochem Cytochem* 1993; **41**: 1273-1278 [PMID: 7687266 DOI: 10.1177/41.8.7687266]

37 **Negoescu A**, Labat-Moleur F, Lorimier P, Lamarcq L, Guillermet C, Chambaz E, Brambilla E. F(ab) secondary antibodies: a general method for double immunolabeling with primary antisera from the same species. Efficiency control by chemiluminescence. *J Histochem Cytochem* 1994; **42**: 433-437 [PMID: 7508473 DOI: 10.1177/42.3.7508473]

38 **Merigo F**, Benati D, Cristofoletti M, Osculati F, Sbarbati A. Glucose transporters are expressed in taste receptor cells. *J Anat* 2011; **219**: 243-252 [PMID: 21592100 DOI: 10.1111/j.1469-7580.2011.01385.x]

39 **Jackson DG**. Biology of the lymphatic marker LYVE-1 and applications in research into lymphatic trafficking and lymphangiogenesis. *APMIS* 2004; **112**: 526-538 [PMID: 15563314 DOI: 10.1111/j.1600-0463.2004.apm11207-0811.x]

40 **Alitalo K**, Tammela T, Petrova TV. Lymphangiogenesis in development and human disease. *Nature* 2005; **438**: 946-953 [PMID: 16355212 DOI: 10.1038/nature04480]

41 **Kerjaschki D**. The lymphatic vasculature revisited. *J Clin Invest* 2014; **124**: 874-877 [PMID: 24590271 DOI: 10.1172/JCI74854]

42 **Geleff S**, Schoppmann SF, Oberhuber G. Increase in podoplanin-expressing intestinal lymphatic vessels in inflammatory bowel disease. *Virchows Arch* 2003; **442**: 231-237 [PMID: 12647212 DOI: 10.1007/s00428-002-0744-4]

43 **Danese S**, Fiocchi C. Etiopathogenesis of inflammatory bowel diseases. *World J Gastroenterol* 2006; **12**: 4807-4812 [PMID: 16937461 DOI: 10.3748/wjg.v12.i30.4807]

44 **Pedica F**, Ligorio C, Tonelli P, Bartolini S, Baccarini P. Lymphangiogenesis in Crohn's disease: an immunohistochemical study using monoclonal antibody D2-40. *Virchows Arch* 2008; **452**: 57-63 [PMID: 18040712 DOI: 10.1007/s00428-007-0540-2]

45 **Kaiserling E**, Kröber S, Geleff S. Lymphatic vessels in the colonic mucosa in ulcerative colitis. *Lymphology* 2003; **36**: 52-61 [PMID: 12926829]

46 **Rahier JF**, De Beauce S, Dubuquoy L, Erdual E, Colombel JF, Jouret-Mourin A, Geboes K, Desreumaux P. Increased lymphatic vessel density and lymphangiogenesis in inflammatory bowel disease. *Aliment Pharmacol Ther* 2011; **34**: 533-543 [PMID: 21736598 DOI: 10.1111/j.1365-2036.2011.04759.x]

47 **Fogt F**, Pascha TL, Zhang PJ, Gausas RE, Rahemtulla A, Zimmerman RL. Proliferation of D2-40-expressing intestinal lymphatic vessels in the lamina propria in inflammatory bowel disease. *Int J Mol Med* 2004; **13**: 211-214 [PMID: 14719125 DOI: 10.3892/ijmm.13.2.211]

48 **Vranova M,** Halin C. Lymphatic Vessels in Inflammation. *J Clin Cell Immunol* 2014; **5**: 250 [DOI: 10.4172/2155-9899.1000250]

49 **Becker F**, Yi P, Al-Kofahi M, Ganta VC, Morris J, Alexander JS. Lymphatic dysregulation in intestinal inflammation: new insights into inflammatory bowel disease pathomechanisms. *Lymphology* 2014; **47**: 3-27 [PMID: 25109166]

50 **Alexander JS**, Chaitanya GV, Grisham MB, Boktor M. Emerging roles of lymphatics in inflammatory bowel disease. *Ann N Y Acad Sci* 2010; **1207** Suppl 1: E75-E85 [PMID: 20961310 DOI: 10.1111/j.1749-6632.2010.05757.x]

51 **Von Der Weid PY**, Rehal S. Lymphatic pump function in the inflamed gut. *Ann N Y Acad Sci* 2010; **1207** Suppl 1: E69-E74 [PMID: 20961308 DOI: 10.1111/j.1749-6632.2010.05715.x]

52 **Linares PM**, Gisbert JP. Role of growth factors in the development of lymphangiogenesis driven by inflammatory bowel disease: a review. *Inflamm Bowel Dis* 2011; **17**: 1814-1821 [PMID: 21744436 DOI: 10.1002/ibd.21554]

53 **D'Alessio S**, Correale C, Tacconi C, Gandelli A, Pietrogrande G, Vetrano S, Genua M, Arena V, Spinelli A, Peyrin-Biroulet L, Fiocchi C, Danese S. VEGF-C-dependent stimulation of lymphatic function ameliorates experimental inflammatory bowel disease. *J Clin Invest* 2014; **124**: 3863-3878 [PMID: 25105363 DOI: 10.1172/JCI72189]

54 **Becker F**, Potepalov S, Shehzahdi R, Bernas M, Witte M, Abreo F, Traylor J, Orr WA, Tsunoda I, Alexander JS. Downregulation of FoxC2 Increased Susceptibility to Experimental Colitis: Influence of Lymphatic Drainage Function? *Inflamm Bowel Dis* 2015; **21**: 1282-1296 [PMID: 25822012 DOI: 10.1097/MIB.0000000000000371]
55 **Edelblum KL**, Turner JR. The tight junction in inflammatory disease: communication breakdown. *Curr Opin Pharmacol* 2009; **9**: 715-720 [PMID: 19632896 DOI: 10.1016/j.coph.2009.06.022]
56 **Berry D**, Reinisch W. Intestinal microbiota: a source of novel biomarkers in inflammatory bowel diseases? *Best Pract Res Clin Gastroenterol* 2013; **27**: 47-58 [PMID: 23768552 DOI: 10.1016/j.bpg.2013.03.005]
57 **Klag T**, Stange EF, Wehkamp J. Defective antibacterial barrier in inflammatory bowel disease. *Dig Dis* 2013; **31**: 310-316 [PMID: 24246980 DOI: 10.1159/000354858]
58 **Lanis JM**, Kao DJ, Alexeev EE, Colgan SP. Tissue metabolism and the inflammatory bowel diseases. *J Mol Med* (Berl) 2017; **95**: 905-913 [PMID: 28528514 DOI: 10.1007/s00109-017-1544-2]
59 **Wirzenius M**, Tammela T, Uutela M, He Y, Odorisio T, Zambruno G, Nagy JA, Dvorak HF, Ylä-Herttuala S, Shibuya M, Alitalo K. Distinct vascular endothelial growth factor signals for lymphatic vessel enlargement and sprouting. *J Exp Med* 2007; **204**: 1431-1440 [PMID: 17535974 DOI: 10.1084/jem.20062642]
60 **Flister MJ**, Wilber A, Hall KL, Iwata C, Miyazono K, Nisato RE, Pepper MS, Zawieja DC, Ran S. Inflammation induces lymphangiogenesis through up-regulation of VEGFR-3 mediated by NF-kappaB and Prox1. *Blood* 2010; **115**: 418-429 [PMID: 19901262 DOI: 10.1182/blood-2008-12-196840]
61 **Johnson LA**, Prevo R, Clasper S, Jackson DG. Inflammation-induced uptake and degradation of the lymphatic endothelial hyaluronan receptor LYVE-1. *J Biol Chem* 2007; **282**: 33671-33680 [PMID: 17884820 DOI: 10.1074/jbc.M702889200]
62 **Beasley NJ**, Prevo R, Banerji S, Leek RD, Moore J, van Trappen P, Cox G, Harris AL, Jackson DG. Intratumoral lymphangiogenesis and lymph node metastasis in head and neck cancer. *Cancer Res* 2002; **62**: 1315-1320 [PMID: 11888898]
63 **Padera TP**, Kadambi A, di Tomaso E, Carreira CM, Brown EB, Boucher Y, Choi NC, Mathisen D, Wain J, Mark EJ, Munn LL, Jain RK. Lymphatic metastasis in the absence of functional intratumor lymphatics. *Science* 2002; **296**: 1883-1886 [PMID: 11976409 DOI: 10.1126/science.1071420]

**P- Reviewer**: Huerta-Franco MR, Maric I, Nakase H, Yu LCH
**S- Editor**: Gong ZM **L- Editor**: A **E- Editor**: Huang Y

World Journal of Gastroenterology

Submit a Manuscript: http://www.f6publishing.com

*World J Gastroenterol* 2018 February 21; 24(7): 794-809

DOI: 10.3748/wjg.v24.i7.794

ISSN 1007-9327 (print) ISSN 2219-2840 (online)

ORIGINAL ARTICLE

Basic Study

# Translational pancreatic cancer research: A comparative study on patient-derived xenograft models

Mercedes Rubio-Manzanares Dorado, Luis Miguel Marín Gómez, Daniel Aparicio Sánchez, Sheila Pereira Arenas, Juan Manuel Praena-Fernández, Juan Jose Borrero Martín, Francisco Farfán López, Miguel Ángel Gómez Bravo, Jordi Muntané Relat, Javier Padillo Ruiz

Mercedes Rubio-Manzanares Dorado, Luis Miguel Marín Gómez, Daniel Aparicio Sánchez, Miguel Ángel Gómez Bravo, Javier Padillo Ruiz, Department of Hepatobiliary and Pancreatic Surgery, Virgen del Rocio University Hospital, Seville 41013, Spain

Sheila Pereira Arenas, Jordi Muntané Relat, Oncology Surgery, Cell Therapy, and Organ Transplantation Group, Institute of Biomedicine of Seville (IBiS), Virgen del Rocio University Hospital, University of Seville, Seville 41013, Spain

Juan Manuel Praena-Fernández, Statistics, Methodology and Evaluation of Research Unit, Virgen del Rocio University Hospital, Seville 41013, Spain

Juan Jose Borrero Martín, Francisco Farfán López, Pathology Department, Virgen del Rocio University Hospital, Seville 41013, Spain

ORCID number: Mercedes Rubio-Manzanares Dorado (0000-0002-0433-1881); Luis Miguel Marín Gómez (0000-0003-3087-7228); Daniel Aparicio Sánchez (0000-0001-7061-345X), Sheila Pereira Arenas (0000-0002-5009-5699); Juan Manuel Praena-Fernández (0000-0001-5728-1024); Juan Jose Borrero Martín (0000-0001-8292-8838); Francisco Farfán López (0000-0002-5555-4655); Miguel Ángel Gómez Bravo (0000-0002-5155-3508); Jordi Muntané Relat (0000-0002-6744-1121); Javier Padillo Ruiz (0000-0002-1220-0822).

Author contributions: Rubio-Manzanares Dorado M, Marín Gómez LM, Aparicio Sánchez D, and Pereira Arenas S contributed substantially to the conception and design of the study and the acquisition of data; Praena-Fernández JM analysed and interpreted the data; Farfán López F and Borrero Martín JJ analysed the anatomopathological samples; Rubio-Manzanares Dorado M wrote the manuscript; and Padillo Ruiz J, Gómez Bravo MÁ and Muntané Relat J drafted the article and made critical revisions related to the intellectual content of the manuscript. All authors approved the final version of the manuscript to be published.

Supported by the Andalusian Public Foundation for the Management of Health Research in Seville (FISEVI).

Institutional review board statement: The study was reviewed and approved by the Ethics Committee of The Seville University of Medicine, Virgen del Rocío Universitary Hospital, Protocol number: CEEA-US2014-013/5.

Conflict-of-interest statement: To the best of our knowledge, no conflict of interest exist.

Data sharing statement: Datasets are available from the corresponding author via email. Participants gave informed consent for data sharing.

ARRIVE guidelines statement: The authors have read the ARRIVE guidelines, and the manuscript was prepared and revised according to the ARRIVE guidelines.



Manuscript source: Unsolicited manuscript

Correspondence to: Mercedes Rubio-Manzanares Dorado, MD, PhD, Staff Physician, Department of Hepatobiliary and Pancreatic Surgery, Virgen del Rocio University Hospital, Manuel Siurot St., Seville 41013, Spain. mercedesrmd@gmail.com
Telephone: +34-609-074420
Fax: +34-955-012317

Received: December 2, 2017

Peer-review started: December 2, 2017
First decision: December 20, 2017
Revised: January 14, 2018
Accepted: January 18, 2018
Article in press: January 18, 2018
Published online: February 21, 2018

## Abstract

***AIM***

To assess the viability of orthotopic and heterotopic patient-derived pancreatic cancer xenografts implanted into nude mice.

***METHODS***

This study presents a prospective experimental analytical follow-up of the development of tumours in mice upon implantation of human pancreatic adenocarcinoma samples. Specimens were obtained surgically from patients with a pathological diagnosis of pancreatic adenocarcinoma. Tumour samples from pancreatic cancer patients were transplanted into nude mice in three different locations (intraperitoneal, subcutaneous and pancreatic). Histological analysis (haematoxylin-eosin and Masson's trichrome staining) and immunohistochemical assessment of apoptosis (TUNEL), proliferation (Ki-67), angiogenesis (CD31) and fibrogenesis (α-SMA) were performed. When a tumour xenograft reached the target size, it was re-implanted in a new nude mouse. Three sequential tumour xenograft generations were generated (F1, F2 and F3).

***RESULTS***

The overall tumour engraftment rate was 61.1%. The subcutaneous model was most effective in terms of tissue growth (69.9%), followed by intraperitoneal (57.6%) and pancreatic (55%) models. Tumour development was faster in the subcutaneous model (17.7 ± 2.6 wk) compared with the pancreatic (23.1 ± 2.3 wk) and intraperitoneal (25.0 ± 2.7 wk) models ($P$ = 0.064). There was a progressive increase in the tumour engraftment rate over successive generations for all three models (F1 28.1% *vs* F2 71.4% *vs* F3 80.9%, $P$ < 0.001). There were no significant differences in tumour xenograft differentiation and cell proliferation between human samples and the three experimental models among the sequential generations of tumour xenografts. However, a progressive decrease in fibrosis, fibrogenesis, tumour vascularisation and apoptosis was observed in the three experimental models compared with the human samples. All three pancreatic patient-derived xenograft models presented similar histological and immunohistochemical characteristics.

***CONCLUSION***

In our experience, the faster development and greatest number of viable xenografts could make the subcutaneous model the best option for experimentation in pancreatic cancer.

**Key words:** Immunohistological analysis; Pancreatic cancer; Patient-derived xenograft; Animal model; Nude mice



**Core tip:** Several investigations have established patient-derived xenograft models for breast, renal, head and neck cancer, and hepatocellular tumours. Some of these models have predicted the clinical response of a specific type of tumour to different chemotherapeutic agents. However, the morphological and histological features of human pancreatic cancer xenografts in experimental models have been poorly studied. In the present study, the effectiveness of three experimental models based on the implantation of patient pancreatic cancer in three different locations (subcutaneous, intraperitoneal and pancreatic) have been assessed for the first time.

Rubio-Manzanares Dorado M, Marín Gómez LM, Aparicio Sánchez D, Pereira Arenas S, Praena-Fernández JM, Borrero Martín JJ, Farfán López F, Gómez Bravo MÁ, Muntané Relat J, Padillo Ruiz J. Translational pancreatic cancer research: A comparative study on patient-derived xenograft models. *World J Gastroenterol* 2018; 24(7): 794-809 Available from: URL: http://www.wjgnet.com/1007-9327/full/v24/i7/794.htm DOI: http://dx.doi.org/10.3748/wjg.v24.i7.794

## INTRODUCTION

The development of chemotherapeutic agents for pancreatic cancer is closely related to the evolution of experimental models. Over the past 50 years, subcutaneous xenografts derived from cancer cell lines grown *in vitro* have been widely used[1-3]. A multitude of anticancer drugs have been tested using these preclinical models[4]. However, drugs that demonstrate benefits in animal models are not necessarily effective in humans[3,5-7].

Since the 1970s, human cancer samples obtained by biopsy or surgery have been implanted directly into mice[5,8-10]. These patient-derived xenografts (PDX), also known as tumour xenografts, were initially abandoned because of their high rejection rate[10]. Recently, this line of research has been reinitiated due to the development of genetically-modified immunodeficient mice, which has increased the success rate of grafting[5,11-13].

This PDX model has become competitive in the study of pancreatic cancer, particularly for predicting the clinical response to chemotherapy, owing to the better clinical predictive ability of this model[5]. Our

**Table 1 Demographic characteristics and anatomopathological diagnosis**

| Code | Sex/Age (yr) | Localization | Surgery | Histology | T | N | M | Stage | Histological grade | Perineural invasion | Neoadjuvant therapy | Subcutaneous engraftment | Intraperitoneal engraftment | Pancreatic engraftment |
|---|---|---|---|---|---|---|---|---|---|---|---|---|---|---|
| H1 | F/75 | Ph | PC | DAC | 4 | X | 1 | Ⅳ | G2 | NO | NO | NO | NO | YES |
| H2 | F/77 | Ph | PC | Periampullary adenocarcinoma | 4 | 0 | 0 | Ⅲ | G2 | YES | NO | YES | YES | YES |
| H3 | M/57 | Ph | PC | DAC | 3 | 0 | 0 | ⅡA | G2 | NO | NO | NO | NO | NO |
| H4 | F/71 | Ph and periaortic node | PC | DAC | X | 1 | 1 | Ⅳ | G2 | NO | YES (nab + paclitaxel + gemcitabine) | YES | NO | NO |
| H5 | M/71 | Ph | PC | DAC | 3 | 1 | 0 | ⅡB | G2 | NO | NO | YES | NO | NO |
| H6 | F/73 | Ph | PC | DAC | 3 | 1 | 0 | ⅡB | G2 | YES | NO | NO | NO | NO |
| H7 | M/50 | Ph | PC | DAC | 3 | 0 | 0 | ⅡA | G2 | YES | NO | NO | NO | NO |
| H8 | M/70 | Ph | PC | Periampullary adenocarcinoma | 3 | 1 | 0 | ⅡB | G2 | NO | NO | YES | YES | NO |
| H9 | M/81 | Pt | DP | DAC | 3 | 0 | 0 | ⅡA | G2 | NO | NO | NO | NO | NO |
| H10 | F/78 | Ph | PC | DAC | 3 | 1 | 0 | ⅡB | G2 | NO | NO | NO | NO | NO |

TNM classification according to the 2010 American Joint Committee on Cancer classification for pancreatic cancer stratification[18]. Histological grade: G1, well differentiated; G2, moderately differentiated; G3, poorly differentiated. PC: Pancreatic cancer; Ph: Pancreas head; Pb: Pancreas body; Pt: Pancreas tail; PD: Pancreatoduodenectomy; DP: Distal pancreatectomy; DAC: Ductal adenocarcinoma.

group has successfully applied this procedure for the implantation of colorectal cancer patient-derived xenografts into nude mice[14]. In the present study, we assessed for the first time the effectiveness of three experimental models based on the implantation of pancreatic cancer PDX in different locations (subcutaneous, intraperitoneal and pancreatic). To date, no studies have investigated the characteristics of a series of pancreatic tumour xenografts placed orthotopically. The aim of this study was to assess the viability of orthotopic (intrapancreatic) and heterotopic (intraperitoneal and subcutaneous) PDX of human pancreatic cancer implanted into nude mice, and to determine which location better maintains human histological and immunohistochemical characteristics.

## MATERIALS AND METHODS

This study presents a prospective experimental analytical follow-up of the development of tumours in mice upon implantation of human pancreatic adenocarcinoma samples. Specimens were obtained surgically from patients with a pathological diagnosis of pancreatic adenocarcinoma. Human cancer samples were implanted as tumour xenografts in three experimental models. All animal experimentation procedures were approved by the Animal Research Committee of the University of Seville, Spain (protocol number CEEA-US2014-013/5).

### *Patients*

We included patients diagnosed with pancreatic adenocarcinoma who underwent an exploratory laparotomy from May 17, 2012 to February 13, 2014 at the Virgen del Rocío University Hospital in Seville, Spain. All patients signed a written informed consent form for inclusion in the study, which had been previously approved by the Ethics Committee. The exclusion criteria for the study were tumours not identified as pancreatic adenocarcinoma, patients under 18 years old, or those who had not given written consent for the use of their samples.

Eleven samples were obtained from a total of 10 patients. Samples were obtained by cephalic pancreatoduodenectomy ($n$ = 9) and distal pancreatectomy ($n$ = 1). Two samples were obtained from the same patient (H4), comprising an interaortocaval lymph node metastasis and a sample extracted from the pancreatic tumour (Table

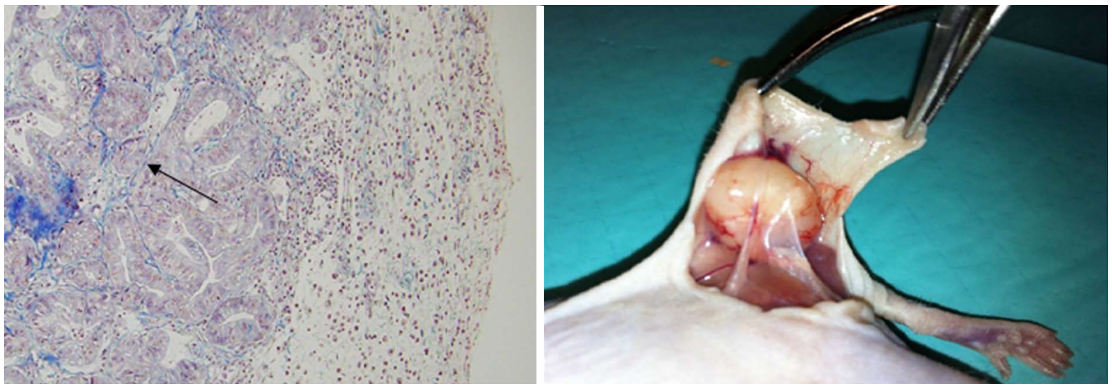

**Figure 1 Masson's trichrome staining of a F2 subcutaneous model (magnification × 500).** Black arrow shows the decreased fibrosis between the tumour glands.

1). Samples were immediately dissected from the surgical specimen by a pathologist, who confirmed the pathological diagnosis of pancreatic adenocarcinoma.

The surgical samples obtained from each patient were divided into five equally sized portions of 3 mm × 3 mm × 3 mm. Samples were placed immediately into culture medium (Nutrient mixture F-10 Ham; Sigma-Aldrich, St. Louis, MO, United States) containing 20% foetal bovine serum that had been previously maintained at 2-8 ℃. Samples were maintained on ice until implantation (from 30 min to 2 h). Three specimens were used as tumour xenograft implants at the subcutaneous, pancreatic and intraperitoneal locations. The remaining two specimens were used for anatomopathological and immunohistochemical analyses.

### *Implantation into nude mice*

Male Hsd:Athymic Nude-Foxn1$^{nu}$ mice (severe combined immunodeficient) aged 6 to 8 wk and weighing 20 to 25 g were purchased from Harlan Laboratories (Barcelona, Spain). Male mice were used to avoid hormonal interference. Mice were anesthetized in a laminar flow cabinet using ketamine (80 mg/kg), xylazine (10 mg/kg) and droperidol (100 mg/kg) intraperitoneally under sterile conditions.

Three experimental models of tissue implantation were developed: (1) Subcutaneous model: A 2–3-mm incision was made with a scalpel on the back of the nude mouse approximately 10 mm from the base of the tail. A subcutaneous pouch was dissected with scissors. The tumour tissue was gently introduced into the corresponding pouch, which was then closed by separated sutures using 3/0 silk (Figure 1); (2) Pancreatic model: The nude mouse was placed in the right lateral decubitus position and a 3-mm left subcostal incision was made 1 mm from the rib cage. The tail of the pancreas was completely exposed using a cotton swab, which helped us to locate the spleen. Using a resorbable 4/0 suture, the tumour xenograft was sutured onto the tail of the mouse pancreas; and (3) Intraperitoneal model: A 3-cm medium laparotomy was performed about 10 mm from the pubis. The musculature was pulled with the dissecting clamp to prevent an accidental enterotomy. The corresponding tumour xenograft was placed intraperitoneally, and the abdominal wall was immediately closed.

### *Establishment of tumour generations*

Mice were monitored daily for discomfort or distress and for tumour growth. Tumours were observed until they reached a maximum length of 10 to 15 mm. At this time, mice were anesthetized and then euthanized by cervical dislocation. All personnel had been properly trained and consistently applied the technique humanely and effectively. The tumour was then harvested under sterile conditions. Animals that showed no tumour growth were euthanised 20 wk after the implantation. An explorative laparotomy was performed to evaluate tumour growth. Tumour xenografts were successively re-implanted into a new nude mouse over three sequential generations (F1, F2 and F3) or cryopreserved in a freezer. In this way, tumour fragments from an F1 generation mouse were re-implanted into three mice at the three different locations in order to establish the F2 generation. Donor mice (bearing F1 tumours) were euthanised by cervical dislocation, and five tumour samples with a size of 3 mm × 3 mm × 3 mm were obtained, of which one was immediately fixed in 4% paraformaldehyde for histological analysis, done was frozen in liquid nitrogen for immunohistochemical analysis, and the other three were maintained in culture medium for re-implantation. Necropsy was performed on donor mice. This process was repeated until implantation of the F3 generation tumour xenograft into the nude mice.

### *Histological analysis of tumours*

The harvested xenograft tumours were fixed in a 10% formalin solution and then embedded in paraffin. The tissue was stained with haematoxylin and eosin and Masson's trichrome stain. For the assessment of samples stained with haematoxylin and eosin and Masson's stain, two different pathologists reviewed all samples twice with a week between each measurement.

Measurements were always performed early in the morning.

### *Tumour differentiation*

Tumour differentiation was evaluated with haematoxylin and eosin staining. Samples were classified as either well differentiated (well-formed tumour glands with a small nucleus relative to the cytoplasm), moderately differentiated (irregular tumour glands with higher cellular atypia and pleomorphic nuclei) and less differentiated (very poorly defined tumour glands, which sometimes acquired a solid pattern, greater architectural and cellular atypia, pleomorphic and large nuclei relative to the cytoplasm and a visible nucleolus).

The World Health Organisation guidelines state that well-differentiated tumours have fewer than five mitoses in 10 high-growth fields; moderately differentiated tumours have from 5 to 10 mitoses; and less differentiated tumours have more than 10 mitoses[15]. The number of mitoses was calculated by counting the number of cells undergoing mitosis in 10 high-magnification fields at 40 × magnification. The same samples were previously examined at 10 × magnification to identify the area in which cells undergoing mitosis were concentrated, and counting began in these areas. Of the two measurements of mitosis for each sample, the highest value was taken.

### *Evaluation of stromal tissue within the tumour*

The degree of fibrosis in the intra- and peritumoral areas was evaluated with Masson's trichrome staining on a scale from 1 to 4, with 1 corresponding to the minimum and 4 to the maximum degree of fibrosis between the tumour glands. There is no published classification system to assess the degree of fibrosis in pancreatic tumours. There is a subjectivity component in this assessment, which can lead to a degree of inter-observer variability[13].

### *Immunohistochemistry*

Different tumour characteristics were assessed by immunohistochemistry, specifically cell proliferation (Ki67), cell death (TUNEL), angiogenesis (CD31) and fibrogenesis (α-smooth muscle actin, or alpha-SMA).

This process involves the use of specific primary antibodies for the detection of Ki-67 (FLEX monoclonal mouse anti-human Ki-67 antigen, clone MIB-1, ref IR626; DAKO Denmark A/S), TUNEL (TACSTM TdT kit, TA4625; R&D Systems, Inc., MN, United States), CD31 (polyclonal anti-CD31, ab28364; Abcam, Cambridge, United States) and α-SMA (polyclonal anti-alpha-SMA, ab5694; Abcam, Cambridge, United States). The fluorescence emitted by a secondary antibody (Alexa 488 anti-rabbit/goat/mouse IgG; Abcam, Cambridge, United States) that was common to all proteins studied was measured using a fluorescence microscope (BX61, Olympus America Inc.) in a darkened room to avoid loss of fluorescence, and analysis was performed using the Cell Sens Dimensions software (Olympus America Inc.). We determined the cut-off level of expression of each protein studied using the Cut-off Finder software version 2.1[16,17].

### *Study variables*

We analysed tumour development (tumour growth greater than 1-1.5 cm or the presence of metastases), disease-free time (time in weeks from tumour xenograft implantation until the tumour had reached the target size), mortality (mice that died spontaneously without intervention by the investigators), postoperative mortality (death during the first 24 h after surgery or on subsequent days as the result of direct failure of the surgical technique) and body weight (weekly weight of the implanted mice measured in grams).

The variables related to histological assessment included differentiation of the tumour and evaluation of the stroma. The variables related to the immunohistochemistry analysis were tumour cell proliferation and stromal cell activation, which was assessed by measuring fibrogenesis, angiogenesis and apoptosis.

### *Statistical analysis*

Statistical analyses were carried out using SPSS® for Windows software version 21.0 (SPSS Inc., Chicago, IL, United States). Quantitative variables are presented as the mean ± SE. Qualitative variables are expressed as frequencies and percentage. The chi-square exact test or the Fisher's exact test were used for the evaluation of tumour development, pathology and immunohistochemistry. A $P$-value $\leqslant 0.05$ was considered significant. The Bonferroni correction was applied for post hoc analysis. The Kaplan-Meir with Log Rank Test was used to analyse disease-free time and tumour development time.

## RESULTS

### *Tumour characteristics*

The demographic and tumour characteristics of the patients, as well as the information regarding F1 engraftment, are summarised in Table 1[18].

The overall tumour engraftment rate was 61.1% (58/95) over the three generations. Tumour xenograft development at F1 (from human to mouse) was significantly lower (28.1%) than in successive implantations, in which the tumour xenograft transplantation was performed from mouse to mouse (F2 71.4% and F3 80.9%; $P < 0.001$). We also observed faster tumour xenograft development in the transplantation between mice (F2 and F3) when compared to the implant from humans to mice (F1 33.7 ± 2.5 wk *vs* F2 15.5 ± 1.8 wk *vs* F3 16.1 ± 1.9 wk, $P < 0.001$, Figure 2).

Analysis of tumour engraftment in the three models showed that the subcutaneous model was the most prolific (69.9%), followed by the intraperitoneal (57.6%) and pancreatic (55.0%) models.

**Table 2 Impact of clinical characteristics on the engraftment of the first generation (F1) xenograft in mice *n* (%)**

| Variables | Number of patients | Number of F1 tumours produced | Impact of clinical characteristics on tumour take rate ($P^1$ value) |
|---|---|---|---|
| Age (yr) | | | |
| < 70 | 2 | 0 (0) | 0.444 |
| ⩾ 70 | 8 | 5 (62.5) | |
| Gender | | | |
| Male | 5 | 2 (40) | 0.999 |
| Female | 5 | 3 (60) | |
| Histology | | | |
| ADCP | 9 | 3 (33.3) | 0.180 |
| Ampulloma | 2 | 2 (100) | |
| Differentiation | | | |
| G1 | 0 | 0 | <0.001 |
| G2 + G3 | 10 | 5 (50) | |
| Staging | | | |
| ⩽ Ⅱ (Ⅰ or Ⅱ) | 7 | 2 (28.6) | 0.160 |
| > Ⅱ (Ⅲ or Ⅳ) | 3 | 3 (100) | |
| Tumour origin | | | |
| Head | 9 | 4 (50) | Not available |
| Tail | 1 | 0 (0) | |
| Body | 0 | 0 | |
| Metastases | 1 | 1 (100) | |
| Perineural invasion | | | |
| Yes | 3 | 1 (33.3) | 0.999 |
| No | 7 | 4 (57.1) | |
| Lymph node metastasis | | | |
| Yes | 6 | 3 (50) | 0.999 |
| No | 4 | 2 (50) | |
| Distant metastases | | | |
| Yes | 2 | 1 (50) | 0.999 |
| No | 8 | 4 (50) | |

[1]Statistical analyses were performed using Fisher's test, with $P < 0.05$ considered statistically significant.

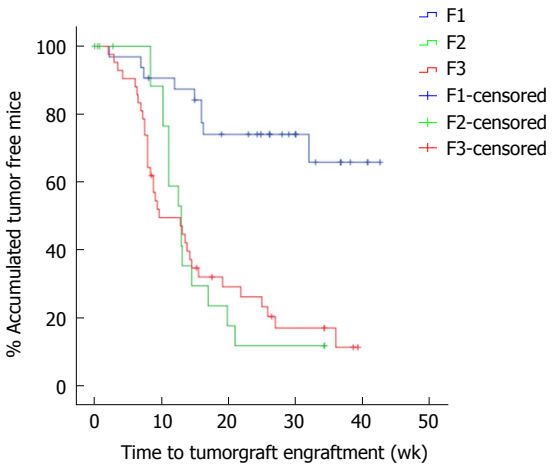


**Figure 2 Time until tumour engraftment for successive re-implants.**

The overall mortality of mice was 13.6%. Post-operative mortality was 4.2%. Mortality was also analysed for each model, for which the lowest mortality was 9.1% in the subcutaneous model, followed by 15.2% in the intraperitoneal model and 17.2% in the pancreatic model.

The time taken to reach the target size of the tumour xenograft (1.5 cm) in the three models was analysed. We observed that the time taken was shorter in the subcutaneous model (17.7 ± 2.6 wk) than in the intraperitoneal (25.0 ± 2.7 wk) and pancreatic (23.1 ± 2.3 wk) models, although there was no significant difference between them ($P = 0.063$).

The probability that a certain patient characteristic could be related to successful engraftment in mice was evaluated (Table 2). Our analysis did not identify any correlation between the progression of engraftment with patient age or gender, tumour stage, tumour differentiation status (histology) or tumour location (head, body or tail of the pancreas or metastases), nor with the presence of lymph nodes metastases, distant metastasis or perineural invasion.

### *Anatomopathological and immunohistochemical assessment of tumour samples*

Tumour differentiation was analysed in all three models. Most of the human samples were moderately differentiated (72.7%) (Figure 3). No significant differences were observed between human pancreatic cancer samples and any of three tumour xenograft models (Table 3).

With regard to the assessment of stromal tissue, the human samples showed higher fibrosis than the mice samples ($P = 0.044$). More than one third (36.3%) of the human samples displayed very high fibrosis (Figure 4). When the experimental models

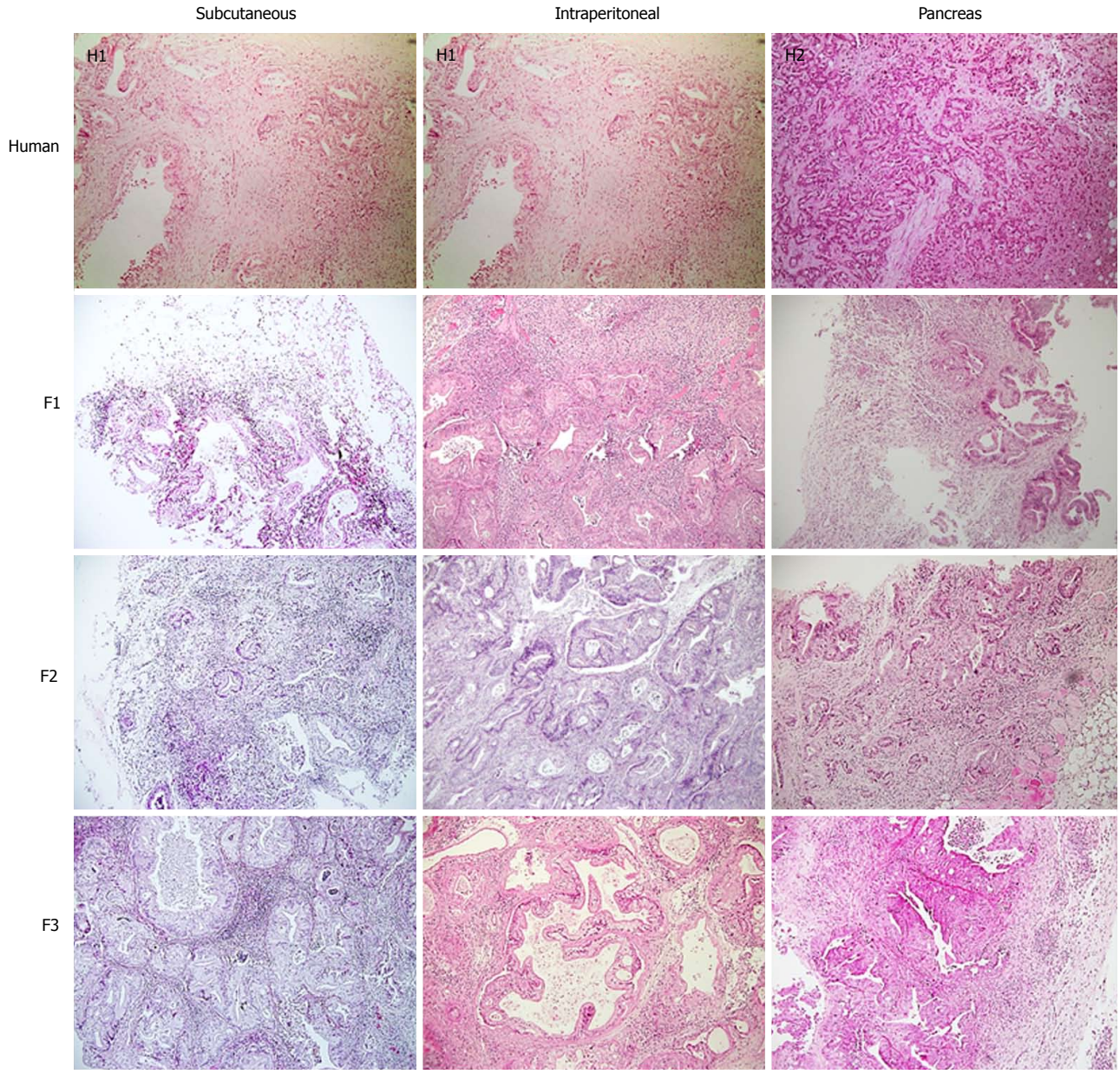


**Figure 3 Haematoxylin-eosin staining through successive generations and PDX models.** Tumour differentiation was maintained with successive re-implants and in the three PDX models (magnification × 500). H1: Sample from Human 1; H2: Sample from Human 2.

were analysed individually, no significant differences were observed compared with the human samples, although the intraperitoneal model seemed to show a trend towards a lower degree of fibrosis (Table 3).

The results of the immunohistochemistry assessment are summarised in Table 4.

Concerning cell proliferation, as indicated by Ki67 staining, no differences were observed between the three experimental models (Figure 5). However, significant differences in fibrogenesis were detected between the human samples and the animal models ($P < 0.001$). All human samples showed high fibrogenesis ($n = 11$) in clear contrast to the PDX models, which showed a lower degree of fibrogenesis (Figure 6). In addition, up to 87.5% of the pancreatic model samples presented low α-SMA expression (Table 4). Similarly, a decrease in angiogenesis was observed in all models, but the reduction was more pronounced in the pancreatic model ($P = 0.0027$; Table 4 and Figure 7). A significant difference in apoptosis was found between the human samples and the animal models (round to $P = 0.001$). Most of the human samples showed elevated apoptosis (72.7%), which was in contrast to the experimental models for which most samples presented only mild apoptosis (Figure 8). In addition, up to 93.8% of the pancreatic model samples presented slight apoptosis (Table 4).

## DISCUSSION

This study was designed to examine the usefulness of a pancreatic tumour xenograft model by focusing on

**Table 3 Impact of histology on experimental models *n* (%)**

| | Human ($n$ = 11) | Subcutaneous ($n$ = 23) | Intraperitoneal ($n$ = 17) | Pancreas ($n$ = 16) | $P^1$ value |
|---|---|---|---|---|---|
| Impact of differentiation | | | | | |
| Differentiated | 2 (18.2) | 7 (30.4) | 5 (29.4) | 3 (18.8) | 0.205 |
| Moderately differentiated | 8 (72.7) | 7 (30.4) | 4 (23.5) | 8 (50) | |
| Undifferentiated | 1 (9.1) | 9 (39.1) | 8 (47.1) | 5 (31.3) | |
| Impact of fibrosis | | | | | |
| Mild | 4 (36.3) | 12 (52.1) | 6 (35.2) | 6 (37.5) | 0.044 |
| Moderate | 3 (27.2) | 5 (21.7) | 9 (52.9) | 3 (18.8) | |
| High | 0 (0) | 4 (17.3) | 2 (11.7) | 5 (31.3) | |
| Very high | 4 (36.3) | 2 (8.6) | 0 (0) | 2 (12.5) | |

[1]Statistical analyses were performed by the $\chi^2$ exact test, with $P < 0.05$ considered statistically significant.

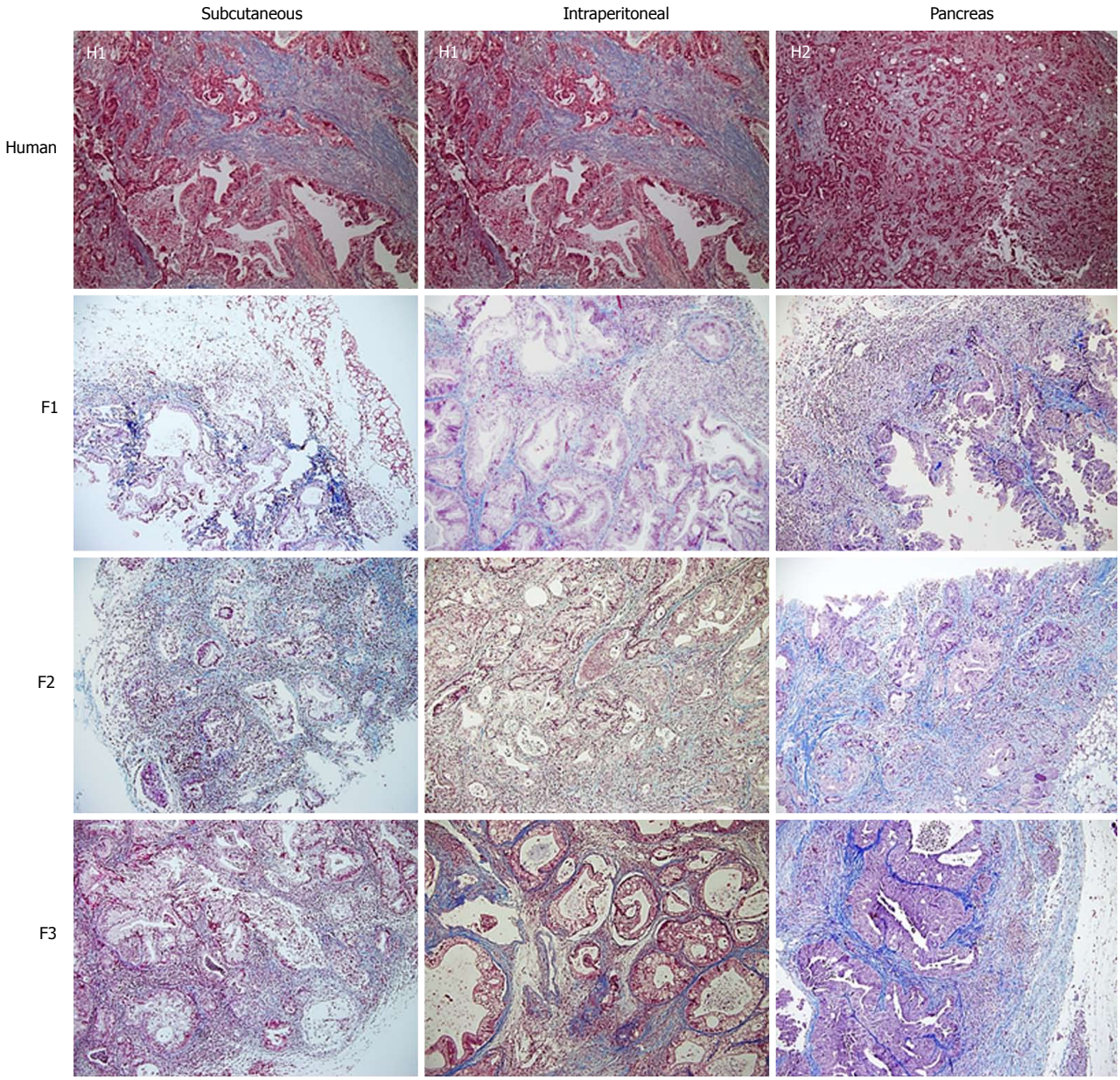


**Figure 4 Masson's trichrome staining through successive generations and PDX models.** The human samples showed higher fibrosis than the mice samples. Tumour stromal tissue was maintained in the three PDX models (magnification × 500). H1: Sample from Human 1; H2: Sample from Human 2.

**Table 4 Impact of immunohistochemistry on experimental models *n* (%)**

| | Human ($n$ = 11) | Subcutaneous ($n$ = 23) | Intraperitoneal ($n$ = 17) | Pancreas ($n$ = 16) | $P^1$ value |
|---|---|---|---|---|---|
| Impact of cell proliferation (Ki67) | | | | | |
| Mild | 4 (36.4) | 13 (56.5) | 10 (58.8) | 8 (50) | 0.650 |
| High | 7 (63.3) | 10 (43.5) | 7 (41.2) | 8 (50) | |
| Impact of fibrogenesis (α-SMA) | | | | | |
| Mild | 0 (0) | 16 (69.6) | 11 (64.7) | 14 (87.5) | < 0.001 |
| High | 11 (100) | 7 (30.4) | 6 (35.3) | 2 (12.5) | |
| Impact of angiogenesis (CD31) | | | | | |
| Mild | 2 (18.2) | 15 (65.2) | 11 (64.7) | 14 (87.5) | < 0.001 |
| High | 9 (81.8) | 8 (34.8) | 6 (35.3) | 2 (12.5) | |
| Impact of apoptosis (TUNEL) | | | | | |
| Mild | 3 (27.3) | 16 (69.6) | 14 (82.4) | 15 (93.8) | < 0.001 |
| High | 8 (72.7) | 7 (30.4) | 3 (17.6) | 1 (6.3) | |

[1]Statistical analyses were performed by the $\chi^2$ exact test, with $P < 0.05$ considered statistically significant. The Bonferroni correction was applied for *post hoc* analysis. The impact of the immunohistochemistry was assessed by Ki67 expression (cell proliferation), α-SMA expression (fibrogenesis), CD31 expression (angiogenesis) and TUNEL expression (apoptosis).

the pathological and immunohistochemical features of subcutaneous, intraperitoneal and pancreatic implantation of human pancreatic cancer tissue fragments into mice. The main findings were: (1) the engraftment rate between mice (F2 and F3) was higher than the engraftment rate from human to mouse (F1); (2) the subcutaneous model developed a higher number of implants, although there were no significant differences in favour of any model; and (3) the tumour xenografts of the three models maintained some human characteristics including differentiation and cell proliferation. While these tumour xenografts presented reduced fibrosis and fibrogenesis, two other features of pancreatic cancer, hypovascularisation and apoptosis, were enhanced.

Our study differs from others published in the literature as we extracted the sample directly from the surgical site[19-21], and tumour cells were not cultured *in vitro*. Neither collagenase nor Matrigel were used to facilitate their implantation[22,23]. These steps, along with rapid implantation, facilitates the procedure and eliminates the influence of factors related to the processing of tumour cells such as DNA aberrations and cell death[24,25].

There was no correlation between the development of F1 tumour xenografts and the clinical characteristics of the patients or the pathological anatomy of the human tumour samples that were implanted into mice (differentiation, fibrosis, cell proliferation, number, fibrogenesis, angiogenesis and apoptosis). The apparent lack of correlation between any of these parameters, together with the rate of engraftment, may reflect a biological phenomenon, or it may be simply be due to an insufficient number of human tumours in some groups. However, similar results have been obtained in other studies[25]. This could be one of the limitations of this study. For this reason, new studies with higher numbers of participants are required. In addition, a genetic assessment of the samples could have enriched the study and might have explained this phenomenon.

Faster tumour development and a greater number of successful engraftments were observed for mouse-to-mouse compared to human-to-mouse transplants. This is probably a result of decreased apoptosis and fibrogenesis with progressing passage, which facilitates tumour development[6,26]. The three experimental models have similar characteristics in terms of differentiation, fibrosis, cell proliferation, fibrogenesis, angiogenesis and apoptosis. Tumour development appeared to occur earlier in the subcutaneous model; however, tumour xenografts that were implanted into the peritoneum or orthotopically in the pancreas were harder to visualise as they were grafted into a distensible cavity. Imaging tests such as nuclear magnetic resonance would probably evidence similar growth to the subcutaneous model[27]. While evaluating the cost-effectiveness of the tumour xenograft was not the purpose of this paper, the shorter time taken for the subcutaneous PDX to reach the target size may reduce the cost of maintenance and experimental duration when compared to other models[6]. The practical utility of tumour xenografts needs to be addressed in terms of engraftment speed and reproducibility. In fact, tumour xenografts show a rather limited engraftment rate and slow tumour growth. However, those models are readily applicable for drug experiment because, once a xenograft has been successfully engrafted, it can be used after several freeze-thaw cycles and several passages[5].

The intraperitoneal and pancreatic models showed a tendency toward higher mortality. Two factors may explain this trend in these two models: firstly, the laparotomy performed in the intraperitoneal model and the subcostal incision in the pancreatic model are more aggressive procedures and more prone to complications (evisceration, unnoticed enterotomy, solid viscera lesion and pancreatitis); and secondly, in both models the tumour xenografts developed inside a cavity where the tumour growth could not be observed. Tumour xenografts could infiltrate vital structures, unnoticed by the researcher, resulting in the death of

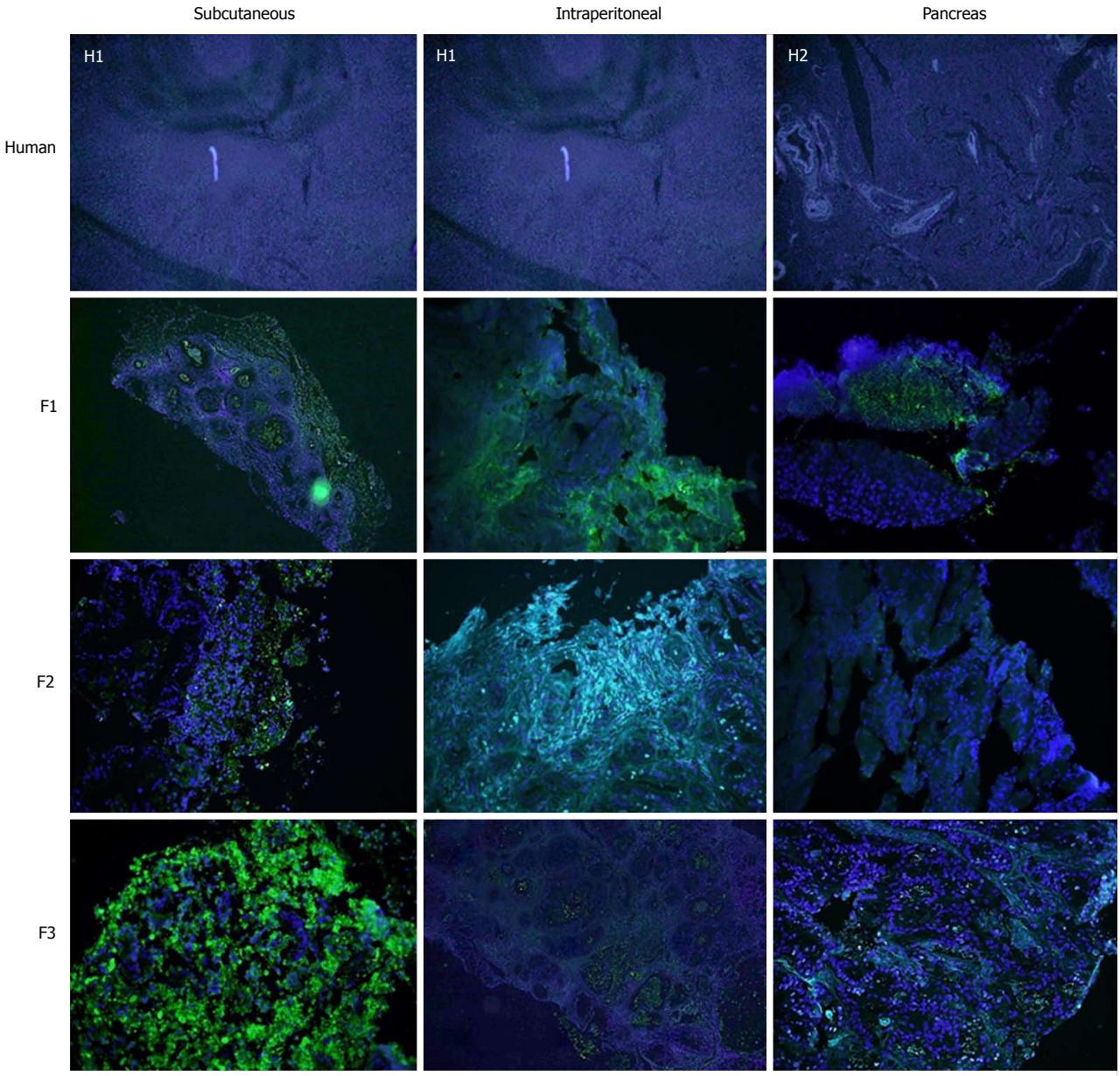


**Figure 5 Immunohistochemical staining of Ki67 through successive generations and PDX models.** Green fluorescence identifies Ki67-positive cells related to proliferation. Blue fluorescence identifies cell nuclei. The Ki67 expression was maintained with successive re-implants and in the three PDX models (magnification × 500). H1: Sample from Human 1; H2: Sample from Human 2.

the mouse. Pancreatic and intraperitoneal models are more invasive and thus might include more suffering/physiological burden in a mouse. That might be one of reasons why the tumour xenograft grows better subcutaneously.

We did not find any significant differences between the differentiation and proliferation of human samples compared to any of the experimental models. Therefore, tumour xenografts in the tested experimental models appear to reproduce human-characteristics independent of the model in which it is implanted (subcutaneous, intraperitoneal or pancreas), suggesting that tumour xenografts could be valid models for the study of chemotherapy[22,25,28,29].

Some authors suggest that the interstitial matrix may act as a physical barrier to the penetration of chemotherapeutics into deeper areas of the tumour[5,30]. These studies conclude that the tumour stroma of tumour xenografts is larger and more similar to human tumour samples than models in which isolated cells are implanted from the human tumour or from *in vitro* cultures[5]. The diffusion of chemotherapeutics in the latter model could be higher than in human tumours; therefore, it is expected that the tumour xenografts will be a more realistic model.

The election in our study of alpha SMA as a marker for fibrogenesis is based on the intense desmoplasia presented by pancreatic tumours. The pancreatic stellate cells involved in tumour desmoplasia are characterized by expressing α-SMA and by the synthesis

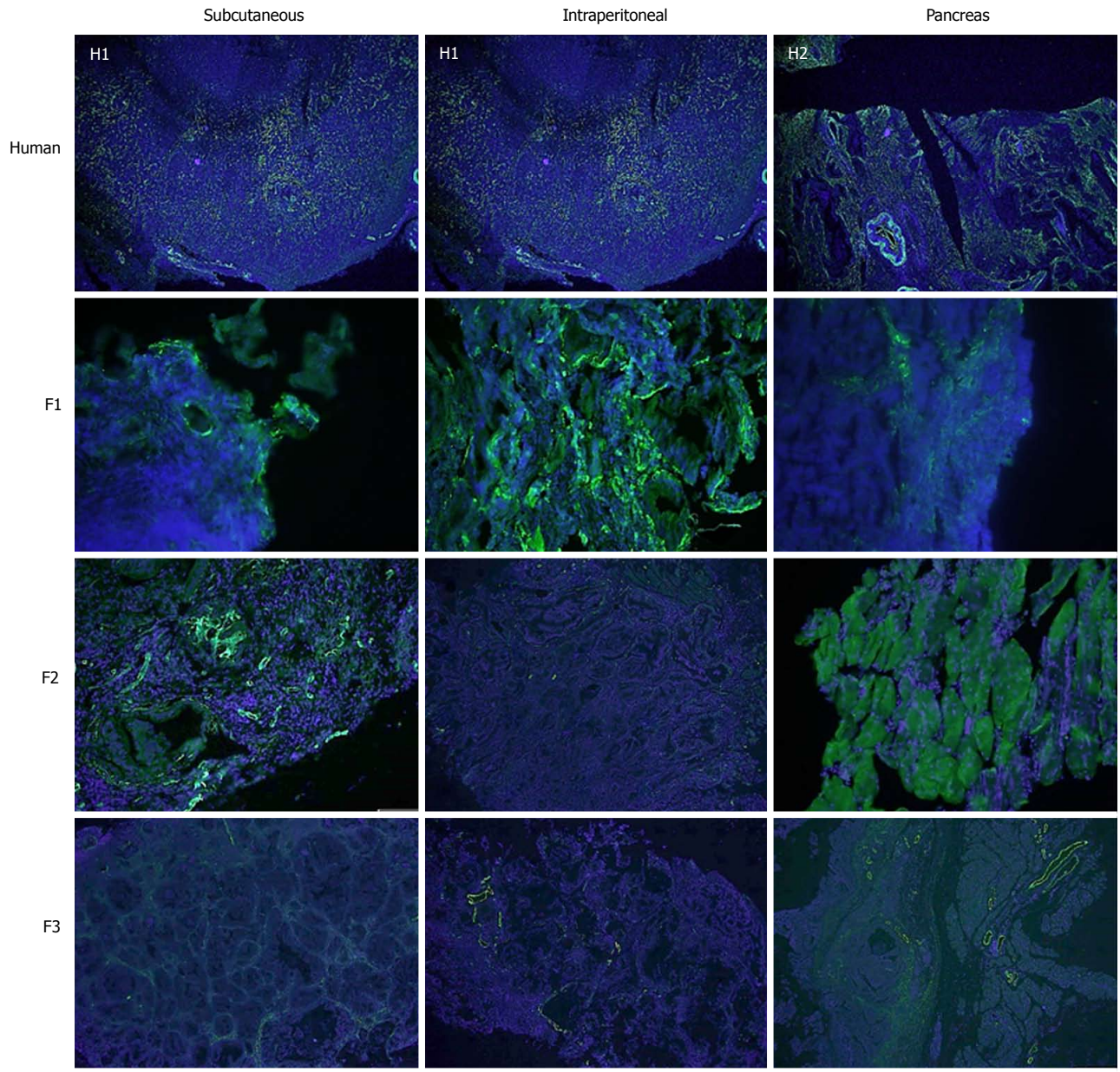


**Figure 6 Immunohistochemical staining of alpha-SMA through successive generations.** Green fluorescence identifies alpha-SMA -positive cells related to fibrogenesis. Blue fluorescence identifies cell nuclei. The alpha-SMA expression was visibly reduced with successive re-implants in all three models, which was more remarkable in the pancreatic model (magnification × 500).

of procollagen α-1T which are the main components of the extracellular matrix that constitute desmoplasia[31,32].

We did not observe any differences in stromal fibrosis in successive tumour xenografts, although there was a tendency toward reduced fibrosis compared to human samples. However, when we analysed fibrogenesis or α-SMA expression, a progressive decline in fibrogenesis was observed throughout the three passages. In the F1 tumour xenografts, there was no difference in fibrogenesis compared to the human specimen; however, in the F2 tumour xenograft there was a significant decrease, and in F3 the decrease was remarkable. This phenomenon may explain the increase in tumorigenesis in successive re-implants[22,23,26].

Finally, by comparing histological fibrosis measured by Masson's staining and α-SMA expression, a decrease in stromal cell activation through successive re-implants was evidenced in all experimental models. The advent of anti-tumour drugs for cancer niches is determined by a variety of factors including drug penetration or diffusion, which is dependent on vascularisation of the tumour and the stromal matrix. Therefore, the distance from cancer cells to the vessels will determine the efficacy of the chemotherapeutic drug[5]. Although a decrease in the activation of myoblasts and fibroblasts may facilitate tumour implantation, we must also consider that this may translate into reduced fibrosis of the tumour stroma. The chemotherapeutic agent may show better diffusion, and thus greater effectiveness, in the animal model than in humans. As such, we

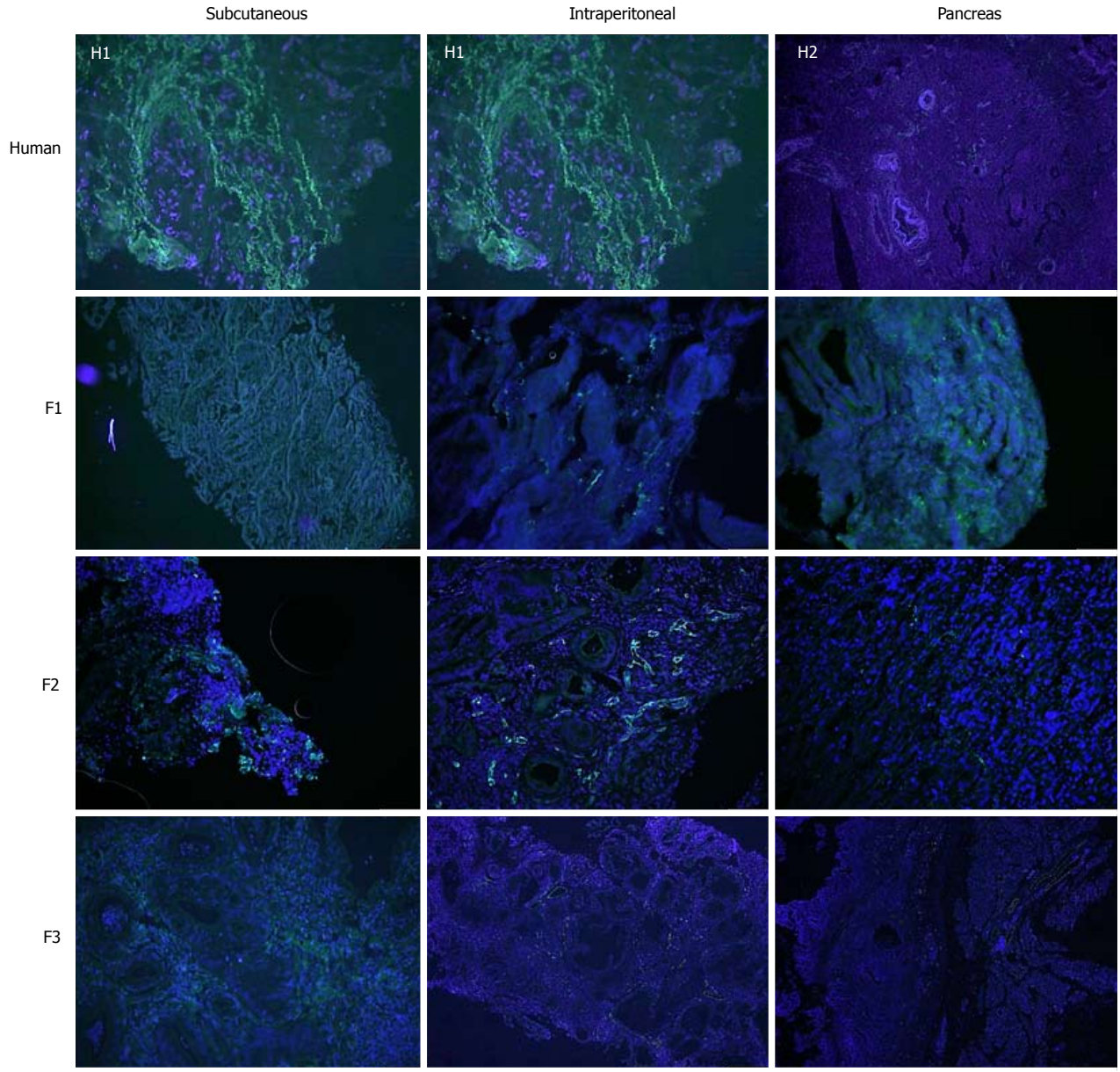


**Figure 7 Immunohistochemical staining of CD31 through successive generations.** Green fluorescence identifies CD31-positive cells related to angiogenesis. Blue fluorescence identifies cell nuclei. The CD31 expression was visibly reduced with successive re-implants (magnification × 500). H1: Sample from Human 1; H2: Sample from Human 2.

must be cautious when testing the pharmacokinetics of chemotherapy drugs, as they may be more effective in animal models than in humans. Hence, further pharmacological studies that compare all three models are mandatory.

Regarding tumour angiogenesis, the evaluation of tumour vascularisation is important in the investigation of pancreatic cancer. The extension of the vascular network is fundamental to assess the response to the treatment of anti-tumour drugs. Multiple authors use a microvessel density analysis system by CD31 expression in pancreatic PDX similar to ours[5,33,34].

A study by Akashi *et al*[5] compared grafts that had been extracted directly from the tumour specimen with those derived from cultured cell lines. The authors observed a higher density of microvessels in the periphery of the tumour xenografts derived from cell lines. In contrast, tumour xenografts derived directly from humans presented areas of low microvessel density, and thus, maintained similar features to those of human basal tumours. Hypovascularisation is a characteristic feature of pancreatic cancer which makes this tumour chemoresistant[5,34,35]. This characteristic was potentiated in our experimental tumour xenografts indicating that these models are representative of human tumours for the purposes of drug testing. Although hypovascularisation is a hallmark of pancreatic cancer, further chemotherapeutic studies are required to determine how tumour xenografts behave against anticancer drugs in order to avoid resistance to chemotherapeutic drugs in preclinical models due to the significant decrease in angiogenesis in tumour

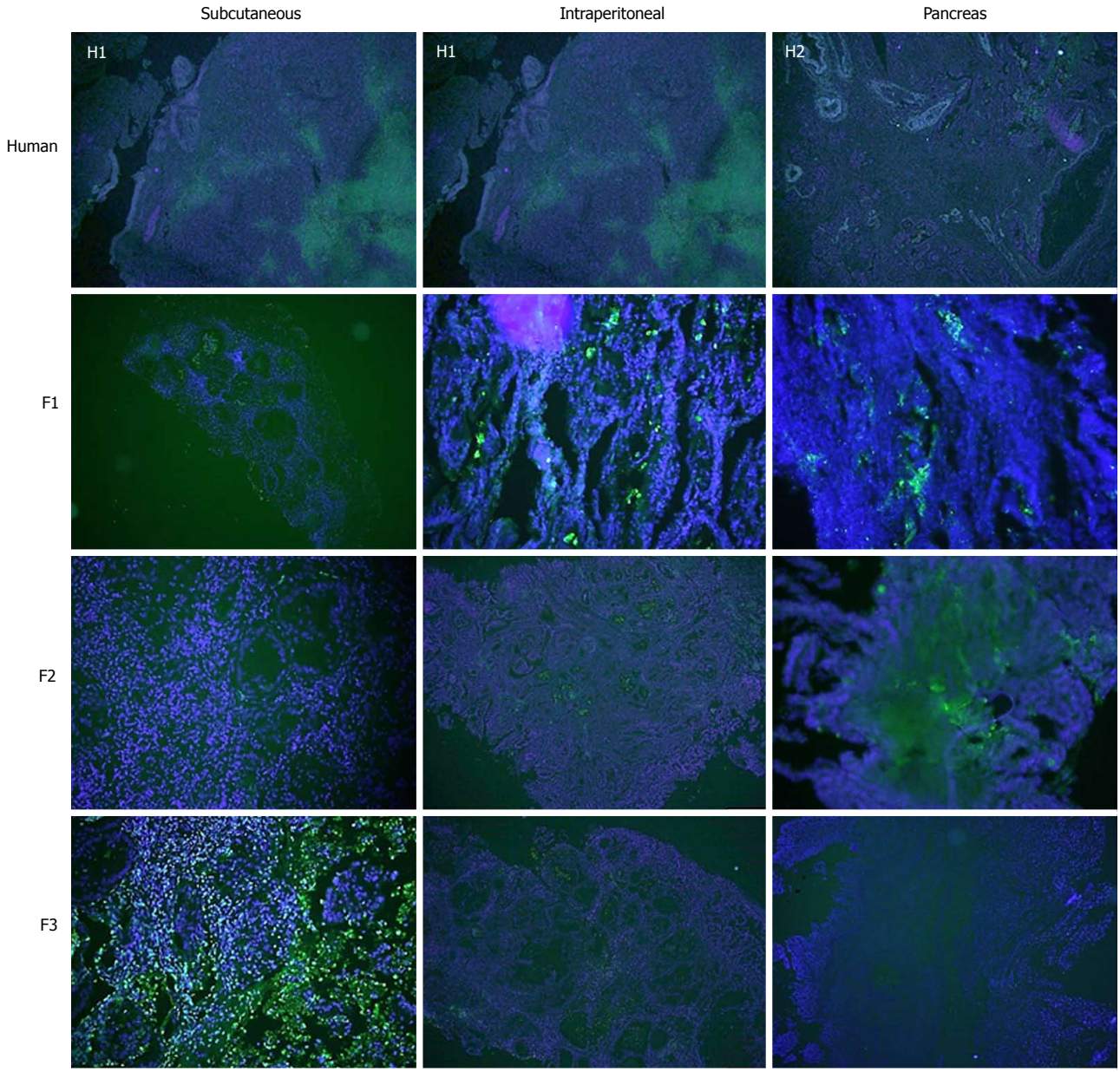


**Figure 8 Immunohistochemical staining of TUNEL through successive generations.** Green fluorescence identifies TUNEL-positive cells related to apoptosis. Blue fluorescence identifies cell nuclei. TUNEL expression was reduced with subsequent re-implants for all three experimental models, which was more remarkable in the intraperitoneal and pancreatic model (magnification × 500).

xenografts.

In addition to a tendency toward hypovascularisation and the development of a strong desmoplastic stroma, human pancreatic cancer has a relatively low apoptosis rate that makes it chemoresistant[36,37]. In our study, there was a trend toward decreasing TUNEL expression with subsequent re-implants for all three experimental models, which was more remarkable in the orthotopic implant and pancreatic model.

In conclusion, The three PDX models have similar characteristics in terms of differentiation, fibrosis, cell proliferation, fibrogenesis, angiogenesis and apoptosis, but tumour development was detected earlier in the subcutaneous model. Intraperitoneal and pancreatic PDX models presented a greater morbidity and mortality than subcutaneous model. There was also a higher number of viable tumour xenografts with the progression of sequential implants in this experimental model. For these reasons, the subcutaneous model may represent the best option for the investigation of anticancer drugs with tumour xenografts.

## ARTICLE HIGHLIGHTS

### *Research background*

Currently, a dozen experimental models are available. The molecular characteristics of these models can vary substantially with the morphology of the lesion, and thus, the selection of the model is not trivial. Multiple laboratories have established models of breast xenografts, head and neck cancer, and hepatocellular tumours that maintain the characteristics of the primary tumour from which they come. Some of these models have predicted

the clinical response of a specific type of tumour to different chemotherapeutic agents. The main advantage of human tumour xenografts in the mouse is that they seem to preserve the pathological and immunohistochemical characteristics of the primary tumour, which may allow us to experiment with drugs with human-like pancreatic cancer models. However, the degree to which periampullary carcinoma implants and ductal adenocarcinoma (DAC) reflect the morphological and histological characteristics of their tumours of origin have been poorly studied and there are few publications on the subject.

## Research motivation

Periampullary carcinomas, and especially DAC, are characterised by early vascular, lymphatic and perineural dissemination, so that some authors consider it to be a systemic disease from the beginning. This implies criteria of unresectability and justifies the ominous prognosis of the disease. At the time of diagnosis, 85% of patients present a macroscopic disease beyond the limits of the organ. The large epidemiological series approximate the incidence of pancreas cancer to their annual mortality. Given the unfortunate prognosis of this disease, the development of new chemotherapy drugs with systemic action that complement the local surgical treatment is fundamental. One of the main problems that researchers find in developing new molecules is the lack of animal models that faithfully reproduce the characteristics of human pancreatic cancer. Both the models developed in genetically modified mice (GEMM) and those induced by carcinogenic substances have facilitated the understanding at the molecular level and the appearance of new anti-tumour drugs with *in vitro* activity. Unfortunately, these treatment lines are often ineffective in humans.

The appearance of immunocompromised nude mice has allowed the resumption of animal models with human xenografts, whose main limitation was the high rejection rate. In this way, we can develop experimental models of human periampullary tumours that preserve the original genotypic and phenotypic characteristics.

The morphological and histological characteristics derived from the xenografts of pancreatic cancer in the experimental models have been poorly studied. In order to make animal models that are more similar to cancer in humans, we have developed this study.

## Research objectives

Following this line of work, we have developed three experimental models through the use of xenografts: subcutaneous, intraperitoneal and pancreatic. The main objective of this study is to assess the viability of orthotopic (intrapancreatic) and heterotopic (intraabdominal and subcutaneous) xenografts of human pancreas cancers implanted in nude mice.

This work is part of a more ambitious line of research that in the future intends to identify molecules or combinations of these with the help of these models to rescue patients for surgery.

## Research methods

A prospective experimental analytical follow-up of the development of tumours in mice upon implantation of human pancreatic adenocarcinoma samples was presents. Specimens surgically from patients with a pathological diagnosis of pancreas adenocarcinoma were obtained. Human cancer samples were implanted as tumour xenografts in three experimental models. The surgical samples were divided into five equally sized portions of 3 mm × 3 mm × 3 mm. Three specimens were used as tumour xenograft implants at the subcutaneous, pancreatic and intraperitoneal locations in nude mice. To date, no study comparing the implantation of a heterotopic pancreatic cancer xenograft with an orthotopic tumour xenograft has been published.

Histological analysis and immunohistochemical assessment of apoptosis, proliferation, angiogenesis and fibrogenesis were performed. When a tumour xenograft got the target size, it was re-implanted in a new nude mouse. Three sequential tumour xenograft generations (F1, F2 and F3) were generated.

## Research results

*The* main findings of this study were: (1) the engraftment rate between mice was higher than the engraftment rate from human to mouse; (2) the subcutaneous model developed a higher number of implants, although there were no significant differences in favour of any model; and (3) the tumour xenograft of the three models maintained some human characteristics including differentiation and cell proliferation. While these tumour xenografts presented reduced fibrosis and fibrogenesis, two other features of pancreatic cancer, hypovascularisation and apoptosis, were enhanced.

The practical utility of tumour grafts needs to be addressed in terms of engraftment speed and reproducibility. In fact, tumour xenografts show a rather limited engraftment rate and slow tumour growth. However, those models are readily applicable for drug experiment because, once a xenograft has been successfully engrafted, it can be used after several freeze-thaw cycles and several passages.

Although these models can develop tumours that are very similar to humans, they are not an exact reflection of them. In this way, chemotherapeutic agents could be more effective in pancreatic PDX models than in human tumours. For this reason, new preclinical studies with chemotherapeutic agents are mandatory in those models.

## Research conclusions

In the establishment of patient-derived xenograft models, samples of primary tumours were implanted in immunodepressed mice subcutaneously, intraperitoneally or orthotopically, with no intermediate step of *in vitro* propagation. Although the subcutaneous model is easy to perform through an incision with the scalpel on the back of the mouse, the microenvironment of the tumour is not exactly the same. We have considered one step further by designing a new intraperitoneal and pancreatic model that may reproduce the natural conditions of human pancreatic cancer. However, in our study, implanted subcutaneous xenografts maintain pathological and immunohistochemical characteristics of the primary tumour from which they derive similarly to the other two developed models.

To date, there has been no study on pancreatic cancer that has determined the best location to develop xenografts in animal models. In our study, the detection of tumour development is earlier in the subcutaneous model, which implies a lower cost compared to the other models. In addition, the subcutaneous model is the one with the highest number of viable xenografts developed throughout the different re-implantations. Taking into account that the three models developed have similar anatomopathological and immunohistochemical characteristics, the subcutaneous model could be the best option for the investigation of anticancer drugs with xenografts. However, more studies are needed to confirm this theory.

## Research perspectives

The majority of works that strive to broaden our knowledge about the diagnosis and treatment of pancreas cancer, are based on xenografts from cell lines cultured *in vitro*. Chemotherapy agents which have good results in these experimental models do not have the same results when they are used in human tumours. In our case, we have established three models of pancreas tumours directly derived from patients and we have compared the morphological and immunological characteristics of the xenografts with the human tumours in order to establish which is the model that most faithfully reflected human tumour characteristics.

In our experience, due to the earliest development and the highest number of viable xenografts, as well as being the experimental model with the lowest morbidity, the subcutaneous model may be the best model for experimentation in pancreatic cancer.

Our intention is to select the best implant route in order to use these models in the future to detect biomarkers of pancreatic cancer and to develop specific chemotherapeutic regimens for each patient.

# REFERENCES


1 **Morton JJ**, Bird G, Refaeli Y, Jimeno A. Humanized Mouse Xenograft Models: Narrowing the Tumor-Microenvironment Gap. *Cancer Res* 2016; **76**: 6153-6158 [PMID: 27587540 DOI: 10.1158/0008-5472.CAN-16-1260]

2 **Jackson SJ**, Thomas GJ. Human tissue models in cancer research: looking beyond the mouse. *Dis Model Mech* 2017; **10**: 939-942 [PMID: 28768734 DOI: 10.1242/dmm.031260]

3 **Voskoglou-Nomikos T**, Pater JL, Seymour L. Clinical predictive value of the in vitro cell line, human xenograft, and mouse allograft preclinical cancer models. *Clin Cancer Res* 2003; **9**: 4227-4239 [PMID: 14519650]

4 **Huynh AS**, Abrahams DF, Torres MS, Baldwin MK, Gillies RJ, Morse DL. Development of an orthotopic human pancreatic cancer xenograft model using ultrasound guided injection of cells. *PLoS One* 2011; **6**: e20330 [PMID: 21647423 DOI: 10.1371/journal.pone.0020330]

5 **Akashi Y**, Oda T, Ohara Y, Miyamoto R, Hashimoto S, Enomoto T, Yamada K, Kobayashi A, Fukunaga K, Ohkochi N. Histological advantages of the tumor graft: a murine model involving transplantation of human pancreatic cancer tissue fragments. *Pancreas* 2013; **42**: 1275-1282 [PMID: 24152953 DOI: 10.1097/MPA.0b013e318296f866]

6 **Olive KP**, Jacobetz MA, Davidson CJ, Gopinathan A, McIntyre D, Honess D, Madhu B, Goldgraben MA, Caldwell ME, Allard D, Frese KK, Denicola G, Feig C, Combs C, Winter SP, Ireland-Zecchini H, Reichelt S, Howat WJ, Chang A, Dhara M, Wang L, Rückert F, Grützmann R, Pilarsky C, Izeradjene K, Hingorani SR, Huang P, Davies SE, Plunkett W, Egorin M, Hruban RH, Whitebread N, McGovern K, Adams J, Iacobuzio-Donahue C, Griffiths J, Tuveson DA. Inhibition of Hedgehog signaling enhances delivery of chemotherapy in a mouse model of pancreatic cancer. *Science* 2009; **324**: 1457-1461 [PMID: 19460966 DOI: 10.1126/science.1171362]

7 **Johnson JI**, Decker S, Zaharevitz D, Rubinstein LV, Venditti JM, Schepartz S, Kalyandrug S, Christian M, Arbuck S, Hollingshead M, Sausville EA. Relationships between drug activity in NCI preclinical in vitro and in vivo models and early clinical trials. *Br J Cancer* 2001; **84**: 1424-1431 [PMID: 11355958 DOI: 10.1054/bjoc.2001.1796]

8 **Garrido-Laguna I**, Uson M, Rajeshkumar NV, Tan AC, de Oliveira E, Karikari C, Villaroel MC, Salomon A, Taylor G, Sharma R, Hruban RH, Maitra A, Laheru D, Rubio-Viqueira B, Jimeno A, Hidalgo M. Tumor engraftment in nude mice and enrichment in stroma- related gene pathways predict poor survival and resistance to gemcitabine in patients with pancreatic cancer. *Clin Cancer Res* 2011; **17**: 5793-5800 [PMID: 21742805 DOI: 10.1158/1078-0432.CCR-11-0341]

9 **Whiteford CC**, Bilke S, Greer BT, Chen Q, Braunschweig TA, Cenacchi N, Wei JS, Smith MA, Houghton P, Morton C, Reynolds CP, Lock R, Gorlick R, Khanna C, Thiele CJ, Takikita M, Catchpoole D, Hewitt SM, Khan J. Credentialing preclinical pediatric xenograft models using gene expression and tissue microarray analysis. *Cancer Res* 2007; **67**: 32-40 [PMID: 17210681 DOI: 10.1158/0008-5472.CAN-06-0610]

10 **Capellá G**, Farré L, Villanueva A, Reyes G, García C, Tarafa G, Lluís F. Orthotopic models of human pancreatic cancer. *Ann N Y Acad Sci* 1999; **880**: 103-109 [PMID: 10415855]

11 **Morton CL**, Houghton PJ. Establishment of human tumor xenografts in immunodeficient mice. *Nat Protoc* 2007; **2**: 247-250 [PMID: 17406581 DOI: 10.1038/nprot.2007.25]

12 **Smith V**, Wirth GJ, Fiebig HH, Burger AM. Tissue microarrays of human tumor xenografts: characterization of proteins involved in migration and angiogenesis for applications in the development of targeted anticancer agents. *Cancer Genomics Proteomics* 2008; **5**: 263-273 [PMID: 19129557]

13 **Galuschka C**, Proynova R, Roth B, Augustin HG, Müller-Decker K. Models in Translational Oncology: A Public Resource Database for Preclinical Cancer Research. *Cancer Res* 2017; **77**: 2557-2563 [PMID: 28507049 DOI: 10.1158/0008-5472.CAN-16-3099]

14 **Perez M**, Lucena-Cacace A, Marín-Gómez LM, Padillo-Ruiz J, Robles-Frias MJ, Saez C, Garcia-Carbonero R, Carnero A. Dasatinib, a Src inhibitor, sensitizes liver metastatic colorectal carcinoma to oxaliplatin in tumors with high levels of phospho-Src. *Oncotarget* 2016; **7**: 33111-33124 [PMID: 27105527 DOI: 10.18632/oncotarget.8880]

15 **Bosman FT**, Carneiro F, Hruban RH, Theise ND. WHO classification of tumours of the digestive system. 4th ed. Geneva: World Health Organisation; 2010

16 **Budczies J**, Klauschen F, Sinn BV, Győrffy B, Schmitt WD, Darb-Esfahani S, Denkert C. Cutoff Finder: a comprehensive and straightforward Web application enabling rapid biomarker cutoff optimization. *PLoS One* 2012; **7**: e51862 [PMID: 23251644 DOI: 10.1371/journal.pone.0051862]

17 **Striefler JK**, Sinn M, Pelzer U, Jühling A, Wislocka L, Bahra M, Sinn BV, Denkert C, Dörken B, Oettle H, Riess H, Bläker H, Lohneis P. P53 overexpression and Ki67-index are associated with outcome in ductal pancreatic adenocarcinoma with adjuvant gemcitabine treatment. *Pathol Res Pract* 2016; **212**: 726-734 [PMID: 27461834 DOI: 10.1016/j.prp.2016.06.001]

18 **Edge SB**, Compton CC. The American Joint Committee on Cancer: the 7th edition of the AJCC cancer staging manual and the future of TNM. *Ann Surg Oncol* 2010; **17**: 1471-1474 [PMID: 20180029 DOI: 10.1245/s10434-010-0985-4]

19 **Arjona-Sánchez A**, Ruiz-Rabelo J, Perea MD, Vázquez R, Cruz A, Muñoz Mdel C, Túnez I, Muntané J, Padillo FJ. Effects of capecitabine and celecoxib in experimental pancreatic cancer. *Pancreatology* 2010; **10**: 641-647 [PMID: 21051919 DOI: 10.1159/000288708]

20 **Ruiz-Rabelo JF**, Vázquez R, Perea MD, Cruz A, González R, Romero A, Muñoz-Villanueva MC, Túnez I, Montilla P, Muntané J, Padillo FJ. Beneficial properties of melatonin in an experimental model of pancreatic cancer. *J Pineal Res* 2007; **43**: 270-275 [PMID: 17803524 DOI: 10.1111/j.1600-079X.2007.00472.x]

21 **Padillo FJ**, Ruiz-Rabelo JF, Cruz A, Perea MD, Tasset I, Montilla P, Túnez I, Muntané J. Melatonin and celecoxib improve the outcomes in hamsters with experimental pancreatic cancer. *J Pineal Res* 2010; **49**: 264-270 [PMID: 20626589 DOI: 10.1111/j.1600-079X.2010.00791.x]

22 **Jiang YJ**, Lee CL, Wang Q, Zhou ZW, Yang F, Jin C, Fu DL. Establishment of an orthotopic pancreatic cancer mouse model: cells suspended and injected in Matrigel. *World J Gastroenterol* 2014; **20**: 9476-9485 [PMID: 25071342 DOI: 10.3748/wjg.v20.i28.9476]

23 **Partecke LI**, Sendler M, Kaeding A, Weiss FU, Mayerle J, Dummer A, Nguyen TD, Albers N, Speerforck S, Lerch MM, Heidecke CD, von Bernstorff W, Stier A. A syngeneic orthotopic murine model of pancreatic adenocarcinoma in the C57/BL6 mouse using the Panc02 and 6606PDA cell lines. *Eur Surg Res* 2011; **47**: 98-107 [PMID: 21720167 DOI: 10.1159/000329413]

24 **Monsma DJ**, Monks NR, Cherba DM, Dylewski D, Eugster E, Jahn H, Srikanth S, Scott SB, Richardson PJ, Everts RE, Ishkin A, Nikolsky Y, Resau JH, Sigler R, Nickoloff BJ, Webb CP. Genomic characterization of explant tumorgraft models derived from fresh patient tumor tissue. *J Transl Med* 2012; **10**: 125 [PMID: 22709571 DOI: 10.1186/1479-5876-10-125]

25 **Garcia PL**, Council LN, Christein JD, Arnoletti JP, Heslin MJ, Gamblin TL, Richardson JH, Bjornsti MA, Yoon KJ. Development and histopathological characterization of tumorgraft models of pancreatic ductal adenocarcinoma. *PLoS One* 2013; **8**: e78183 [PMID: 24194913 DOI: 10.1371/journal.pone.0078183]

26 **Grippo PJ**, Tuveson DA. Deploying mouse models of pancreatic cancer for chemoprevention studies. *Cancer Prev Res (Phila)* 2010; **3**: 1382-1387 [PMID: 21045161 DOI: 10.1158/1940-6207.CAPR-10-0258]

27 **Qiu W**, Su GH. Development of orthotopic pancreatic tumor mouse models. *Methods Mol Biol* 2013; **980**: 215-223 [PMID: 23359156 DOI: 10.1007/978-1-62703-287-2_11]

28 **Hruban RH**, Adsay NV, Albores-Saavedra J, Anver MR, Biankin AV, Boivin GP, Furth EE, Furukawa T, Klein A, Klimstra DS, Kloppel G, Lauwers GY, Longnecker DS, Luttges J, Maitra A, Offerhaus GJ, Pérez-Gallego L, Redston M, Tuveson DA. Pathology of genetically engineered mouse models of pancreatic exocrine cancer: consensus report and recommendations. *Cancer Res* 2006; **66**: 95-106 [PMID: 16397221 DOI: 10.1158/0008-5472.CAN-05-2168]

29 **Hidalgo M**, Amant F, Biankin AV, Budinská E, Byrne AT, Caldas C, Clarke RB, de Jong S, Jonkers J, Mælandsmo GM, Roman-Roman S, Seoane J, Trusolino L, Villanueva A. Patient-derived xenograft models: an emerging platform for translational cancer research. *Cancer Discov* 2014; **4**: 998-1013 [PMID: 25185190 DOI: 10.1158/2159-8290.CD-14-0001]

30 **Jain RK**, Stylianopoulos T. Delivering nanomedicine to solid tumors. *Nat Rev Clin Oncol* 2010; **7**: 653-664 [PMID: 20838415 DOI: 10.1038/nrclinonc.2010.139]
31 **Ernsting MJ**, Hoang B, Lohse I, Undzys E, Cao P, Do T, Gill B, Pintilie M, Hedley D, Li SD. Targeting of metastasis-promoting tumor-associated fibroblasts and modulation of pancreatic tumor-associated stroma with a carboxymethylcellulose-docetaxel nanoparticle. *J Control Release* 2015; **206**: 122-130 [PMID: 25804872 DOI: 10.1016/j.jconrel.2015.03.023]
32 **Xu Q**, Wang Z, Chen X, Duan W, Lei J, Zong L, Li X, Sheng L, Ma J, Han L, Li W, Zhang L, Guo K, Ma Z, Wu Z, Wu E, Ma Q. Stromal-derived factor-1α/CXCL12-CXCR4 chemotactic pathway promotes perineural invasion in pancreatic cancer. *Oncotarget* 2015; **6**: 4717-4732 [PMID: 25605248 DOI: 10.18632/oncotarget.3069]
33 **Li JA**, Xu XF, Han X, Fang Y, Shi CY, Jin DY, Lou WH. Nab-Paclitaxel Plus S-1 Shows Increased Antitumor Activity in Patient-Derived Pancreatic Cancer Xenograft Mouse Models. *Pancreas* 2016; **45**: 425-433 [PMID: 26495780 DOI: 10.1097/MPA.0000000000000501]
34 **Saito K**, Matsuo Y, Imafuji H, Okubo T, Maeda Y, Sato T, Shamoto T, Tsuboi K, Morimoto M, Takahashi H, Ishiguro H, Takiguchi S. Xanthohumol inhibits angiogenesis by suppressing nuclear factor-κB activation in pancreatic cancer. *Cancer Sci* 2018; **109**: 132-140 [PMID: 29121426 DOI: 10.1111/cas.13441]
35 **Baxter LT**, Jain RK. Transport of fluid and macromolecules in tumors. II. Role of heterogeneous perfusion and lymphatics. *Microvasc Res* 1990; **40**: 246-263 [PMID: 2250603]
36 **Baish JW**, Gazit Y, Berk DA, Nozue M, Baxter LT, Jain RK. Role of tumor vascular architecture in nutrient and drug delivery: an invasion percolation-based network model. *Microvasc Res* 1996; **51**: 327-346 [PMID: 8992232 DOI: 10.1006/mvre.1996.0031]
37 **Beyer K**, Partecke LI, Roetz F, Fluhr H, Weiss FU, Heidecke CD, von Bernstorff W. LPS promotes resistance to TRAIL-induced apoptosis in pancreatic cancer. *Infect Agent Cancer* 2017; **12**: 30 [PMID: 28572836 DOI: 10.1186/s13027-017-0139-4]

**P- Reviewer**: Sukocheva OA **S- Editor**: Wang JL **L- Editor**: A
**E- Editor**: Huang Y

World Journal of Gastroenterology

Submit a Manuscript: http://www.f6publishing.com

*World J Gastroenterol* 2018 February 21; 24(7): 810-818

DOI: 10.3748/wjg.v24.i7.810

ISSN 1007-9327 (print) ISSN 2219-2840 (online)

ORIGINAL ARTICLE

Basic Study

# Cryopreservation for delayed circulating tumor cell isolation is a valid strategy for prognostic association of circulating tumor cells in gastroesophageal cancer

Daniel Brungs, David Lynch, Alison WS Luk, Elahe Minaei, Marie Ranson, Morteza Aghmesheh, Kara L Vine, Martin Carolan, Mouhannad Jaber, Paul de Souza, Therese M Becker

Daniel Brungs, Elahe Minaei, Marie Ranson, Morteza Aghmesheh, Kara L Vine, Martin Carolan, Illawarra Health and Medical Research Institute, University of Wollongong, Wollongong 2500, Australia

Daniel Brungs, Elahe Minaei, Marie Ranson, Kara L Vine, School of Biological Sciences, University of Wollongong, Wollongong 2500, Australia

Daniel Brungs, Morteza Aghmesheh, Martin Carolan, Mouhannad Jaber, Illawarra Cancer Centre, Wollongong Hospital, Wollongong 2500, Australia

Daniel Brungs, David Lynch, Alison WS Luk, Elahe Minaei, Marie Ranson, Morteza Aghmesheh, Kara L Vine, Martin Carolan, Mouhannad Jaber, Paul de Souza, Therese M Becker, CONCERT-Translational Cancer Research Centre, New South Wales 2000, Australia

David Lynch, Paul de Souza, Therese M Becker, Centre for Circulating Tumor Cell Diagnostics and Research, Ingham Institute for Applied Medical Research, Liverpool Hospital, Sydney 2170, Australia

Paul de Souza, Therese M Becker, School of Medicine, University of Western Sydney, Sydney 2170, Australia

Paul de Souza, Therese M Becker, South Western Medical School, University of New South Wales, Sydney 2170, Australia

ORCID number: Daniel Brungs (0000-0002-8154-6966); David Lynch (0000-0002-9589-4478); Alison WS Luk (0000-0003-1221-7023); Elahe Minaei (0000-0002-8674-6801); Marie Ranson (0000-0002-5570-9645); Morteza Aghmesheh (0000-0003-1664-4743); Kara L Vine (0000-0001-6871-1149); Martin Carolan (0000-0001-6671-029X); Mouhannad Jaber (0000-0001-6991-9507); Paul de Souza (0000-0002-7380-1170); Therese M Becker (0000-0002-5636-9902).

Institutional review board statement: This study was approved by South Western Sydney Local Health District Human Research Ethics Committee (Project Number 15/072). A written informed consent was obtained from each participant before sample collection.

Conflict-of-interest statement: All authors have no conflicts of interest to declare.

Data sharing statement: No additional data are available.



Manuscript source: Unsolicited manuscript

Correspondence to: Daniel Brungs, BSc, MBBS, Doctor, Illawarra Cancer Care Centre, Wollongong Hospital, 348 Crown St, Wollongong NSW 2500, Australia. daniel.brungs@health.nsw.gov.au
Telephone: +61-2-42225200
Fax: +61-2-42225243

Received: November 6, 2017
Peer-review started: November 7, 2017
First decision: November 30, 2017
Revised: December 11, 2017
Accepted: December 19, 2017
Article in press: December 19, 2017
Published online: February 21, 2018

## Abstract

***AIM***

To demonstrate the feasibility of cryopreservation of peripheral blood mononuclear cells (PBMCs) for prognostic circulating tumor cell (CTC) detection in gastroesophageal cancer.

***METHODS***

Using 7.5 mL blood samples collected in EDTA tubes from patients with gastroesopheagal adenocarcinoma, CTCs were isolated by epithelial cell adhesion molecule based immunomagnetic capture using the IsoFlux platform. Paired specimens taken during the same blood draw ($n$ = 15) were used to compare number of CTCs isolated from fresh and cryopreserved PBMCs. Blood samples were processed within 24 h to recover the PBMC fraction, with PBMCs used for fresh analysis immediately processed for CTC isolation. Cryopreservation of PBMCs lasted from 2 wk to 25.2 mo (median 14.6 mo). CTCs isolated from pre-treatment cryopreserved PBMCs ($n$ = 43) were examined for associations with clinicopathological variables and survival outcomes.

***RESULTS***

While there was a significant trend to a decrease in CTC numbers associated with cryopreserved specimens (mean number of CTCs 34.4 *vs* 51.5, $P$ = 0.04), this was predominately in samples with a total CTC count of > 50, with low CTC count samples less affected ($P$ = 0.06). There was no significant association between the duration of cryopreservation and number of CTCs. In cryopreserved PBMCs from patient samples prior to treatment, a high CTC count (> 17) was associated with poorer overall survival (OS) ($n$ = 43, HR = 4.4, 95%CI: 1.7-11.7, $P$ = 0.0013). In multivariate analysis, after controlling for sex, age, stage, ECOG performance status, and primary tumor location, a high CTC count remained significantly associated with a poorer OS (HR = 3.7, 95%CI: 1.2-12.4, $P$ = 0.03).

***CONCLUSION***

PBMC cryopreservation for delayed CTC isolation is a valid strategy to assist with sample collection, transporting and processing.


**Key words:** Cryopreservation; Circulating tumor cells; Liquid biopsy; Gastroesophageal cancer; Gastric cancer



**Core tip:** This study demonstrates a novel and robust protocol for the cryopreservation and thawing of patient blood samples, demonstrating reliable circulating tumor cell isolation and characterisation after the long term storage of patient samples. Using the largest patient cohort reported to date, we validated our method by confirming the independent prognostic association of circulating tumor cell (CTC) enumeration from cryopreserved peripheral blood mononuclear cells. Cryopreservation may assist with the wider incorporation of CTC collection and analysis in biobanking, retrospective studies, and large international clinical trials, by facilitating specimen storage, bulk transporting, and batch processing.

Brungs D, Lynch D, Luk AW, Minaei E, Ranson M, Aghmesheh M, Vine KL, Carolan M, Jaber M, de Souza P, Becker TM. Cryopreservation for delayed circulating tumor cell isolation is a valid strategy for prognostic association of circulating tumor cells in gastroesophageal cancer. *World J Gastroenterol* 2018; 24(7): 810-818 Available from: URL: http://www.wjgnet.com/1007-9327/full/v24/i7/810.htm DOI: http://dx.doi.org/10.3748/wjg.v24.i7.810

## INTRODUCTION

Circulating tumor cell (CTC) analysis continues to be a rapidly developing field in oncology, offering a promising tool to both prognosticate and guide managements for patients[1]. Despite recent advancements in the field, one persisting challenge to the widespread adoption of CTC analysis for translational clinical trials or routine clinical care is the limited time frame considered best for blood processing and CTC isolation. Usually fresh blood is processed for CTCs within 24 h after blood draw, requiring prompt transfer to specialised centres for CTC isolation and analysis, which offers significant logistical challenges[2]. To overcome this issue, some studies use blood collection tubes that contain fixatives. Fixation of blood samples can allow CTC processing delayed by several days which has proven very useful for some CTC analyses[3,4]. However, fixatives may interfere with down-stream molecular analyses that require isolation of nucleic acids[5]. An alternative is the use of cryopreservation protocols for peripheral blood mononuclear cells (PBMCs) to allow delayed CTC isolation from these cells followed by CTC analysis. Cryopreservation should overcome fixation related analysis limitations and allow far more flexible time frames for batched CTC processing. However, a defined, robust cryopreservation protocol that is proven to enable analysis of the same or at least a relevant proportion of CTCs to that found in fresh samples, needs to be adopted and confirmation is needed whether cryopreserved CTCs can still predict disease outcome.

The advantage of cryopreservation of PBMCs is that it requires only minimal local processing, possible in most diagnostic settings, as well as feasible cryostorage and frozen transport of PBMC samples.

While there are a large number of approaches used to isolate and identify circulating tumor cells (recently

reviewed by van der Toom *et al*[6]), the best established and most widely used is the CellSearch™ system (Menarini-Silicon Biosystems), which uses positive immunomagnetic isolation of epithelial cell adhesion molecule (EpCAM, an epithelial cell marker) expressing cells followed by cytokeratin (CK), CD45, and DAPI staining[2]. The CTCs are then identified with automated immunofluorescence microscopy, defined by an EpCAM/CK/DAPI positive and CD45 negative phenotype. Cell Search CTC counts have shown to be prognostic in large patient series in a variety of cancers[7-9], including gastroesophageal cancer[10-12], but the instrument offers limited sensitivity in resectable gastroesophageal cancer, with CTCs detected in less than 15% of patients[10,13]. The IsoFlux system (Fluxion) uses a similar definition of CTCs to CellSearch (EpCAM/CK/DAPI positive, CD45 negative phenotype), but has shown a greater sensitivity for CTC detection[14-16]. This platform uses EpCAM targeted immunomagnetic isolation of CTCs within a microfluidic setting, improving isolation of CTCs with lower EpCAM expression, minimising leukocyte contamination, and allowing downstream applications including staining, enumeration, or sequencing, as shown for fresh blood samples[16].

Here, we use a viable method of PBMC cryopreservation that allows subsequent isolation and immunocytochemical analysis of CTCs. We demonstrate the feasibility of PBMC cryopreservation for delayed CTC isolation using paired cryopreserved and freshly processed blood samples drawn at the same time from patients with gastroesophageal adenocarcinoma. Importantly, we also provide data confirming that cryopreserved CTCs remain clinically applicable as a circulating prognostic marker for overall survival (OS).

## MATERIALS AND METHODS

### *Patient population*

Blood samples were collected from patients with histologically confirmed distal oesophageal, gastroesophageal junction, or gastric adenocarcinomas treated at Wollongong Hospital, Australia. Blood samples were collected in 7.5 mL EDTA Vacutainer tubes (Sarstedt AG & Co.) and maintained at room temperature until processing.

In the initial cohort (Cohort 1) to confirm the feasibility of cryopreservation, 15 patients with gastroesophageal carcinomas had 2 specimens taken during the one blood draw, one processed within 24 h ("fresh" specimen), and one cryopreserved with delayed CTC isolation and analysis ("cryopreserved" specimen). Pretreatment blood samples were cryopreserved from a second, larger cohort of patients for correlation with clinical outcomes (Cohort 2). The study was approved by South Western Sydney Local Health District Human Research Ethics Committee (Project Number 15/072). A written informed consent was obtained from each participant before sample collection.

### *Sample preparation*

Blood samples were processed within 24 h to recover the PBMC fraction using 50 mL SepMate tubes and Lymphoprep according to manufacturer's instructions (Stemcell Technologies, Vancouver, BC, Canada).

PBMCs used for fresh analysis were resuspended in Isoflux Binding Buffer and immediately processed for CTC isolation (see below).

PBMCs for cryopreservation were well resuspended in 1 mL of diluted plasma (the supernatant of the PBMC preparation from the matching patient) with the addition of 7.5% final DMSO, and stored at -80 ℃ until further processing. Cryopreserved samples were thawed according to the protocol from Fluxion Biosciences, San Francisco, California, United States[17]. In brief, warmed (37 ℃) thawing buffer, consisting of RPMI 1640 with 10% Fetal Bovine Serum (FBS, Bovogen Biologicals, Australia) and 50 Unit/mL Benzonase (Sigma-Aldrich, Germany), was added to thawed samples, washed once in thawing buffer, and resuspended in IsoFlux Binding Buffer with 5% FBS.

### *Circulating tumor cell isolation, staining, and imaging*

As per the Fluxion protocol, immunomagnetic beads preconjugated with anti-EpCAM antibodies (CTC Enrichment Kit; Fluxion Biosciences Inc) were added to PBMCs suspended in IsoFlux Binding Buffer, and incubated for 90 min at 4 ℃ with passive mixing on a rotator. Samples were then loaded into the sample well of the microfluidic cartridge and underwent immunomagnetic isolation of CTCs with the IsoFlux using the standard protocol (Fluxion Biosciences Inc).

Recovered CTCs were blocked with a final concentration of 1.2 μg/μL mouse IgG in binding buffer (Jackson ImmunoResearch, Baltimore, PA, United States) for 30 min, washed and fixed in fixing solution (Fluxion Biosciences Inc). The CTCs were then blocked in 10% FBS in binding buffer for 15 min, then underwent immunofluorence staining for anti-CD45 antibody conjugated to Alexa Fluor 647 (Biolegend, Clone HI30). The CTCs were also stained for urokinase plasminogen activator receptor (uPAR, CD87), a key receptor in the plasminogen activator system and clinically relevant biomarker in primary gastroesophageal cancer[18], using anti-uPAR antibody conjugated to AF594 (ThermoFischer, Clone R4). After permeabilization with 0.1% Triton X-100, cells were probed with anti-cytokeratin antibody conjugated to FITC (Sigma-Aldrich, Clone PCK-26). CTCs were finally stained with Hoechst and mounted using Isoflux mounting media to 24-well glass bottom plates (MoBioTec, Goettingen, Germany) for imaging.

Imaging was performed with an inverted epifluorescence microscope (Leica DMi8, Leica Microsystems Pty Ltd) using the Leica Application Suite. Cells were considered CTCs if they were CK positive, CD45

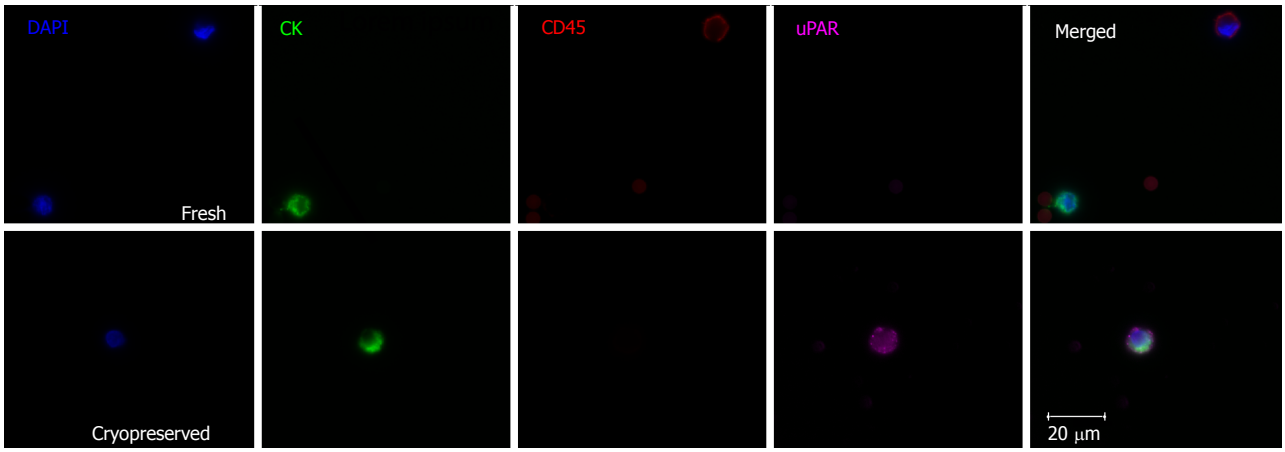


**Figure 1 Representative images of circulating tumor cell isolation from fresh and cryopreserved samples demonstrating preservation of leukocyte and circulating tumor cell morphology.** The fresh sample demonstrates a nucleated CK+/CD45- CTC which is uPAR negative, as well as a CK-/CD45+ leukocyte. The cryopreserved sample shows a uPAR positive CTC. CTC: Circulating tumor cell.

negative, nucleated and morphologically intact. The proportion of uPAR positive CTCs was recorded.

### *Statistical analysis*

The CTC recovery from matched cryopreserved and fresh samples were compared with the paired *t*-test. Correlation between cryopreservation time and CTC number was described with a Pearson correlation coefficient, and the Fisher exact test and *t*-test were used to compare the status of CTCs with categorical clinicopathologic factors.

For survival analyses, in the absence of established cut-offs for prognostic CTC numbers, the median CTC count (17) was used as the discriminator between high and low CTC counts. Survival analyses are conducted using Kaplan-Meier methods, with median survival reported. Unadjusted and multivariable Cox proportional hazards regression analyses were used to estimate the association between CTC counts and survival, and to calculate corresponding hazard ratios (HRs) and 95% confidence intervals (CIs). The following variables were included in the multivariate model: age, sex, ECOG, TNM stage, primary tumor location, and CTC count. All statistical analyses were performed using SAS 9.2 software (SAS Institute, Inc., Cary, NC, United States).

## RESULTS

### *Matched fresh and cryopreserved specimens (cohort 1)*

Matching parallel blood samples, collected from 15 gastroesophageal cancer patients (10 patients had blood taken prior to treatment, 5 patients were already on treatment), that had either been cryopreserved before CTC processing or were processed fresh, were compared. Cryopreservation of PBMCs lasted from 2 wk to 25.2 mo (median 14.6 mo). There was no significant correlation between cryopreservation time and CTC number (Pearson r -0.25, $P$ = 0.09). CTCs isolated from cryopreserved samples appeared morphologically similar to fresh samples (Figure 1). There was a significant difference between CTC numbers isolated from the cryopreserved samples compared to fresh samples (mean number of CTCs 34.4 cryopreserved *vs* 51.5 fresh, $P$ = 0.04, Figure 2), however this difference was predominately attributable to a larger fall in CTC numbers in samples with very high CTC counts (> 50 CTCs in the fresh specimen). There was no significant difference in CTC count between cryopreserved and fresh samples for specimens with CTC count less than 50 ($n$ = 11 patients, mean number of CTCs 10.7 *vs* 16.3, $P$ = 0.06). Thus CTC loss by cryopreservation in patient samples with low CTC counts appears relatively minor (mean proportion of CTCs lost in cryopreserved samples = 23.95%).

### *Cryopreserved circulating tumor cell and clinical outcomes (cohort 2)*

A larger cohort of 43 gastroesophageal cancer patients (cohort 2) was analyzed to validate whether detectable CTC counts post cryopreservation correlated to disease outcomes. All patient samples were taken prior to treatment commencement and had undergone cryopreservation before CTC isolation. Cohort 2 included the 10 treatment naive patients from cohort 1. Patient characteristics of cohort 2 are summarised in Table 1. Twenty-four patients had resectable disease (Stage Ⅱ or Ⅲ). Post CTC evaluation, 11 of these patients received neoadjuvant chemoradiotherapy prior to resection (CROSS regimen), 3 received perioperative chemotherapy (MAGIC regimen), and 10 had surgery alone. Nineteen patients had metastatic disease (stage Ⅳ). Most of these patients received chemotherapy (7 patients: platinum and capecitabine doublet, 3 patients: anthracycline, capecitabine, and platinum triplet, 1 patient: irinotecan or paclitaxel monotherapy), immunotherapy (2 patients), and 6 patients received no active systemic treatments.

CTCs were detected in 42/43 patients (95.5%),

**Table 1 Characteristics of patients in cohort 2 *n* (%)**

| | All patients *n* = 43 | CTC count | |
|---|---|---|---|
| | | Low (CTC ⩽ 17) *n* = 23 | High (CTC > 17) *n* = 20 |
| Age | | | |
| Mean (range) | 64 (39-89) | 65 (39-89) | 64 (48-83) |
| Sex | | | |
| Male | 32 (74.4) | 15 (65.2) | 20 (85.0) |
| Female | 11 (25.6) | 8 (34.8) | 3 (15.0) |
| ECOG | | | |
| 0-1 | 36 (83.7) | 22 (95.6) | 14 (70.0) |
| 2-4 | 7 (16.3) | 1 (4.3) | 6 (30.0) |
| Primary tumor location | | | |
| Distal oesophageal | 12 (27.9) | 8 (34.8) | 4 (20.0) |
| Gastroesophageal junction | 14 (32.6) | 4 (17.4) | 10 (50.0) |
| Gastric | 17 (37.5) | 11 (47.8) | 6 (30.0) |
| Stage | | | |
| Ⅱ | 18 (41.9) | 13 (56.5) | 5 (25.0) |
| Ⅲ | 6 (14.0) | 4 (17.4) | 2 (10.0) |
| Ⅳ | 19 (44.2) | 6 (26.1) | 13 (65.0) |

CTC: Circulating tumor cell; ECOG: Eastern cooperative oncology group performance status.

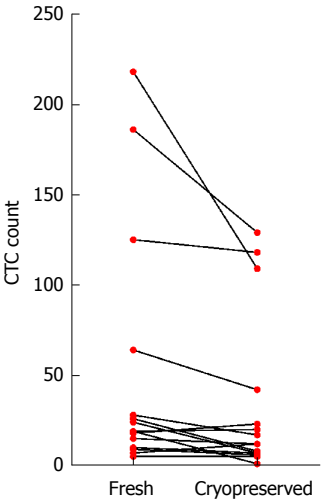


**Figure 2 Circulating tumor cell enumeration by processing method.** Mean number of CTCs isolated in the fresh specimens were higher than in the matched cryopreserved sample (mean difference in CTCs 17.1 95%CI: 0.7-33.6, *P* = 0.043). This difference was mostly driven by larger falls in CTC counts in samples with high numbers of CTCs (> 50 CTCs in fresh samples), with no significant difference in CTC counts for samples with less than 50 CTC in the fresh specimen (*P* = 0.06).

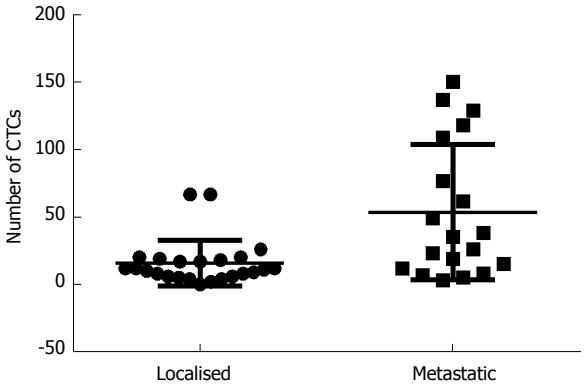


**Figure 3 Circulating tumor cell count by stage.** CTC processing post cryopreservation produced a higher mean CTC count in metastatic patients compared to the resectable patients (mean CTC in metastatic 53.8 *vs* resectable 15.8, *P* = 0.0013). CTC: Circulating tumor cell.

with a median CTC of 17 (interquartile range 8-38). Patients with metastatic disease had a higher number of CTCs than those with resectable disease (Figure 3, mean CTC count 53.8 *vs* 15.8, *P* = 0.0013).

Currently there are no established cut-offs for prognostic CTC numbers detected using the IsoFlux in gastroesophageal adenocarcinoma. Therefore we opted to divide our patients by their CTC counts, above versus equal or lower than the median CTC count, to test for any correlation with clinical outcomes. Patients with a high CTC count (> 17) had a poorer OS than those with a lower CTC count (⩽ 17) (Figure 4, median OS 2.8 mo *vs* 23.2 mo, HR = 4.4, 95%CI: 1.7-11.7, *P* = 0.0013). In multivariate analysis, after controlling for sex, age, stage, ECOG performance status, and primary tumor location, a high CTC count remained an independent prognostic factor associated with poor OS (Table 2, HR = 3.7, 95%CI: 1.2-12.4, *P* = 0.03). This association was stronger when the analysis was restricted to patients with metastatic disease (*n* = 19, HR = 5.5, 95%CI: 1.2-25.5, *P* = 0.01), but not observed in patients with resectable disease (*n* = 24, *P* = 0.39), although a high CTC count (> 17) was associated with a non-significant trend to shorter recurrence free survival in these patients (HR = 3.1, 95%CI: 0.8-12.6, *P* = 0.09).

Most patients had some uPAR positive CTCs (40/43, 93.0%), however the proportion of uPAR positive CTCs was similar between patients with localised and metastatic disease (mean proportion uPAR positive CTCs 48.8% *vs* 47.7% respectively, *P* = 0.89), and there was no association with survival outcomes (Supplementary

**Table 2 Univariate and multivariate analysis for overall survival for cohort 2 (*n* = 43)**

| Factor | Univariate | | Multivariate | |
|---|---|---|---|---|
| | HR (95%CI) | *P* value | HR (95%CI) | *P* value |
| CTC count (high *vs* low) | 4.4 (1.7-11.7) | 0.001 | 3.7 (1.2-12.4) | 0.03 |
| Age (≥ 65 *vs* <65 yr old) | 0.7 (0.3-1.8) | 0.46 | 1.0 (0.9-1.1) | 0.76 |
| ECOG (2-4 *vs* 0-1) | 7.2 (2.2-23.7) | 0.0002 | 2.3 (0.5-10.1) | 0.14 |
| Sex (male *vs* female) | 1.2 (0.4-3.8) | 0.7 | 0.7 (0.2-2.1) | 0.49 |
| Stage (Ⅳ *vs* Ⅱ-Ⅲ) | 10.0 (3.3-30.8) | < 0.0001 | 9.9 (2.9-33.8) | 0.0003 |
| Primary tumor location (gastric *vs* oesophageal/GOJ) | 0.3 (0.1-1.01) | 0.05 | 0.4 (0.2-1.6) | 0.22 |

Significant values are italicised. In both univariate and multivariate analysis, a high CTC count (> 17) remained statistically significant as an independent factor associated with poorer overall survival. CTC: Circulating tumor cell; ECOG: Eastern cooperative oncology group performance status; GOJ: Gastroesophageal junction.

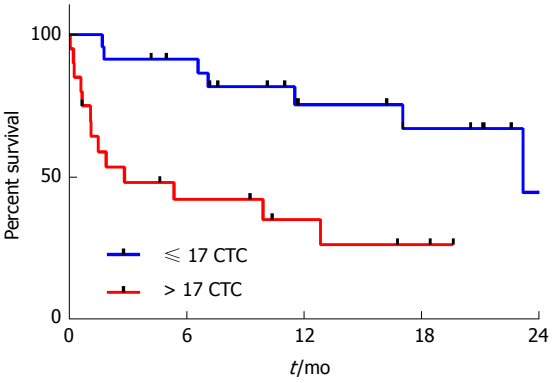


**Figure 4 Overall survival by circulating tumor cell count.** Patients with > 17 CTCs isolated from cryopreserved specimens had a poorer overall survival compared to those with ≤ 17 CTCs (median OS 2.8 mo *vs* 23.2 mo, HR = 4.4, 95%CI: 1.7-11.7, *P* = 0.0013). OS: Overall survival; CTC: Circulating tumor cell.

Figure 1, median OS 17.0 mo *vs* 12.8 mo, *P* = 0.6).

## DISCUSSION

In this study we report the reliable isolation, immunocytochemical identification, and enumeration of gastroesophageal cancer CTCs from cryopreserved PBMCs using the IsoFlux platform. The included cohort is the largest reported study analysing cryopreservation of patient PBMCs for CTC detection. Our data confirms that CTCs isolated from cryopreserved samples remain an independent prognostic factor associated with OS.

The timely processing of patient samples for CTC isolation, usually is recommended within 24 h for most isolation methods[19], presenting significant logistical challenges for researchers and prohibits inclusion of patients from remote areas into clinical trials that would rely on CTCs as outcome measures. This is mainly because current methods of CTC analysis require significant expertise, instrumentation, time and laboratory resources, usually performed in specialised research centres. Protocols using isolation of CTCs from cryopreserved specimens would require some basic processing and cryopreservation at the site of blood draw, but offer many advantages, including the ability to biobank patient samples for prolonged periods of time before central processing. This would be a huge benefit for larger scale clinical trials as it would allow inclusion of geographically separated sites.

Previous work has shown that the immunochemical properties of CK, EpCAM and CD45, central to the isolation and identification of CTCs, are not affected by cryopreservation and thawing[20,21]. In agreement, our results demonstrate a similar morphological and immunofluorescent profile between cryopreserved and fresh CTCs and leukocytes, suggesting current techniques are suitable for cryopreserved samples. This approach is further supported by other work showing close concordance in genetic alterations seen on paired fresh and frozen CTCs[21].

Our results also show that enumeration of CTCs isolated from cryopreserved PMBCs is a valid prognostic biomarker in gastroesophageal cancer. Patients with metastatic disease had a significantly higher number of CTCs than those with resectable disease (mean CTC count 53.8 *vs* 15.8, *P* = 0.0013). Moreover, patients with a high CTC count (> 17) had a much poorer OS than those with a lower CTC count (≤ 17) (HR = 4.4, *P* = 0.0013). High CTC count remained significant in the multivariate analysis as an independent predictor of poorer OS (HR = 3.7, *P* = 0.03), after controlling for age, ECOG, sex, stage and primary tumour location, particularly when analysis was restricted to patients with metastatic disease only (HR = 5.5, *P* = 0.01). These results are concordant with other studies which confirm CTC enumeration as an important prognostic factor in gastroesophageal cancer[10-12].

Given our previous findings that the uPA system is a clinically relevant biomarker in primary gastroesophageal cancer[18], we undertook and successfully probed for uPAR expression in CTCs derived from cryopreserved and fresh samples. We previously have shown that higher expression of uPA, uPAR and PAI-1 in the primary tumour is associated with higher risk disease and poorer prognosis. However, in this study, there was no correlation between CTC uPAR expression with disease parameters. This suggests that the selection of epithelial (EpCAM-positive) CTCs might have affected any correlation of uPAR with patient outcome, as CTCs that present mesenchymal phenotypes, such as

uPAR expressing cells, can escape standard methods of isolation reliant on epithelial markers[22]. Indeed Vishnoi *et al*[23]. has previously reported the isolation of subsets of EpCAM-negative, uPAR and integrin β1 positive breast cancer CTCs, which further supports the concept of CTC heterogeneity[23]. Ultimately, we have successfully stained for a novel biomarker, uPAR, which further supports our cryopreservation method as a valid CTC isolation approach.

One important concern with cryopreservation is the potential for loss of CTCs due to cell loss during freezing, storage, or thawing. In a study by Nejlund *et al*[20], tumor cell recovery from cryopreserved spiked tumor cells in normal controls was variable, with up to a 40% tumor cell loss. However in clinical samples using matched fresh and cryopreserved specimens from the same patient, there was no consistent loss of CTCs, with the variation in CTC enumeration similar to those seen in paired fresh samples in other studies[2,20]. Friedlander *et al*[21] found that cryopreservation of PBMCs had no significant effect on the cell recovery from patients with metastatic prostate cancer. We noted a small loss of CTCs associated with cryopreservation, however this was predominately in samples with large numbers of CTCs (> 50), where loss of some CTCs is more acceptable than samples with low CTC counts. We noted samples with high numbers of CTCs were more prone to cell clumping despite benzonase. This is normally due to the release of viscous DNA from cell lysis on thawing, leading to aggregates which prevent accurate CTC counting. We speculate that the higher disease burden in these patients, coupled with a corresponding systemic inflammatory response, lead to poorer cell integrity within the PBMCs of high CTC-count samples. Some loss of CTCs in these samples will have little impact for prognostic and down-stream biomarker analysis purposes. There was no significant loss of CTCs in samples were the total CTC count was $\leqslant$ 50 ($P$ = 0.06).

Similar to previously published work, we found that the duration of cryopreservation was not correlated with number of isolated CTCs[20]. Moreover, we were able to isolate CTCs from specimens stored at -80 ℃ for over two years, suggesting cryopreservation is a suitable approach for long term projects that involve biobanking of patient samples.

Even when using cryopreservation prior to CTC isolation, we found higher numbers of CTCs (median CTC count 17) and a higher number of patient samples with CTCs (98%) compared to other studies using EpCAM based CTC capture in gastroesophageal cancer[10-12,24]. The correlation of CTC numbers with disease progression implies that the CTCs we identified are indeed disease related. Increased CTC counts are consistent with the higher reported sensitivity of the IsoFlux system compared to other platforms, particularly in isolating CTCs with a lower expression of EpCAM[14-16]. Our results confirm, in the largest cohort of patients reported to date, that a high CTC count (> 17) in cryopreserved specimen was an independent prognostic factor associated with poorer OS (HR = 3.7). As expected from the minimal CTC loss during cryopreservation, these data indicate that indeed our method is suitable for delayed and centralised CTC analysis which could help recruiting patients for major clinical trials. In this setting it would be advantageous compared to fixation of blood which allows CTC processing delayed by only several days rather than long term biobanking. We are currently testing if cryopreservation is also able to overcome limitations associated with using fixative for molecular down-stream analysis of CTCs that involves nucleic acid extraction[4,5].

In conclusion, we have tested a robust PBMC cryopreservation protocol that allows successful CTC isolation even 2 years post freezing. Cryopreservation of CTCs is feasible, with a small loss of tumor cells predominantly in samples with a high CTC load. Enumeration of CTCs from cryopreserved samples remained a clinically important prognostic biomarker. Cryopreservation may assist with the wider incorporation of CTC collection and analysis in biobanking, retrospective studies, and large international clinical trials, by facilitating specimen storage, bulk transporting, and batch processing. It may also help to develop diagnostic settings that can service even remote patients with diagnostic CTC data potentially relevant for their disease management.

## ARTICLE HIGHLIGHTS

### *Research background*

A persisting challenge to the field of circulating tumor cell (CTC) research is the requirement for prompt analysis of samples at specialised centres. This has presented significant logistical challenges to researchers, compounded by the significant expertise, time and laboratory resources required for CTC analysis.

### *Research motivation*

Current methods to overcome this issue, such as fixation of blood samples, extend the time for CTC processing for several days, but may interfere with downstream molecular analyses.

Cryopreservation of patient samples permits the wider incorporation of CTC collection and analysis in biobanking, retrospective studies, and large international clinical trials, by facilitating specimen storage, bulk transporting, and batch processing. However, up to now, there has been little research in how cryopreservation affects CTC recovery, and whether cryopreservation retains predictive value of CTCs.

### *Research objectives*

The primary objective of our study was to investigate the feasibility and reliability of delayed CTC isolation from cryopreserved peripheral blood mononuclear cells (PBMCs) layer. This was determined by percentage of CTC loss during cryopreservation and thawing, and clinical validity of CTC enumeration from cryopreserved samples.

### *Research methods*

CTCs were isolated from 7.5 mL blood samples collected from patients with gastroesophageal adenocarcinoma using EpCAM based immunomagnetic capture with the IsoFlux platform. CTC loss with cryopreservation was determined by comparing CTC enumeration from matched cryopreserved

and freshly processed blood samples collected during the same blood draw. CTCs isolated from pre-treatment cryopreserved PBMCs were examined for association with clinicopathological variables and survival outcomes.

### Research results

We found a minor loss of tumor cells in matched cryopreserved and freshly processed samples, mostly in samples with high CTC counts. A high CTC count isolated from cryopreserved PBMCs remained a statistically significant independent prognostic factor in gastroesophageal cancer.

### Research conclusions

Our study demonstrates a feasible and robust protocol facilitating CTC isolation from cryopreserved PBMCs even after 2 years post freezing. Our results have immediate applicability in the design and conduct of translational studies, as it facilitates incorporation of CTC analysis in large international trials and biobanking projects.

### Research perspectives

There is an increasing variety of techniques used for CTC isolation described in the literature. While the current work confirms the reliability of CTC isolation from cryopreserved samples using immunomagnetic separation, further work needs to be undertaken to confirm its suitability for other isolation approaches.

## REFERENCES


1 **Alix-Panabières C**, Pantel K. Challenges in circulating tumour cell research. *Nat Rev Cancer* 2014; **14**: 623-631 [PMID: 25154812 DOI: 10.1038/nrc3820]

2 **Allard WJ**, Matera J, Miller MC, Repollet M, Connelly MC, Rao C, Tibbe AG, Uhr JW, Terstappen LW. Tumor cells circulate in the peripheral blood of all major carcinomas but not in healthy subjects or patients with nonmalignant diseases. *Clin Cancer Res* 2004; **10**: 6897-6904 [PMID: 15501967 DOI: 10.1158/1078-0432.ccr-04-0378]

3 **Qin J**, Alt JR, Hunsley BA, Williams TL, Fernando MR. Stabilization of circulating tumor cells in blood using a collection device with a preservative reagent. *Cancer Cell Int* 2014; **14**: 23 [PMID: 24602297 DOI: 10.1186/1475-2867-14-23]

4 **Yee SS**, Lieberman DB, Blanchard T, Rader J, Zhao J, Troxel AB, DeSloover D, Fox AJ, Daber RD, Kakrecha B, Sukhadia S, Belka GK, DeMichele AM, Chodosh LA, Morrissette JJ, Carpenter EL. A novel approach for next-generation sequencing of circulating tumor cells. *Mol Genet Genomic Med* 2016; **4**: 395-406 [PMID: 27468416 DOI: 10.1002/mgg3.210]

5 **Luk AWS**, Ma Y, Ding PN, Young FP, Chua W, Balakrishnar B, Dransfield DT, Souza P, Becker TM. CTC-mRNA (AR-V7) Analysis from Blood Samples-Impact of Blood Collection Tube and Storage Time. *Int J Mol Sci* 2017; **18**: pii: E1047 [PMID: 28498319 DOI: 10.3390/ijms18051047]

6 **van der Toom EE**, Verdone JE, Gorin MA, Pienta KJ. Technical challenges in the isolation and analysis of circulating tumor cells. *Oncotarget* 2016; **7**: 62754-62766 [PMID: 27517159 DOI: 10.18632/oncotarget.11191]

7 **Bidard FC**, Peeters DJ, Fehm T, Nolé F, Gisbert-Criado R, Mavroudis D, Grisanti S, Generali D, Garcia-Saenz JA, Stebbing J, Caldas C, Gazzaniga P, Manso L, Zamarchi R, de Lascoiti AF, De Mattos-Arruda L, Ignatiadis M, Lebofsky R, van Laere SJ, Meier-Stiegen F, Sandri MT, Vidal-Martinez J, Politaki E, Consoli F, Bottini A, Diaz-Rubio E, Krell J, Dawson SJ, Raimondi C, Rutten A, Janni W, Munzone E, Carañana V, Agelaki S, Almici C, Dirix L, Solomayer EF, Zorzino L, Johannes H, Reis-Filho JS, Pantel K, Pierga JY, Michiels S. Clinical validity of circulating tumour cells in patients with metastatic breast cancer: a pooled analysis of individual patient data. *Lancet Oncol* 2014; **15**: 406-414 [PMID: 24636208 DOI: 10.1016/s1470-2045(14)70069-5]

8 **Lim SH**, Becker TM, Chua W, Caixeiro NJ, Ng WL, Kienzle N, Tognela A, Lumba S, Rasko JE, de Souza P, Spring KJ. Circulating tumour cells and circulating free nucleic acid as prognostic and predictive biomarkers in colorectal cancer. *Cancer Lett* 2014; **346**: 24-33 [PMID: 24368189 DOI: 10.1016/j.canlet.2013.12.019]

9 **Miyamoto DT**, Sequist LV, Lee RJ. Circulating tumour cells-monitoring treatment response in prostate cancer. *Nat Rev Clin Oncol* 2014; **11**: 401-412 [PMID: 24821215 DOI: 10.1038/nrclinonc.2014.82]

10 **Uenosono Y**, Arigami T, Kozono T, Yanagita S, Hagihara T, Haraguchi N, Matsushita D, Hirata M, Arima H, Funasako Y, Kijima Y, Nakajo A, Okumura H, Ishigami S, Hokita S, Ueno S, Natsugoe S. Clinical significance of circulating tumor cells in peripheral blood from patients with gastric cancer. *Cancer* 2013; **119**: 3984-3991 [PMID: 23963829 DOI: 10.1002/cncr.28309]

11 **Reeh M**, Effenberger KE, Koenig AM, Riethdorf S, Eichstädt D, Vettorazzi E, Uzunoglu FG, Vashist YK, Izbicki JR, Pantel K, Bockhorn M. Circulating Tumor Cells as a Biomarker for Preoperative Prognostic Staging in Patients With Esophageal Cancer. *Ann Surg* 2015; **261**: 1124-1130 [PMID: 25607767 DOI: 10.1097/sla.0000000000001130]

12 **Lee SJ**, Lee J, Kim ST, Park SH, Park JO, Park YS, Lim HY, Kang WK. Circulating tumor cells are predictive of poor response to chemotherapy in metastatic gastric cancer. *Int J Biol Markers* 2015; **30**: e382-e386 [PMID: 26044775 DOI: 10.5301/jbm.5000151]

13 **Hiraiwa K**, Takeuchi H, Hasegawa H, Saikawa Y, Suda K, Ando T, Kumagai K, Irino T, Yoshikawa T, Matsuda S, Kitajima M, Kitagawa Y. Clinical significance of circulating tumor cells in blood from patients with gastrointestinal cancers. *Ann Surg Oncol* 2008; **15**: 3092-3100 [PMID: 18766405 DOI: 10.1245/s10434-008-0122-9]

14 **Alva A**, Friedlander T, Clark M, Huebner T, Daignault S, Hussain M, Lee C, Hafez K, Hollenbeck B, Weizer A, Premasekharan G, Tran T, Fu C, Ionescu-Zanetti C, Schwartz M, Fan A, Paris P. Circulating Tumor Cells as Potential Biomarkers in Bladder Cancer. *J Urol* 2015; **194**: 790-798 [PMID: 25912492 DOI: 10.1016/j.juro.2015.02.2951]

15 **Sánchez-Lorencio MI**, Ramirez P, Saenz L, Martínez Sánchez MV, De La Orden V, Mediero-Valeros B, Veganzones-De-Castro S, Baroja-Mazo A, Revilla Nuin B, Gonzalez MR, Cascales-Campos PA, Noguera-Velasco JA, Minguela A, Díaz-Rubio E, Pons JA, Parrilla P. Comparison of Two Types of Liquid Biopsies in Patients With Hepatocellular Carcinoma Awaiting Orthotopic Liver Transplantation. *Transplant Proc* 2015; **47**: 2639-2642 [PMID: 26680058 DOI: 10.1016/j.transproceed.2015.10.003]

16 **Harb W**, Fan A, Tran T, Danila DC, Keys D, Schwartz M, Ionescu-Zanetti C. Mutational Analysis of Circulating Tumor Cells Using a Novel Microfluidic Collection Device and qPCR Assay. *Transl Oncol* 2013; **6**: 528-538 [PMID: 24151533 DOI: 10.1593/tlo.13367]

17 Cryopreservation of CTC samples for biobanking and sample storage. Available from: URL: https://liquidbiopsy.fluxionbio.com/application-notes

18 **Brungs D**, Chen J, Aghmesheh M, Vine KL, Becker TM, Carolan MG, Ranson M. The urokinase plasminogen activation system in gastroesophageal cancer: A systematic review and meta-analysis. *Oncotarget* 2017; **8**: 23099-23109 [PMID: 28416743 DOI: 10.18632/oncotarget.15485]

19 **Fehm T**, Solomayer EF, Meng S, Tucker T, Lane N, Wang J, Gebauer G. Methods for isolating circulating epithelial cells and criteria for their classification as carcinoma cells. *Cytotherapy* 2005; **7**: 171-185 [PMID: 16040397 DOI: 10.1080/14653240510027082]

20 **Nejlund S**, Smith J, Kraan J, Stender H, Van MN, Langkjer ST, Nielsen MT, Sölétormos G, Hillig T. Cryopreservation of Circulating Tumor Cells for Enumeration and Characterization. *Biopreserv Biobank* 2016; **14**: 330-337 [PMID: 27092845 DOI: 10.1089/bio.2015.0074]

21 **Friedlander TW**, Ngo VT, Dong H, Premasekharan G, Weinberg V, Doty S, Zhao Q, Gilbert EG, Ryan CJ, Chen WT, Paris PL. Detection and characterization of invasive circulating tumor cells derived from men with metastatic castration-resistant prostate cancer. *Int J Cancer* 2014; **134**: 2284-2293 [PMID: 24166007 DOI: 10.1002/ijc.28561]

22 **Königsberg R**, Obermayr E, Bises G, Pfeiler G, Gneist M, Wrba F, de Santis M, Zeillinger R, Hudec M, Dittrich C. Detection of EpCAM positive and negative circulating tumor cells in metastatic breast cancer patients. *Acta Oncol* 2011; **50**: 700-710 [PMID: 21261508 DOI: 10.3109/0284186x.2010.549151]

23 **Vishnoi M**, Peddibhotla S, Yin W, T Scamardo A, George GC, Hong DS, Marchetti D. The isolation and characterization of CTC subsets related to breast cancer dormancy. *Sci Rep* 2015; **5**: 17533 [PMID: 26631983 DOI: 10.1038/srep17533]

24 **Matsusaka S**, Chìn K, Ogura M, Suenaga M, Shinozaki E, Mishima Y, Terui Y, Mizunuma N, Hatake K. Circulating tumor cells as a surrogate marker for determining response to chemotherapy in patients with advanced gastric cancer. *Cancer Sci* 2010; **101**: 1067-1071 [PMID: 20219073 DOI: 10.1111/j.1349-7006.2010.01492.x]

**P- Reviewer**: Dumitrascu DL **S- Editor**: Chen K **L- Editor**: A
**E- Editor**: Huang Y

World Journal of Gastroenterology

Submit a Manuscript: http://www.f6publishing.com

*World J Gastroenterol* 2018 February 21; 24(7): 819-832

DOI: 10.3748/wjg.v24.i7.819

ISSN 1007-9327 (print) ISSN 2219-2840 (online)

ORIGINAL ARTICLE

Basic Study

# Metformin attenuates motility, contraction, and fibrogenic response of hepatic stellate cells *in vivo* and *in vitro* by activating AMP-activated protein kinase

Zhen Li, Qian Ding, Li-Ping Ling, Ying Wu, Dong-Xiao Meng, Xiao Li, Chun-Qing Zhang

Zhen Li, Qian Ding, Li-Ping Ling, Ying Wu, Dong-Xiao Meng, Xiao Li, Chun-Qing Zhang, Department of Gastroenterology, Shandong Provincial Hospital Affiliated to Shandong University, Jinan 250021, Shandong Province, China

Zhen Li, Li-Ping Ling, Ying Wu, Dong-Xiao Meng, Xiao Li, Shandong Provincial Engineering and Technological Research Center for Liver Disease Prevention and Control, Jinan 250021, Shandong Province, China

ORCID number: Zhen Li (0000-0003-1860-3048); Qian Ding (0000-0002-2301-8487); Li-Ping Ling (0000-0002-1738-830X); Ying Wu (0000-0002-7813-7862); Dong-Xiao Meng (0000-0003-4558-8760); Xiao Li (0000-0003-1992-3529); Chun-Qing Zhang (0000-0001-8711-1579).

Author contributions: Li Z, Ding Q, Ling LP, Wu Y and Meng DX performed the study; Li Z, Ding Q and Li X collected and analyzed the data and edited the manuscript; Li Z and Zhang CQ designed the study and wrote the manuscript.

Supported by National Natural Science Foundation of China, No. 81370590.

Institutional review board statement: The study was reviewed and approved by the Institutional Review Board of Shandong Provincial Hospital Affiliated to Shandong University.

Institutional animal care and use committee statement: The consent procedure and study protocol were approved by the Animal Medical Ethics Committee of Shandong Provincial Hospital Affiliated to Shandong University (No. 2017-228).

Conflict-of-interest statement: The authors declare no conflict of interest related to this manuscript.

Data sharing statement: No additional unpublished data are available.



Manuscript source: Unsolicited manuscript

Correspondence to: Chun-Qing Zhang, PhD, Chief Doctor, Department of Gastroenterology, Shandong Provincial Hospital Affiliated to Shandong University, 324 Jingwu Weiqi Road, Jinan 250021, Shandong Province, China. zhangchunqing_sdu@163.com
Telephone: +86-531-68773293
Fax: +86-531-87906348

Received: November 21, 2017
Peer-review started: November 21, 2017
First decision: December 6, 2017
Revised: December 12, 2017
Accepted: December 26, 2017
Article in press: December 26, 2017
Published online: February 21, 2018

## Abstract

### *AIM*

To investigate the effect of metformin on activated hepatic stellate cells (HSCs) and the possible signaling pathways involved.

### *METHODS*

A fibrotic mouse model was generated by intraperitoneal injection of carbon tetrachloride ($CCl_4$) and subsequent treatment with or without metformin. The level of fibrosis was detected by hematoxylin-eosin staining, Sirius Red staining, and immunohistochemistry. The HSC cell line LX-2 was used for *in vitro* studies. The effect of metformin on cell proliferation (CCK8 assay),

motility (scratch test and Transwell assay), contraction (collagen gel contraction assay), extracellular matrix (ECM) secretion (Western blot), and angiogenesis (ELISA and tube formation assay) was investigated. We also analyzed the possible signaling pathways involved by Western blot analysis.

***RESULTS***

Mice developed marked liver fibrosis after intraperitoneal injection with $CCl_4$ for 6 wk. Metformin decreased the activation of HSCs, reduced the deposition of ECM, and inhibited angiogenesis in $CCl_4$-treated mice. Platelet-derived growth factor (PDGF) promoted the fibrogenic response of HSCs *in vitro*, while metformin inhibited the activation, proliferation, migration, and contraction of HSCs, and reduced the secretion of ECM. Metformin decreased the expression of vascular endothelial growth factor (VEGF) in HSCs through inhibition of hypoxia inducible factor (HIF)-1$\alpha$ in both PDGF-BB treatment and hypoxic conditions, and it down-regulated VEGF secretion by HSCs and inhibited HSC-based angiogenesis in hypoxic conditions *in vitro*. The inhibitory effects of metformin on activated HSCs were mediated by inhibiting the Akt/mammalian target of rapamycin (mTOR) and extracellular signal-regulated kinase (ERK) pathways *via* the activation of adenosine monophosphate-activated protein kinase (AMPK).

***CONCLUSION***

Metformin attenuates the fibrogenic response of HSCs *in vivo* and *in vitro*, and may therefore be useful for the treatment of chronic liver diseases.

**Key words:** Hepatic stellate cell; Intrahepatic vascular resistance; Angiogenesis; Contraction; Liver fibrosis; Adenosine monophosphate-activated protein kinase



**Core tip:** Activation of hepatic stellate cells (HSCs) contributes to liver fibrosis and portal hypertension. In this study, we examined the effect of metformin on activated HSCs *in vivo* and *in vitro*. Metformin decreased the activation of HSCs, reduced the deposition of extracellular matrix (ECM), and inhibited angiogenesis in $CCl_4$-treated mice. Moreover, metformin inhibited the activation, proliferation, motility, and contraction of activated HSCs, reduced the secretion of ECM, and decreased HSC-based angiogenesis, thus providing a new therapeutic approach to the treatment of liver fibrosis and portal hypertension.

Li Z, Ding Q, Ling LP, Wu Y, Meng DX, Li X, Zhang CQ. Metformin attenuates motility, contraction, and fibrogenic response of hepatic stellate cells *in vivo* and *in vitro* by activating AMP-activated protein kinase. *World J Gastroenterol* 2018; 24(7): 819-832 Available from: URL: http://www.wjgnet.com/1007-9327/full/v24/i7/819.htm DOI: http://dx.doi.org/10.3748/wjg.v24.i7.819

## INTRODUCTION

Liver fibrosis is a common pathological condition resulting from chronic liver injury stemming from a variety of etiological factors. Hepatic stellate cells (HSCs) play a key role in the progression of liver fibrosis, and are thought to be its primary effector cells[1]. In chronic liver diseases (CLDs), quiescent HSCs are activated and change to myofibroblast-like cells, which are proliferative, contractile, and secrete increased levels of more extracellular matrix (ECM)[2]. Angiogenesis is widely noted in CLDs, and influences liver fibrosis and portal hypertension (PHT)[3]. HSCs are liver-specific pericytes that participate in angiogenesis and sinusoidal remodeling. The primary pathological feature of sinusoidal remodeling is sinusoidal capillarization and coverage of the vessels with contractile HSCs[4]. HSCs reduce the diameter of sinusoids after contraction, causing a functional change in modulating the hepatic tone and increasing intrahepatic vascular resistance (IHVR), ultimately contributing to PHT[5]. HSCs occupy a crossroad at the intersection between inflammation, angiogenesis, and fibrosis[6], and activation of HSCs is a key event mediating increased IHVR[7]. Thus, activated HSCs are a potent therapeutic target for the treatment of CLDs.

Metformin is the first-line drug recommended for the treatment of diabetes. Previous studies have demonstrated that metformin has a wide range of pharmacological activities beyond its antidiabetic effects. The beneficial effects of metformin in hepatic disorders have been previously confirmed for reducing fibrosis[8,9], IHVR, and therefore PHT in cirrhosis[10], and decreasing hepatocellular carcinoma risk[11]. Metformin is a potent therapeutic approach for CLDs, but the mechanisms underlying its effects are still unclear, especially in the treatment of PHT. Further studies are needed to investigate the effect of metformin in CLDs.

Platelet-derived growth factor (PDGF) signaling is among the most well characterized pathways of HSC activation. It induces activation of the extracellular signal-regulated kinase (ERK) and the Akt/mammalian target of rapamycin (mTOR) pathways, which are associated with cellular proliferation and migration[12]. Studies have also linked ERK and mTOR signaling to vascular endothelial gowth factor (VEGF) expression during angiogenesis[13,14]. Activation of adenosine monophosphate-activated protein kinase (AMPK) inhibits the proliferation and migration of HSCs induced by PDGF, and this effect is related to the inhibition of the Akt and ERK pathways[15]. Metformin is known to activate AMPK, therefore, we speculated that metformin may regulate the fibrogenic response of HSCs and have an anti-angiogenic effect.

In the present study, we investigated the effect of metformin on activated HSCs. The inhibitory effects of metformin on the activation, proliferation, motility, contraction, and ECM secretion of HSCs and HSC-based angiogenesis were evaluated. We also investigated the

underlying mechanisms, with a focus on AMPK and the downstream AKT/mTOR and ERK signaling pathways.

## MATERIALS AND METHODS

### Animals

Thirty male C57BL/6 mice weighing 20-22 g were purchased from the Central Animal Care Facility of Shandong University and randomly divided into three groups (a control group, a $CCl_4$ group, and a metformin group, $n$ = 10 in each group). The animals were housed in an air-conditioned room at 23-25 ℃ with a light/dark (12 h:12 h) cycle for one week prior to the initiation of the experiment. All animals received appropriate care during the study, with free access to chow and water. The liver fibrosis model was induced by intraperitoneal injection of carbon tetrachloride ($CCl_4$, 1 μL/g, Sinopharm, Beijing, China) dissolved 1:1 (v/v) in olive oil twice per week, while the control mice were injected with olive oil alone. Mice in the metformin group were treated with metformin (Sigma-Aldrich, Saint Louis, MO, United States) in drinking water (1 g/L) at the same time. All mice were sacrificed at the end of 6 wk. A portion of liver tissue was fixed in 4% paraformaldehyde and then embedded in paraffin. The other liver tissues were stored at -80 ℃.

### Cell culture

The HSC cell line LX-2 (a kind gift from Professor Wei-fen Xie, Changzheng Hospital, the Second Military Medical University) and human umbilical vascular endothelial cells (HUVECs, ATCC, Manassas, VA, United States) were cultured in Dulbecco's modified Eagle's medium (DMEM; Gibco, Grand Island, NY, United States) supplemented with 10% fetal bovine serum (FBS; Gibco) in an incubator at 37 ℃ with 5% $CO_2$ and 90% humidity.

### CCK-8 assay

First, 5 × $10^3$ LX-2 cells were seeded in 96-well plates and incubated overnight, and then the medium was changed to fresh medium containing different concentrations of metformin. After incubation for 24 h, 10 μL of CCK-8 (Dojindo, Japan) was added to each well. The optical density (OD) values were measured every 30 min with a spectrophotometer (Thermo Fisher, Finland) at 450 nm. The OD values at 2 h were chosen for analysis.

### Migration and invasion assay

A scratch test was used for HSC migration assay. Cells (5 × $10^5$) were seeded in 6-well plates, incubated overnight to cover the full plate, and then serum-starved for 8 h. After making scratch wounds, plates were washed three times with PBS. Cells were treated with or without 10 ng/mL PDGF-BB (PeproTech, Rocky Hill, NJ, United States) for 24 h. Different concentrations of metformin were added to the medium 2 h before the PDGF-BB addition. Images were acquired at 0 and 24 h. The Transwell (8 μm pore size, Costar) assay was used to test the invasive ability of HSCs. HSCs were serum-free for 6 h and then harvested. Cells (1 × $10^5$) in 100 μL serum-free medium were seeded in the upper chambers with the Matrigel (BD Bioscience, Bedford, MA, United States) membrane and different concentrations of metformin, and the lower chambers were loaded with DMEM with or without 10% FBS. After incubation for 24 h, cells that migrated through the membrane were fixed and stained with hematoxylin. Cell numbers were counted under a microscope (Olympus, Japan).

### Collagen gel contraction assay

Rat tail tendon collagen type Ⅰ was obtained from Sybio (Hangzhou, China). The collagen gel was prepared in 24-well plates. We used 0.1 mol/L NaOH to adjust the pH and 10 × PBS to adjust the solution to physiological strength. The mixed solution (500 μL) was added to each plate and incubated at 37 ℃ for 1 h to allow gelatinization. LX-2 cells (1 × $10^5$) in 1000 μL of medium were seeded on the gel and incubated overnight. Cells were starved for 8 h in DMEM, and then the DMEM was replaced with fresh medium with 1% FBS and different concentrations of metformin. PDGF-BB (10 ng/mL) was added to the medium, except in the control group, 2 h after metformin addition. The tip of a 200 μL pipette was used to gently detach the gel from the plates. After incubation for 24 h, the areas of the gels were measured.

### Enzyme-linked immunosorbent assay

First, 4 × $10^5$ LX-2 cells were seeded in 6-well plates and incubated overnight. Cells were starved in DMEM for 8 h. The DMEM was changed to 1 mL of fresh medium with 1% FBS and different concentrations of metformin. Cobalt (Ⅱ) chloride hexahydrate ($CoCl_2 \cdot 6H_2O$, 150 μmol/L, Sigma-Aldrich, Saint Louis, MO, United States) was added to the medium, except for the control group, 2 h after metformin addition. After 12 h of incubation, the supernatant was collected and centrifuged at 1000 rpm for 4 min. VEGF was measured with an ELISA kit (Boster, Wuhan, China). The ELISA protocol was performed according to the manufacturer's instructions.

### Tube formation assay

A 96-well plate was coated with 50 μL of Matrigel, and then placed in an incubator at 37 ℃ for 1 h. Cells were treated in the same way as in the ELISA assay, and the supernatant was collected. Conditioned medium was generated from supernatant diluted 4:1 (v/v) in DMEM with 10% FBS. HUVECs were harvested and suspended in the conditioned medium. HUVECs (2 × $10^4$) in 100 μL of conditioned medium were seeded in 96-well plates and incubated at 37 ℃. The cells were

**Table 1 The primers used for RT-PCR analysis**

| Primer (Mouse) | Sequence (5'-3') |
|---|---|
| *GAPDH* F | AAATGGTGAAGGTCGGTGTGAAC |
| *GAPDH* R | CAACAATCTCCACTTTGCCACTG |
| *α-SMA* F | GACAATGGCTCTGGGCTCTGTA |
| *α-SMA* R | TTTGGCCCATTCCAACCATTA |
| *COL1A1* F | GACATGTTCAGCTTTGTGGACCTC |
| *COL1A1* R | GGGACCCTTAGGCCATTGTGTA |

α-SMA: Alpha-smooth muscle actin; COL1A1: Collagen type 1 alpha 1.

monitored every 2 h for 12 h under a microscope. Images of the tube formation were acquired at 8 h.

### Western blot analysis

Total protein was extracted with RIPA buffer, and the protein concentration was measured by the bicinchoninic acid method. Equal amounts of proteins were loaded and separated by SDS-PAGE, and then transferred onto a PVDF membrane. The membrane was blocked in TBST buffer with 5% non-fat milk for 1 h and incubated with different antibodies overnight at 4 ℃. Primary antibodies against α-SMA (14395-1-AP), fibronectin (66042-1-IG), and collagen type Ⅰ (14695-1-AP) were obtained from Proteintech (Wuhan, China). Primary antibodies against p-ERK1/2 (#4376), p-Akt (#4060), p-AMPK (#2535), p-mTOR (#5536), ERK1/2 (#4695), Akt (#4691), AMPK (#5832), and mTOR (#2983) were obtained from CST (Boston, MA, United States). Primary antibody against VEGF (ab46154) was obtained from Abcam (Cambridge, CA, United States). Primary antibody against HIF-1α (NB100-105) was obtained from Novus (Littleton, CO, United States). Primary antibody against glyceraldehyde 3-phosphate dehydrogenase (GAPDH) and horseradish peroxidase (HRP)-conjugated secondary antibody were obtained from Zhongshan Golden Bridge (Beijing, China). The HRP-conjugated secondary antibodies were goat anti-rabbit or anti-mouse antibody depending on the primary antibodies. AICAR (an AMPK activator) and rapamycin (an mTOR inhibitor) were obtained from Selleck (Houston, TX, United States). PD98059 (an ERK inhibitor) and LY294002 (an AKT inhibitor) were obtained from MCE (Monmouth Junction, NJ, United States). Antibody bands were detected by enhanced chemiluminescence with Amersham Imager 600 (GE Healthcare, United States). GAPDH in the same membrane was used as an internal control, and all bands were normalized to its expression.

### Reverse transcription-polymerase chain reaction

Total RNA was extracted with TRIzol reagent (Takara, Japan) from frozen liver tissues and was reverse-transcribed to cDNA using an RT reagent kit (Takara, Japan). Amplifications were detected using a the SYBR Premix Ex Taq kit (Takara, Japan) on a LightCycler 480 Real-Time PCR system (Roche Diagnostics, United States). The primers used in this study are presented in Table 1. Expression of target genes was normalized to expression of GAPDH by the $2^{-\Delta CT}$ method.

### Histopathological and immunohistochemical analyses

Liver specimens embedded in paraffin were cut into 4 μm-thick sections. The specimens were stained with hematoxylin and eosin and Sirius Red. Immunohistochemistry (IHC) was performed using a 2-step plus Poly-HRP Anti-Mouse/Rabbit IgG Detection system (Zhongshan Golden Bridge, Beijing, China), according to the manufacturer's instructions. Sections were incubated with antibodies against α-SMA, fibronectin, and VEGF, and the blots were developed with a DAB kit (Zhongshan Golden Bridge, Beijing, China).

### Statistical analysis

All data are presented as the mean ± SEM from at least three independent experiments. Statistics were analyzed using GraphPad Prism 5.0 and SPSS19.0 software. Statistical significance was determined by one-way analysis of variance (ANOVA) followed by Dunnett's test. A $P$-value < 0.05 was considered statistically significant.

## RESULTS

### Metformin decreases the activation of HSCs, reduces the deposition of ECM, and inhibits angiogenesis in $CCl_4$-treated mice

Liver specimens from mice exposed to $CCl_4$ showed hepatocellular degeneration with excessive accumulation of connective tissue, the formation of fibrotic septa, and infiltration of inflammatory cells. Metformin treatment attenuated the fibrotic level of the fibrotic tissue, the appearance of degenerated hepatocytes, and inflammatory cell infiltration (Figure 1A). Increased collagen deposition was observed in $CCl_4$-induced fibrotic mice, which could be suppressed by metformin (Figure 1B). A similar effect of metformin on fibronectin was seen in IHC (Figure 1D). As shown in Figure 1E, fibrotic mice expressed more VEGF, indicating more intrahepatic angiogenesis than the control group. Treatment with metformin significantly suppressed expression of VEGF.

Mice exposed to $CCl_4$ increased α-SMA at both the protein and mRNA levels, while co-treatment with metformin reduced this effect (Figure 2A and B), which was also confirmed by IHC (Figure 1C). The $CCl_4$-induced increase in collagen I mRNA expression was reduced by co-treatment with metformin. Taken together, metformin decreased the activation of HSCs, reduced the deposition of ECM, and inhibited angiogenesis in $CCl_4$-treated mice. Therefore, metformin attenuated $CCl_4$-induced liver fibrosis in mice.

### Metformin inhibits the proliferation of activated HSCs

HSCs were treated with different concentrations

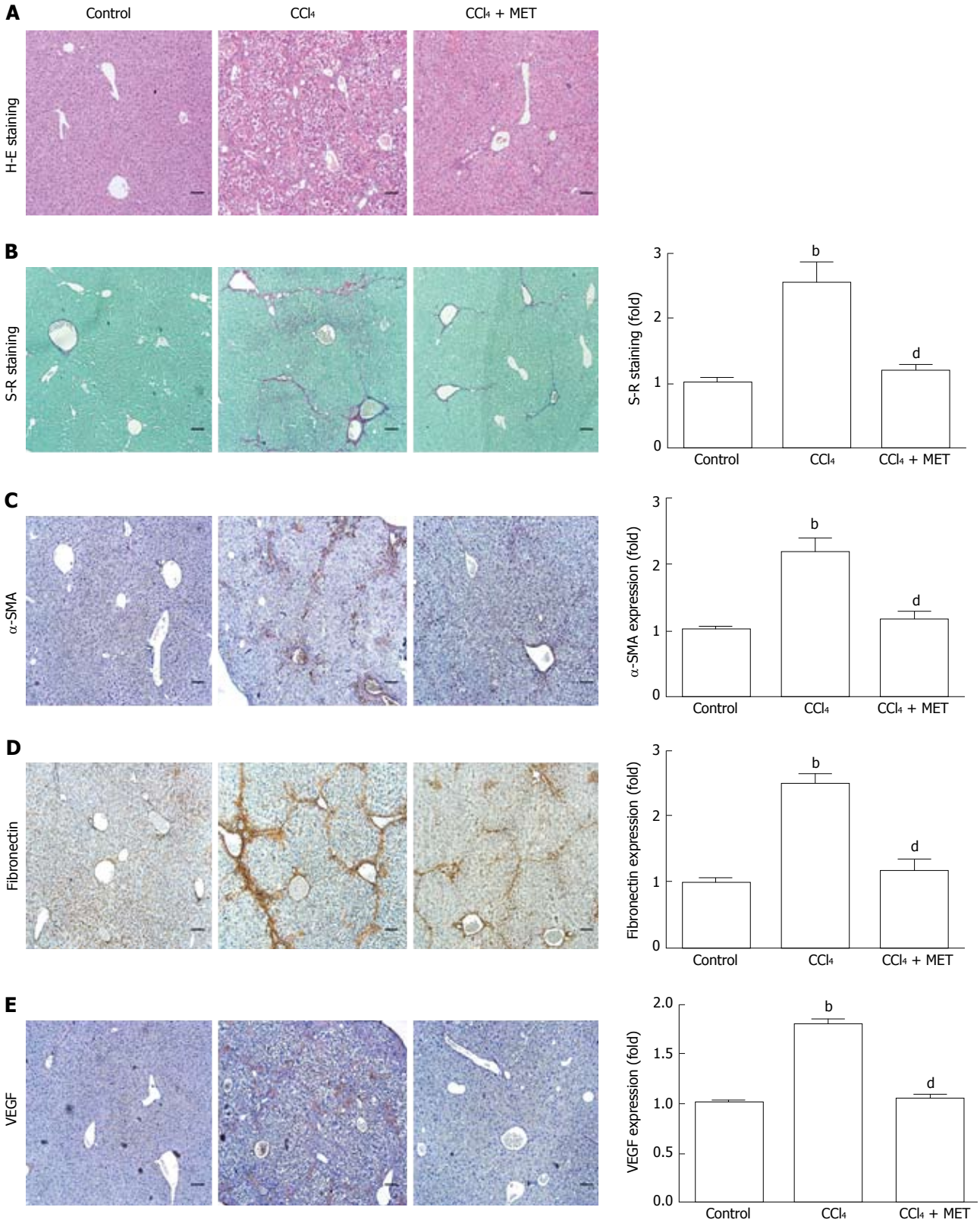


**Figure 1 Effect of metformin in $CCl_4$-induced fibrotic mice.** A fibrotic mouse model was induced by intraperitoneal injection of $CCl_4$ (1 μL/g) dissolved in olive oil ($CCl_4$:olive oil = 1:1, v/v) twice per week for 6 weeks. A and B: Histological changes were assessed by hematoxylin-eosin (H-E) staining and Sirius Red (S-R) staining (100 × magnification); C-E: Expression levels of α-SMA, fibronectin, and VEGF in the liver tissues were measured by immunohistochemistry (100 × magnification). Sirius Red staining was analyzed with ImageJ and immunohistochemical staining was analyzed with Image-Pro Plus 6.0. (Scale bar = 200 μm, $n = 5$, $^bP < 0.01$ *vs* the control group, $^dP < 0.01$ *vs* the $CCl_4$ group).

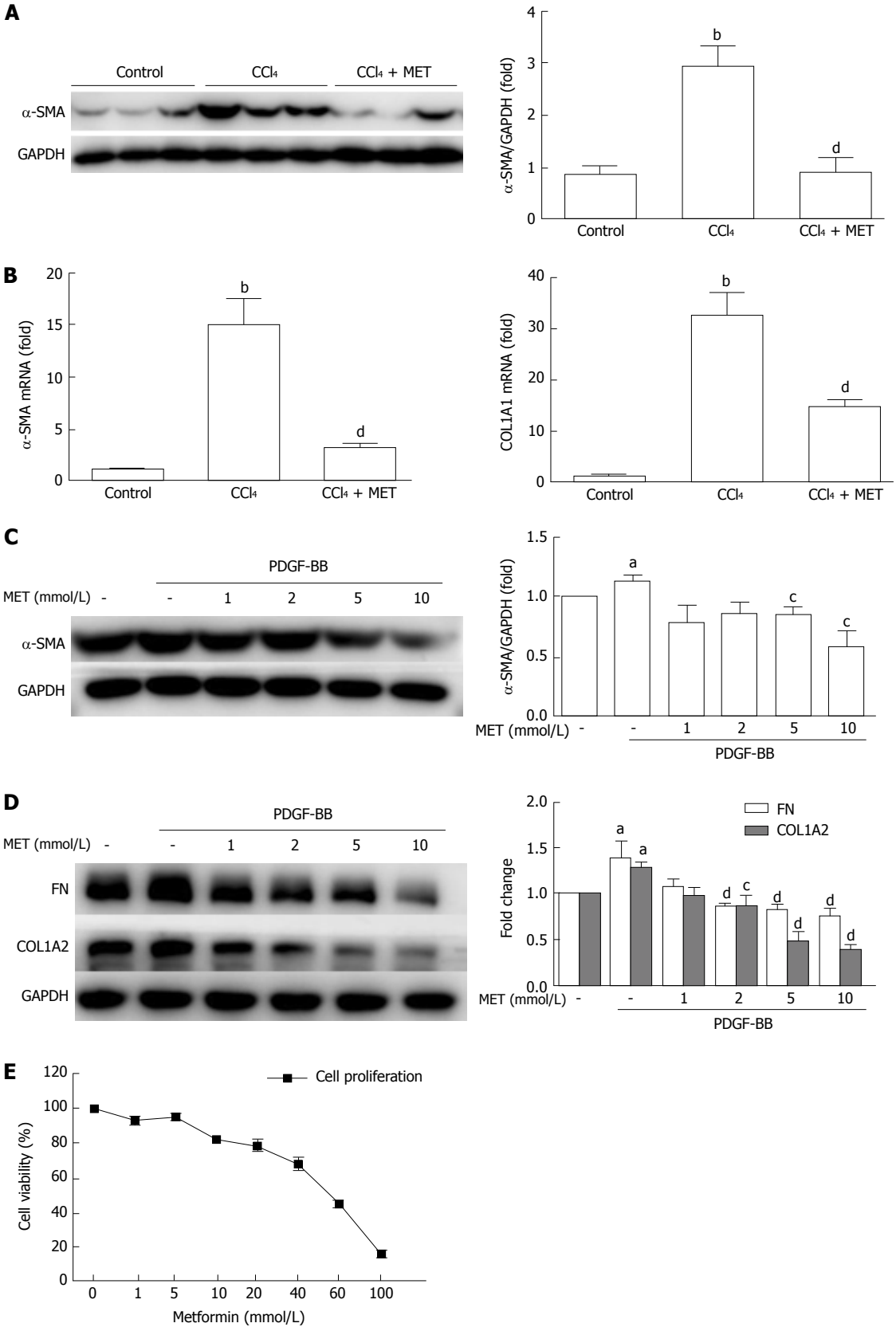


**Figure 2 Effect of metformin on the activation, proliferation, and extracellular matrix secretion of hepatic stellate cells.** A: Measurement of α-SMA levels in murine liver tissues by Western blot; B: Measurement of hepatic α-SMA and collagen type Ⅰ mRNA expression levels by quantitative real-time PCR ($n$ = 5, $^{b}P < 0.01$ *vs* the control group, $^{d}P < 0.01$ *vs* the $CCl_4$ group); C and D: HSCs were treated with or without 10 ng/mL PDGF-BB for 24 h, and the effect of metformin (1, 2, 5, and 10 mmol/L) on the expression levels of α-SMA, collagen type Ⅰ ,and fibronectin (FN) were measured by Western blot ($^{a}P < 0.05$ *vs* the control group, $^{c}P < 0.05$ and $^{d}P < 0.01$ *vs* the PDGF-BB only group); E: HSCs were treated with a series of concentrations ranging from 1 mmol/L to 100 mmol/L of metformin for 24 h, and the proliferation was measured by CCK-8 assays. HSCs: Hepatic stellate cells.

(1 mmol/L to 100 mmol/L) of metformin for 24 h (Figure 2E). The proliferation of HSCs was inhibited by metformin in a dose-dependent manner, and the $IC_{50}$ was 50.01 mmol/L.

### *Metformin suppresses the activation of HSCs and decreases the expression of ECM in vitro*

The protein levels of α-SMA, collagen type Ⅰ ,and fibronectin were measured by Western blot (Figure 2C and D). PDGF-BB up-regulated the expression of α-SMA, while treatment with metformin at 5 mmol/L and 10 mmol/L suppressed this increase, from 113.5% ± 4.66% to 84.87% ± 6.63% and 58.79% ± 12.64%, respectively ($P < 0.05$). Collagen type I and fibronectin are the major components of the ECM, and HSCs expressed increased levels of these protein after co-incubation with PDGF-BB. Metformin decreased the protein levels at doses of 2, 5, and 10 mmol/L. These results indicated that metformin suppressed the activation of HSCs and the secretion of ECM *in vitro*.

### *Metformin decreases the migration and invasion of HSCs*

The migration rate of HSCs was significantly increased by PDGF-BB treatment compared with that of the control group (26.38% ± 2.98% to 48.05% ± 3.67%, $P < 0.01$). Treatment with metformin at 5 mmol/L and 10 mmol/L reduced PDGF-BB-induced migration, from 48.05% ± 3.67% to 21.67% ± 2.73% and 14.99% ± 0.25% ($P < 0.01$), respectively (Figure 3A and C). As shown in Figure 3B, cells that migrated through the matrigel membrane decreased from 1352% ± 62.87% to 748.0% ± 76.18%, 453.0% ± 4.58%, and 190.0% ± 14.73% ($P < 0.01$) compared with the control group when treated with metformin at 1, 5, and 10 mmol/L, respectively (Figure 3D). These findings indicated that metformin decreased the motility of HSCs.

### *Metformin inhibits the contraction of HSCs*

We assessed the inhibitory effect of metformin on the contractility of HSCs by collagen gel contraction assay. PDGF-BB caused a significant increase in cell contractility, while co-culture with metformin neutralized these effects (Figure 4A and C). PDGF-BB treatment enhanced the contraction rate of HSCs from 47.43% ± 2.13% to 70.25% ± 1.35% ($P < 0.01$), while treatment with metformin at 1, 5, and 10 mmol/L attenuated the contraction rate to 49.70% ± 6.59% ($P < 0.05$), 44.73% ± 4.65%, and 42.26% ± 3.28% ($P < 0.01$), respectively.

### *Metformin decreases the expression of VEGF in HSCs through inhibition of HIF-1α in both PDGF-BB and hypoxic conditions*

$CoCl_2 \cdot 6H_2O$ (150 μmol/L) was added to the medium to mimic hypoxic conditions[16,17]. HSCs expressed more VEGF when incubated with PDGF-BB or $CoCl_2$ compared with the control group, and this effect was associated with an increased level of HIF-1α (Figure 5A and B). Metformin decreased the level of HIF-1α and further reduced the expression of VEGF in HSCs. Treatment with metformin at 5 and 10 mmol/L had an inhibitory effect on VEGF expression in both PDGF-BB and hypoxic conditions.

### *Metformin down-regulates VEGF secretion by HSCs and inhibits angiogenesis in hypoxic conditions in vitro*

The VEGF protein level in the supernatant was increased from 148.96 ± 50.62 pg/mL to 343.52 ± 25.91 pg/mL ($P < 0.01$) when $CoCl_2$ (150 μmol/L) was added to the medium, but co-culture with metformin at 5 mmol/L and 10 mmol/L decreased VEGF levels to 254.40 ± 16.91 pg/mL and 229.04 ± 1.62 pg/mL, respectively ($P < 0.01$) (Figure 5C). Tube formation of HUVECs on Matrigel can be used to analyze angiogenesis *in vitro*. HUVECs were cultured in conditioned medium on Matrigel-coated plates. The conditioned medium from $CoCl_2$-treated HSCs significantly increased tube formation, while conditioned medium from HSCs co-treated with $CoCl_2$ and metformin decreased tube formation. AICAR mimicked the effect of metformin on tube formation (Figure 5D and E).

### *Metformin inhibits the fibrogenic response of HSCs through inhibition of the Akt/mTOR and ERK pathways via the activation of AMPK*

Metformin increased the phosphorylation of AMPK in a dose-dependent manner (Figure 6C). After stimulation with PDGF-BB, the levels of p-Akt, p-mTOR, and p-ERK were significantly increased compared with those of the control group, while co-treatment with metformin decreased these effects (Figure 6A and E). The Akt/mTOR and ERK pathways are associated with cell proliferation, migration, and phenotypic change in HSCs. To further confirm these effects, we used various indicated inhibitors to treat HSCs (Figure 7A and C). LY294002 (an Akt inhibitor, 20 μmol/L) and rapamycin (an mTOR inhibitor, 100 nmol/L) inhibited the activation of HSCs, decreased ECM secretion, and reduced the expression of HIF-1α and VEGF. Moreover, LY294002 inhibited the contraction of HSCs (Figure 4B and D). PD98059 (an ERK inhibitor, 10 μmol/L) had a similar effect as LY294002, except that it could not decrease the secretion of collagen type I. Additionally, AICAR (500 μmol/L), another AMPK activator, mimicked the effect of metformin. In conclusion, PDGF-BB increased the fibrogenic response of HSCs through activating the downstream Akt/mTOR and ERK pathways, while metformin inhibited these effects *via* activation of AMPK.

### *Metformin decreases VEGF expression by activated HSCs by down-regulating the mTOR/HIF-1α and ERK/HIF-1α pathways under hypoxic conditions*

The levels of p-mTOR and p-ERK were significantly increased when compared with the control group under hypoxic conditions, while no change was found in the

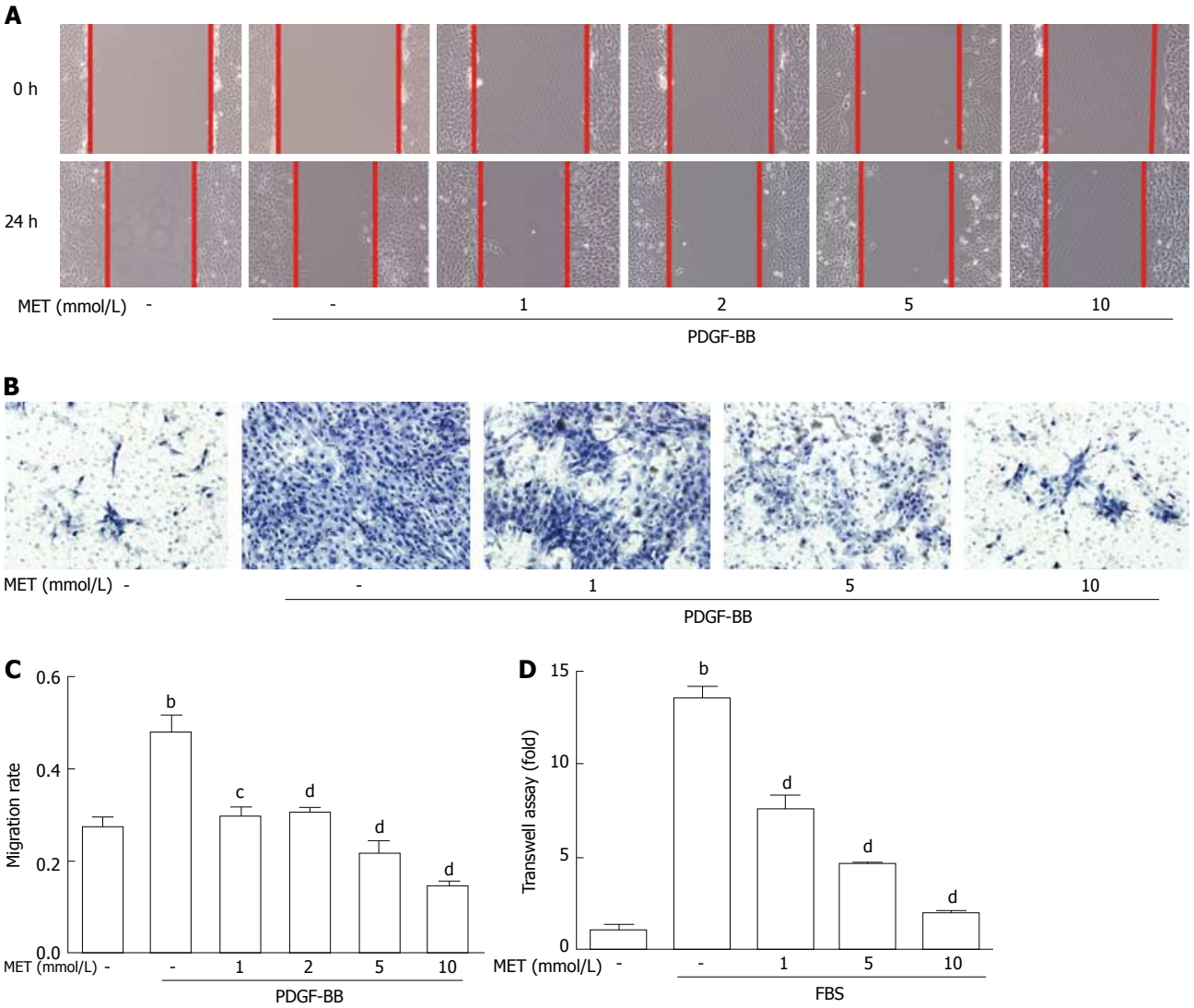


**Figure 3 Effect of metformin on hepatic stellate cell migration and invasion.** Scratch tests were used to determine cell migration, and Transwell assays were used to evaluate cell invasion. A: HSCs were scraped and then incubated with or without PDGF-BB (10 ng/mL) and metformin (1, 2, 5, and 10 mmol/L). Images were acquired at 0 and 24 h (100 × magnification); B: HSCs were seeded in the upper chamber with a Matrigel membrane, and various concentrations of metformin (0, 1, 5, and 10 mmol/L) were added to the medium. The lower chambers were loaded with DMEM with or without 10% FBS. Cells that migrated through the membrane were fixed and stained with hematoxylin at 24 h; C: The migration ability was quantified by measuring the distance of the scratch edge; D: Cells that migrated through the membrane were counted and quantified. ($^{b}P < 0.01$ *vs* the control group, $^{c}P < 0.05$ and $^{d}P < 0.01$ *vs* the PDGF-BB or FBS only groups). HSCs: Hepatic stellate cells.

phosphorylation of Akt (Figure 6B and D). Metformin increased the phosphorylation of AMPK and inhibited the activation of p-mTOR and p-ERK. PD98059 and rapamycin decreased the expression of HIF-1α and VEGF. LY294002 inhibited the activation of p-Akt and the downstream p-mTOR, which therefore decreased the expression of HIF-1α and VEGF. AICAR had a similar effect as metformin under these conditions (Figure 7D and F). These results indicated that metformin decreased VEGF expression by activated HSCs by down-regulating the mTOR/HIF-1α and ERK/HIF-1α signaling pathways under hypoxic conditions.

## DISCUSSION

The prime determinant of PHT is increased IHVR, which is thought to be generated by the following two factors: structural (distortion of the liver vascular architecture caused by fibrosis, scarring, and nodule formation) and functional (hepatic sinusoidal cellular alterations that promote constriction of the hepatic sinusoids) components[18]. Research has shown that activation of HSCs is a key event mediating augmented IHVR[7]. We designed this study to investigate the role of metformin in activated HSCs. We found that metformin could attenuate the fibrogenic response of HSCs and decrease IHVR. Our research indicated that metformin treatment may be a potent therapeutic approach to treating liver fibrosis and PHT.

First, we used a fibrotic mouse model to determine whether metformin had effects on liver fibrosis. Mice injected with $CCl_4$ for 6 wk developed marked fibrosis compared with the control group, while co-treatment with metformin attenuated histopathologic features

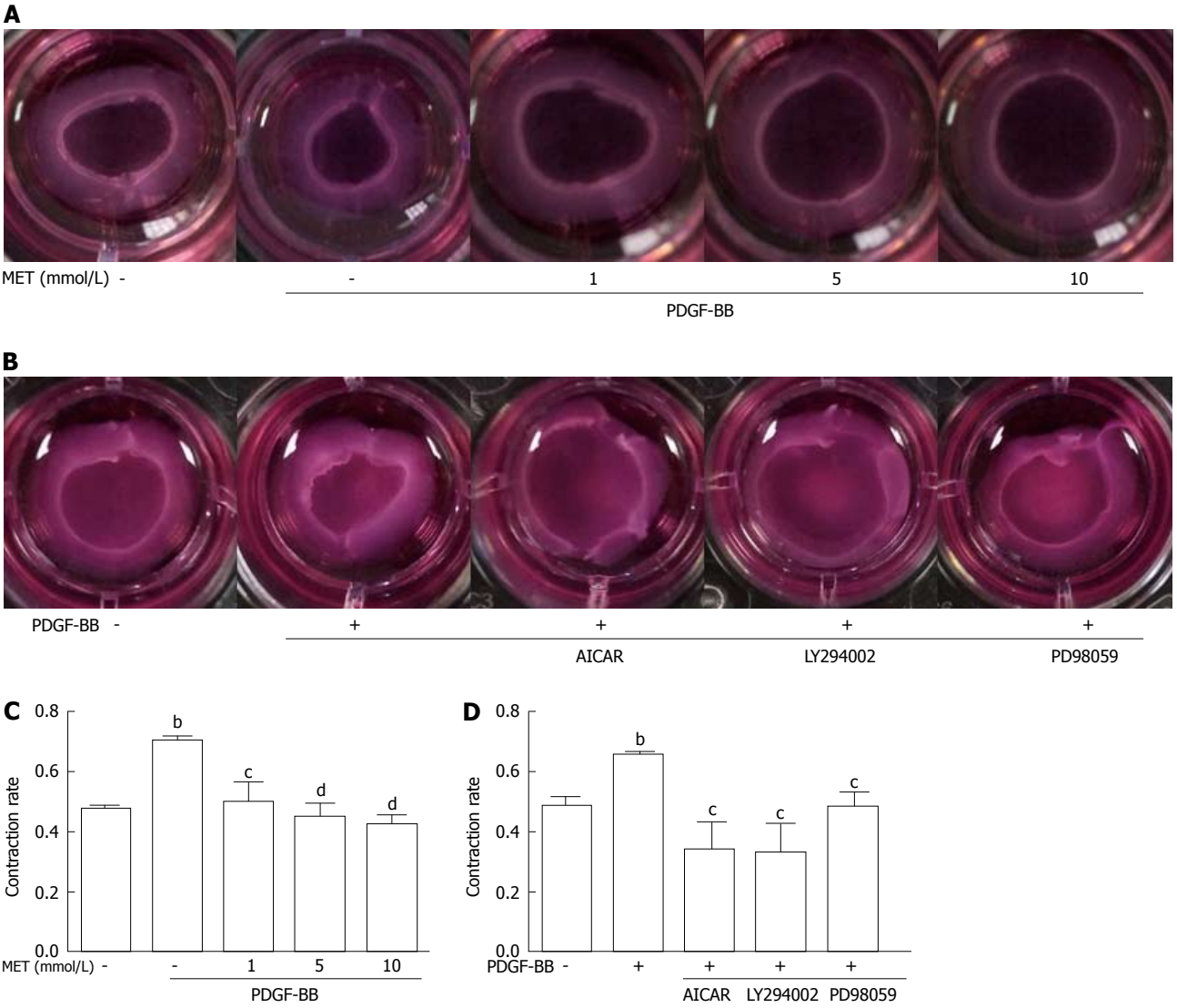


**Figure 4 Effect of metformin on hepatic stellate cell contraction.** Collagen gels were prepared in 24-well plates. A: HSCs were seeded on the collagen gel with or without PDGF-BB (10 ng/mL) and metformin (1, 5, and 10 mmol/L); B: Metformin was changed to AICAR (500 μmol/L), LY294002 (20 μmol/L), and PD98059 (10 μmol/L); C and D: After incubation for 24 h, the areas of the collagen gel were measured for analysis. ($^{b}P < 0.01$ *vs* the control group, $^{c}P < 0.05$ and $^{d}P < 0.01$ *vs* the PDGF-BB only group). HSCs: Hepatic stellate cells.

of fibrosis. α-SMA, a marker of HSC activation, was inhibited by metformin at both the protein and mRNA levels. Sirius Red staining showed that collagen deposition was also decreased, as well as the mRNA level of collagen type Ⅰ. Moreover, VEGF expression was up-regulated in fibrotic mice, which was decreased by metformin treatment. Therefore, metformin could alleviate the progression of liver fibrosis in fibrotic mice. A recent study also showed that metformin mitigated $CCl_4$-induced liver fibrosis in mice. The anti-fibrogenic response was reported to primarily involve suppression of ECM deposition, and this effect might have resulted from suppressed TGF-β1/Smad3 signaling[8]; this was supported by a previous *in vitro* study[9]. In our study, we found that metformin could also inhibit the angiogenesis in liver fibrosis, indicating that metformin may attenuate liver fibrosis in other ways. The PDGF signaling pathway is among the most well characterized pathways involved in HSC activation; PDGF-BB is the most potent stimulator of HSC growth and intracellular signaling[1], and blocking of PDGF signaling ameliorates experimental liver fibrogenesis[19]. As described above, we speculated that metformin could regulate the fibrogenic response of HSCs and have an anti-angiogenic effect *via* PDGF and its downstream pathways. Therefore, we performed an *in vitro* study to further explain the effect of metformin on activated HSCs and investigate the possible signaling pathways involved.

We used PDGF-BB to stimulate HSCs *in vitro*. PDGF-BB up-regulated the expression of α-SMA, as well as type Ⅰ collagen and fibronectin, in HSCs, while these protein levels were decreased when treated with metformin. These results are in agreement with our animal experiments. Caligiuri showed that activation of AMPK modulated the activated phenotype change

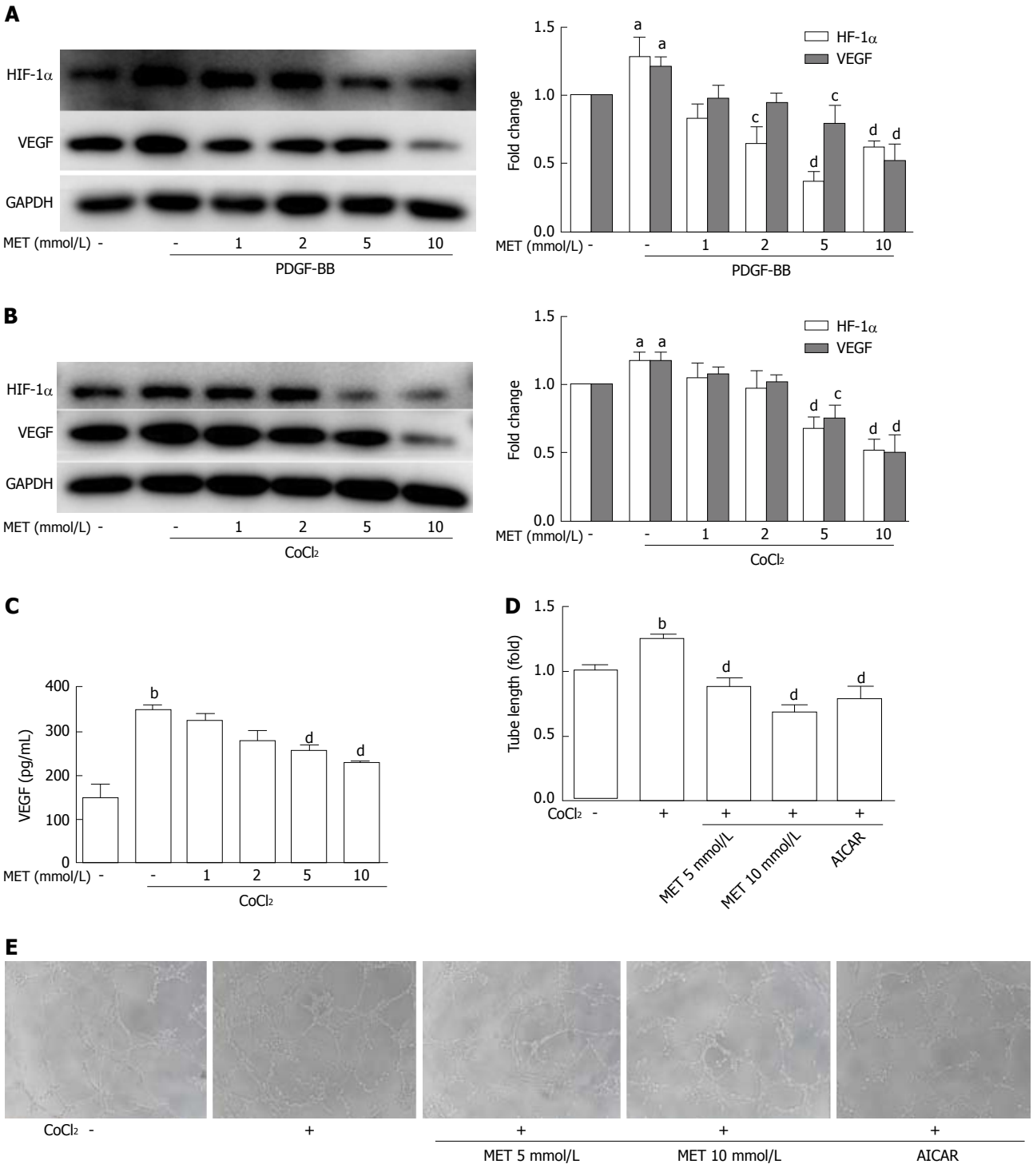


**Figure 5 Effect of metformin on VEGF expression and secretion of hepatic stellate cells and angiogenesis *in vitro*.** A and B: HSCs were incubated with or without PDGF-BB (10 ng/mL) for 24 h or $CoCl_2$ (150 μmol/L) for 12 h and metformin (1, 2, 5, and 10 mmol/L). The expression levels of HIF-1α and VEGF were measured by Western blot analysis, and the results were quantified; C: Cells were treated as in panel B, and the supernatant was collected. The protein level of VEGF was measured by ELISA assay; D and E: HSCs were pretreated with metformin (5 and 10 mmol/L) or AICAR (500 μmol/L) for 2 h, and then incubated with or without $CoCl_2$ (150 μmol/L) for 12 h. The supernatant was collected and diluted 4:1 (v/v) in DMEM with 10% FBS to form conditioned medium. HUVECs were harvested and suspended in the conditioned medium, and then seeded on Matrigel. Images were acquired at 8 h (100 × magnification), and tube lengths were calculated with ImageJ and quantified. $^aP < 0.05$ and $^bP < 0.01$ *vs* the control group, $^cP < 0.05$ and $^dP < 0.01$ *vs* the PDGF-BB or $CoCl_2$ only groups. HSCs: Hepatic stellate cells.

of HSCs caused by PDGF-BB[15]. In this study, PDGF induced activation of the downstream molecules ERK and Akt/mTOR in activated HSCs, which are associated with cellular proliferation, migration, and phenotype changes. Metformin inhibited the activation of ERK and Akt/mTOR by activating AMPK. To further analyze the role of the signaling pathways, we used various indicated inhibitors to determine whether the signaling pathways could affect activated HSCs. LY294002 and rapamycin inhibited the expression of α-SMA,

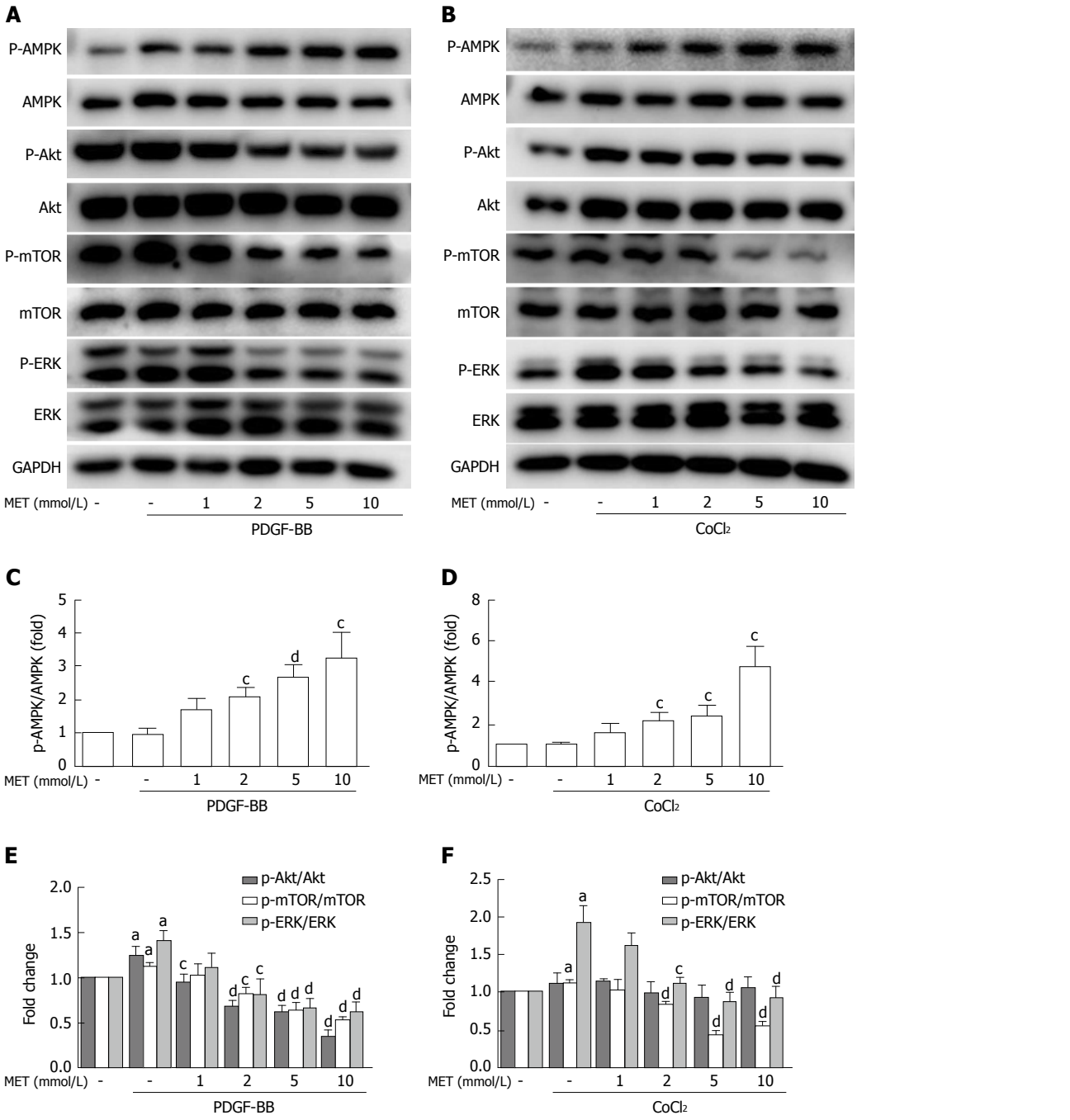


**Figure 6 Effect of metformin on AMPK, Akt/mTOR, and ERK signaling in hepatic stellate cells.** A and B: HSCs were pretreated with metformin (1, 2, 5 and 10 mmol/L) for 2 h and then incubated with PDGF-BB (10 ng/mL) for 24 h or $CoCl_2$ (150 μmol/L) for 12 h. AMPK, Akt/mTOR, and ERK signaling pathways were assessed by Western blot analysis; C and D: The results were quantified. $^{a}P < 0.05$ *vs* the control group, $^{c}P < 0.05$ and $^{d}P < 0.01$ *vs* the PDGF-BB or $CoCl_2$ only groups. HSCs: Hepatic stellate cells.

collagen Ⅰ,and fibronectin. PD98059 had a similar effect, except for the expression of collagen type Ⅰ. Furthermore, AICAR, another AMPK activator, could imitate the effect of metformin on activated HSCs. Metformin inhibited activation and ECM secretion of HSCs. This effect was mediated by the activation of AMPK, thereby inhibiting the activation of ERK and Akt/mTOR by PDGF-BB.

In liver cirrhosis, an imbalance between vasoconstrictors and vasodilators makes HSCs more contractile, which increases IHVR and aggravates PHT. Metformin has been reported to attenuate contractile responses in rat aortas[20], and to reduce pulmonary artery contraction in pulmonary arterial hypertension[21]. Therefore, we used a collagen gel contraction assay to evaluate the effect of metformin on the contraction of HSCs. Our results showed that metformin inhibited the contraction of HSCs caused by PDGF-BB. The RhoA/Rock pathway is the contractile pathway in vascular smooth muscle that is also expressed in HSCs[22]. Sorafenib can down-regulate Rho kinase by inhibiting the ERK pathway in secondary biliary cirrhotic rats and further reduce portal

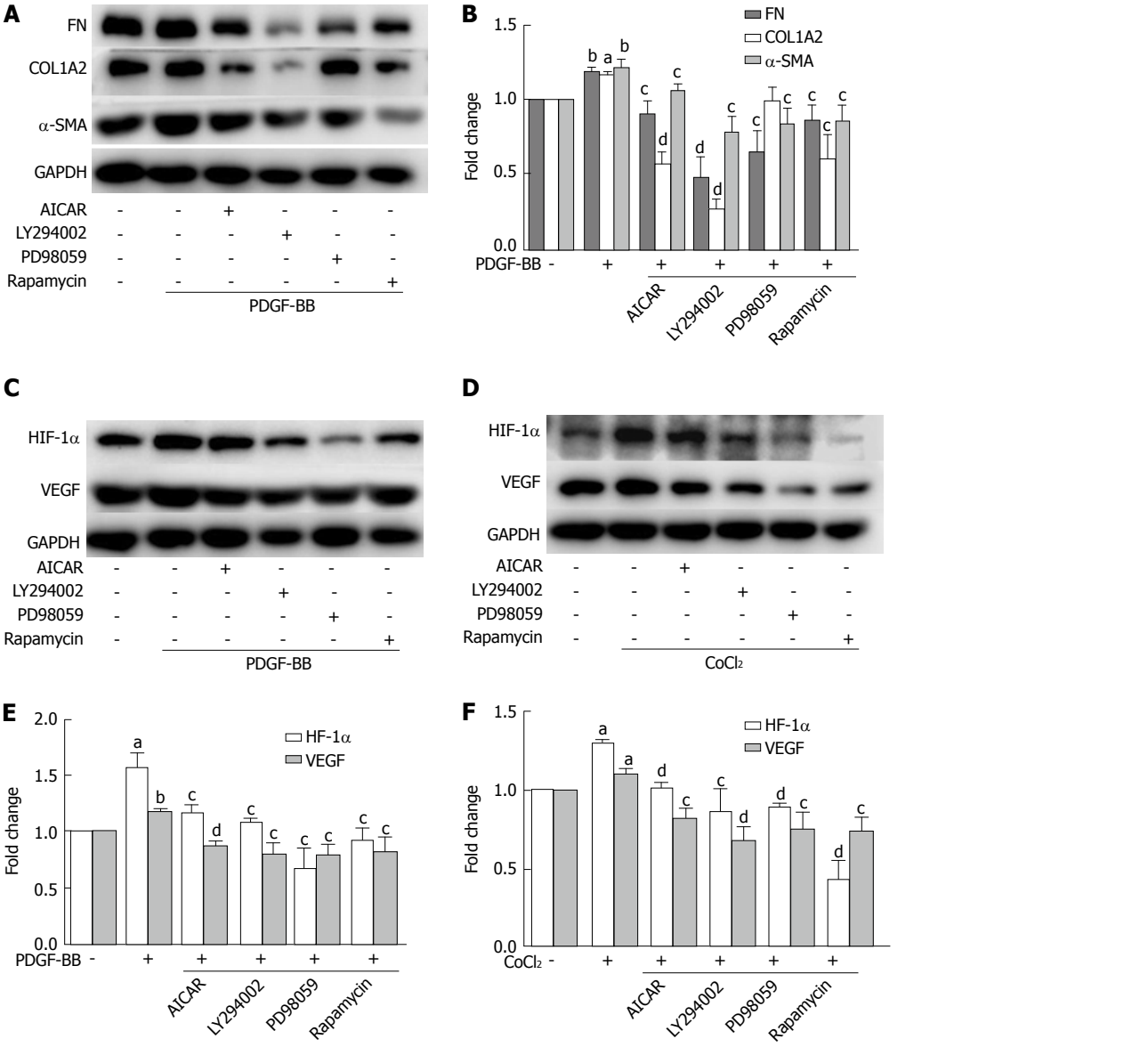


**Figure 7 The inhibitory effects of metformin on activated hepatic stellate cells were associated with activation of AMPK and subsequent down-regulation of the Akt/mTOR and ERK signaling pathways.** A and B: HSCs were pretreated with AICAR (500 μmol/L), LY294002 (20 μmol/L), PD98059 (10 μmol/L), or rapamycin (100 nmol/L) for 2 h and then incubated with PDGF-BB (10 ng/mL) for 24 h. Expression levels of fibronectin (FN), collagen type Ⅰ (COL1A2), and α-SMA were measured by Western blot analysis and the results were quantified; C and D: HSCs were pretreated with AICAR (500 μmol/L), LY294002 (20 μmol/L), PD98059 (10 μmol/L), or rapamycin (100 nmol/L) for 2 h and then incubated with or without $CoCl_2$ (150 μmol/L) for 12 h. Expression levels of HIF-1α and VEGF were measured by Western blot analysis; E and F: The results were quantified. ($^aP < 0.05$ and $^bP < 0.01$ *vs* the control group, $^cP < 0.05$ and $^dP < 0.01$ *vs* the PDGF-BB or $CoCl_2$ only groups). HSCs: Hepatic stellate cells.

pressure[23]. Metformin can decrease the activation of ERK caused by PDGF-BB; therefore, we speculated that the inhibitory effect of metformin on the contraction of HSCs were due in part to the inhibition of the ERK pathway. To confirm this effect, we used PD98059 to treat HSCs stimulated with PDGF-BB. PD98059 inhibited the contraction of HSCs, as expected. There have also been studies that linked the inhibition of the Akt pathway to attenuation of contraction[24,25], and this effect may be associated with the Akt/L-type calcium channel and the Akt/RhoA/Rho kinase pathways[26,27]. In our research, LY294002 could also inhibit the contraction of HSCs, indicating that the Akt pathway was also involved in modulating the contraction of HSCs. In addition, AICAR had a similar effect to metformin on the contraction of HSCs. Thus, metformin inhibits the contraction of activated HSCs, which can decrease IHVR and lower portal pressure.

PDGF can promote HSCs to develop an angiogenic phenotype *via* modulating HSC-based vascular tube formation and increasing coverage of sinusoids, with resulting effects on vascular permeability, vessel mutation, and portal pressure regulation[6,28]. Activated HSC recruitment to liver sinusoidal epithelial cells is an important step in sinusoidal remodeling, and PDGF may be the most important growth factor in this process[29]. In our study, metformin decreased the motility of HSCs. Moreover, metformin decreased the level of VEGF

secreted by HSCs, and inhibited angiogenesis *in vitro*. Taken together, we showed that metformin could inhibit the angiogenic properties of HSCs.

VEGF plays a predominant role in the initial stages of angiogenesis[3]. Reports have shown that PDGF can increase the HIF-1α and VEGF protein levels in activated HSCs[30]. PDGF can also stimulate VEGF expression and HSC-driven vascularization through signals mediated by ERK and mTOR[31]. In our study, the AKT/mTOR and ERK pathways were up-regulated by PDGF and caused increased levels of HIF-1α and VEGF in HSCs. The activation of AMPK by metformin decreased the up-regulation of VEGF by PDGF. This result was partly in agreement with the research by Zhang *et al*[32], who found that curcumin interrupted the PDGF-βR/ERK and mTOR pathways, leading to reductions in VEGF expression in HSCs. As hypoxia is the most potent stimulus for VEGF expression, we further used $CoCl_2$ to mimic a hypoxic environment. Hypoxia stabilized HIF-1α and up-regulated the expression of VEGF in our study. The protein level of VEGF in the HSCs and the medium was significantly higher than that in the control group, and the phosphorylation of ERK and mTOR was also increased. Co-treatment with the AMPK activator metformin inhibited the increase of HIF-1α, VEGF, and the activation of ERK and mTOR. In addition, AICAR, LY294002, PD98059, and rapamycin could also inhibit the expression of HIF-1α and VEGF. These results indicated that metformin could decrease the VEGF levels secreted by HSCs, and this effect was partly mediated by the ERK/HIF-1α and mTOR/HIF-1α pathways. Finally, we used tube formation assays to analyze angiogenesis *in vitro*. When HUVECs were cultured with conditioned medium from HSCs treated with metformin under hypoxic conditions, tube formation was less than that in medium without metformin. AICAR had a similar effect to metformin. Therefore, metformin could inhibit PDGF and hypoxia-induced VEGF expression in HSCs, thus decreasing HSC-based angiogenesis. These effects were mediated through the inhibition of the ERK/HIF-1α and mTOR/HIF-1α pathways by activation of AMPK.

In conclusion, metformin can inhibit the activation, proliferation, motility, and contraction of HSCs, reduce the secretion of ECM, attenuate HSC angiogenic properties, and decrease HSC-based angiogenesis. Metformin has effects on both structural and functional components of IHVR, suggesting a novel therapeutic approach for the treatment of liver fibrosis and PHT.

## ARTICLE HIGHLIGHTS

### Research background

Activation of hepatic stellate cells (HSCs) contributes to liver fibrosis and portal hypertension, and it is a therapeutic target for the treatment of chronic liver diseases (CLDs). Previous studies have demonstrated that metformin has a wide range of pharmacological activities beyond its antidiabetic effects. It may therefore represent a potent therapeutic approach to CLDs, but the mechanisms underlying its effects are still unclear.

### Research motivation

This study was performed to investigate the effect of metformin on activated HSCs and clarify its molecular mechanisms.

### Research objectives

The inhibitory effects of metformin on the activation, proliferation, motility, contraction, extracellular matrix (ECM) secretion of HSCs and HSC-based angiogenesis were evaluated. We also characterized its underlying mechanisms with a focus on AMPK and downstream AKT/mTOR and ERK signaling pathways.

### Research methods

The effect of metformin on activated HSCs were investigated *in vivo* and *in vitro*. A fibrotic mouse model was treated with or without metformin, and the effect of metformin on liver fibrosis was evaluated. The HSC cell line LX-2 was used for *in vitro* studies. The effect of metformin on cell proliferation was detected by CCK8 assay. Cell motility was measured by scratch tests and Transwell assays. Collagen gel contraction assays were performed to assess the effect of metformin on cell contraction. Expression of α-SMA, collagen type Ⅰ, and fibronectin was determined by Western blot analysis. We also analyzed the effect of metformin on HSC-based angiogenesis in both PDGF and hypoxic conditions. The phosphorylation levels of AMPK, AKT, mTOR, and ERK were measured by Western blot analysis. We also used the indicated pharmacologic inhibitors and agonists to confirm our findings.

### Research results

Metformin decreased the activation of HSCs, reduced the deposition of ECM, and inhibited angiogenesis in fibrotic mice. PDGF-BB promoted the fibrogenic response of HSCs, while metformin inhibited the activation, proliferation, migration, and contraction of HSCs, reduced their secretion of ECM, and decreased HSC-based angiogenesis. These inhibitory effects were mediated by inhibition of the Akt/mTOR and ERK pathways *via* the activation of AMPK.

### Research conclusions

Metformin attenuates the fibrogenic response of HSCs *in vivo* and *in vitro*, and may therefore be useful for the treatment of chronic liver diseases.

### Research perspective

This study investigated the inhibitory effect of metformin on activated HSCs and the possible signaling pathways involved. The results strongly confirmed the potential use of metformin for the treatment of CLDs. In future studies, we will provide more evidence for the use of metformin, especially in the treatment of portal hypertension. The effect of metformin on liver sinusoidal endothelial cells will also be analyzed.

## ACKNOWLEDGMENTS

We gratefully thank Dr. Edward C Mignot, Shandong University, for linguistic advice.

## REFERENCES

1 **Lee UE**, Friedman SL. Mechanisms of hepatic fibrogenesis. *Best Pract Res Clin Gastroenterol* 2011; **25**: 195-206 [PMID: 21497738 DOI: 10.1016/j.bpg.2011.02.005]
2 **Elpek GÖ**. Cellular and molecular mechanisms in the pathogenesis of liver fibrosis: An update. *World J Gastroenterol* 2014; **20**: 7260-7276 [PMID: 24966597 DOI: 10.3748/wjg.v20.i23.7260]
3 **Fernández M**, Semela D, Bruix J, Colle I, Pinzani M, Bosch J. Angiogenesis in liver disease. *J Hepatol* 2009; **50**: 604-620 [PMID: 19157625 DOI: 10.1016/j.jhep.2008.12.011]
4 **Thabut D**, Shah V. Intrahepatic angiogenesis and sinusoidal remodeling in chronic liver disease: new targets for the treatment of portal hypertension? *J Hepatol* 2010; **53**: 976-980 [PMID: 20800926 DOI: 10.1016/j.jhep.2010.07.004]

5 **Gracia-Sancho J**, Maeso-Díaz R, Fernández-Iglesias A, Navarro-Zornoza M, Bosch J. New cellular and molecular targets for the treatment of portal hypertension. *Hepatol Int* 2015; **9**: 183-191 [PMID: 25788198 DOI: 10.1007/s12072-015-9613-5]

6 **Bocca C**, Novo E, Miglietta A, Parola M. Angiogenesis and Fibrogenesis in Chronic Liver Diseases. *Cell Mol Gastroenterol Hepatol* 2015; **1**: 477-488 [PMID: 28210697 DOI: 10.1016/j.jcmgh.2015.06.011]

7 **Fernandez M**. Molecular pathophysiology of portal hypertension. *Hepatology* 2015; **61**: 1406-1415 [PMID: 25092403 DOI: 10.1002/hep.27343]

8 **Fan K**, Wu K, Lin L, Ge P, Dai J, He X, Hu K, Zhang L. Metformin mitigates carbon tetrachloride-induced TGF-β1/Smad3 signaling and liver fibrosis in mice. *Biomed Pharmacother* 2017; **90**: 421-426 [PMID: 28390311 DOI: 10.1016/j.biopha.2017.03.079]

9 **Lim JY**, Oh MA, Kim WH, Sohn HY, Park SI. AMP-activated protein kinase inhibits TGF-β-induced fibrogenic responses of hepatic stellate cells by targeting transcriptional coactivator p300. *J Cell Physiol* 2012; **227**: 1081-1089 [PMID: 21567395 DOI: 10.1002/jcp.22824]

10 **Tripathi DM**, Erice E, Lafoz E, García-Calderó H, Sarin SK, Bosch J, Gracia-Sancho J, García-Pagán JC. Metformin reduces hepatic resistance and portal pressure in cirrhotic rats. *Am J Physiol Gastrointest Liver Physiol* 2015; **309**: G301-G309 [PMID: 26138461 DOI: 10.1152/ajpgi.00010.2015]

11 **Chen HP**, Shieh JJ, Chang CC, Chen TT, Lin JT, Wu MS, Lin JH, Wu CY. Metformin decreases hepatocellular carcinoma risk in a dose-dependent manner: population-based and in vitro studies. *Gut* 2013; **62**: 606-615 [PMID: 22773548 DOI: 10.1136/gutjnl-2011-301708]

12 **Pinzani M**. PDGF and signal transduction in hepatic stellate cells. *Front Biosci* 2002; **7**: d1720-d1726 [PMID: 12133817]

13 **Berra E**, Pagès G, Pouysségur J. MAP kinases and hypoxia in the control of VEGF expression. *Cancer Metastasis Rev* 2000; **19**: 139-145 [PMID: 11191053]

14 **Karar J**, Maity A. PI3K/AKT/mTOR Pathway in Angiogenesis. *Front Mol Neurosci* 2011; **4**: 51 [PMID: 22144946 DOI: 10.3389/fnmol.2011.00051]

15 **Caligiuri A**, Bertolani C, Guerra CT, Aleffi S, Galastri S, Trappoliere M, Vizzutti F, Gelmini S, Laffi G, Pinzani M, Marra F. Adenosine monophosphate-activated protein kinase modulates the activated phenotype of hepatic stellate cells. *Hepatology* 2008; **47**: 668-676 [PMID: 18098312 DOI: 10.1002/hep.21995]

16 **Tadakawa M**, Takeda T, Li B, Tsuiji K, Yaegashi N. The anti-diabetic drug metformin inhibits vascular endothelial growth factor expression via the mammalian target of rapamycin complex 1/hypoxia-inducible factor-1α signaling pathway in ELT-3 cells. *Mol Cell Endocrinol* 2015; **399**: 1-8 [PMID: 25179820 DOI: 10.1016/j.mce.2014.08.012]

17 **Al Qahtani A**, Holly J, Perks C. Hypoxia negates hyperglycaemia-induced chemo-resistance in breast cancer cells: the role of insulin-like growth factor binding protein 2. *Oncotarget* 2017; **8**: 74635-74648 [PMID: 29088813 DOI: 10.18632/oncotarget.20287]

18 **Garcia-Tsao G**, Abraldes JG, Berzigotti A, Bosch J. Portal hypertensive bleeding in cirrhosis: Risk stratification, diagnosis, and management: 2016 practice guidance by the American Association for the study of liver diseases. *Hepatology* 2017; **65**: 310-335 [PMID: 27786365 DOI: 10.1002/hep.28906]

19 **Borkham-Kamphorst E**, Weiskirchen R. The PDGF system and its antagonists in liver fibrosis. *Cytokine Growth Factor Rev* 2016; **28**: 53-61 [PMID: 26547628 DOI: 10.1016/j.cytogfr.2015.10.002]

20 **Pyla R**, Osman I, Pichavaram P, Hansen P, Segar L. Metformin exaggerates phenylephrine-induced AMPK phosphorylation independent of CaMKKβ and attenuates contractile response in endothelium-denuded rat aorta. *Biochem Pharmacol* 2014; **92**: 266-279 [PMID: 25179145 DOI: 10.1016/j.bcp.2014.08.024]

21 **Agard C**, Rolli-Derkinderen M, Dumas-de-La-Roque E, Rio M, Sagan C, Savineau JP, Loirand G, Pacaud P. Protective role of the antidiabetic drug metformin against chronic experimental pulmonary hypertension. *Br J Pharmacol* 2009; **158**: 1285-1294 [PMID: 19814724 DOI: 10.1111/j.1476-5381.2009.00445.x]

22 **Trebicka J**, Hennenberg M, Laleman W, Shelest N, Biecker E, Schepke M, Nevens F, Sauerbruch T, Heller J. Atorvastatin lowers portal pressure in cirrhotic rats by inhibition of RhoA/Rho-kinase and activation of endothelial nitric oxide synthase. *Hepatology* 2007; **46**: 242-253 [PMID: 17596891 DOI: 10.1002/hep.21673]

23 **Hennenberg M**, Trebicka J, Stark C, Kohistani AZ, Heller J, Sauerbruch T. Sorafenib targets dysregulated Rho kinase expression and portal hypertension in rats with secondary biliary cirrhosis. *Br J Pharmacol* 2009; **157**: 258-270 [PMID: 19338580 DOI: 10.1111/j.1476-5381.2009.00158.x]

24 **Liu H**, Chen Z, Liu J, Liu L, Gao Y, Dou D. Endothelium-independent hypoxic contraction of porcine coronary arteries may be mediated by activation of phosphoinositide 3-kinase/Akt pathway. *Vascul Pharmacol* 2014; **61**: 56-62 [PMID: 24685819 DOI: 10.1016/j.vph.2014.03.005]

25 **Liegl R**, Wertheimer C, Kernt M, Docheva D, Kampik A, Eibl-Lindner KH. Attenuation of human lens epithelial cell spreading, migration and contraction via downregulation of the PI3K/Akt pathway. *Graefes Arch Clin Exp Ophthalmol* 2014; **252**: 285-292 [PMID: 24263529 DOI: 10.1007/s00417-013-2524-z]

26 **Carnevale D**, Vecchione C, Mascio G, Esposito G, Cifelli G, Martinello K, Landolfi A, Selvetella G, Grieco P, Damato A, Franco E, Haase H, Maffei A, Ciraolo E, Fucile S, Frati G, Mazzoni O, Hirsch E, Lembo G. PI3Kγ inhibition reduces blood pressure by a vasorelaxant Akt/L-type calcium channel mechanism. *Cardiovasc Res* 2012; **93**: 200-209 [PMID: 22038741 DOI: 10.1093/cvr/cvr288]

27 **Miao L**, Dai Y, Zhang J. Mechanism of RhoA/Rho kinase activation in endothelin-1- induced contraction in rabbit basilar artery. *Am J Physiol Heart Circ Physiol* 2002; **283**: H983-H989 [PMID: 12181127 DOI: 10.1152/ajpheart.00141.2002]

28 **Coulon S**, Heindryckx F, Geerts A, Van Steenkiste C, Colle I, Van Vlierberghe H. Angiogenesis in chronic liver disease and its complications. *Liver Int* 2011; **31**: 146-162 [PMID: 21073649 DOI: 10.1111/j.1478-3231.2010.02369.x]

29 **Lee JS**, Semela D, Iredale J, Shah VH. Sinusoidal remodeling and angiogenesis: a new function for the liver-specific pericyte? *Hepatology* 2007; **45**: 817-825 [PMID: 17326208 DOI: 10.1002/hep.21564]

30 **Aleffi S**, Navari N, Delogu W, Galastri S, Novo E, Rombouts K, Pinzani M, Parola M, Marra F. Mammalian target of rapamycin mediates the angiogenic effects of leptin in human hepatic stellate cells. *Am J Physiol Gastrointest Liver Physiol* 2011; **301**: G210-G219 [PMID: 21252047 DOI: 10.1152/ajpgi.00047.2010]

31 **Zhang F**, Kong D, Chen L, Zhang X, Lian N, Zhu X, Lu Y, Zheng S. Peroxisome proliferator-activated receptor-γ interrupts angiogenic signal transduction by transrepression of platelet-derived growth factor-β receptor in hepatic stellate cells. *J Cell Sci* 2014; **127**: 305-314 [PMID: 24259663 DOI: 10.1242/jcs.128306]

32 **Zhang F**, Zhang Z, Chen L, Kong D, Zhang X, Lu C, Lu Y, Zheng S. Curcumin attenuates angiogenesis in liver fibrosis and inhibits angiogenic properties of hepatic stellate cells. *J Cell Mol Med* 2014; **18**: 1392-1406 [PMID: 24779927 DOI: 10.1111/jcmm.12286]


**P- Reviewer**: Shin T, Siddiqui I **S- Editor**: Gong ZM
**L- Editor**: Wang TQ **E- Editor**: Li D

World Journal of Gastroenterology

Submit a Manuscript: http://www.f6publishing.com

*World J Gastroenterol* 2018 February 21; 24(7): 833-843

DOI: 10.3748/wjg.v24.i7.833

ISSN 1007-9327 (print) ISSN 2219-2840 (online)

ORIGINAL ARTICLE

Basic Study

# Fish oil alleviates liver injury induced by intestinal ischemia/reperfusion *via* AMPK/SIRT-1/autophagy pathway

Hui-Rong Jing, Fu-Wen Luo, Xing-Ming Liu, Xiao-Feng Tian, Yun Zhou

Hui-Rong Jing, Fu-Wen Luo, Xing-Ming Liu, Xiao-Feng Tian, Department of General Surgery, Second Affiliated Hospital of Dalian Medical University, Dalian 116023, Liaoning Province, China

Yun Zhou, Department of Clinical Nutrition, Second Affiliated Hospital of Dalian Medical University, Dalian 116023, Liaoning Province, China

ORCID number: Hui-Rong Jing (0000-0003-2725-1785); Fu-Wen Luo (0000-0002-4891-535X); Xing-Ming Liu (0000-0001-9875-9573); Xiao-Feng Tian (0000-0001-9219-1868); Yun Zhou (0000-0003-0036-0332).

Author contributions: Jing HR and Luo FW performed the majority of experiments and almost equally contributed to the present study; Luo FW and Liu XM provided vital reagents and analytical tools and were also involved in editing the manuscript; Jing HR coordinated and provided the collection of all the human material in addition to providing financial support for this work; Tian XF and Zhou Y designed the study and wrote the manuscript.

Supported by the National Natural Science Foundation of China, No. 81600446; Natural Science Foundation of Liaoning Province, China, No. 201102048; and Natural Science Foundation of Dalian Medical Association, No. WSJ/KJC-01-JL-01.

Institutional review board statement: The study was reviewed and approved by the review board of Dalian Medical University, Liaoning Province, China.

Institutional animal care and use committee statement: All procedures involving animals were reviewed and approved by the Institutional Animal Care and Use Committee of the Dalian Medical University (Permit number: SCXK 2008-0002).

Conflict-of-interest statement: There is no conflict of interest in this study.

Data sharing statement: No additional data are available.



Manuscript source: Unsolicited manuscript

Correspondence to: Yun Zhou, MD, Doctor, Department of Clinical Nutrition, Second Affiliated Hospital of Dalian Medical University, No. 467, Zhongshan Road, Shahekou District, Dalian 116023, Liaoning Province, China. zydy2ynutrition@126.com
Telephone: +86-411-84690722
Fax: +86-411- 84672130

Received: October 28, 2017
Peer-review started: October 30, 2017
First decision: November 15, 2017
Revised: December 25, 2017
Accepted: January 15, 2018
Article in press: January 15, 2018
Published online: February 21, 2018

## Abstract

### *AIM*

To evaluate whether fish oil (FO) can protect liver injury induced by intestinal ischemia/reperfusion (I/R) *via* the AMPK/SIRT-1/autophagy pathway.

### *METHODS*

Ischemia in Wistar rats was induced by superior mesenteric artery occlusion for 60 min and reperfusion for 240 min. One milliliter per day of FO emulsion or normal saline was administered by intraperitoneal injection for 5 consecutive days to each animal. Animals were sacrificed at the end of reperfusion. Blood and

tissue samples were collected for analyses. AMPK, SIRT-1, and Beclin-1 expression was determined in lipopolysaccharide (LPS)-stimulated HepG2 cells with or without FO emulsion treatment.

***RESULTS***

Intestinal I/R induced significant liver morphological changes and increased serum alanine aminotransferase and aspartate aminotransferase levels. Expression of p-AMPK/AMPK, SIRT-1, and autophagy markers was decreased whereas tumor necrosis factor-α (TNF-α) and malonaldehyde (MDA) were increased. FO emulsion blocked the changes of the above indicators effectively. Besides, in LPS-stimulated HepG2 cells, small interfering RNA (siRNA) targeting AMPK impaired the FO induced increase of p-AMPK, SIRT-1, and Beclin-1 and decrease of TNF-α and MDA. SIRT-1 siRNA impaired the increase of SIRT-1 and Beclin-1 and the decrease of TNF-α and MDA.

***CONCLUSION***

Our study indicates that FO may protect the liver against intestinal I/R induced injury through the AMPK/SIRT-1/autophagy pathway.

**Key words:** Fish oil; AMPK/SIRT1/autophagy; Liver injury; Intestinal ischemia/reperfusion



**Core tip:** Intestinal ischemia/reperfusion (I/R) injury is a remarkable problem in many clinical conditions. Increased evidence indicates AMPK/SIRT-1 pathway linked autophagy exhibits a protective effect in liver diseases. Fish oil (FO) emulsion improves outcomes in patients with parenteral nutrition associated liver injury. We aimed to evaluate whether FO can protect liver injury induced by intestinal I/R *via* the AMPK/SIRT-1/autophagy pathway. Our results indicate that FO may protect the liver against intestinal I/R induced injury through the AMPK/SIRT-1/autophagy pathway. To our knowledge, we maybe for the first time present that FO attenuated intestinal I/R induced liver injury by inducing autophagy both *in vivo* and *in vitro* through the AMPK/SIRT-1 signaling pathway.

Jing HR, Luo FW, Liu XM, Tian XF, Zhou Y. Fish oil alleviates liver injury induced by intestinal ischemia/reperfusion *via* AMPK/SIRT-1/autophagy pathway. *World J Gastroenterol* 2018; 24(7): 833-843 Available from: URL: http://www.wjgnet.com/1007-9327/full/v24/i7/833.htm DOI: http://dx.doi.org/10.3748/wjg.v24.i7.833

## INTRODUCTION

Ischemia-reperfusion (I/R) injury of the intestine is a remarkable problem in many clinical conditions. Patients who suffer from conditions including abdominal aortic aneurysm surgery, cardiopulmonary bypass, intestinal transplantation, necrotizing enterocolitis, strangulated hernias, collapse of systemic circulation, and hypovolemic and septic shock have a potential risk for intestinal I/R[1-3]. Intestinal I/R is associated with a high morbidity and mortality[4]. Despite intensive study efforts over the past decades, pharmacologic therapies for liver injury induced by intestinal I/R have remained ineffective and controversial[5]. Patients who underwent persistent intestinal ischemia are often accompanied with the complication of septic shock, which eventually induces multiorgan dysfunction syndrome (MODS) and death[6].

The liver is the first organ which is affected by intestinal I/R because of the washout of toxic substances from the re-perfused intestine[7]. In addition, it is presumably due to the fact that the vasculature of the liver is associated with the intestine[8]. The gut-liver axis with cytokine cascade may play an important role in the liver injury induced by intestinal I/R[9]. The pathophysiology of acute liver injury is unclear; however, the prominent neutrophil infiltration and other related injury models suggest that oxygen radical species and inflammatory cascade crosstalk in this pathogenesis, which eventually results in final liver failure and even MODS[6].

Autophagy is a regulated cellular pathway involved in the turnover of cytoplasmic organelles and proteins through a lysosome-dependent degradation process[10]. Recent studies indicated that autophagy deficiency promoted inflammatory reaction and oxidative stress[11,12], implicating a protective function. In addition, autophagy can be modulated by several pathways, the most crucial one of which is the adenosine 5'-monophosphate-activated protein kinase/sirtuin 1 (AMPK/SIRT-1) pathway[13]. Increasing evidence indicates that AMPK/SIRT-1 pathway linked autophagy plays a protective effect in various diseases including liver injury. Studies also reported that resveratrol, a kind of natural polyphenol, regulates autophagy by activating the AMPK/SIRT-1 signaling pathway in neuroblastoma and endothelial cells[14]. Furthermore, inducing autophagy by activating AMPK/SIRT-1 alleviates oxidized low-density lipoprotein (oxLDL)-induced human umbilical vein endothelial cell injury[15]. However, the role of the AMPK/SIRT-1/autophagy pathway in intestinal I/R-challenged liver injury is still unknown.

Fish oil (FO), containing major ingredients as ω-3 polyunsaturated fatty acids including eicosapentaenoic acid (EPA) and docosahexaenoic acid (DHA), has been widely used as a therapeutic intervention in critical care settings[16]. Parenteral FO improves outcomes in patients with parenteral nutrition associated-liver injury[17]. FO has been shown to be a potent activator of the AMPK/SIRT-1 pathway against lung injury induced

by intestinal I/R[16]. Herein, we hypothesized that FO could be an appropriate agent for intestinal I/R-induced liver injury *via* the AMPK/SIRT-1/autophagy pathway.

## MATERIALS AND METHODS

### Animals

Male Wistar rats weighing 180-220 g from the Animal Center of Dalian Medical University were used in this study, and maintained under standard laboratory conditions. All rats were fed standard laboratory food and water. Rats were housed in a barrier system at 25 ℃ with 12 h light-12 h dark cycles and acclimated for 1 wk before experimentation. All procedures were carried out in strict accordance with the recommendations in the Guide for the Care and Use of Laboratory Animals of the National Institutes of Health. The protocol was approved by the Committee on the Ethics of Animal Experiments of Dalian Medical University (Permit number: SCXK 2008-0002). All surgery was performed under sodium pentobarbital anesthesia, and all efforts were made to minimize animal suffering.

### Experimental design

Intestinal I/R was induced in rats according to a previously standardized method[16]. Briefly, after a midline laparotomy was performed, the superior mesenteric artery was gently isolated and occluded with an atraumatic microvascular clamp for 60 min and then followed by reperfusion for 240 min. When mesenteric pulsations ceased and the intestine became pale in color, occlusion was confirmed. And reperfusion was confirmed when the pusatile flow returned to the mesenteric artery and its branches. For sham operation, the superior mesenteric artery was only isolated without occlusion.

The rats were randomly divided into three groups ($n$ = 8 each): (1) sham group; (2) I/R group; and (3) FO group. In the FO group, rats were pretreated intraperitoneally with 1 mL/d of FO emulsion (100 mL of FO emulsion contained 2.82 g of EPA and 3.09 g of DHA; Fresenius Kabi, Bad Homburg, Germany) for five consecutive days, and then surgery was performed as that in the I/R group. The same volume of normal saline was administered in the sham group and I/R group.

The dose of FO emulsion pretreatment was selected according to a previous study[16], and a pilot study has been performed. All animals were sacrificed at the end of reperfusion and tissue and blood samples were obtained for further analysis.

### Intestinal and liver morphological assessment

Intestinal and liver tissues were fixed in 10% formalin, embedded in paraffin, cut into 4-μm sections, and stained with hematoxylin and eosin (H&E) for light microscopy. Scores of liver and intestine pathology were evaluated according to previous studies[7-9].

### Measurement of serum aspartate aminotransferase, alanine aminotransferase, tumor necrosis factor-α, and liver malonaldehyde

Serum was obtained from blood samples by centrifugation (1000 *g*, 10 min, 4 ℃) and stored at -80 ℃ for assessment. Serum alanine aminotransferase (ALT) and aspartate aminotransferase (AST) levels were measured with an OLYMPUS AU1000 automatic analyzer (Aus Bio Laboratories Co., Ltd., Beijing, China). Serum tumor necrosis factor-α (TNF-α) was quantified using a rat enzyme-linked immunosorbent assay kit (BOSTER Bioengineering Co Ltd, Wuhan, China). Liver tissues were harvested and homogenized immediately on ice in five volumes of normal saline. Homogenates were centrifuged at 1200 *g* for 10 min. Liver malonaldehyde (MDA) concentration in the supernatant was determined using an assay kit (Nanjing Jiancheng Corp., Nanjing, China), according to the manufacturer's recommendations. The activity of MDA is expressed in nmol/mg prot.

### Cell culture and treatment

HepG2 cells were cultured in Dulbecco's Modified Eagle's Medium (Gibco, CA, United States) supplemented with 10% fetal bovine serum. The cells were kept at 37 ℃ in a humidified atmosphere with 5% $CO_2$, 100 units/mL of penicillin, and 10 μg/mL of streptomycin. Media were collected and centrifuged 48 h after treatment with lipopolysaccharide (LPS; 10 μg/mL, Sigma-Aldrich, United States) in the presence or absence of FO (50 mmol/L EPA/50 mmol/L DHA each mixture) and TNF-α was measured with a specific ELISA kit (Jiancheng, Nanjing, China) according to the manufacturer's protocol.

The doses of FO and LPS pretreatment were selected according to previous studies[16,18], and a pilot study has been performed.

### Western blot analysis of p-AMPK, SIRT-1, LC3 Ⅱ, Beclin-1, and P62 in liver tissue and HepG2 cells

For detecting p-AMPK, SIRT-1, LC3 Ⅱ, Beclin-1, and P62 contents in liver tissue, 30 μg of protein was separated by 12% or 15% SDS-PAGE (Bio-Rad, Hercules, United States), and transferred to polyvinylidene difluoride membranes (Millipore, Bedford, United States). The membranes were then incubated with primary anti-p-AMPK (Abcam Ltd., Cambridge, United Kingdom), anti-SIRT-1 (Abcam Ltd., Hong Kong, China), anti-LC3 Ⅰ, anti-LC3 Ⅱ, anti-P62, anti-Beclin-1, or anti-β-actin antibody (Santa Cruz Biotechnology, United States) in Tris buffered solution (TBS) containing 5% skimmed milk overnight at 4 ℃. After washing three times in TBS with 0.1% Tween 20 (TTBS), the membranes were incubated with biotinylated secondary antibody diluted 1:1000 in PBST containing 5% skimmed milk for 2 h at 37 ℃. After extensive washing with TTBS, the membranes were exposed to enhanced

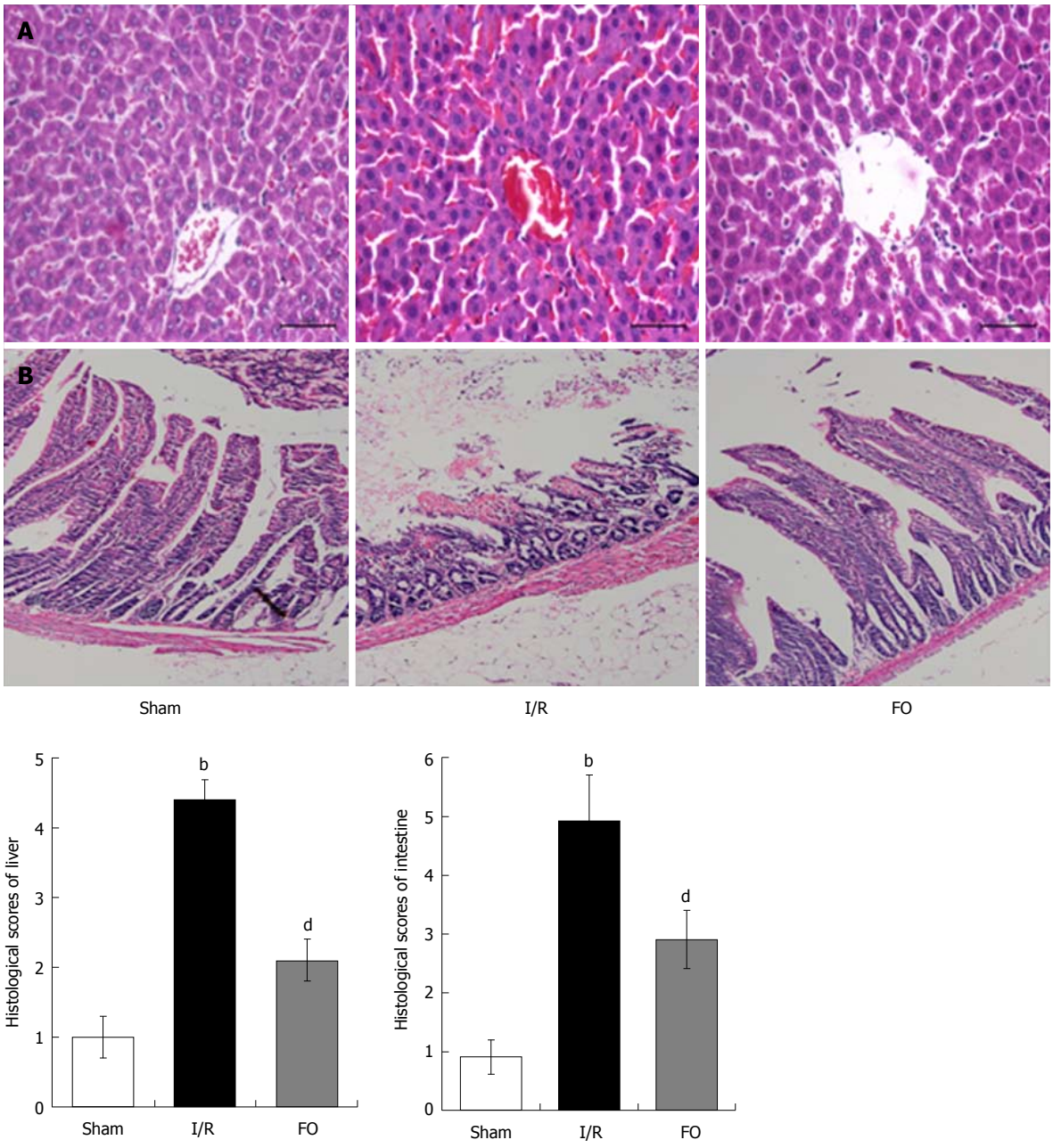


**Figure 1 Fish oil emulsion improves I/R induced liver and intestinal injury histopathologically.** Pathologic changes of liver (A) and intestinal (B) tissues in different groups (mean ± SD, $n = 8$). $^{b}P < 0.01$ *vs* sham group; $^{d}P < 0.01$ *vs* I/R group.

chemiluminescence-plus reagents (Beyotime Institute of Biotechnology, Hangzhou, China). Emitted light was documented with a BioSpectrum-410 multispectral imaging system with a Chemi HR camera 410 (UVP, Upland, CA, United States) and analyzed with Gel-Pro Analyzer Version 4.0 (Media Cybernetics, Bethesda, United States).

### *Quantitative real-time polymerase chain reaction (RT-PCR) analysis of liver AMPK and SIRT-1 mRNA levels*

Total RNA was extracted from rat liver using Trizol reagent (Invitrogen, Carlsbad, CA, United States) according to the manufacturer's instructions. Reverse transcription into cDNA was performed using a TaKaRa RNA polymerase chain reaction (PCR) kit Version 3.0 (TaKaRa, Dalian, China) for PCR analysis; primers are shown as follows: AMPK forward, 5'-GTGGTGTTATCCTGTATGCCCTTCT-3' and reverse, 5'-CTGTTTAAACCATTCATGCTCTCGT-3'; SIRT-1 forward, 5'-AGCTGGGGTTTCTGTTTCCTGTGG-3' and reverse, 5'-CGAACATGGCTTGAGGATCTGGGA-3'; β-actin forward, 5'-AGAGGGAAATCGTGCGTGAC-3' and reverse, 5'-CAATAGTGATGACCTGGCCGT-3'. RT-PCR was performed with the SYBR Premix Ex Taq kit (Takara, Dalian, China) for fluorescence detection during amplification on an ABI 7500 Fast Real-Time PCR System (Applied Biosystems). PCR cycling was performed under the following conditions: initial denaturation at 95 ℃ for 30 s and 40 thermal cycles of 95 ℃ for 5 s, 60 ℃ for 34 s, and 72 ℃ for 30 s.

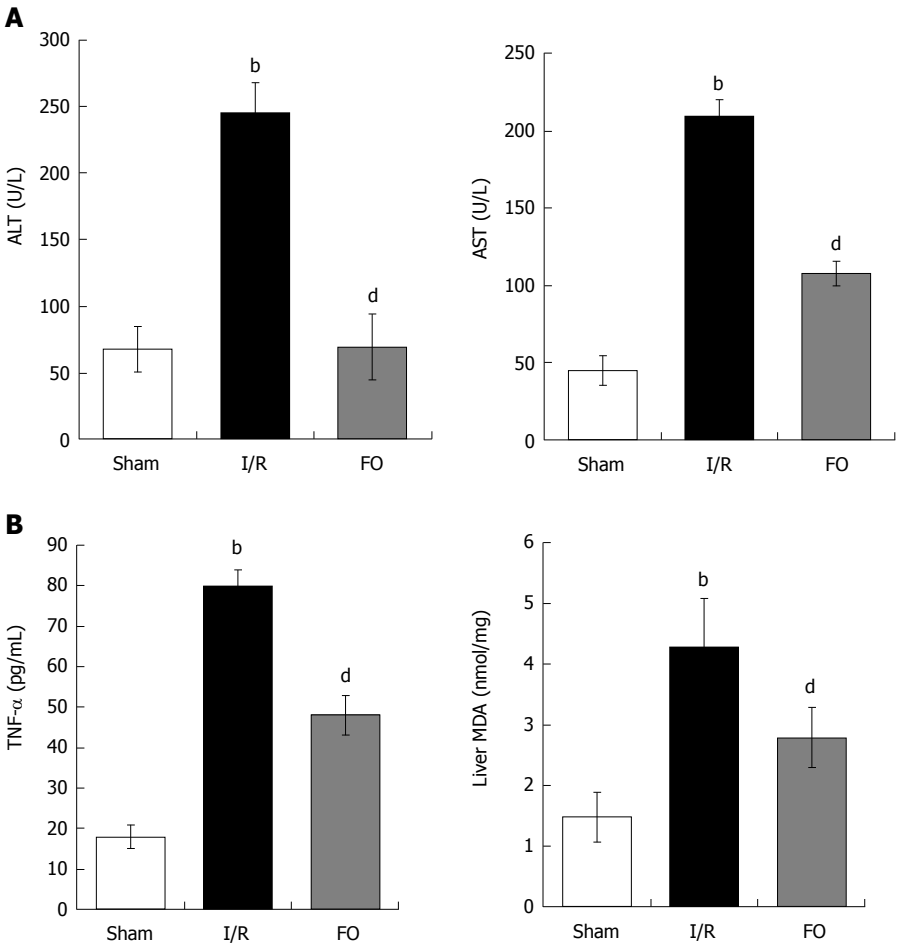


**Figure 2 Alanine aminotransferase and aspartate aminotransferase (A) as well as TNF-α and liver MDA levels (B) in different groups (mean ± SD, *n* = 8).** $^{b}P < 0.01$ *vs* sham group; $^{d}P < 0.01$ *vs* I/R group.

### *RNA interference*

HepG2 cells were transfected with small interfering RNAs (siRNAs) directed against AMPK α1 and SIRT-1, with scrambled siRNAs used as controls. Both specific and control siRNAs were obtained from GenePharma (Shanghai, China), and transient siRNA transfection was performed as previously described. After siRNA transfection for 48 h, the cells were treated with FO for an additional 6 h. The cells were then collected for the protein and mRNA analyses.

## RESULTS

### *Effect of FO emulsion on intestinal and liver injury induced by intestinal I/R*

Histopathological analysis of the liver in the I/R group showed apparent injury compared with the sham group, which was manifested as edema, hemorrhage, and neutrophil infiltration (Figure 1A). However, liver injury was significantly improved by pretreatment with FO emulsion, and the histopathological score was significantly reduced compared with the I/R group (Figure 1A, $P < 0.01$).

Compared with the sham group, intestinal mucosal injury was also found in the I/R group with apparent hemorrhage and loss of lamina propria villi and glands (Figure 1B). Pretreatment with FO emulsion significantly reduced the intestinal damage and histopathology score (Figure 1B, $P < 0.01$).

### *Effect of FO emulsion on serum ALT, AST, TNF-α, and liver MDA levels*

In the I/R group, there was a significant increase in serum ALT and AST levels compared with the sham group. However, pretreatment with FO significantly decreased serum levels of both ALT and AST compared with the I/R group (Figure 2A, $P < 0.01$). This indicated that FO emulsion was effective in improving liver function.

Moreover, serum TNF-α and liver MDA increased significantly after intestinal I/R compared with the sham group ($P < 0.01$). Furthermore, FO emulsion pretreatment dramatically reduced proinflammatory cytokine levels (Figure 2B, $P < 0.01$).

### *Effect of FO emulsion on LC3 Ⅱ, Beclin-1, and P62 expression in liver tissue after intestinal I/R*

Western blot analysis was performed to examine the expression of LC3 Ⅱ, Beclin-1, and P62 in liver tissue. Compared with the sham group, both LC3 Ⅱ

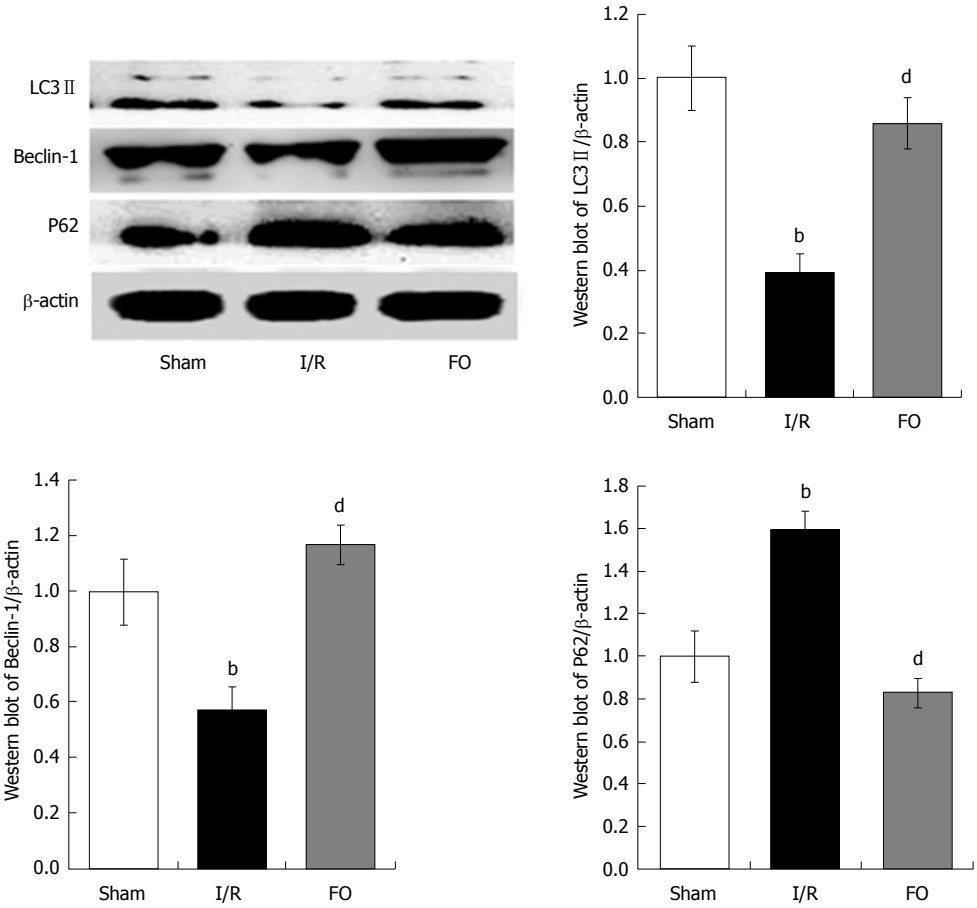


**Figure 3 Western blot analysis of liver autophagy (LC3 II, Beclin-1, and P62) levels in different groups (mean ± SD, *n* = 8).** $^{b}P < 0.01$ *vs* sham group; $^{d}P < 0.01$ *vs* I/R group.

and Beclin-1 expression was markedly decreased but P62 expression increased in the I/R group. However, pretreatment with FO emulsion markedly increased the expression of both LC3 Ⅱ and Beclin-1, and decreased the expression of P62 compared with the I/R group (Figure 3, $P < 0.01$), indicating that FO emulsion activated autophagy in intestinal I/R-induced liver injury.

### *Effect of AMPK/SIRT-1 activation by FO emulsion in liver tissue after intestinal I/R*

Western blot and RT-PCR analyses were performed to determine AMPK and SIRT-1 protein and mRNA contents in the liver. After intestinal I/R, the ratio of p-AMPK/AMPK protein and AMPK mRNA in the liver was dramatically decreased compared with the sham group (Figure 4A, $P < 0.01$). Similarly, both SIRT-1 protein and mRNA expression in the liver were dramatically decreased compared with the sham group (Figure 4B, $P < 0.01$). Nevertheless, not only the ratio of p-AMPK/AMPK protein and AMPK mRNA, but also the SIRT-1 protein and mRNA expression in the liver were dramatically increased by pretreatment with FO emulsion compared with the I/R group (Figure 4A and B, $P < 0.01$, $P < 0.05$).

### *FO emulsion ameliorates LPS induced HepG2 cell damage through the AMPK/SIRT-1/autophagy pathway*

To investigate the role of the AMPK/SIRT-1/autophagy pathway affected by FO emulsion in intestinal I/R-induced liver injury, HepG2 cells were employed and challenged with LPS to mimic the circumstance *in vivo.* Western blot analysis was then performed to examine the AMPK, SIRT-1, and Beclin-1 expression in LPS-stimulated HepG2 cells. Further, TNF-α and MDA were determined using experimental kits according to the manufacturer's protocols. Compared with the con group (control + LPS), the expression of p-AMPK, SIRT-1, and Beclin-1 was significantly increased in the FO group (FO + LPS) (Figure 5A, $P < 0.05$). This was associated with a significant decrease of TNF-α and MDA levels (Figure 5B, $P < 0.01$). However, p-AMPK, SIRT-1, and Beclin-1 expression was decreased significantly in the FO + siA (FO + AMPK siRNA + LPS) group compared with the FO group. Moreover, reduced SIRT-1 and Beclin-1 expression was observed in the FO + siS (FO + siRNA of SIRT-1 + LPS) group compared with the FO group (Figure 5A, $P < 0.05$). This was associated with a significant increase of TNF-α and MDA levels in HepG2 cells, although there was no change of p-AMPK (Figure

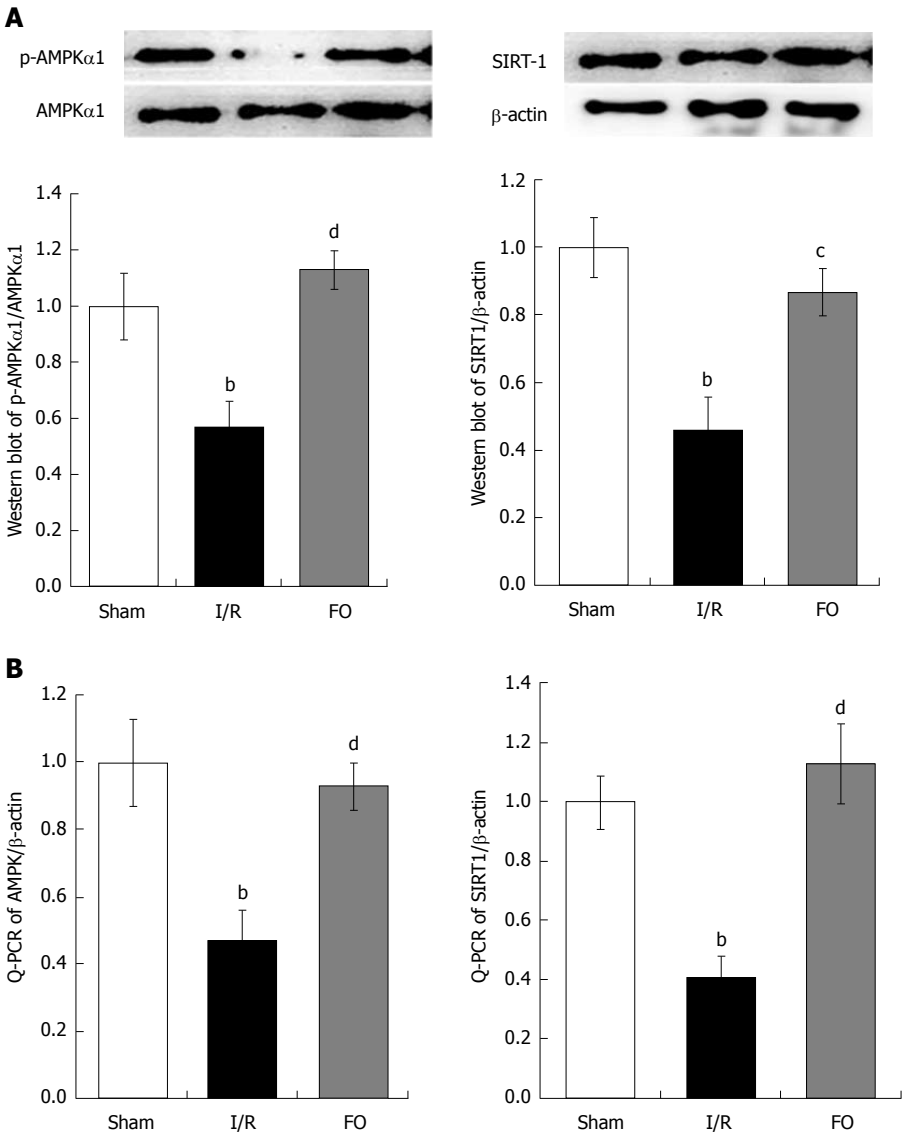


**Figure 4 Western blot analysis (A) of liver p-AMPKα1/AMPKα1 and qRT-PCR analysis (B) of liver AMPK expression in different groups (mean ± SD, *n* = 8).** [b]*P* < 0.01 *vs* sham group; [c]*P* < 0.05, [d]*P* < 0.01 *vs* I/R group.

5B, *P* < 0.05). Thus, FO emulsion may ameliorate liver injury induced by intestinal I/R through the AMPK/SIRT-1/autophagy pathway.

## DISCUSSION

To our knowledge, we may provide the first evidence of the protective effect of AMPK/SIRT-1/autophagy activated by FO in intestinal I/R induced liver injury. In the present study, we demonstrated that intestinal I/R caused significant liver injury, which was evidenced by: (1) apparent liver tissue edema, hemorrhage, and neutrophil infiltration; (2) liver dysfunction (increased serum AST and ALT levels) associated with increased TNF-α and MDA; (3) decreased protein and mRNA expression of p-AMPK/AMPK and SIRT-1 associated with autophagy (decreased LC3 Ⅱ and Beclin-1 expression but increased P62 expression); (4) FO emulsion restored the balance of the factors and alleviated liver injury; and (5) in LPS-stimulated HepG2 cells, AMPK siRNA impaired the FO-induced increase of p-AMPK, SIRT-1, and Beclin-1 but the decrease of TNF-α and MDA. SIRT-1 siRNA impaired the FO-induced increase of SIRT-1 and Beclin-1 but the decrease of TNF-α and MDA.

Intestinal I/R injury is the initiator of MODS and the promoter of distant organ injury[6]. Elucidating the series of events which lead to distant organ injury and a lethal consequence may provide clues to the pathogenesis of MODS and may further improve survival in critically ill patients. The liver is the most vulnerable organ even beyond the intestine *per se* when suffering intestinal I/R[7-9]. Liver malfunction often indicates a poor prognosis in MODS patients[9].

Oxidative stress and inflammatory cascade are two critical pathogeneses in liver injury induced by intestinal I/R. Intestinal I/R can induce leukocyte (including neutrophils and lymphocytes) infiltration

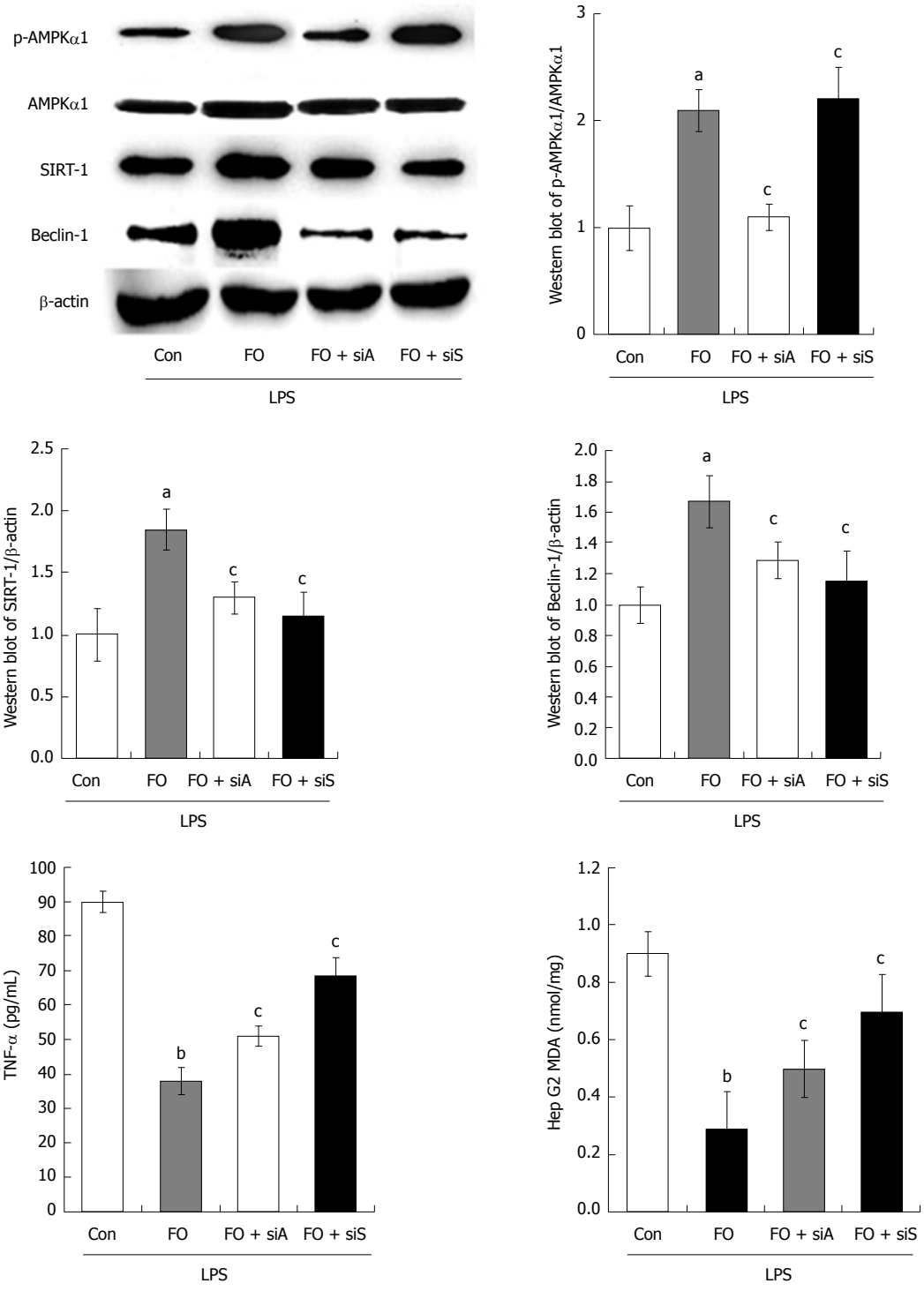


**Figure 5 p-AMPK, AMPK, SIRT-1, Beclin-1, TNF-α, and MDA expression in HepG2 cells challenged with LPS, LPS + FO, LPS + FO + siAMPK, or LPS + FO + siSIRT-1 (mean ± SD, *n* = 3).** $^{a}P < 0.05$, $^{b}P < 0.01$ *vs* control; $^{c}P < 0.05$ *vs* FO.

into the liver and results in an oxidative stress in sinusoids that contributes to subsequent hepatocellular injury[19]. It has been proposed that activated Kupffer cells and infiltrating neutrophils producing oxygen radicals and chemical inflammatory mediators such as TNF-α and IL-6 are involved in the gut I/R induced neutrophil accumulation in the liver[9]. TNF-α is regarded as the most important proinflammatory cytokine which contributes to both morbidity and mortality in inflammation cascade. Because the biological effects of TNF-α both in the liver and elsewhere, it has been widely used as an indicator of liver injury[9]. Further, MDA as an indicator of lipid peroxidation was determined in the present study[19]. We now demonstrated that serum TNF-α and liver MDA were increased after intestinal I/R. This is consistent with previous studies from our and other laboratories[7-9].

Autophagy is a lysosome-mediated degradative

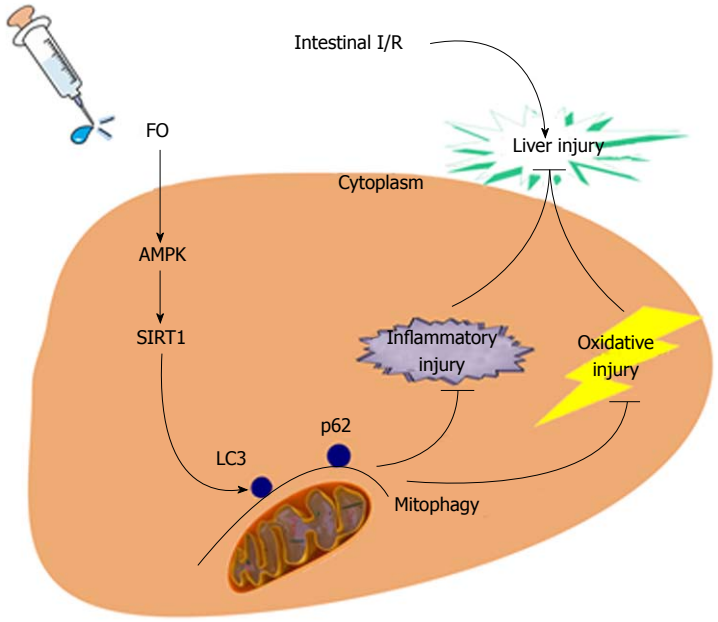


**Figure 6 Schematic representation of the novel potential protective mechanism of fish oil in liver injury induced by intestinal I/R through the AMPK/SIRT-1/autophagy pathway.**

pathway of cellular mechanisms for degrading misfolded proteins[10]. The execution of autophagy involves three critical proteins including LC3 Ⅱ, P62/SQSTM1, and Beclin 1[20-22]. Autophagy not only plays a crucial role in normal liver but also diseased liver. Moderate autophagy is benefit for cell survival against various stress stimulations. Nevertheless, excessive activation of autophagy results in cell death[23,24]. Autophagy also exhibits dual roles in different disease circumstances and also links to oxidative stress and inflammatory reaction[11,12]. Previous studies indicated that autophagy is a cellular self-protective mechanism against oxLDL-induced injury[13]. In the current study, decreased expression of essential autophagy regulators (decrease of Beclin 1 and LC3 Ⅱ and increase of P62) was observed in rat liver challenged by intestinal I/R. FO induced this self-protective mechanism, which manifested as an increase of rat liver autophagy in case of intestinal I/R. Similarly, FO also induced this self-protective mechanism in HepG2 cells in the presence of I/R. Our results suggested that FO conferred liver protection and amplified the activation of autophagy during intestinal I/R.

In addition, we identified the role of AMPK and SIRT-1 in FO stimulated autophagy in liver injury induced by intestinal I/R. SIRT-1 belongs to the mammalian family of sirtuins, a highly conserved family of NAD-dependent deacetylases that regulate cellular energy and lifespan in mammals[25]. A study of SIRT-1 knockout mice showed that SIRT-1 is an important regulator of autophagy[26]. SIRT-1 interacts with several essential components of the autophagy machinery and elevates autophagy. We and others have demonstrated that AMPK can enhance the activity of SIRT-1, which is associated with the cellular energy balance in animal models of stroke[26,27]. It has been reported that AMPK phosphorylation regulates SIRT-1 activity[16]. Herein, we found that a decrease of p-AMPK/AMPK and SIRT-1 protein and mRNA expression in rat liver suffering from intestinal I/R. However, FO promoted AMPK phosphorylation and SIRT-1 expression in intestinal I/R-induced liver injury. This is parallel with the autophagy levels but contradictory with TNF-α and MDA expression. This is consistent with a previous study indicating that AMPK decreases after cold I/R injury of intestinal preservation for transplantation and may be because of energy deprivation under ischemic conditions[28,29]. In addition, knockdown of AMPK impaired the FO-induced increase of p-AMPK, SIRT-1, and Beclin-1 but the decrease of TNF-α and MDA induced by in LPS-stimulated HepG2 cells, and knockdown of SIRT-1 impaired the FO-induced increase of SIRT-1 and Beclin-1 but the decrease of TNF-α and MDA. These indicated that FO stimulated autophagy through the AMPK/SIRT-1 signaling pathway in liver injury induced by intestinal I/R.

To our knowledge, we presented here, maybe for the first time, that FO attenuated intestinal I/R induced liver injury by inducing autophagy both *in vivo* and *in vitro* through the AMPK/SIRT-1 signaling pathway (Figure 6). Our results provide experimental evidence for future clinical applications of FO or FO-related products to prevent intestinal I/R associated liver disease. This study has some limitations, and further studies should be performed using gene knockout animals and clinical application should be concentrated.

## ARTICLE HIGHLIGHTS

### *Research background*

The liver is the most vulnerable organ after intestinal ischemia/reperfusion (I/R)

because the liver and intestine share the anatomical common pathway such as coupled vasculature. The mechanism is obscure and has multiple overlapping pathways. Increased evidence indicates that the AMPK/SIRT-1/autophagy pathway may be involved in this process. Fish oil (FO) may regulate the AMPK/SIRT-1/autophagy pathway to affect liver injury induced by intestinal I/R.

### Research motivation

Understanding and regulating AMPK/SIRT-1/autophagy pathway using a safe and effective substance like FO will be an important area of future research.

### Research objectives

This study aimed to provide evidence that FO can attenuate intestinal I/R induced liver injury by inducing autophagy through the AMPK/SIRT-1 pathway. This will provide a therapeutic target for future clinical applications of FO to prevent intestinal I/R associated liver disease.

### Research methods

This research was performed using Wistar rats challenged by intestinal I/R and HepG2 cells stimulated with LPS to mimic the *in vivo* pathogenesis. Further, RNA interference has been employed, which laid a foundation for the future gene knockout animal study.

### Research results

Intestinal I/R induced apparent liver injury, including histopathological injury and liver dysfunction, and this was associated with increased TNF-α and MDA, and decreased AMPK/SIRT-1/autophagy molecular function. FO emulsion restored the balance of the factors and alleviated liver injury. The similar results were observed in HepG2 cells stimulated with LPS.

### Research conclusions

Intestinal I/R induced liver injury is associated with decreased AMPK/SIRT-1/autophagy (LC3 Ⅱ, Beclin-1, and P62 expression) molecular function. FO emulsion restored the beneficial factors and alleviated liver injury. Similar results were observed in HepG2 cells. We present a novel theory here that FO can prevent intestinal I/R associated liver disease *via* the AMPK/SIRT-1/autophagy pathway. This may be a potential novel target for patients. We may provide the first evidence of AMPK/SIRT-1/autophagy regulated by FO in liver injury induced by intestinal I/R. Our hypothesis was confirmed using rat models and HepG2 cells treated with LPS and RNA interfere to mimic the conditions *in vivo*. Thus, FO and FO-related products may have novel clinical applications to prevent intestinal I/R associated liver disease in future.

### Research perspectives

This study has some limitations and further studies should be performed using gene knockout animals and clinical application should be concentrated.

## REFERENCES


1 **Mainous MR**, Ertel W, Chaudry IH, Deitch EA. The gut: a cytokine-generating organ in systemic inflammation? *Shock* 1995; **4**: 193-199 [PMID: 8574754]

2 **Pastores SM**, Katz DP, Kvetan V. Splanchnic ischemia and gut mucosal injury in sepsis and the multiple organ dysfunction syndrome. *Am J Gastroenterol* 1996; **91**: 1697-1710 [PMID: 8792684]

3 **Valentine RJ**, Hagino RT, Jackson MR, Kakish HB, Bengtson TD, Clagett GP. Gastrointestinal complications after aortic surgery. *J Vasc Surg* 1998; **28**: 404-411; discussion 411-412 [PMID: 9737449]

4 **Schütz A**, Eichinger W, Breuer M, Gansera B, Kemkes BM. Acute mesenteric ischemia after open heart surgery. *Angiology* 1998; **49**: 267-273 [PMID: 9555929 DOI: 10.1177/000331979804900404]

5 **Carrico CJ**, Meakins JL, Marshall JC, Fry D, Maier RV. Multiple-organ-failure syndrome. *Arch Surg* 1986; **121**: 196-208 [PMID: 3484944]

6 **Wilmore DW**, Smith RJ, O'Dwyer ST, Jacobs DO, Ziegler TR, Wang XD. The gut: a central organ after surgical stress. *Surgery* 1988; **104**: 917-923 [PMID: 3055397]

7 **Towfigh S**, Heisler T, Rigberg DA, Hines OJ, Chu J, McFadden DW, Chandler C. Intestinal ischemia and the gut-liver axis: an in vitro model. *J Surg Res* 2000; **88**: 160-164 [PMID: 10644483 DOI: 10.1006/jsre.1999.5767]

8 **Jing H**, Shen G, Wang G, Zhang F, Li Y, Luo F, Yao J, Tian XF. MG132 alleviates liver injury induced by intestinal ischemia/reperfusion in rats: involvement of the AhR and NFκB pathways. *J Surg Res* 2012; **176**: 63-73 [PMID: 22079846 DOI: 10.1016/j.jss.2011.09.001]

9 **Kaplan N**, Yagmurdur H, Kilinc K, Baltaci B, Tezel S. The protective effects of intravenous anesthetics and verapamil in gut ischemia/reperfusion-induced liver injury. *Anesth Analg* 2007; **105**: 1371-1378, table of contents [PMID: 17959968 DOI: 10.1213/01.ane.0000284696.99629.3a]

10 **Pandey UB**, Nie Z, Batlevi Y, McCray BA, Ritson GP, Nedelsky NB, Schwartz SL, DiProspero NA, Knight MA, Schuldiner O, Padmanabhan R, Hild M, Berry DL, Garza D, Hubbert CC, Yao TP, Baehrecke EH, Taylor JP. HDAC6 rescues neurodegeneration and provides an essential link between autophagy and the UPS. *Nature* 2007; **447**: 859-863 [PMID: 17568747 DOI: 10.1038/nature05853]

11 **Swanson MS**, Molofsky AB. Autophagy and inflammatory cell death, partners of innate immunity. *Autophagy* 2005; **1**: 174-176 [PMID: 16874072]

12 **Scherz-Shouval R**, Shvets E, Fass E, Shorer H, Gil L, Elazar Z. Reactive oxygen species are essential for autophagy and specifically regulate the activity of Atg4. *EMBO J* 2007; **26**: 1749-1760 [PMID: 17347651 DOI: 10.1038/sj.emboj.7601623]

13 **Jin X**, Chen M, Yi L, Chang H, Zhang T, Wang L, Ma W, Peng X, Zhou Y, Mi M. Delphinidin-3-glucoside protects human umbilical vein endothelial cells against oxidized low-density lipoprotein-induced injury by autophagy upregulation via the AMPK/SIRT1 signaling pathway. *Mol Nutr Food Res* 2014; **58**: 1941-1951 [PMID: 25047736 DOI: 10.1002/mnfr.201400161]

14 **Wu Y**, Li X, Zhu JX, Xie W, Le W, Fan Z, Jankovic J, Pan T. Resveratrol-activated AMPK/SIRT1/autophagy in cellular models of Parkinson's disease. *Neurosignals* 2011; **19**: 163-174 [PMID: 21778691 DOI: 10.1159/000328516]

15 **Guo H**, Chen Y, Liao L, Wu W. Resveratrol protects HUVECs from oxidized-LDL induced oxidative damage by autophagy upregulation via the AMPK/SIRT1 pathway. *Cardiovasc Drugs Ther* 2013; **27**: 189-198 [PMID: 23358928 DOI: 10.1007/s10557-013-6442-4]

16 **Jing H**, Yao J, Liu X, Fan H, Zhang F, Li Z, Tian X, Zhou Y. Fish-oil emulsion (omega-3 polyunsaturated fatty acids) attenuates acute lung injury induced by intestinal ischemia-reperfusion through Adenosine 5'-monophosphate-activated protein kinase-sirtuin1 pathway. *J Surg Res* 2014; **187**: 252-261 [PMID: 24231522 DOI: 10.1016/j.jss.2013.10.009]

17 **Puder M**, Valim C, Meisel JA, Le HD, de Meijer VE, Robinson EM, Zhou J, Duggan C, Gura KM. Parenteral fish oil improves outcomes in patients with parenteral nutrition-associated liver injury. *Ann Surg* 2009; **250**: 395-402 [PMID: 19661785 DOI: 10.1097/SLA.0b013e3181b36657]

18 **Dumoutier L**, Van Roost E, Colau D, Renauld JC. Human interleukin-10-related T cell-derived inducible factor: molecular cloning and functional characterization as an hepatocyte-stimulating factor. *Proc Natl Acad Sci USA* 2000; **97**: 10144-10149 [PMID: 10954742 DOI: 10.1073/pnas.170291697]

19 **Fan Z**, Jing H, Yao J, Li Y, Hu X, Shao H, Shen G, Pan J, Luo F, Tian X. The protective effects of curcumin on experimental acute liver lesion induced by intestinal ischemia-reperfusion through inhibiting the pathway of NF-κB in a rat model. *Oxid Med Cell Longev* 2014; **2014**: 191624 [PMID: 25215173 DOI: 10.1155/2014/191624]

20 **Liang XH**, Jackson S, Seaman M, Brown K, Kempkes B, Hibshoosh H, Levine B. Induction of autophagy and inhibition of tumorigenesis by beclin 1. *Nature* 1999; **402**: 672-676 [PMID: 10604474 DOI: 10.1038/45257]

21 **Bjørkøy G**, Lamark T, Johansen T. p62/SQSTM1: a missing link between protein aggregates and the autophagy machinery.

*Autophagy* 2006; **2**: 138-139 [PMID: 16874037]
22 **Tanida I**, Minematsu-Ikeguchi N, Ueno T, Kominami E. Lysosomal turnover, but not a cellular level, of endogenous LC3 is a marker for autophagy. *Autophagy* 2005; **1**: 84-91 [PMID: 16874052]
23 **Czaja MJ**, Ding WX, Donohue TM Jr, Friedman SL, Kim JS, Komatsu M, Lemasters JJ, Lemoine A, Lin JD, Ou JH, Perlmutter DH, Randall G, Ray RB, Tsung A, Yin XM. Functions of autophagy in normal and diseased liver. *Autophagy* 2013; **9**: 1131-1158 [PMID: 23774882 DOI: 10.4161/auto.25063]
24 **Rautou PE**, Mansouri A, Lebrec D, Durand F, Valla D, Moreau R. Autophagy in liver diseases. *J Hepatol* 2010; **53**: 1123-1134 [PMID: 20810185 DOI: 10.1016/j.jhep.2010.07.006]
25 **Cantó C**, Gerhart-Hines Z, Feige JN, Lagouge M, Noriega L, Milne JC, Elliott PJ, Puigserver P, Auwerx J. AMPK regulates energy expenditure by modulating NAD+ metabolism and SIRT1 activity. *Nature* 2009; **458**: 1056-1060 [PMID: 19262508 DOI: 10.1038/nature07813]
26 **Lee IH**, Cao L, Mostoslavsky R, Lombard DB, Liu J, Bruns NE, Tsokos M, Alt FW, Finkel T. A role for the NAD-dependent deacetylase Sirt1 in the regulation of autophagy. *Proc Natl Acad Sci USA* 2008; **105**: 3374-3379 [PMID: 18296641 DOI: 10.1073/pnas.0712145105]
27 **Wang LM**, Wang YJ, Cui M, Luo WJ, Wang XJ, Barber PA, Chen ZY. A dietary polyphenol resveratrol acts to provide neuroprotection in recurrent stroke models by regulating AMPK and SIRT1 signaling, thereby reducing energy requirements during ischemia. *Eur J Neurosci* 2013; **37**: 1669-1681 [PMID: 23461657 DOI: 10.1111/ejn.12162]
28 **Salehi P**, Walker J, Madsen KL, Sigurdson GT, Strand BL, Christensen BE, Jewell LD, Churchill TA. Relationship between energetic stress and pro-apoptotic/cytoprotective kinase mechanisms in intestinal preservation. *Surgery* 2007; **141**: 795-803 [PMID: 17560256 DOI: 10.1016/j.surg.2007.01.018]
29 **Zaouali MA**, Boncompagni E, Reiter RJ, Bejaoui M, Freitas I, Pantazi E, Folch-Puy E, Abdennebi HB, Garcia-Gil FA, Roselló-Catafau J. AMPK involvement in endoplasmic reticulum stress and autophagy modulation after fatty liver graft preservation: a role for melatonin and trimetazidine cocktail. *J Pineal Res* 2013; **55**: 65-78 [PMID: 23551302 DOI: 10.1111/jpi.12051]

**P- Reviewer**: Beltowski J, Dai ZJ **S- Editor**: Gong ZM
**L- Editor**: Wang TQ **E- Editor**: Huang Y

World Journal of Gastroenterology

Submit a Manuscript: http://www.f6publishing.com

*World J Gastroenterol* 2018 February 21; 24(7): 844-851

DOI: 10.3748/wjg.v24.i7.844

ISSN 1007-9327 (print) ISSN 2219-2840 (online)

ORIGINAL ARTICLE

Retrospective Cohort Study

# Elderly patients had more severe postoperative complications after pancreatic resection: A retrospective analysis of 727 patients

Ying-Tai Chen, Fu-Hai Ma, Cheng-Feng Wang, Dong-Bing Zhao, Ya-Wei Zhang, Yan-Tao Tian

Ying-Tai Chen, Fu-Hai Ma, Cheng-Feng Wang, Dong-Bing Zhao, Yan-Tao Tian, Department of Pancreatic and Gastric Surgery, National Cancer Center/Cancer Hospital, Chinese Academy of Medical Sciences and Peking Union Medical College, Beijing 100021, China

Ya-Wei Zhang, Department of Surgery, Yale School of Medicine, New Haven, CT 06520, United States

ORCID number: Ying-Tai Chen (0000-0003-4980-6315); Fu-Hai Ma (0000-0003-2437-6881); Cheng-Feng Wang (0000-0002-2349-0415); Dong-Bing Zhao (0000-0002-3011-5277); Ya-Wei Zhang (0000-0001-5248-4754); Yan-Tao Tian (0000-0001-6479-7547).

Author contributions: Tian YT contributed to study conception and design; Ma FH, Chen YT and Zhang YW contributed to data acquisition, analysis and interpretation, and writing of the article; Wang CF, Zhao DB and Tian YT performed the operations.

Supported by National Natural Science Foundation of China, No. 81401947; Beijing Nova Program, No. xxjh2015A090.

Institutional review board statement: The study was reviewed and approved by the Cancer Hospital of the Chinese Academy of Medical Sciences.

Informed consent statement: All study participants provided informed written consent prior to study enrolment.

Conflict-of-interest statement: The authors declare that they have no conflicts of interest.

Data sharing statement: The original anonymized dataset is available upon request from the corresponding author at tyt67@163.com.



Manuscript source: Unsolicited manuscript

Correspondence to: Yan-Tao Tian, MD, Professor, Department of Pancreatic and Gastric Surgery, National Cancer Center/Cancer Hospital, Chinese Academy of Medical Sciences and Peking Union Medical College, No. 17 Panjiayuan Nanli, Beijing 100021, China. tyt67@163.com
Telephone: +86-10-87787120
Fax: +86-10-87787120

Received: December 3, 2017
Peer-review started: December 4, 2017
First decision: December 20, 2017
Revised: January 3, 2018
Accepted: January 15, 2018
Article in press: January 15, 2018
Published online: February 21, 2018

## Abstract

### *AIM*

To examine the impact of aging on the short-term outcomes following pancreatic resection (PR) in elderly patients.

### *METHODS*

A retrospective cohort study using prospectively collected data was conducted at the China National Cancer Center. Consecutive patients who underwent PR from January 2004 to December 2015 were identified

and included. 'Elderly patient' was defined as ones age 65 and above. Comorbidities, clinicopathology, perioperative variables, and postoperative morbidity and mortality were compared between the elderly and young patients. Univariate and multivariate analyses were performed using the Cox proportional hazard model for severe postoperative complications (grades Ⅲb-Ⅴ).

***RESULTS***

A total of 454 (63.4%) patients were < 65-years-old and 273 (36.6%) patients were ⩾ 65-years-old, respectively. Compared to patients < 65-years-old, elderly patients had worse American Society of Anesthesiologists scores ($P$ = 0.007) and more comorbidities (62.6% *vs* 32.4%, $P$ < 0.001). Elderly patients had more severe postoperative complications (16.8% *vs* 9.0%, $P$ = 0.002) and higher postoperative mortality rates (5.5% *vs* 0.9%, $P$ < 0.001). In the multivariate Cox proportional hazards model for severe postoperative complications, age ⩾ 65 years [hazard ratio (HR) = 1.63; 95% confidence interval (CI): 1.18-6.30], body mass index ⩾ 24 kg/m$^2$ (HR = 1.20, 95%CI: 1.07-5.89), pancreaticoduodenectomy (HR = 4.86, 95%CI: 1.20-8.31) and length of operation ⩾ 241 min (HR = 2.97; 95%CI: 1.04-6.14) were significant ($P$ = 0.010, $P$ = 0.041, $P$ = 0.017 and $P$ = 0.012, respectively).

***CONCLUSION***

We found that aging is an independent risk factor for severe postoperative complications after PR. Our results might contribute to more informed decision-making for elderly patients.

**Key words:** Pancreatectomy; Aged; Pancreatic cancer; Postoperative complications; Mortality



**Core tip:** Pancreatic resection is the only treatment with curative potential for pancreatic cancer and periampullary cancer, and it is a useful treatment for other benign diseases. But, compromised physiological reserve and comorbidities may counterindicate pancreatic resection in elderly patients. We found that aging is an independent risk factor for severe postoperative complications (grades Ⅲb-Ⅴ). The potential deleterious effect of age on severe complications translates to a need for improvement in surgical management of elderly patients undergoing pancreatic resection. Our results might contribute to informed decision-making for elderly patients.

Chen YT, Ma FH, Wang CF, Zhao DB, Zhang YW, Tian YT. Elderly patients had more severe postoperative complications after pancreatic resection: A retrospective analysis of 727 patients. *World J Gastroenterol* 2018; 24(7): 844-851 Available from: URL: http://www.wjgnet.com/1007-9327/full/v24/i7/844.htm DOI: http://dx.doi.org/10.3748/wjg.v24.i7.844

## INTRODUCTION

The aging population worldwide is growing at a remarkable rate. It is predicted that the proportion of the population aged 65 or above, in developed and developing nations alike, will rise until at least 2050[1]. The incidence of pancreatic and periampullary cancer is strongly age-related, and elderly patients represent 60% of all diagnosed cases[2]. Pancreatic resection is the only treatment with curative potential for pancreatic and periampullary cancer, and it is a useful treatment for other benign diseases[3]. Thus, pancreatic surgeons will increasingly face decisions on whether to perform a pancreatic resection on elderly patients.

Over the last decade, several reports described outcomes for pancreatic resection on elderly patients; however, the results are inconsistent. Some studies[2,4-15] reported a positive association between age and the postoperative complications after pancreatic resections, whereas others[3,16-27] found no association. Moreover, the majority of such studies were conducted in developed countries. For developing countries, the data was scarce. As such, we conducted a single-center, large-scale retrospective study to examine the association between age and postoperative complications after pancreatic resections in Chinese patients.

## MATERIALS AND METHODS

Patients who underwent pancreatic resection at the Cancer Hospital of the Chinese Academy of Medical Sciences, China National Cancer Center from January 2004 to December 2015 were identified and included in the study. All pancreatic resections including pancreaticoduodenectomy ($n$ = 385), distal pancreatectomy ($n$ = 281) and middle-segment pancreatectomy ($n$ = 51) were reviewed. The patients were divided into those at the age of 65-years-old or above and those younger than 65 years. The patients aged at 65-years-old or above were defined as "elderly patients". All study procedures were approved by the Institutional Review Board at the Cancer Hospital of the Chinese Academy of Medical Sciences.

The following factors were compared between two groups: demographic characteristics, smoking and alcohol consumption, body mass index (BMI), hemoglobin and serum albumin levels, American Society of Anesthesiologists (ASA) score, preoperative biliary drainage, comorbidities (diabetes, coronary artery

disease, hypertension, chronic obstructive pulmonary disease, hepatitis B), previous history of cancer, previous abdominal surgery, family history of cancer, surgical procedure, intraoperative data (operative time, intraoperative blood loss), pathologic data, postoperative hospital stay, cost, perioperative complications and perioperative mortality.

Perioperative mortality was defined as in-hospital death within 30 d after surgery. The specific complications studied include delayed gastric emptying, pancreatic fistula, bile leak, gastrointestinal hemorrhage, cholangitis, pneumonia, wound infection, urinary tract infection, intraabdominal abscess, central line infection, and cerebrovascular accident. Postoperative complications were defined according to the Clavien-Dindo classification, and severe complications were defined as complications grade Ⅲb and greater[28,29]. Length of stay was calculated from the date of operation to the date of hospital discharge.

### Statistical analysis

$\chi^2$ tests (for categorical variables) or *t*-tests (for continuous variables) were used to examine the differences in patients' characteristics between the elderly and young groups. Univariate and multivariate Cox proportional hazards regression models were performed to identify independent predictors for severe postoperative complications (grades Ⅲb-Ⅴ). A *P*-value of less than 0.05 was considered statistically significant. Statistical analyses were conducted using SAS software version 9.3 (SAS Institute Inc., Cary, NC, United States).

## RESULTS

### Patient demographics and comorbidities

Pancreatic resection was performed in 454 elderly patients (63.4%) and 273 young patients (36.6%). The elderly patients had significantly higher male:female ratio and alcohol consumption (Table 1). Compared to the young patients, the elderly patients had statistically higher preoperative ASA scores, with 48.4% of these patients within Ⅲ/Ⅳ classes compared to 19.6% in the young patients ($P$ = 0.007), and had a higher rate of preoperative biliary drainage ($P$ = 0.011). The elderly patients had more comorbidities (62.6% *vs* 32.4%, $P$ < 0.001). The incidences of diabetes, hypertension and coronary artery disease were significantly higher in elderly patients (Table 1). Depending on the primary tumor localization, pancreaticoduodenectomy ($n$ = 385), middle-segment pancreatectomy ($n$ = 51) or distal pancreatectomy ($n$ = 281) were performed. The most common malignancies were pancreatic ductal adenocarcinoma in 45 (60.8%), and the rate of pancreatic ductal adenocarcinoma was higher in the elderly than in the young patients ($P$ < 0.001).

### Patient age and postoperative complications

Although overall complication rate was comparable between two groups (39.6% *vs* 33%, $P$ = 0.075), the incidence of postoperative severe complications (grades Ⅲb-Ⅴ) was significantly higher in elderly patients (16.8% *vs* 9.0%, $P$ = 0.002). Gastrointestinal hemorrhage and urinary tract infection was more frequent in the elderly patients. There was no significant difference in the incidence of delayed gastric emptying, pancreatic fistula, bile leak, cholangitis, pneumonia, wound infection, intraabdominal abscess, central line infection and cerebrovascular accident between the two groups. Postoperative mortality was significantly higher in the elderly patients (5.5% *vs* 0.9%, $P$ < 0.001) (Table 2).

### Patient age and operative variables/length of hospital stay

Age did not show a significant association with operative time, cost of hospitalization or postoperative hospital stay (Table 3). Intraoperative blood loss (median: 468 mL) was comparable between groups, whereas the number of individuals receiving blood transfusions was significantly greater among elderly patients (129/273 *vs* 169/454).

### Risk factors for severe postoperative complications (grades Ⅲb-Ⅴ) in elderly patients

Univariate Cox proportional hazards regression models identified the following risk factors for severe postoperative complications (grades Ⅲb-Ⅴ): age ⩾ 65 ($P$ = 0.002), BMI ⩾ 24 kg/m$^2$ ($P$ = 0.012), ASA score Ⅲ/Ⅳ ($P$ = 0.038), PD ($P$ < 0.001), and length of operation (⩾ 241 min) ($P$ = 0.004). In multivariate analysis, independent factors were age ⩾ 65 years [$P$ = 0.010; odds ratio (OR) = 1.63; 95% confidence interval (CI): 1.18-6.30], BMI ⩾ 24 kg/m$^2$ ($P$ = 0.041; OR = 1.20; 95%CI: 1.07-5.89), PD ($P$ = 0.017; OR = 4.86; 95%CI: 1.20-8.31), and length of operation ($P$ = 0.12; OR = 2.97; 95%CI: 1.04-6.14) (Table 4).

## DISCUSSION

Pancreatic resection is recognized as a highly invasive surgery. Despite recent advances in surgical technique, devices and perioperative care, elderly patients undergoing pancreatic resection remain a challenge, mainly due to compromised physiological reserve and comorbidities, which may negatively impact the postoperative outcomes[27].

In our study, we found that the incidence of severe postoperative complications (grades Ⅲb-Ⅴ) was significantly higher in elderly patients (16.8% *vs* 9.0%, $P$ = 0.002), although the overall complication rate was comparable between the two groups (39.6% *vs* 33%, $P$ = 0.075). Recently, centers in developed counties have started to report their results after pancreatic resection in the elderly. The majority of studies reported statistically higher postoperative complication rates

**Table 1 Demographic, comorbidity, operation type, and pathology data in patients grouped according to age**

| Variable | < 65 yr, *n* = 454 | ≥ 65 yr, *n* = 273 | Total, *n* = 727 | *P* value |
|---|---|---|---|---|
| Sex | | | | |
| Male | 202 | 159 | 361 | |
| Female | 252 | 114 | 366 | |
| Male:female ratio | 0.8 | 1.4 | 1.0 | 0.0003 |
| Mean BMI in kg/m$^2$ | 23.1 | 23.4 | 23.2 | 0.351 |
| Smoking | | | | 0.129 |
| Never | 323 | 180 | 503 | |
| Ever | 130 | 93 | 223 | |
| Mean smoking amount. in packs/yr | 50 | 53 | 51 | 0.127 |
| Mean smoking time in yr | 22.1 | 26.1 | 23.7 | 0.101 |
| Alcohol | | | | 0.017 |
| Never | 367 | 200 | 567 | |
| Ever | 87 | 73 | 160 | |
| Mean preoperative TBIL in μmol/L | 31.4 | 42.8 | 36.3 | 0.134 |
| Preoperative serum albumin in g/L | 39.7 | 37.8 | 38.9 | 0.111 |
| ASA category Ⅲ + Ⅳ | 89 | 77 | 166 | 0.007 |
| Preoperative biliary drainage | 51 | 49 | 100 | 0.011 |
| Comorbidity | | | | |
| Patients with any comorbidity | 147 | 171 | 318 | < 0.001 |
| Diabetes | 89 | 73 | 162 | 0.025 |
| Coronary artery disease | 18 | 57 | 75 | < 0.001 |
| Hypertension | 77 | 63 | 140 | 0.043 |
| COPD | 11 | 12 | 23 | 0.141 |
| HBV | 26 | 9 | 35 | 0.138 |
| HCV | 11 | 4 | 15 | 0.379 |
| Previous history of cancer | 3 | 6 | 9 | 0.070 |
| Previous abdominal surgery | 61 | 37 | 98 | 0.964 |
| Family history of cancer | 49 | 50 | 99 | 0.004 |
| Operation type | | | | |
| Pancreaticoduodenectomy | 232 | 153 | 385 | 0.196 |
| Distal pancreatectomy | 169 | 112 | 281 | 0.308 |
| Middle-segment pancreatectomy | 43 | 8 | 51 | 0.0008 |
| Pathology data | | | | |
| Pancreatic duct adenocarcinoma | 94 | 101 | 195 | < 0.001 |
| Others[1] | 360 | 172 | 532 | |

[1]Distal bile duct adenocarcinoma, ampulla adenocarcinoma, gall bladder adenocarcinoma, duodenal adenocarcinoma, intraductal papillary mucinous neoplasm, neuroendocrine neoplasm, pancreatic metastasis, solid pseudopapillary tumor, benign neoplasm, pancreatitis. ASA: American Society of Anesthesiologists; BMI: Body mass index; COPD: Chronic obstructive pulmonary disease; HBV: Hepatitis B virus; HCV: Hepatitis C virus; TBIL: Total bilirubin.

in the group they defined as elderly patients when compared to young patients. Lahat *et al*[8] reported that elderly patients (age ≥ 70 years) had more postoperative complications (41% *vs* 29%, *P* = 0.01), longer hospital stays (26.2 d *vs* 19.7 d, *P* < 0.0001) and higher incidences of perioperative mortality (5.4% *vs* 1.4%, *P* = 0.01). Adham *et al*[2] found that elderly patients had higher postoperative mortality rates (12.9% *vs* 3.9%, *P* = 0.04) and demonstrated age ≥ 70 years [hazard ratio (HR) = 3.5; 95%CI: 1.3-9.3] as an independent predictor of postoperative mortality. Ayman *et al*[14] showed that the incidence of complications was higher in elderly patients (25.9% in patients aged < 65 years, 36.8% in those aged at 65 to 69 years, and 37.5% in those aged ≥ 70 years, *P* = 0.006) and postoperative hospital mortality was comparable. Kow *et al*[10] found that morbidity rate in elderly patients was higher (56% *vs* 44%, *P* = 0.04) for age ≥ 70 years, but the mortality rate was comparable (0% *vs* 3%, *P* = 0.28). Riall *et al*[5] described increasing age as an independent risk factor for mortality after pancreatic resection by using a large population-based cohort. Another population-based study[15] in the Netherlands found that postoperative length of stay in hospital was longer and morbidity rate was higher (56% *vs* 44%, *P* = 0.04) among elderly patients, and also showed that elderly patient groups (≥ 70 years) exhibited a higher short-term mortality risk compared to patients under 70-years-old. Several studies did not show a statistical difference in overall morbidity or mortality rates between the older and younger groups. Our study is one of the largest studies, and our data is consistent with those from population-based studies.

Beside age, we also found BMI ≥ 24 kg/m$^2$, pancreaticoduodenectomy and length of operation ≥ 241 min (median) were independent risk factors for severe postoperative complications (grades Ⅲb-Ⅴ). Taken together, age alone should not be the only

**Table 2 Postoperative complications in patients grouped according to age**

| Complication | < 65 yr, *n* = 454 | ≥ 65 yr, *n* = 273 | Total, *n* = 727 | *P* value |
|---|---|---|---|---|
| Patients with any complication | 150 (33.0) | 108 (39.6) | 258 (35.5) | 0.075 |
| Patients with severe complication (grades Ⅲb-Ⅴ) | 41 (9.0) | 46 (16.8) | 87 (12.0) | 0.002[a] |
| Pancreatic fistula | 72 (15.9) | 55 (20.1) | 127 (17.5) | 0.140 |
| Delayed gastric emptying | 45 (9.9) | 35 (12.8) | 80 (11.0) | 0.225 |
| Bile leak | 15 (3.3) | 14 (5.1) | 29 (4.0) | 0.224 |
| Reoperation | 12 (2.6) | 11 (4.0) | 23 (3.2) | 0.301 |
| Readmission | 4 (0.9) | 1 (0.4) | 5 (0.7) | 0.416 |
| Gastrointestinal hemorrhage | 9 (2.0) | 13 (4.8) | 22 (3.0) | 0.034[a] |
| Wound infection | 18 (4.0) | 12 (4.4) | 30 (4.1) | 0.777 |
| Cholangitis | 6 (1.3) | 5 (1.8) | 11 (1.5) | 0.585 |
| Urinary tract infection | 12 (2.6) | 16 (5.9) | 28 (3.9) | 0.029[a] |
| Pneumonia | 7 (1.5) | 10 (3.7) | 17 (2.3) | 0.067 |
| Intraabdominal abscess | 13 (2.9) | 7 (2.6) | 20 (2.8) | 0.811 |
| Bacteremia | 7 (1.5) | 9 (3.3) | 16 (2.2) | 0.118 |
| Central line infection | 12 (2.6) | 10 (3.7) | 22 (3.0) | 0.437 |
| Pulmonary embolus | 0 (0) | 1 (0.4) | 1 (0.1) | 0.197 |
| Deep venous thrombosis | 1 (0.2) | 3 (1.1) | 4 (0.5) | 0.121 |
| Arrhythmia | 10 (2.2) | 11 (4.0) | 21 (2.9) | 0.154 |
| Cerebrovascular accident | 1 (0.2) | 1 (0.4) | 2 (0.3) | 0.716 |
| Mortality | 4 (0.9) | 15 (5.5) | 19 (2.6) | < 0.001[a] |

Data are presented as *n* (%). [a]Statistical significance.

**Table 3 Association among operative difficulty, postoperative hospital stay and cost with age**

| Variable | < 65 yr, *n* = 454 | ≥ 65 yr, *n* = 273 | Total, *n* = 727 | *P* value |
|---|---|---|---|---|
| Mean operative time in min | 239.8 | 247.5 | 243.1 | 0.330 |
| Mean intraoperative blood loss in mL | 461.0 | 479.1 | 468.0 | 0.650 |
| Blood transfusion, *n* | 169 | 129 | 298 | 0.008 |
| Mean postoperative hospital stay in d | 21.1 | 22.7 | 21.9 | 0.150 |
| Mean cost in RMB | 76411 | 73610 | 74717 | 0.790 |

**Table 4 Univariate and multivariate Cox proportional hazards models for severe postoperative complications (grades Ⅲb-Ⅴ)**

| Variable | Subgroup | Univariate | Multivariate | |
|---|---|---|---|---|
| | | *P* value | *P* value | HR (95%CI) |
| Medical risk factors | | | | |
| Age in yr | < 65 *vs* ≥ 65 | 0.002 | 0.010 | 1.63 (1.18-6.30) |
| BMI | < 24 kg/m$^2$ *vs* ≥ 24 kg/m$^2$ | 0.012 | 0.041 | 1.20 (1.07-5.89) |
| ASA classification | Ⅰ / Ⅱ *vs* Ⅲ / Ⅳ | 0.038 | 0.271 | - |
| Surgical risk factors | | | | |
| Pancreaticoduodenectomy | Yes *vs* No | < 0.001 | 0.017 | 4.86 (1.20-8.31) |
| Length of operation | < 241 min *vs* ≥ 241 min (median) | 0.004 | 0.012 | 2.97 (1.04-6.14) |

ASA: American Society of Anesthesiologists; BMI: Body mass index; CI: Confidence interval; HR: Hazard ratio.

contraindication to pancreatic resection. It is important for surgeons to recognize that elderly patients have higher severe postoperative complications. In order to allow the proper selection of those patients best suited for surgery, a more comprehensive evaluation of the comorbidities, BMI, complexity of the surgical procedure and type of surgical procedure is required.

The age groups studied vary among the published studies. Some studies[10,19] set 65-years-old as the cut-off for elderly patients, while others set the ages of 70 years[2,8,13,15,21,23,25,27], 75 years[3,18,22] or even 80 years[7,11,16,20] as cut-offs. We accepted the age of 65 years as a definition of elderly. Compared to patients aged < 65 years, those elderly patients had statistically higher preoperative ASA scores and more comorbidities, such as diabetes, hypertension and coronary artery disease. In the present series, the elderly patients had a higher rate of preoperative biliary drainage ($P$ = 0.011), which is in line with a previous study[21] that found most physicians might reduce the threshold of acceptable preoperative bilirubin in the elderly, fearing the well-known impact of sustained jaundice on nutritional status and renal function in elderly patients. The elderly patients also

had a higher rate of pancreatic duct adenocarcinoma; this could be explained by age-dependent biological differences.

The study has several strengths. First, to our knowledge, this is one of the largest studies in developing countries evaluating the effect of age on short-term outcomes after pancreatic resection. Second, our study used the Clavien-Dindo classification system to classify the complications associated with pancreatic resection, and we found that aging is an independent risk factor for severe postoperative complications (grades Ⅲb-Ⅴ), which have negative effects on health-related quality of life, length of stay and resource utilization[30,31]. Our study may provide a more realistic view of complications following pancreatic resection. As for the current study, there are several limitations. The retrospective nature of this study can be associated with selection bias. The study also took place over a 12-year period, during which advances in surgical technique, devices and perioperative care likely improved outcomes in elderly patients. In addition, all patients were analyzed from a single institution, so the findings may not be generalizable to other settings. The limited sample size makes it difficult to further perform subcategory analysis based on age.

In conclusion, increasing age is an independent risk factor for severe postoperative complications (grades Ⅲb-Ⅴ) after pancreatic resection. Therefore, pancreatic surgery should be considered with caution in elderly patients. Our results may contribute to informed decision-making for elderly patients.

## ARTICLE HIGHLIGHTS

### Research background

Pancreatic resection is the only treatment with curative potential for pancreatic cancer and periampullary cancer, and it is also a useful treatment for other benign diseases. But, compromised physiological reserve and comorbidities may counterindicate pancreatic resection on elderly patients. Over the last decade, several reports described outcomes for pancreatic resection on elderly patients; however the results are inconsistent. Some studies reported a positive association between age and the postoperative complications after pancreatic resections, whereas others found no association. Moreover, the majority of such studies were conducted in developed countries. For developing countries, the data was scarce.

### Research motivation

The aging population worldwide is growing at a remarkable rate. It is predicted that the proportion of the population aged 65 or above, in developed and developing nations alike, will rise until at least 2050. The incidence of pancreatic and periampullary cancer is strongly age-related, and elderly patients represent 60% of all diagnosed cases. Pancreatic resection is the only treatment with curative potential for pancreatic and periampullary cancer, and it is also a useful treatment for other benign diseases. Thus, pancreatic surgeons will increasingly face decisions on whether to perform a pancreatic resection on elderly patients. As such, we conducted a single-center, large-scale retrospective study to examine the association between age and postoperative complications after pancreatic resections in Chinese patients.

### Research objectives

The aim of this study is to examine the impact of aging on the short-term outcomes following pancreatic resection in elderly patients.

### Research methods

A retrospective cohort study using prospectively collected data was conducted at the Cancer Hospital of the Chinese Academy of Medical Sciences, China National Cancer Center. The patients were divided into those at the age of 65-years-old or above and those younger than 65 years. The patients aged at 65-years-old or above were defined as 'elderly patients'. The following factors were compared between two groups: demographic characteristics, smoking and alcohol consumption, body mass index (BMI), hemoglobin and serum albumin levels, American Society of Anesthesiologists (ASA) score, preoperative biliary drainage, comorbidities (diabetes, coronary artery disease, hypertension, chronic obstructive pulmonary disease, hepatitis B), previous history of cancer, previous abdominal surgery, family history of cancer, surgical procedure, intraoperative data (operative time, intraoperative blood loss), pathologic data, postoperative hospital stay, cost, perioperative complications and perioperative mortality.

### Research results

Compared to patients < 65-years-old, elderly patients had worse ASA scores ($P$ = 0.007) and more comorbidities (62.6% *vs* 32.4%, $P$ < 0.001). Operative time, intraoperative blood loss, postoperative hospital stay and cost were comparable. Elderly patients had more severe postoperative complications (grades Ⅲb-Ⅴ) (16.8% *vs* 9.0%, $P$ = 0.002) and higher postoperative mortality rates (5.5% *vs* 0.9%, $P$ < 0.001). In the multivariate Cox proportional hazards model for severe postoperative complications (grades Ⅲb-Ⅴ), age ⩾ 65 years, BMI ⩾ 24 kg/m$^2$, pancreaticoduodenectomy and length of operation ⩾ 241 min were significant.

### Research conclusions

Increasing age is an independent risk factor for severe postoperative complications (grades Ⅲb-Ⅴ) after pancreatic resection. Therefore, pancreatic surgery should be considered with caution in elderly patients. Our results may contribute to informed decision-making for elderly patients. Aging is an independent risk factor for severe postoperative complications after pancreatic resection. We found that aging is an independent risk factor for severe postoperative complications after pancreatic resection. Our results might contribute to more informed decision-making for elderly patients. We found that aging is an independent risk factor for severe postoperative complications (grades Ⅲb-Ⅴ) after pancreatic resection. Our results might contribute to more informed decision-making for elderly patients.

The association between age and postoperative complications after pancreatic resections in Chinese patients is unknown. Our study used the Clavien-Dindo classification system to classify the complications associated with pancreatic resection, and we found that aging is an independent risk factor for severe postoperative complications (grades Ⅲb-Ⅴ). Our study may provide a more realistic view of complications following pancreatic resection.

Elderly patients had more severe postoperative complications and higher postoperative mortality rates. Age ⩾ 65 years is an independent risk factor for severe postoperative complications (grades Ⅲb-Ⅴ) after pancreatic resection. Outcomes for pancreatic resection on elderly patients are inconsistent. This potential deleterious effect of age on severe complications needs improvement for surgical management of elderly patients undergoing pancreatic resection.

### Research perspectives

We found that aging is an independent risk factor for severe postoperative complications (grades Ⅲb-Ⅴ) after pancreatic resection. Our results might contribute to more informed decision-making for elderly patients.

## REFERENCES

1 **Fukuoka H**, Afshari NA. The impact of age-related cataract on measures of frailty in an aging global population. *Curr Opin Ophthalmol* 2017; **28**: 93-97 [PMID: 27820747 DOI: 10.1097/ICU.0000000000000338]

2 **Adham M**, Bredt LC, Robert M, Perinel J, Lombard-Bohas C, Ponchon T, Valette PJ. Pancreatic resection in elderly patients: should it be denied? *Langenbecks Arch Surg* 2014; **399**: 449-459 [PMID: 24671518 DOI: 10.1007/s00423-014-1183-9]
3 **Ballarin R**, Spaggiari M, Di Benedetto F, Montalti R, Masetti M, De Ruvo N, Romano A, Guerrini GP, De Blasiis MG, Gerunda GE. Do not deny pancreatic resection to elderly patients. *J Gastrointest Surg* 2009; **13**: 341-348 [PMID: 18784970 DOI: 10.1007/s11605-008-0601-0]
4 **Kang CM**, Kim JY, Choi GH, Kim KS, Choi JS, Lee WJ, Kim BR. Pancreaticoduodenectomy of pancreatic ductal adenocarcinoma in the elderly. *Yonsei Med J* 2007; **48**: 488-494 [PMID: 17594158 DOI: 10.3349/ymj.2007.48.3.488]
5 **Riall TS**, Reddy DM, Nealon WH, Goodwin JS. The effect of age on short-term outcomes after pancreatic resection: a population-based study. *Ann Surg* 2008; **248**: 459-467 [PMID: 18791366 DOI: 10.1097/SLA.0b013e318185e1b3]
6 **Pratt WB**, Gangavati A, Agarwal K, Schreiber R, Lipsitz LA, Callery MP, Vollmer CM Jr. Establishing standards of quality for elderly patients undergoing pancreatic resection. *Arch Surg* 2009; **144**: 950-956 [PMID: 19841364 DOI: 10.1001/archsurg.2009.107]
7 **Khan S**, Sclabas G, Lombardo KR, Sarr MG, Nagorney D, Kendrick ML, Donohue JH, Que FG, Farnell MB. Pancreatoduodenectomy for ductal adenocarcinoma in the very elderly; is it safe and justified? *J Gastrointest Surg* 2010; **14**: 1826-1831 [PMID: 20714937 DOI: 10.1007/s11605-010-1294-8]
8 **Lahat G**, Sever R, Lubezky N, Nachmany I, Gerstenhaber F, Ben-Haim M, Nakache R, Koriansky J, Klausner JM. Pancreatic cancer: surgery is a feasible therapeutic option for elderly patients. *World J Surg Oncol* 2011; **9**: 10 [PMID: 21272335 DOI: 10.1186/1477-7819-9-10]
9 **Sukharamwala P**, Thoens J, Szuchmacher M, Smith J, DeVito P. Advanced age is a risk factor for post-operative complications and mortality after a pancreaticoduodenectomy: a meta-analysis and systematic review. *HPB* (Oxford) 2012; **14**: 649-657 [PMID: 22954000 DOI: 10.1111/j.1477-2574.2012.00506.x]
10 **Kow AW**, Sadayan NA, Ernest A, Wang B, Chan CY, Ho CK, Liau KH. Is pancreaticoduodenectomy justified in elderly patients? *Surgeon* 2012; **10**: 128-136 [PMID: 22525414 DOI: 10.1016/j.surge.2011.02.005]
11 **Oguro S**, Shimada K, Kishi Y, Nara S, Esaki M, Kosuge T. Perioperative and long-term outcomes after pancreaticoduodenectomy in elderly patients 80 years of age and older. *Langenbecks Arch Surg* 2013; **398**: 531-538 [PMID: 23462741 DOI: 10.1007/s00423-013-1072-7]
12 **Casadei R**, Ricci C, Lazzarini E, Taffurelli G, D'Ambra M, Mastroroberto M, Morselli-Labate AM, Minni F. Pancreatic resection in patients 80 years or older: a meta-analysis and systematic review. *Pancreas* 2014; **43**: 1208-1218 [PMID: 25333405 DOI: 10.1097/MPA.0000000000000182]
13 **Schlottmann F**, Iovaldi ML, Capitanich P, McCormack L. Outcomes of pancreatic surgery in patients older than 70 years. *Cir Esp* 2015; **93**: 638-642 [PMID: 25944478 DOI: 10.1016/j.ciresp.2015.03.010]
14 **El Nakeeb A**, Atef E, El Hanafy E, Salem A, Askar W, Ezzat H, Shehta A, Abdel Wahab M. Outcomes of pancreaticoduodenectomy in elderly patients. *Hepatobiliary Pancreat Dis Int* 2016; **15**: 419-427 [PMID: 27498583]
15 **van der Geest LG**, Besselink MG, van Gestel YR, Busch OR, de Hingh IH, de Jong KP, Molenaar IQ, Lemmens VE. Pancreatic cancer surgery in elderly patients: Balancing between short-term harm and long-term benefit. A population-based study in the Netherlands. *Acta Oncol* 2016; **55**: 278-285 [PMID: 26552841 DOI: 10.3109/0284186X.2015.1105381]
16 **Lee MK**, Dinorcia J, Reavey PL, Holden MM, Genkinger JM, Lee JA, Schrope BA, Chabot JA, Allendorf JD. Pancreaticoduodenectomy can be performed safely in patients aged 80 years and older. *J Gastrointest Surg* 2010; **14**: 1838-1846 [PMID: 20824366 DOI: 10.1007/s11605-010-1345-1]
17 **de Franco V**, Frampas E, Wong M, Meurette G, Charvin M, Leborgne J, Regenet N. Safety and feasibility of pancreatico-duodenectomy in the elderly: a matched study. *Pancreas* 2011; **40**: 920-924 [PMID: 21747313 DOI: 10.1097/MPA.0b013e31821fd70b]
18 **Ito Y**, Kenmochi T, Irino T, Egawa T, Hayashi S, Nagashima A, Kitagawa Y. The impact of surgical outcome after pancreaticoduodenectomy in elderly patients. *World J Surg Oncol* 2011; **9**: 102 [PMID: 21906398 DOI: 10.1186/1477-7819-9-102]
19 **Barbas AS**, Turley RS, Ceppa EP, Reddy SK, Blazer DG 3rd, Clary BM, Pappas TN, Tyler DS, White RR, Lagoo SA. Comparison of outcomes and the use of multimodality therapy in young and elderly people undergoing surgical resection of pancreatic cancer. *J Am Geriatr Soc* 2012; **60**: 344-350 [PMID: 22211710 DOI: 10.1111/j.1532-5415.2011.03785.x]
20 **Melis M**, Marcon F, Masi A, Pinna A, Sarpel U, Miller G, Moore H, Cohen S, Berman R, Pachter HL, Newman E. The safety of a pancreaticoduodenectomy in patients older than 80 years: risk vs. benefits. *HPB* (Oxford) 2012; **14**: 583-588 [PMID: 22882194 DOI: 10.1111/j.1477-2574.2012.00484.x]
21 **Turrini O**, Paye F, Bachellier P, Sauvanet A, Sa Cunha A, Le Treut YP, Adham M, Mabrut JY, Chiche L, Delpero JR; French Surgical Association (AFC). Pancreatectomy for adenocarcinoma in elderly patients: postoperative outcomes and long term results: a study of the French Surgical Association. *Eur J Surg Oncol* 2013; **39**: 171-178 [PMID: 22999411 DOI: 10.1016/j.ejso.2012.08.017]
22 **Suzuki S**, Kaji S, Koike N, Harada N, Suzuki M. Pancreatico-duodenectomy can be safely performed in the elderly. *Surg Today* 2013; **43**: 620-624 [PMID: 23104552 DOI: 10.1007/s00595-012-0383-6]
23 **Oliveira-Cunha M**, Malde DJ, Aldouri A, Morris-Stiff G, Menon KV, Smith AM. Results of pancreatic surgery in the elderly: is age a barrier? *HPB* (Oxford) 2013; **15**: 24-30 [PMID: 23216776 DOI: 10.1111/j.1477-2574.2012.00549.x]
24 **Usuba T**, Takeda Y, Murakami K, Tanaka Y, Hanyu N. Clinical outcomes after pancreaticoduodenectomy in elderly patients at middle-volume center. *Hepatogastroenterology* 2014; **61**: 1762-1766 [PMID: 25436376]
25 **Frakes JM**, Strom T, Springett GM, Hoffe SE, Balducci L, Hodul P, Malafa MP, Shridhar R. Resected pancreatic cancer outcomes in the elderly. *J Geriatr Oncol* 2015; **6**: 127-132 [PMID: 25555451 DOI: 10.1016/j.jgo.2014.11.005]
26 **Marsoner K**, Kornprat P, Sodeck G, Schagerl J, Langeder R, Csengeri D, Wagner D, Mischinger HJ, Haybaeck J. Pancreas Cancer Surgery in Octogenarians - Should We or Should We Not? *Anticancer Res* 2016; **36**: 1979-1984 [PMID: 27069190]
27 **Ansari D**, Aronsson L, Fredriksson J, Andersson B, Andersson R. Safety of pancreatic resection in the elderly: a retrospective analysis of 556 patients. *Ann Gastroenterol* 2016; **29**: 221-225 [PMID: 27065736 DOI: 10.20524/aog.2016.0016]
28 **DeOliveira ML**, Winter JM, Schafer M, Cunningham SC, Cameron JL, Yeo CJ, Clavien PA. Assessment of complications after pancreatic surgery: A novel grading system applied to 633 patients undergoing pancreaticoduodenectomy. *Ann Surg* 2006; **244**: 931-937; discussion 937-939 [PMID: 17122618 DOI: 10.1097/01.sla.0000246856.03918.9a]
29 **Clavien PA**, Barkun J, de Oliveira ML, Vauthey JN, Dindo D, Schulick RD, de Santibañes E, Pekolj J, Slankamenac K, Bassi C, Graf R, Vonlanthen R, Padbury R, Cameron JL, Makuuchi M. The Clavien-Dindo classification of surgical complications: five-year experience. *Ann Surg* 2009; **250**: 187-196 [PMID: 19638912 DOI: 10.1097/SLA.0b013e3181b13ca2]
30 **Kamphues C**, Bova R, Schricke D, Hippler-Benscheidt M, Klauschen F, Stenzinger A, Seehofer D, Glanemann M, Neuhaus P, Bahra M. Postoperative complications deteriorate long-term

outcome in pancreatic cancer patients. *Ann Surg Oncol* 2012; **19**: 856-863 [PMID: 21879265 DOI: 10.1245/s10434-011-2041-4]
31 **Petermann D**, Demartines N, Schäfer M. Severe postoperative complications adversely affect long-term survival after R1 resection for pancreatic head adenocarcinoma. *World J Surg* 2013; **37**: 1901-1908 [PMID: 23564215 DOI: 10.1007/s00268-013-2023-8]

**P- Reviewer**: Araujo RLC, Boeckxstaens GE, Lee MW
**S- Editor**: Gong ZM **L- Editor**: Filipodia **E- Editor**: Huang Y

World Journal of Gastroenterology

Submit a Manuscript: http://www.f6publishing.com

*World J Gastroenterol* 2018 February 21; 24(7): 852-861

DOI: 10.3748/wjg.v24.i7.852

ISSN 1007-9327 (print) ISSN 2219-2840 (online)

ORIGINAL ARTICLE

Retrospective Study

# Predictors of functional benefit of hepatitis C therapy in a 'real-life' cohort

Niels Steinebrunner, Kerstin Stein, Catharina Sandig, Thomas Bruckner, Wolfgang Stremmel, Anita Pathil

Niels Steinebrunner, Catharina Sandig, Wolfgang Stremmel, Anita Pathil, Department of Internal Medicine IV, University Hospital Heidelberg, Heidelberg 69120, Germany

Kerstin Stein, Department of Gastroenterology, Hepatology and Infectious Diseases, University Hospital of Magdeburg, Magdeburg 39120, Germany

Thomas Bruckner, Department of Medical Biometry, Institute of Medical Biometry and Informatics (IMBI), Heidelberg 69120, Germany

ORCID number: Niels Steinebrunner (0000-0003-1520-9707); Kerstin Stein (0000-0002-4940-5856); Catharina Sandig (0000-0003-1836-602X); Thomas Bruckner (0000-0001-9342-3456); Wolfgang Stremmel (0000-0002-8545-1753); Anita Pathil (0000-0002-3670-8209).

Author contributions: Steinebrunner N, Stein K, Sandig C and Pathil A drafted the original manuscript, contributed to the study design, interpreted the results and collected the data; Bruckner T performed the statistical analyses; Stremmel W critically revised the manuscript. All authors read and approved the final manuscript.

Institutional review board statement: The institutional Ethics Committee (Ethikkommission der Medizinischen Fakultät Heidelberg) approved the protocol.

Informed consent statement: Informed consent to participate in the study was obtained from each subject.

Conflict-of-interest statement: Steinebrunner N received travel support from BMS and Gilead; Stein K received lecturer fees from Roche and Gilead; and Pathil A received travel support from AbbVie and BMS and lecturer fees from AbbVie, BMS and Gilead.

Data sharing statement: Statistical code and datasets analysed during the current study are available from the corresponding author on reasonable request via e-mail (anita.pathil-warth@med.uni-heidelberg.de); Consent for data sharing was not obtained but the presented data are anonymized and risk of identification is low.



Manuscript source: Unsolicited manuscript

Correspondence to: Anita Pathil, MD, Doctor, Department of Internal Medicine Ⅳ, Gastroenterology and Hepatology, University of Heidelberg, Im Neuenheimer Feld 410, Heidelberg 69120, Germany. anita.pathil-warth@med.uni-heidelberg.de
Telephone: +49-6221-5638102
Fax: +49-6221-565697

Received: October 22, 2017
Peer-review started: October 25, 2017
First decision: November 22, 2017
Revised: December 31, 2017
Accepted: January 15, 2018
Article in press: January 15, 2018
Published online: February 21, 2018

## Abstract

### *AIM*

To define predictors of functional benefit of direct-acting antivirals (DAAs) in patients with chronic hepatitis C virus (HCV) infection and liver cirrhosis.

### *METHODS*

We analysed a cohort of 199 patients with chronic HCV genotype 1, 2, 3 and 4 infection involving previously treated and untreated patients with compensated (76%) and decompensated (24%) liver cirrhosis at two tertiary centres in Germany. Patients were included with

treatment initiation between February 2014 and August 2016. All patients received a combination regimen of one or more DAAs for either 12 or 24 wk. Predictors of functional benefit were assessed in a univariable as well as multivariable model by binary logistic regression analysis.

***RESULTS***

Viral clearance was achieved in 88% (175/199) of patients. Sustained virological response (SVR) 12 rates were as follows: among 156 patients with genotype 1 infection the SVR 12 rate was 90% (*n* = 141); among 7 patients with genotype 2 infection the SVR 12 rate was 57% (*n* = 4); among 30 patients with genotype 3 infection the SVR 12 rate was 87% (*n* = 26); and among 6 patients with genotype 4 infection the SVR 12 rate was 67% (*n* = 4). Follow-up MELD scores were available for 179 patients. A MELD score improvement was observed in 37% (65/179) of patients, no change of MELD score in 41% (74/179) of patients, and an aggravation was observed in 22% (40/179) of patients. We analysed predictors of functional benefit from antiviral therapy in our patients beyond viral eradication. We identified the Child-Pugh score, the MELD score, the number of platelets and the levels of albumin and bilirubin as significant factors for functional benefit.

***CONCLUSION***

Our data may contribute to the discussion of potential risks and benefits of antiviral therapy with individual patients infected with HCV and with advanced liver disease.

**Key words:** Functional benefit; Direct acting antiviral; Hepatitis C; Cirrhosis; Real-life data



**Core tip:** Therapeutic regimens for patients with chronic hepatitis C virus (HCV) infection have substantially improved over the last few years. However real-life data in patients with cirrhosis are still limited, and predictors of functional benefit of direct-acting antivirals are not well defined. We analysed data from patients with HCV infection and liver cirrhosis to evaluate predictors of functional benefit for identifying patients profiting most from antiviral therapy beyond HCV eradication.

Steinebrunner N, Stein K, Sandig C, Bruckner T, Stremmel W, Pathil A. Predictors of functional benefit of hepatitis C therapy in a 'real-life' cohort. *World J Gastroenterol* 2018; 24(7): 852-861 Available from: URL: http://www.wjgnet.com/1007-9327/full/v24/i7/852.htm DOI: http://dx.doi.org/10.3748/wjg.v24.i7.852

## INTRODUCTION

The introduction of all oral direct-acting antivirals (DAAs) based hepatitis C virus (HCV) therapy has dramatically increased the number of patients who are eligible for anti-viral therapy[1-4] and high response rates can be achieved with various combinational treatment regimens[5-7]. However, patients infected with HCV and suffering from liver cirrhosis remain a challenging subgroup with lower sustained virological response (SVR) rates compared with those patients with mild or moderate hepatic impairment[7,8]. An estimated 25% of patients with HCV infection in the United States have cirrhosis, and this number is expected to rise to 37% by 2020[9-11]. These patients are at risk of disease-related complications, including hepatocellular carcinoma, liver decompensation, end-stage liver disease and finally the need for liver transplantation[7,12,13]. Liver decompensation and hepatocellular carcinoma associated with infection of HCV are the most common causes for liver transplantation in Europe and North America. Several trials have shown an early and long-term improvement of liver function associated with successful anti-viral treatment in the majority of cases[14-21]. However, a certain number of patients with compensated and decompensated liver cirrhosis show a deterioration of liver function in spite of successful viral clearance[17,22,23]. In this subset of patients with advanced liver disease, the prediction of functional benefit of anti-viral therapy in an individual patient is not well established. Therefore, in our real-life observational study, we analysed patients with HCV infection and liver cirrhosis to evaluate predictors for identifying those patients profiting most from antiviral therapy beyond HCV eradication with significant clinical improvement of hepatic function.

## MATERIALS AND METHODS

### *Patient population and study design*

We analysed clinical and laboratory data sets of all consecutive patients aged 18 years or over with chronic HCV genotype 1, 2, 3 or 4 infection and liver cirrhosis receiving DAA-based antiviral therapy. Patients were included with treatment initiation between February 2014 and August 2016 in a retrospective, longitudinal study at two investigative sites in Germany. One patient with HCV genotype 1b infection on a 12-wk regimen of paritaprevir/ritonavir (PTV/r) + ombitasvir (OMV) + dasabuvir (DSV) ± ribavirin (RBV) prematurely terminated treatment due to deterioration of liver function and subsequently received a liver transplant. After liver transplantation, the viral load remained negative on follow-up. Another patient with HCV genotype 1b infection on a 12-wk regimen of sofosbuvir (SOF) + daclatasvir (DCV) prematurely terminated treatment due to myalgia. At the point of treatment discontinuation, the patient had no detectable viral load and it remained negative on follow-up. In two patients with HCV genotype 1b infection on a 12-wk regimen of SOF + simeprevir (SMV) + RBV the dose of RBV

was discontinued after four weeks and after six weeks respectively, due to anaemia. Both patients showed SVR on follow-up. One patient was non-adherent to the antiviral treatment plan and showed no SVR. Three patients were started on antiviral therapy and failed to attend their follow-ups. These were, respectively, two patients with a 12-wk regimen of SOF + ledipasvir (LDV) + RBV (genotype 1a and genotype 1b) and one patient with a 12-wk regimen of SOF + DCV + RBV (genotype 3). These patients were classified as treatment failures. All patients were included in the intention-to-treat (ITT) analysis.

Patients received a combination treatment of one or more DAAs with or without RBV for either 12 or 24 wk, depending on genotype, pre-treatment history or contraindications according to local guidelines[1]. SOF was administered at 400 mg once daily or in combination with LDV 90 mg as a single tablet co-formulation. DCV was applied once daily at a dosing of 60 mg, with dose adjustment to 30 mg or 90 mg per day as recommended for patients with relevant potential drug-drug interactions. SMV was applied at a dosing of 150 mg once daily. Another treatment combination was PTV/r 150 mg/100 mg plus OMV 25 mg (once daily) and DSV 250 mg (twice daily) with or without RBV. RBV was administered twice daily, with the dose determined according to body weight (1000 mg per day for patients with a body weight of < 75 kg and 1200 mg per day in patients with a body weight ⩾ 75 kg), according to the individual treatment protocol.

Patients were reviewed at treatment weeks 4, 12 and 24 and at additional time points, if deemed necessary, as well as 12 wk after the end of treatment. Serum HCV-RNA and standard laboratory tests were regularly assessed at baseline and at the following clinical visits. The lower limit of quantification (LLOQ) was 12 IU/mL [Abbott Real Time (ART) HCV assay (Abbott Molecular, Des Plaines, IL, United States)]. Liver cirrhosis was confirmed by liver histology or conducted by evaluation of data sets from non-invasive tests, comprising transient elastography (TE) (FibroScan, Echosens, Paris, France), with a cut-off value for cirrhosis of ⩾ 12.5 kPa, ultrasound examination, imaging by computed tomography or magnetic resonance, presence of oesophageal varices and laboratory values. Classification was according to the Child-Pugh score. Liver stiffness measurements were performed according to current EASL guidelines[5,24] at baseline and 12 wk after the end of DAA treatment. The study was conducted in accordance with the Guidelines for Good Clinical Practice and the Declaration of Helsinki.

### Statistical analysis

Continuous data were expressed by mean values and standard deviation. Categorical variables were expressed as absolute and relative numbers. Continuous data were analysed with t-test and categorical data with the chi-square test. Predictors of functional benefit were assessed in a non-stepwise method for multivariable binary logistic regression analysis. To maintain the validity of the logistic regression analysis relative to the number of outcome events, a maximum of 7 variables was selected[25]. Variables were chosen due to clinical relevance. These variables were selected based on the clinical experience of the authors, as well as based on the data of other publications[23] and were used for univariable as well as for multivariable analyses. MELD score and Child-Pugh score were assessed for interaction and showed none. We performed the Hosmer-Lemeshow test, which showed significance ($P$ = 0.02) and therefore demonstrated a low goodness of fit. The removal of creatinine from the multivariable assessments improved the goodness of fit considerably ($P$ = 0.43) and therefore was excluded from further analyses. A $P$-value < 0.05 was considered statistically significant. Statistical analysis was performed using SPSS software (IBM SPSS Statistics 24, Armonk, NY, United States) with additional analysis performed using SAS 9.4 (SAS Institute, Cary, NC, United States).

## RESULTS

### Patient characteristics

We enrolled 199 patients with chronic HCV infection and liver cirrhosis at two tertiary sites in Germany. HCV genotype 1 was present in 78% ($n$ = 156) of patients, followed by genotype 3 in 15% ($n$ = 30), genotype 2 in 4% ($n$ = 7) and genotype 4 in 3% ($n$ = 6) of patients. Our patient sample reflects existing data for the distribution of genotypes in Central Europe: Approximately 70% for genotype 1, followed by 21% for genotype 3, 3% for genotype 2 and 5% for genotype 4[26,27]. Of all patients, 56% ($n$ = 112) were treatment experienced, and 4% ($n$ = 8) had received a protease inhibitor in a previous therapy. At treatment initiation, 152 (76%) patients had compensated cirrhosis and 47 (24%) had decompensated cirrhosis. Baseline characteristics of the study cohort are shown in Table 1. A combination treatment of SOF+RBV was administered to 18% ($n$ = 36) of patients, and 47% ($n$ = 93) of patients received a therapy regime of SOF + LDV ± RBV. A therapy regime of SOF + DCV ± RBV was administered to 19% ($n$ = 38) of patients. 18 patients (9%) were treated with a regimen of SOF + SMV ± RBV. A therapy regime of PTV/r + OMV + DSV ± RBV was applied in 7% ($n$ = 14) of patients. Treatment duration was either 12 or 24 wk, depending on the individual treatment protocol. Details on the treatment protocols with respect to the different genotypes are shown in Table 2.

### Efficacy of antiviral therapies

Viral clearance was achieved in 88% (175/199) of patients. The SVR 12 rates according to the HCV genotype were as follows: 90% of patients with genotype 1 infection (141/156) and 57% of patients

**Table 1 Baseline characteristics of the study population**

| Demographics | Value |
|---|---|
| Age (yr) | 59 ± 10 (27-83) |
| Male gender | 133 (67) |
| HCV genotype | |
| 1a | 47 (23) |
| 1b | 100 (50) |
| 1 (no confirmed subtype) | 9 (5) |
| 2 | 7 (4) |
| 3 | 30 (15) |
| 4 | 6 (3) |
| Viral load $10^6$ (IU/mL) | 2.04 ± 3.46 (0.01-34.50) |
| Treatment history | |
| Treatment naive | 86 (43) |
| Treatment experienced | 113 (57) |
| Protease inhibitor experienced | 8 (4) |
| Liver/renal status | |
| Platelets ($10^3$/μL) | 116 ± 61 (26-341) |
| Total bilirubin (mg/dL) | 1.4 ± 0.9 (0.2-5.7) |
| INR | 1.34 ± 0.78 (0.40-5.70) |
| Creatinine (mg/dL) | 0.80 ± 0.22 (0.43-1.96) |
| TE score (kPa)[1] | 24.5 ± 12.5 (5.5-75) |
| Average MELD score | 9 ± 3 (6-23) |
| MELD score | |
| < 10 | 130 (65) |
| 10-15 | 59 (30) |
| > 15 | 10 (5) |
| Child-Pugh score | |
| A | 152 (76) |
| B | 40 (20) |
| C | 7 (4) |

Data are expressed as *n* (%) or means ± SD (range). [1]Data available for 112 patients.

with genotype 2 infection (4/7) reached SVR 12. Among 30 patients with genotype 3 infection, the SVR 12 rate was 87% (26/30) and among 6 patients with genotype 4 infection, the SVR 12 rate was 67% (4/6) (Figure 1). Anti-viral treatment in our patient group was well tolerated. However, one patient treated with PTV/r + OMV + DSV ± RBV presented with acute liver failure within 10 d of treatment initiation. Therefore, antiviral therapy was terminated at this time. Deterioration of liver function was associated with a worsening of the MELD score from 12 to 29. This patient received a liver transplant within a short period of time with subsequently undetectable HCV RNA on follow-ups.

### *Changes in liver function*

The MELD score consists of international normalized ratio (INR), serum bilirubin and creatinine levels[28]. At treatment initiation, the mean MELD score in our cohort was 9 ± 3 and the respective variables were as follows: INR was 1.34 ± 0.78; bilirubin was 1.4 ± 0.9 mgdl-1 and creatinine 0.80 ± 0.22 mgdl-1. Of all patients, 130 (65%) had a MELD score <10; 59 (30%) had a MELD score in the range of 10-15; and 10 (5%) had a MELD score >15. At 12 wk post-treatment, laboratory data were available for 179 patients. The average MELD score in the total number of our studied patients remained unchanged with 9 ± 3 at 12 wk post-treatment and the respective variables were as follows: INR was 1.13 ± 0.23; bilirubin was 1.4 ± 1.0 mgdl-1 and creatinine 0.80 ± 0.21 mgdl-1. A MELD score decrease was observed in 37% (65/179) of patients, no change of MELD score in 41% (74/179), and an increase was observed in 22% (40/179). In the subgroup of patients with a MELD decrease, 16% (11/65) experienced a relapse, compared to 25% (10/40) in the subgroup with a MELD increase. The difference between these groups for this parameter could not be deemed to be significant ($P$ = 0.315). The highest increase of the MELD score was +8 in one patient, the largest reduction of the MELD score was -6 in four patients (Figure 2A). In one patient, the increase of the MELD score was 17 (from 12 to 29) within 10 d of treatment initiation. In this patient, antiviral treatment was terminated prematurely. Of the baseline factors examined (age, Child-Pugh score, MELD score, creatinine, platelets, albumin and bilirubin), the Child-Pugh score, the MELD score, the number of platelets and the levels of albumin and bilirubin were significant factors for functional benefit in the univariable analyses. Multivariable analyses showed a trend for MELD ($P$ = 0.082) and for albumin ($P$ = 0.057), however significance at the level of 5% was not reached (Table 3 and Figure 3).

### *Changes in transient elastography*

Mean TE scores before treatment initiation were 24.5 ± 12.5 kPa. After antiviral therapy, TE scores decreased in 75% of patients (33/44) and increased in 20% of patients (9/44) 12 wk post-treatment. Two patients (5%) had no change in TE scores. Four patients had a relapse of HCV infection as well as a decrease in liver stiffness measured at that time (Figure 2B).

## DISCUSSION

Interferon-free combinations of DAAs have profoundly improved the efficacy and safety of HCV treatment in patients with cirrhosis, which is the group of patients most difficult to cure. Overall response rates to DAA-based therapies in our patient group were high at 88% (175/199). This is consistent with previously published data of DAA treatment regimens in patients with an advanced stage of liver disease. However, there is restricted comparability of SVR rates of our patients with previously published trials, due to differences in study populations, including clinical characteristics of patients, pre-treatment history and the specific treatment plans and treatment duration. For patients with genotype 1 infection treated with SOF + LDV for 12 wk, in the ION-1 trial SVR was achieved in 97% of previously untreated patients and in the ION-2 trial in 93% of treatment-experienced patients. However, the ION-1 and ION-2 trial included only 15%-20% of patients with cirrhosis[29,30]. In the TURQUOISE-II trial, 191 (92%) of 208 treatment-naive or treatment-

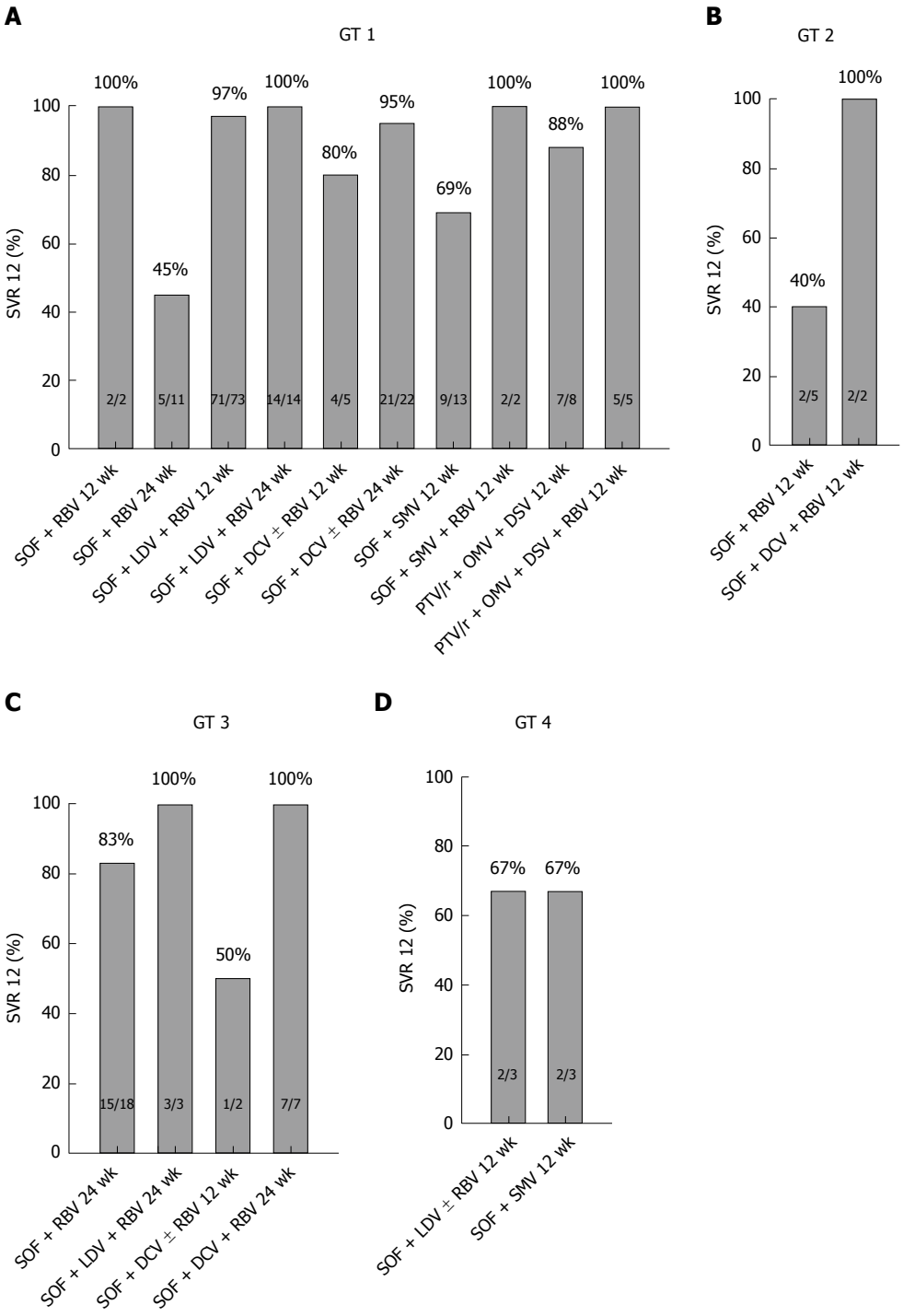


**Figure 1 Efficacy of treatment.** Sustained virological response rates 12 wk after the end of treatment (SVR 12) are shown for patients with HCV genotype 1, 2, 3 or 4 (A-D). Patients were sub-classified for therapy regime and treatment duration.

experienced patients with compensated cirrhosis treated for 12 wk with ritonavir-boosted PTV + OMV + DSV achieved SVR[31]. In the SOLAR-1 and SOLAR-2 trials, including patients with cirrhosis with HCV genotype 1 or 4 treated with SOF/LDV + RBV for 12 or 24 wk, SVR rates were 86% to 89%[22,32]. In the SOLAR trials, viral eradication was associated with an improvement of MELD scores, but it is unclear whether the benefits were related to viral eradication alone or due to a more stringent care of patients at specialized centres in the setting of a clinical trial[22,32].

In general, randomized controlled trials involve a more homogenous cohort of patients with typically extensive inclusion and exclusion criteria, while real-life cohorts represent a more diverse spectrum of patients with fewer restrictions. Thus, these cohorts help to better understand the risk of virological failure in a real-life clinical setting.

It has to be emphasised that current DAA treatments are expensive. Therefore, stratification and

**Table 2 Therapy regime and treatment duration**

| Therapy regime | Treatment duration (wk) | GT 1 | GT 2 | GT 3 | GT 4 |
|---|---|---|---|---|---|
| SOF + RBV | 12 | 2 (1) | 5 (3) | | |
| SOF + RBV | 24 | 11 (5) | | 18 (9) | |
| SOF + LDV | 12 | | | | 1 (1) |
| SOF + LDV + RBV | 12 | 73 (36) | | | 2 (1) |
| SOF + LDV + RBV | 24 | 14 (6) | | 3 (2) | |
| SOF + DCV | 12 | 2 (1) | | 1 (1) | |
| SOF + DCV | 24 | 19 (9) | | | |
| SOF + DCV + RBV | 12 | 3 (2) | 2 (1) | 1 (1) | |
| SOF + DCV + RBV | 24 | 3 (2) | | 7 (3) | |
| SOF + SMV | 12 | 13 (6) | | | 3 (2) |
| SOF + SMV + RBV | 12 | 2 (1) | | | |
| PTV/r + OMV + DSV | 12 | 8 (4) | | | |
| PTV/r + OMV + DSV + RBV | 12 | 6 (3) | | | |

Data are expressed as number of patients for each therapy regime (percent of total patients). GT: Genotype, SOF: Sofosbuvir; RBV: Ribavirin; LDV: Ledipasvir; DCV: Daclatasvir; SMV: Simeprevir; PTV/r: Paritaprevir/ritonavir; OMV: Ombitasvir; DSV: Dasabuvir.

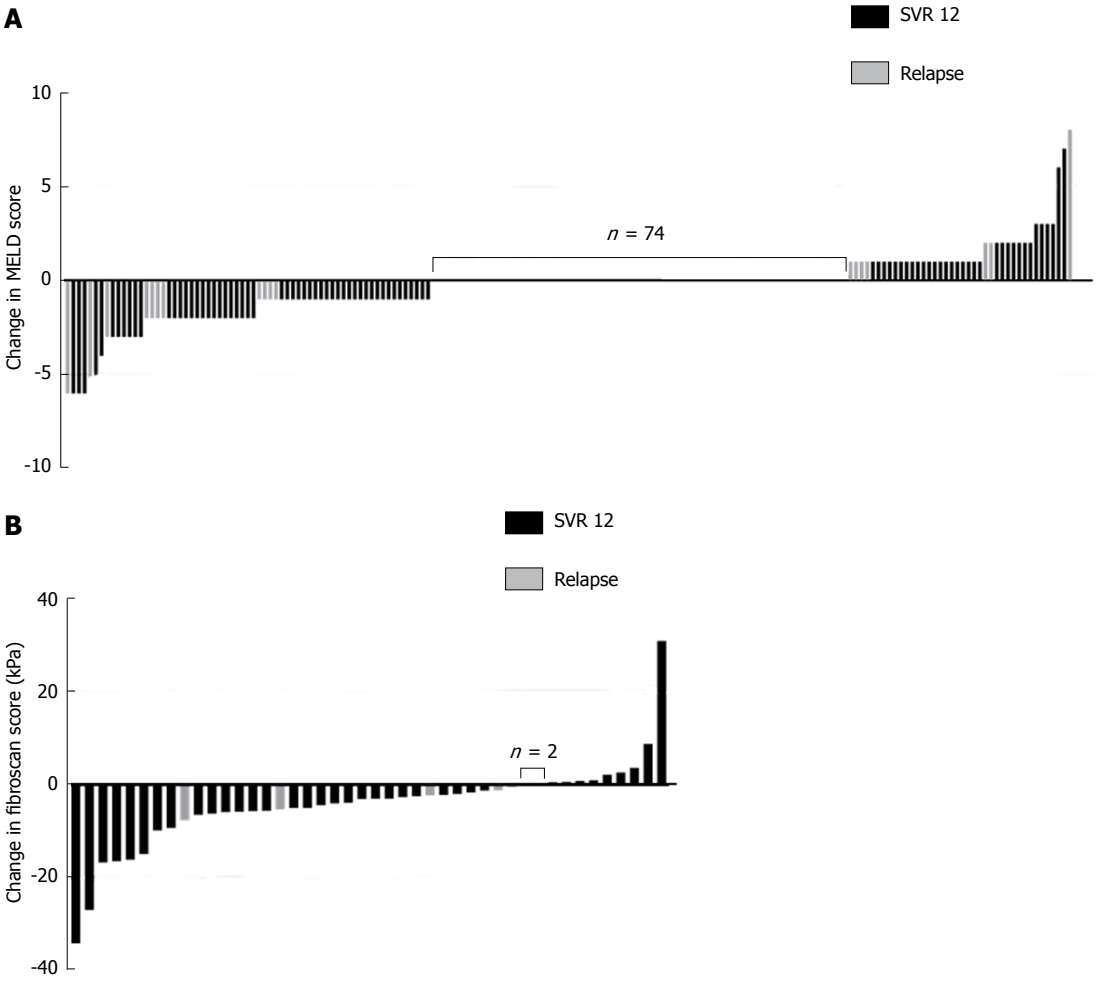


**Figure 2 Change in MELD score (A) and liver stiffness (B) from baseline to 12 wk post-therapy.** A: Baseline and follow-up data at 12 wk after the end of treatment was available for *n* = 179 patients. Each bar represents an individual patient. Patients with a relapse in follow-up are highlighted in pale grey. B: Baseline and follow-up data at 12 wk after the end of treatment was available for *n* = 44 patients. Each bar represents an individual patient. Patients with a relapse in follow-up are highlighted in pale grey.

prioritisation of patients by identifying those with the most urgent need for therapy and the most likely to benefit from therapy are important until treatment costs decrease as several effective drugs offering a cure are introduced[7].

SVR has been shown to reduce both all-cause and liver-related mortality from HCV infection among patients with cirrhosis[21,33] and also an improvement of

**Table 3 Predictors of functional benefit (MELD score decrease) following antiviral therapy based on patient baseline characteristics**

| Baseline parameters | MELD decrease | | *P* value (univariable) | *P* value (multivariable[3]) | OR (95%CI) |
|---|---|---|---|---|---|
| | Yes (*n* = 78, 44%) | No (*n* = 101, 56%) | | | |
| Age (yr) | 59 ± 9 | 59 ± 9 | 0.978[1] | 0.815 | 0.996 (0.961-1.032) |
| Child-Pugh A | 53 (38) | 86 (62) | 0.006[2] | 0.592 | 1.327 (0.472-3.725) |
| Child-Pugh B/C | 25 (62) | 15 (38) | | | |
| MELD | 10 ± 3 | 8 ± 3 | < 0.001[1] | 0.082 | 1.177 (0.980-1.414) |
| Creatinine (mg/dL) | 0.8 ± 0.3 | 0.9 ± 0.8 | 0.344[1] | - | - |
| Platelets (/nL) | 104 ± 56 | 126 ± 64 | 0.014[1] | 0.617 | 0.998 (0.992-1.005) |
| Albumin (g/L) | 36.7 ± 5.2 | 39.9 ± 4.9 | < 0.001[1] | 0.057 | 0.928 (0.860-1.002) |
| Bilirubin (mg/dL) | 1.6 ± 1.0 | 1.1 ± 0.8 | < 0.001[1] | 0.739 | 1.096 (0.638-1.883) |

Data are expressed as *n* (%) or means ± SD (range). Baseline and follow-up data at 12 wk after the end of treatment was available for *n* = 179 patients. [1]*t*-test; [2]Chi-square-test; [3]Multivariable logistic regression.

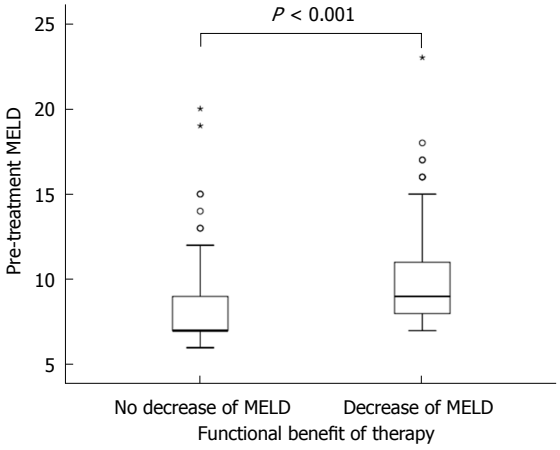


**Figure 3 MELD score as a predictor of functional benefit of antiviral therapy.**

the MELD score has been reported[22]. In the SOLAR-2 study including patients with advanced cirrhosis with Child-Pugh class B and C, a majority of patients showed an improvement of the MELD score under successful DAA therapy[32]. Nevertheless, some patients showed no change or even a deterioration of the MELD score despite viral clearance.

Considering that not all patients with cirrhosis benefit from HCV therapy despite SVR, the key question is which patients profit. The Child-Pugh score is a prognostic model for liver cirrhosis, which has been a useful clinical tool in day-to-day clinical practice for over 50 years[34]. However, the Child-Pugh score includes subjective criteria (ascites and encephalopathy) besides the laboratory values of INR, bilirubin and albumin. Furthermore, the Child-Pugh score is not as accurate in predicting mortality of patients with liver cirrhosis as is the MELD score. In contrast to the Child-Pugh score, the MELD score has been derived from prospectively collected data rather than empirically constructed data. Also, the MELD score increases as the three variables (INR, bilirubin and creatinine) deteriorate, whereas the constituent parameters in the Child-Pugh score remain fixed once a defined threshold has been reached[35]. Therefore, the MELD score has been established as a classification system to determine the urgency for liver transplantation. Consequently, we suggest that the MELD score also might be a valuable tool in assessing the risk and benefit of DAA treatment and might be more reliable than the Child-Pugh score. This is in line with the results of the study by Foster *et al*[23], including patients with HCV and decompensated cirrhosis treated with SOF + LDV or SOF + DCV either with or without RBV for a total of 12 wk. This study analysed patient characteristics to identify patients most likely to benefit from therapy. Regression analysis of baseline characteristics and association with MELD change yielded baseline MELD score as the only significant independent factor[23].

However, it should be mentioned that benefits, including mortality, even in non-advanced liver disease such as low-grade fibrosis have been found in long-term studies following antiviral treatment[36,37].

In a study of the Irish Early Access Programme, 101 patients with advanced cirrhosis with HCV genotype 1, 3 or 4 were treated with SOF + LDV ± RBV for 12 wk. The overall SVR 12 rate for this cohort was 74.3%. This data depicts high SVR rates in this difficult to treat patient group. However, the authors also reported 8 deaths, representing an on-treatment mortality in patients with Child-Pugh B score at a baseline of 6% (4/67), and in patients with Child-Pugh C score at a baseline of 21% (4/19). The causes of death for the eight patients were: liver failure (*n* = 2), intracerebral haemorrhage (*n* = 2), sepsis (*n* = 2), complications from a pre-existing hepatocellular carcinoma (*n* = 1) and cardiac arrest (*n* = 1)[38]. However, with efficacy and safety of DAA therapy established in large patient cohorts, it appears that in these cases of adverse events were caused by the underlying disease process[39]. The data of our study support the general statement that DAA treatment is safe, even in patients with advanced liver disease.

As there was no significant difference in the rate of relapse in the group of patients with a MELD score increase compared to the group with no change in MELD score or with a decrease of the MELD score, the risk of a relapse seems to be independent of functional

hepatic changes during therapy.

Transient elastography measurements are established for fibrosis and cirrhosis assessment in patients with HCV infection[5,6,40,41]. However, experience in the change of transient elastography following antiviral therapy is still limited. We observed a decrease of transient elastography measures in 75% of patients (33/44) following antiviral therapy. A recent study showed a significant reduction of liver stiffness assessed by transient elastography only for patients who achieve SVR[42]. However, in our patient cohort, four patients with a relapse presented with a decrease of transient elastography measures. It remains to be further examined whether the changes in liver stiffness indicate a regression of fibrosis or an attenuation of chronic liver inflammation caused by HCV replication. These results have to be validated in a larger cohort of patients, and it has to be determined whether these early changes persist with a longer follow-up time interval.

In conclusion, novel treatment algorithms with DAAs for chronic HCV infection yield excellent results even in a patient population with cirrhosis. However, it may be useful to pinpoint parameters to identify those patients who will actually benefit clinically from antiviral therapy beyond viral eradication. Our results suggest that the Child-Pugh score, the MELD score, the number of platelets and the levels of albumin and bilirubin may be predictors of functional benefit from DAA-based therapy. This association may serve as another tool for health care providers to discuss treatment options and assess the risks and benefits of antiviral therapy with patients on an individual basis.

## ARTICLE HIGHLIGHTS

### *Research background*

To improve patient care by assisting health care professionals in the decision-making process for treatment of patients infected with hepatitis C virus (HCV).

### *Research motivation*

Direct-acting antivirals (DAAs) have recently opened up promising new therapeutic options for patients with chronic HCV infection. Nevertheless, in order to study the efficacy of these regimens, especially in difficult-to-treat patient populations, such as patients with liver cirrhosis, real-life data is needed.

### *Research objectives*

We investigated patients in our real-life cohort from two tertiary referral centres in Germany. We analysed data from patients with HCV infection and liver cirrhosis to evaluate predictors of functional benefit for identifying patients profiting most of antiviral therapy beyond HCV eradication.

### *Research methods*

Predictors of functional benefit were determined in a univariable as well as multivariable model assessed by binary logistic regression analysis. For reasons of validity of the logistic regression analysis (relative to the number of outcome events), a maximum of 7 clinically relevant variables was selected.

### *Research results*

Our results indicate that the Child-Pugh score, the MELD score, the number of platelets and the levels of albumin and bilirubin may be predictors of functional benefit from DAA-based therapy, so that these variables may serve as another tool to guide antiviral therapy in affected patients.

### *Research conclusions*

With the introduction of DAAs, the indication for therapy for patients with HCV infection and with liver cirrhosis has dramatically expanded with vast improvements of SVR. However, it remains unclear, which patients profit most from antiviral therapy. Therefore, a simple and feasible clinical index may be beneficial to evaluate the presumed effect of antiviral therapy before treatment initiation. Based on the parameters studied, we suggest the MELD score as part of such an evaluation system.

### *Research perspectives*

The ultimate goal of antiviral therapy in patients with HCV infection is to avoid hepatic complications such as the development of hepatocellular carcinoma or hepatic decompensation. Further research with large patient groups and longer observation periods is warranted to define and confirm predictive markers to identify patients, which profit clinically most from antiviral therapy beyond viral eradication

## REFERENCES


1 **Lin H**, Zeng J, Xie R, Schulz MJ, Tedesco R, Qu J, Erhard KF, Mack JF, Raha K, Rendina AR, Szewczuk LM, Kratz PM, Jurewicz AJ, Cecconie T, Martens S, McDevitt PJ, Martin JD, Chen SB, Jiang Y, Nickels L, Schwartz BJ, Smallwood A, Zhao B, Campobasso N, Qian Y, Briand J, Rominger CM, Oleykowski C, Hardwicke MA, Luengo JI. Discovery of a Novel 2,6-Disubstituted Glucosamine Series of Potent and Selective Hexokinase 2 Inhibitors. *ACS Med Chem Lett* 2015; **7**: 217-222 [PMID: 26985301 DOI: 10.1021/acsmedchemlett.5b00214]

2 **European Association for Study of Liver**. EASL Recommendations on Treatment of Hepatitis C 2015. *J Hepatol* 2015; **63**: 199-236 [PMID: 25911336 DOI: 10.1016/j.jhep.2015.03.025]

3 **European Association for the Study of the Liver**. EASL recommendations on treatment of hepatitis C 2014. *J Hepatol* 2014; **61**: 373-395 [PMID: 24818984 DOI: 10.1016/j.jhep.2014.05.001]

4 **European Association for the Study of the Liver**. EASL Recommendations on Treatment of Hepatitis C 2016. *J Hepatol* 2017; **66**: 153-194 [PMID: 27667367 DOI: 10.1016/j.jhep.2016.09.001]

5 **European Association for Study of Liver**; Asociacion Latinoamericana para el Estudio del Higado. EASL-ALEH Clinical Practice Guidelines: Non-invasive tests for evaluation of liver disease severity and prognosis. *J Hepatol* 2015; **63**: 237-264 [PMID: 25911335 DOI: 10.1016/j.jhep.2015.04.006]

6 **Friedrich-Rust M**, Ong MF, Martens S, Sarrazin C, Bojunga J, Zeuzem S, Herrmann E. Performance of transient elastography for the staging of liver fibrosis: a meta-analysis. *Gastroenterology* 2008; **134**: 960-974 [PMID: 18395077 DOI: 10.1053/j.gastro.2008.01.034]

7 **Staton-Tindall M**, Webster JM, Oser CB, Havens JR, Leukefeld CG. Drug use, hepatitis C, and service availability: perspectives of incarcerated rural women. *Soc Work Public Health* 2015; **30**: 385-396 [PMID: 25950907 DOI: 10.1080/19371918.2015.1021024]

8 **Nelson DR**, Cooper JN, Lalezari JP, Lawitz E, Pockros PJ, Gitlin N, Freilich BF, Younes ZH, Harlan W, Ghalib R, Oguchi G, Thuluvath PJ, Ortiz-Lasanta G, Rabinovitz M, Bernstein D, Bennett M, Hawkins T, Ravendhran N, Sheikh AM, Varunok P, Kowdley KV, Hennicken D, McPhee F, Rana K, Hughes EA; ALLY-3 Study Team. All-oral 12-week treatment with daclatasvir plus sofosbuvir in patients with hepatitis C virus genotype 3 infection: ALLY-3 phase III study. *Hepatology* 2015; **61**: 1127-1135 [PMID: 25614962 DOI: 10.1002/hep.27726]

9 **Davis GL**, Alter MJ, El-Serag H, Poynard T, Jennings LW. Aging of hepatitis C virus (HCV)-infected persons in the United States: a multiple cohort model of HCV prevalence and disease progression. *Gastroenterology* 2010; **138**: 513-521, 521.e1-521.e6 [PMID: 19861128 DOI: 10.1053/j.gastro.2009.09.067]

10 **Hajarizadeh B**, Grebely J, Dore GJ. Epidemiology and natural history of HCV infection. *Nat Rev Gastroenterol Hepatol* 2013; **10**:

553-562 [PMID: 23817321 DOI: 10.1038/nrgastro.2013.107]
11 **Razavi H**, Elkhoury AC, Elbasha E, Estes C, Pasini K, Poynard T, Kumar R. Chronic hepatitis C virus (HCV) disease burden and cost in the United States. *Hepatology* 2013; **57**: 2164-2170 [PMID: 23280550 DOI: 10.1002/hep.26218]
12 **Steinebrunner N**, Sandig C, Sommerer C, Hinz U, Giese T, Stremmel W, Zahn A. Reduced residual gene expression of nuclear factor of activated T cells-regulated genes correlates with the risk of cytomegalovirus infection after liver transplantation. *Transpl Infect Dis* 2014; **16**: 379-386 [PMID: 24666466 DOI: 10.1111/tid.12206]
13 **Steinebrunner N**, Sandig C, Sommerer C, Hinz U, Giese T, Stremmel W, Zahn A. Pharmacodynamic monitoring of nuclear factor of activated T cell-regulated gene expression in liver allograft recipients on immunosuppressive therapy with calcineurin inhibitors in the course of time and correlation with acute rejection episodes--a prospective study. *Ann Transplant* 2014; **19**: 32-40 [PMID: 24457606 DOI: 10.12659/AOT.889809]
14 **Backus LI**, Boothroyd DB, Phillips BR, Belperio P, Halloran J, Mole LA. A sustained virologic response reduces risk of all-cause mortality in patients with hepatitis C. *Clin Gastroenterol Hepatol* 2011; **9**: 509-516.e1 [PMID: 21397729 DOI: 10.1016/j.cgh.2011.03.004]
15 **Bruno S**, Crosignani A, Facciotto C, Rossi S, Roffi L, Redaelli A, de Franchis R, Almasio PL, Maisonneuve P. Sustained virologic response prevents the development of esophageal varices in compensated, Child-Pugh class A hepatitis C virus-induced cirrhosis. A 12-year prospective follow-up study. *Hepatology* 2010; **51**: 2069-2076 [PMID: 20196120 DOI: 10.1002/hep.23528]
16 **Butt AA**, Wang X, Moore CG. Effect of hepatitis C virus and its treatment on survival. *Hepatology* 2009; **50**: 387-392 [PMID: 19591128 DOI: 10.1002/hep.23000]
17 **Curry MP**, O'Leary JG, Bzowej N, Muir AJ, Korenblat KM, Fenkel JM, Reddy KR, Lawitz E, Flamm SL, Schiano T, Teperman L, Fontana R, Schiff E, Fried M, Doehle B, An D, McNally J, Osinusi A, Brainard DM, McHutchison JG, Brown RS Jr, Charlton M; ASTRAL-4 Investigators. Sofosbuvir and Velpatasvir for HCV in Patients with Decompensated Cirrhosis. *N Engl J Med* 2015; **373**: 2618-2628 [PMID: 26569658 DOI: 10.1056/NEJMoa1512614]
18 **George SL**, Bacon BR, Brunt EM, Mihindukulasuriya KL, Hoffmann J, Di Bisceglie AM. Clinical, virologic, histologic, and biochemical outcomes after successful HCV therapy: a 5-year follow-up of 150 patients. *Hepatology* 2009; **49**: 729-738 [PMID: 19072828 DOI: 10.1002/hep.22694]
19 **Mira JA**, Rivero-Juárez A, López-Cortés LF, Girón-González JA, Téllez F, de los Santos-Gil I, Macías J, Merino D, Márquez M, Ríos-Villegas MJ, Gea I, Merchante N, Rivero A, Torres-Cornejo A, Pineda JA; Grupo Andaluz para el Estudio de las Hepatitis Víricas de la Sociedad Andaluza de Enfermedades Infecciosas. Benefits from sustained virologic response to pegylated interferon plus ribavirin in HIV/hepatitis C virus-coinfected patients with compensated cirrhosis. *Clin Infect Dis* 2013; **56**: 1646-1653 [PMID: 23429381 DOI: 10.1093/cid/cit103]
20 **Poordad F**, Schiff ER, Vierling JM, Landis C, Fontana RJ, Yang R, McPhee F, Hughes EA, Noviello S, Swenson ES. Daclatasvir with sofosbuvir and ribavirin for hepatitis C virus infection with advanced cirrhosis or post-liver transplantation recurrence. *Hepatology* 2016; **63**: 1493-1505 [PMID: 26754432 DOI: 10.1002/hep.28446]
21 **van der Meer AJ**, Veldt BJ, Feld JJ, Wedemeyer H, Dufour JF, Lammert F, Duarte-Rojo A, Heathcote EJ, Manns MP, Kuske L, Zeuzem S, Hofmann WP, de Knegt RJ, Hansen BE, Janssen HL. Association between sustained virological response and all-cause mortality among patients with chronic hepatitis C and advanced hepatic fibrosis. *JAMA* 2012; **308**: 2584-2593 [PMID: 23268517 DOI: 10.1001/jama.2012.144878]
22 **Charlton M**, Everson GT, Flamm SL, Kumar P, Landis C, Brown RS Jr, Fried MW, Terrault NA, O'Leary JG, Vargas HE, Kuo A, Schiff E, Sulkowski MS, Gilroy R, Watt KD, Brown K, Kwo P, Pungpapong S, Korenblat KM, Muir AJ, Teperman L, Fontana RJ, Denning J, Arterburn S, Dvory-Sobol H, Brandt-Sarif T, Pang PS, McHutchison JG, Reddy KR, Afdhal N; SOLAR-1 Investigators. Ledipasvir and Sofosbuvir Plus Ribavirin for Treatment of HCV Infection in Patients With Advanced Liver Disease. *Gastroenterology* 2015; **149**: 649-659 [PMID: 25985734 DOI: 10.1053/j.gastro.2015.05.010]
23 **Foster GR**, Irving WL, Cheung MC, Walker AJ, Hudson BE, Verma S, McLauchlan J, Mutimer DJ, Brown A, Gelson WT, MacDonald DC, Agarwal K; HCV Research, UK. Impact of direct acting antiviral therapy in patients with chronic hepatitis C and decompensated cirrhosis. *J Hepatol* 2016; **64**: 1224-1231 [PMID: 26829205 DOI: 10.1016/j.jhep.2016.01.029]
24 **Castera L**, Forns X, Alberti A. Non-invasive evaluation of liver fibrosis using transient elastography. *J Hepatol* 2008; **48**: 835-847 [PMID: 18334275 DOI: 10.1016/j.jhep.2008.02.008]
25 **Peduzzi P**, Concato J, Kemper E, Holford TR, Feinstein AR. A simulation study of the number of events per variable in logistic regression analysis. *J Clin Epidemiol* 1996; **49**: 1373-1379 [PMID: 8970487]
26 **Messina JP**, Humphreys I, Flaxman A, Brown A, Cooke GS, Pybus OG, Barnes E. Global distribution and prevalence of hepatitis C virus genotypes. *Hepatology* 2015; **61**: 77-87 [PMID: 25069599 DOI: 10.1002/hep.27259]
27 **Petruzziello A**, Marigliano S, Loquercio G, Cacciapuoti C. Hepatitis C virus (HCV) genotypes distribution: an epidemiological up-date in Europe. *Infect Agent Cancer* 2016; **11**: 53 [PMID: 27752280 DOI: 10.1186/s13027-016-0099-0]
28 **Kamath PS**, Wiesner RH, Malinchoc M, Kremers W, Therneau TM, Kosberg CL, D'Amico G, Dickson ER, Kim WR. A model to predict survival in patients with end-stage liver disease. *Hepatology* 2001; **33**: 464-470 [PMID: 11172350 DOI: 10.1053/jhep.2001.22172]
29 **Afdhal N**, Reddy KR, Nelson DR, Lawitz E, Gordon SC, Schiff E, Nahass R, Ghalib R, Gitlin N, Herring R, Lalezari J, Younes ZH, Pockros PJ, Di Bisceglie AM, Arora S, Subramanian GM, Zhu Y, Dvory-Sobol H, Yang JC, Pang PS, Symonds WT, McHutchison JG, Muir AJ, Sulkowski M, Kwo P; ION-2 Investigators. Ledipasvir and sofosbuvir for previously treated HCV genotype 1 infection. *N Engl J Med* 2014; **370**: 1483-1493 [PMID: 24725238 DOI: 10.1056/NEJMoa1316366]
30 **Afdhal N**, Zeuzem S, Kwo P, Chojkier M, Gitlin N, Puoti M, Romero-Gomez M, Zarski JP, Agarwal K, Buggisch P, Foster GR, Bräu N, Buti M, Jacobson IM, Subramanian GM, Ding X, Mo H, Yang JC, Pang PS, Symonds WT, McHutchison JG, Muir AJ, Mangia A, Marcellin P; ION-1 Investigators. Ledipasvir and sofosbuvir for untreated HCV genotype 1 infection. *N Engl J Med* 2014; **370**: 1889-1898 [PMID: 24725239 DOI: 10.1056/NEJMoa1402454]
31 **Poordad F**, Hezode C, Trinh R, Kowdley KV, Zeuzem S, Agarwal K, Shiffman ML, Wedemeyer H, Berg T, Yoshida EM, Forns X, Lovell SS, Da Silva-Tillmann B, Collins CA, Campbell AL, Podsadecki T, Bernstein B. ABT-450/r-ombitasvir and dasabuvir with ribavirin for hepatitis C with cirrhosis. *N Engl J Med* 2014; **370**: 1973-1982 [PMID: 24725237 DOI: 10.1056/NEJMoa1402869]
32 **Manns M**, Samuel D, Gane EJ, Mutimer D, McCaughan G, Buti M, Prieto M, Calleja JL, Peck-Radosavljevic M, Müllhaupt B, Agarwal K, Angus P, Yoshida EM, Colombo M, Rizzetto M, Dvory-Sobol H, Denning J, Arterburn S, Pang PS, Brainard D, McHutchison JG, Dufour JF, Van Vlierberghe H, van Hoek B, Forns X; SOLAR-2 investigators. Ledipasvir and sofosbuvir plus ribavirin in patients with genotype 1 or 4 hepatitis C virus infection and advanced liver disease: a multicentre, open-label, randomised, phase 2 trial. *Lancet Infect Dis* 2016; **16**: 685-697 [PMID: 26907736 DOI: 10.1016/S1473-3099(16)00052-9]
33 **Bruno S**, Stroffolini T, Colombo M, Bollani S, Benvegnù L, Mazzella G, Ascione A, Santantonio T, Piccinino F, Andreone P, Mangia A, Gaeta GB, Persico M, Fagiuoli S, Almasio PL; Italian Association of the Study of the Liver Disease (AISF). Sustained

virological response to interferon-alpha is associated with improved outcome in HCV-related cirrhosis: a retrospective study. *Hepatology* 2007; **45**: 579-587 [PMID: 17326216 DOI: 10.1002/hep.21492]

34 **Child CG**, Turcotte JG. Surgery and portal hypertension. *Major Probl Clin Surg* 1964; **1**: 1-85 [PMID: 4950264]

35 **Malinchoc M**, Kamath PS, Gordon FD, Peine CJ, Rank J, ter Borg PC. A model to predict poor survival in patients undergoing transjugular intrahepatic portosystemic shunts. *Hepatology* 2000; **31**: 864-871 [PMID: 10733541 DOI: 10.1053/he.2000.5852]

36 **Zahnd C**, Salazar-Vizcaya L, Dufour JF, Müllhaupt B, Wandeler G, Kouyos R, Estill J, Bertisch B, Rauch A, Keiser O; Swiss HIV; Swiss Hepatitis C Cohort Studies. Modelling the impact of deferring HCV treatment on liver-related complications in HIV coinfected men who have sex with men. *J Hepatol* 2016; **65**: 26-32 [PMID: 26921687 DOI: 10.1016/j.jhep.2016.02.030]

37 **McCombs J**, Matsuda T, Tonnu-Mihara I, Saab S, Hines P, L' italien G, Juday T, Yuan Y. The risk of long-term morbidity and mortality in patients with chronic hepatitis C: results from an analysis of data from a Department of Veterans Affairs Clinical Registry. *JAMA Intern Med* 2014; **174**: 204-212 [PMID: 24193887 DOI: 10.1001/jamainternmed.2013.12505]

38 **Gray E**, O'Leary A, Stewart S, Bergin C, Cannon M, Courtney G, Crosbie O, De Gascun CF, Fanning LJ, Feeney E, Houlihan DD, Kelleher B, Lambert JS, Lee J, Mallon P, McConkey S, McCormick A, McKiernan S, McNally C, Murray F, Sheehan G, Norris S; Irish Hepatitis C Outcomes and Research Network (ICORN). High mortality during direct acting antiviral therapy for hepatitis C patients with Child's C cirrhosis: Results of the Irish Early Access Programme. *J Hepatol* 2016; **65**: 446-448 [PMID: 27130842 DOI: 10.1016/j.jhep.2016.03.022]

39 **Curry MP**. Direct acting antivirals for decompensated cirrhosis. Efficacy and safety are now established. *J Hepatol* 2016; **64**: 1206-1207 [PMID: 26948496 DOI: 10.1016/j.jhep.2016.02.041]

40 **Sandrin L**, Fourquet B, Hasquenoph JM, Yon S, Fournier C, Mal F, Christidis C, Ziol M, Poulet B, Kazemi F, Beaugrand M, Palau R. Transient elastography: a new noninvasive method for assessment of hepatic fibrosis. *Ultrasound Med Biol* 2003; **29**: 1705-1713 [PMID: 14698338]

41 **Degos F**, Perez P, Roche B, Mahmoudi A, Asselineau J, Voitot H, Bedossa P; FIBROSTIC study group. Diagnostic accuracy of FibroScan and comparison to liver fibrosis biomarkers in chronic viral hepatitis: a multicenter prospective study (the FIBROSTIC study). *J Hepatol* 2010; **53**: 1013-1021 [PMID: 20850886 DOI: 10.1016/j.jhep.2010.05.035]

42 **Bachofner JA**, Valli PV, Kröger A, Bergamin I, Künzler P, Baserga A, Braun D, Seifert B, Moncsek A, Fehr J, Semela D, Magenta L, Müllhaupt B, Terziroli Beretta-Piccoli B, Mertens JC. Direct antiviral agent treatment of chronic hepatitis C results in rapid regression of transient elastography and fibrosis markers fibrosis-4 score and aspartate aminotransferase-platelet ratio index. *Liver Int* 2017; **37**: 369-376 [PMID: 27678216 DOI: 10.1111/liv.13256]

**P- Reviewer**: Inoue K, Marcos M **S- Editor**: Gong ZM
**L- Editor**: A **E- Editor**: Huang Y

World Journal of Gastroenterology

Submit a Manuscript: http://www.f6publishing.com

*World J Gastroenterol* 2018 February 21; 24(7): 862-869

DOI: 10.3748/wjg.v24.i7.862

ISSN 1007-9327 (print) ISSN 2219-2840 (online)

ORIGINAL ARTICLE

Retrospective Study

# Predictors of post-treatment stenosis in cervical esophageal cancer undergoing high-dose radiotherapy

Jun Won Kim, Tae Hyung Kim, Jie-Hyun Kim, Ik Jae Lee

Jun Won Kim, Tae Hyung Kim, Ik Jae Lee, Department of Radiation Oncology, Gangnam Severance Hospital, Yonsei University College of Medicine, Seoul 06273, South Korea

Jie-Hyun Kim, Department of Internal Medicine, Gangnam Severance Hospital, Yonsei University College of Medicine, Seoul 06273, South Korea

ORCID number: Jun Won Kim (0000-0003-1358-364X); Tae Hyung Kim (0000-0002-5205-3775); Jie-Hyun Kim (0000-0002-9198-3326); Ik Jae Lee (0000-0001-7165-3373).

Author contributions: All authors helped to perform the research; Kim JW contributed to manuscript writing, data analysis and drafting design; Kim TH contributed to data analysis; Kim JH contributed to performing procedures; and Lee IJ contributed to drafting concept and design and performing procedures.

Supported by Basic Science Research Program through the National Research Foundation of Korea (NRF) funded by the Ministry of Education, No. 2017R1D1A1B03035047; and the National Research Foundation of Korea Grant funded by the Korean Government, No. NRF-2017M2A2A4A03083634.

Institutional review board statement: This study was reviewed and approved by the Ethics Committee of Gangnam Severance Hospital.

Informed consent statement: Patients were not required to give informed consent to the study because the analysis used anonymous clinical data that were obtained after each patient agreed to treatment by written consent.

Conflict-of-interest statement: All authors declare no conflicts-of-interest related to this article.

Data sharing statement: No additional data are available.



Manuscript source: Unsolicited manuscript

Correspondence to: Ik Jae Lee, MD, PhD, Associate Professor, Department of Radiation Oncology, Gangnam Severance Hospital, Yonsei University College of Medicine, 211 Eonju-ro, Gangnam-gu, Seoul 06273, South Korea. ikjae412@yuhs.ac
Telephone: +82-2-20193158
Fax: +82-2-20194855

Received: December 11, 2017
Peer-review started: December 11, 2017
First decision: December 20, 2017
Revised: December 25, 2017
Accepted: January 16, 2018
Article in press: January 16, 2018
Published online: February 21, 2018

## Abstract

### *AIM*

To evaluate toxicity and treatment outcome of high-dose radiotherapy (RT) for cervical esophageal cancer (CEC).

### *METHODS*

We reviewed a total of 62 consecutive patients who received definitive RT for stage Ⅰ to Ⅲ cervical esophageal cancer between 2001 and 2015. Patients who received < 45 Gy, treated for lesions below sternal notch, treated with palliative aim, treated with subsequent surgical resection, or diagnosed with synchronous hypopharyngeal cancer were excluded. Treatment failures were divided into local (occurring within the RT field), outfield-esophageal, and regional [occurring in regional lymph node(s)] failures. Factors predictive of esophageal stenosis requiring endoscopic dilation were analyzed.

***RESULTS***

Grade 1, 2, and 3 esophagitis occurred in 19 (30.6%), 39 (62.9%), and 4 patients (6.5%), respectively, without grade ⩾ 4 toxicities. Sixteen patients (25.8%) developed post-RT stenosis, of which 7 cases (43.8%) were malignant. Four patients (6.5%) developed tracheoesophageal fistula (TEF), of which 3 (75%) cases were malignant. Factors significantly correlated with post-RT stenosis were stage T3/4 ($P$ = 0.001), complete circumference involvement ($P$ < 0.0001), stenosis at diagnosis ($P$ = 0.024), and endoscopic complete response ($P$ = 0.017) in univariate analysis, while complete circumference involvement was significant in multivariate analysis ($P$ = 0.003). A higher dose (⩾ 60 Gy) was not associated with occurrence of post-RT stenosis or TEF. With a median follow-up of 24.3 (range, 3.4-152) mo, the 2 y local control, outfield esophageal control, progression-free survival, and overall survival (OS) rates were 78.9%, 90.2%, 49.6%, and 57.3%, respectively. Factors significantly correlated with OS were complete circumference involvement ($P$ = 0.023), stenosis at diagnosis ($P$ < 0.0001), and occurrence of post-RT stenosis or TEF ($P$ < 0.001) in univariate analysis, while stenosis at diagnosis ($P$ = 0.004) and occurrence of post-RT stenosis or TEF ($P$ = 0.023) were significant in multivariate analysis.

***CONCLUSION***

Chemoradiation for CEC was well tolerated, and a higher dose was not associated with stenosis. Patients with complete circumferential involvement require close follow-up.

**Key words:** Chemoradiotherapy; Post-radiotherapy stenosis; High-dose radiotherapy; Cervical esophageal cancer



**Core tip:** This study reports the outcome and toxicity of high dose (median 63 Gy) radiotherapy for cervical esophageal cancer. Post-RT stenosis and tracheoesophageal fistula rates were 26% and 6.5%, respectively. Stenosis at diagnosis and post-RT stenosis/fistula was significantly associated with overall survival. Complete circumference involvement was significantly associated with post-RT stenosis but dose higher than 60 Gy was not.

Kim JW, Kim TH, Kim JH, Lee IJ. Predictors of post-treatment stenosis in cervical esophageal cancer undergoing high-dose radiotherapy. *World J Gastroenterol* 2018; 24(7): 862-869 Available from: URL: http://www.wjgnet.com/1007-9327/full/v24/i7/862.htm DOI: http://dx.doi.org/10.3748/wjg.v24.i7.862

## INTRODUCTION

Carcinoma of the cervical esophagus is uncommon and accounts for 2%-10% of all esophageal carcinomas[1]. Squamous cell carcinoma (SCC) is predominant in the proximal esophagus, and the highest rates of SCC are found in East Asia and Southern Africa[2]. There are no prospective clinical trials to establish the standard care for cervical esophageal cancer (CEC). Because CEC is located between the cricopharyngeal muscle and the sternal notch, the surgical procedure to CEC is extensive, such as pharyngo-laryngo-esophagectomy[3], resulting in permanent tracheostomy and significant deterioration of quality of life[4]. Concurrent chemo-radiotherapy (CRT) has emerged as the preferred treatment modality for CEC[5]. Common toxic effects of definitive CRT for CEC include dysphagia, dehydration, mucositis, esophagitis, dermatitis, and fatigue[6]. Late toxic effects, such as stricture and fistulas may also occur[7,8].

Because of its anatomical proximity to the hypopharynx, CRT protocols for CEC are somewhat analogous to those for hypopharyngeal cancer[6]. However, unlike locally advanced SCC of the hypopharynx which requires 70 Gy in 35 fractions for definitive CRT[9], the standard dose of CRT for esophageal cancer remains 50 Gy[5,10]. Although a higher-than-standard dose of 50 Gy is suggested for CEC[5], the increased dose to the esophagus may lead to a higher incidence of severe toxicities, including ulcer, perforation, and stenosis[11]. Organs at risk for RT planning depend on the site of treatment. Radiation pneumonitis and fibrosis are of major concern when planning for the thoracic esophagus but are of less importance for CEC. Esophageal toxicity information from hypopharyngeal cancer treatment is of limited value; the radiation field for hypopharyngeal cancer includes only a small segment of the cervical esophagus, while RT for CEC includes a large segment of the esophagus because of expansion of the craniocaudal margins from the gross tumor and the entire esophageal circumference. Reports on the high-dose radiation-induced toxicity of CEC are scarce, although information can be inferred from the retrospective data on head and neck cancer patients experiencing toxicities of the proximal esophagus[12]. A toxicity evaluation is required before the administration of dose-escalated protocols.

We report the outcome and toxicity of definitive radiotherapy (RT) for CEC, with an emphasis on the identification of clinical variables associated with the occurrence of post-RT esophageal stenosis and tracheo-esophageal fistulas (TEF).

## MATERIALS AND METHODS

### *Patients*

We retrospectively reviewed a total of 62 consecutive patients who received definitive RT for pathologically confirmed stage Ⅰ-Ⅲ (American Joint Committee on Cancer 7$^{th}$ edition) CEC between 2001 and 2015. CEC was defined as a tumor of the esophagus located between the inferior border of the cricoid cartilage and

the thoracic inlet (suprasternal notch). Tumors with the epicenter located below the sternal notch were generally considered non-CEC for this study. Patients treated with a palliative aim, those who received < 45 Gy, those treated with subsequent surgical resection, or those diagnosed with synchronous hypopharyngeal cancer were excluded. All procedures were performed in accordance with the Helsinki Declaration of 1975, as revised in 1983. This study was approved by the institutional review board (4-2017-0027).

### Treatment

All patients were treated according to institutional protocols, consisting of platinum-based concurrent CRT or RT alone if patients could not tolerate chemotherapy. The gross tumor volume (GTV) was defined as a visible tumor in the esophagus and gross regional lymph node metastasis. The initial clinical target volume (CTV1) was defined by expansion of the GTV by 4 cm craniocaudally and 1-2 cm laterally, as well as bilateral supraclavicular lymph nodes inclusion for elective nodal irradiation. The initial planning target volume (PTV1) was defined as CTV1 plus a 0.5 cm margin in all directions, and 36-45 Gy in a conventional daily fractionation of 1.8 Gy was prescribed for PTV1. The boost CTV (CTV2) included the GTV plus a 3-4 cm craniocaudal margin and a 1-2 cm lateral margin, excluding the elective nodal field. PTV2 was obtained by adding a 0.5 cm margin to CTV2 in all directions and received a total dose of up to 50.4 Gy, while limiting the maximum spinal cord dose under 45 Gy. For patients receiving a total dose higher than 50.4 Gy, an additional boost dose was delivered to PTV3, which comprised the GTV with a narrow margin of 0.5-1 cm in all directions. Cisplatin (or carboplatin) and 5-fluorouracil (5-FU) based chemotherapy was used. Two cycles of chemotherapy were administered concurrently with RT, followed by 1-6 cycles of consolidation chemotherapy[13].

### Follow-up and evaluation

Upon completion of concurrent CRT, patients were evaluated every 3 mo for the first year and every 6 mo thereafter with a physical examination, toxicity assessment, upper gastrointestinal endoscopy, computed tomography (CT) scans of the neck, chest, and abdomen, and, when necessary, positron emission tomography-CT. Acute and late toxicity was assessed using the Radiation Therapy Oncology Group (RTOG) criteria. Esophageal stenosis was evaluated using esophagography or endoscopy, and significant stenosis was defined as symptomatic stenosis requiring endoscopic dilatation and/or stent insertion. Endoscopic complete remission (CR) of the primary tumor was defined when all visible tumors disappeared on endoscopy and a negative biopsy was conducted, with these outcomes lasting for more than 4 wk. Treatment failures were divided into local (occurring within the RT field), outfield-esophageal, and regional [occurring in regional lymph node(s)] failures. Factors predictive of esophageal stenosis requiring endoscopic dilation and TEF were analyzed.

### Statistical analysis

Survival time was measured from the date of diagnosis to the date of the first event or the date of death. Survival curves were estimated using the Kaplan-Meier method, and multivariate analysis was performed using the Cox proportional hazard model. Correlation between clinical variables and post-RT occurrence of esophageal stenosis/TEF was performed using the $\chi^2$ test. A $P$ value < 0.05 was indicative of statistical significance.

## RESULTS

### Patient characteristics

The median age was 66 (range, 29-86) years, and SCC was predominant (90.3%). The numbers of patients with T1, T2, T3, and T4 disease were 14 (22.6%), 6 (9.7%), 30 (48.4%), and 12 (19.3%), respectively. The median length of tumor involvement of the esophagus was 5.0 (range, 1-14) cm, and 22 patients had a tumor involving 100% of the esophageal circumference. The median biologically equivalent RT dose in 1.8-Gy fraction was 63 (range, 45-90) Gy. Two of the patients received a total dose of 81 Gy and 90 Gy each because a boost RT (18-27 Gy) was delivered to the residual tumor 1-2 mo after 63 Gy. Sixty patients (96.8%) were treated with concurrent chemotherapy (Table 1).

### Toxicity and risk factors

Grade 1, 2, and 3 esophagitis occurred in 19 (30.6%), 39 (62.9%), and 4 patients (6.5%), respectively, without grade 4 or 5 toxicities. Sixteen patients (25.8%) developed stenosis requiring dilation within a median of 5.5 mo (range 1.1-22.5) after RT, among which 7 cases (11.3%) were malignant strictures. Four patients (6.5%) developed TEF within a median of 2.6 mo (range 1.8-5.8) after RT, 3 (4.8%) of which were malignant fistulas (Table 2). Factors showing a significant correlation with post-RT stenosis requiring dilation were T3/4 disease (*vs* T1/2) ($P$ = 0.001), 100% circumference involvement (*vs* < 100%) ($P$ < 0.0001), stenosis at diagnosis (*vs* none) ($P$ = 0.024), and endoscopic CR (*vs* < CR) ($P$ = 0.017) in univariate analysis. A higher dose (≥ 60 Gy) was not associated with post-RT stenosis ($P$ = 0.515). Only 100% circumference involvement was significantly associated with stenosis in multivariate analysis ($P$ = 0.003) (Table 3). Factors showing significant correlation with either post-RT stenosis requiring dilatation or TEF were T3/4 (*vs* T1/2) ($P$ < 0.0001), 100% circumference involvement (*vs* < 100%) ($P$ < 0.0001), stenosis at diagnosis (*vs* none) ($P$ = 0.023), and endoscopic CR (*vs* < CR) ($P$ = 0.001) in univariate analysis. Higher dose (≥ 60 Gy) was not associated with post-RT

**Table 1 Demographic and treatment data (*n* = 62)**

| Characteristics | | *n* (%) |
|---|---|---|
| Sex | Female:Male | 4:58 (6.5:93.5) |
| Age | | Median 66 yr (range 29-86) |
| Pathology | Squamous cell carcinoma | 56 (90.3) |
| | Adenocarcinoma | 2 (3.2) |
| | Other | 4 (6.5) |
| T stage | T1 | 14 (22.6) |
| | T2 | 6 (9.7) |
| | T3 | 30 (48.4) |
| | T4 | 12 (19.3) |
| Regional node metastasis | N0 | 14 (22.6) |
| | N+ | 48 (77.4) |
| Tumor length | | Median 5.0 cm (range 1-14) |
| Total length of skip lesions | | Median 5.0 cm (range 1-20) |
| Involved circumference | < 100% | 40 (64.5) |
| | 100% | 22 (35.5) |
| Stenosis at diagnosis | No | 45 (72.6) |
| | Yes | 17 (27.4) |
| Radiation dose (EQD1.8) | | Median 63 Gy (range 45-90) |
| Concurrent chemotherapy | Yes | 60 (96.8) |
| | No | 2 (3.2) |
| Endoscopic response | CR | 39 (62.9) |
| | < CR | 23 (37.1) |

EQD1.8: Biologically equivalent dose in 1.8 Gy fractions; CR: Complete response.

**Table 2 Post-radiotherapy toxicity profile**

| Toxicity | | *n* (%) | RT-event interval (mo) |
|---|---|---|---|
| Esophagitis | RTOG Gr 1 | 19 (30.6) | |
| | RTOG Gr 2 | 39 (62.9) | |
| | RTOG Gr 3 | 4 (6.5) | |
| RT stenosis[1] | All | 16 (25.8) | Median 5.5 (range 1.1-22.5) |
| | Malignant | 7 (11.3) | |
| T-E fistula | All | 4 (6.5) | Median 2.6 (range 1.8-5.8) |
| | Malignant | 3 (4.8) | |

[1]Stenosis requiring dilatation. RTOG: Radiation therapy oncology group; T-E: Tracheoesophageal; Gr: Grade; RT: Radiotherapy.

stenosis or TEF ($P$ = 0.259). Both 100% circumference involvement ($P$ = 0.002) and endoscopic CR ($P$ = 0.035) were significantly associated with the occurrence of post-RT stenosis or TEF in multivariate analysis (Supplementary Table 1). Table 4 summarizes the clinical variables and treatment outcomes among the 19 patients who developed post-RT stenosis requiring dilatation or TEF. Nine of these patients had endoscopic findings of total esophageal obstruction at the time of diagnosis and 10 patients had dysphagia symptoms only. Seven of the 8 patients (87.5%) who developed non-malignant post-RT stenosis and 5 of the 7 patients (71.4%) who developed malignant post-RT stenosis initially had 100% circumferential esophageal involvement by the tumor. Four patients with post-RT TEF showed a CR or partial response (PR) and developed fistulas within 6 mo after completion of RT. Of the 17 patients who initially had endoscopic finding of total obstruction at the time of diagnosis, post-RT stenosis requiring dilatation was reported in 8 patients (3 malignant stenosis) and malignant TEF in 2 patients (Supplementary Table 2).

### *Treatment outcome and prognostic factors*

Twenty-seven patients were alive at the time of diagnosis. The median follow-up was 24.3 (range, 3.4-152) mo for all patients and 67.8 (range, 17.8-152) mo for surviving patients. An endoscopic CR was achieved in 39 patients (62.9%). A total of 34 patients experienced treatment failures: 7 local, 3 outfield esophageal, 6 regional, 11 distant, 2 concurrent local and regional, 1 concurrent outfield esophageal and regional, 3 concurrent local and distant, and 1 concurrent outfield esophageal, regional, and distant failure (Supplementary figure 1). The 2-year local failure-free (LFFS), outfield esophageal failure-free, regional failure-free, distant metastasis-free, progression-free, and overall survival (OS) rates were 78.9%, 90.2%, 79.5%, 72.7%, 49.6%, and 57.3%, respectively. T3/4 stage ($P$ = 0.050), stenosis at diagnosis ($P$ = 0.025), and RT stenosis or TEF ($P$ = 0.001) showed a correlation with LFFS in univariate analysis. Only the occurrence of RT stenosis

**Table 3 Factors influencing occurrence of post-radiotherapy stenosis *n* (%)**

| Characteristics | No. of Patients | Stenosis | | *P* value | |
|---|---|---|---|---|---|
| | | No | Yes | Univariate | Multivariate |
| Age | | | | | |
| ≤ 65 | 30 | 24 (80) | 6 (20) | 0.236 | |
| > 65 | 32 | 22 (69) | 10 (31) | | |
| T stage | | | | | |
| T1/2 | 20 | 20 (100) | 0 | 0.001 | 0.998 |
| T3/4 | 42 | 26 (62) | 16 (38) | | |
| Involved circumference | | | | | |
| < 100% | 40 | 37 (93) | 3 (7) | < 0.0001 | 0.003 |
| 100% | 22 | 9 (41) | 13 (59) | | |
| Total length | | | | | |
| < 5.0 | 28 | 22 (79) | 6 (921) | 0.338 | |
| ≥ 5.0 | 34 | 24 (71) | 10 (29) | | |
| Stenosis at diagnosis | | | | | |
| No | 45 | 37 (82) | 8 (18) | 0.024 | 0.995 |
| Yes | 17 | 9 (53) | 8 (47) | | |
| Dysphagia at diagnosis | | | | | |
| ≤ 1 mo | 36 | 30 (83) | 6 (17) | 0.051 | |
| > 1 mo | 26 | 16 (62) | 10 (38) | | |
| RT dose | | | | | |
| ≥ 60 Gy | 37 | 27 (73) | 10 (27) | 0.515 | |
| < 60 Gy | 25 | 19 (76) | 6 (24) | | |
| Endoscopic response | | | | | |
| CR | 39 | 33 (85) | 6 (15) | 0.017 | 0.740 |
| < CR | 23 | 13 (56) | 10 (44) | | |

RT: Radiotherapy; CR: Complete response.

**Table 4 Patients with post-radiotherapy stenosis or tracheoesophageal fistula (*n* = 19)**

| Age/Sex | T stage | Involve circumf | Initial stenosis/ management | RT (Gy) | Response | Toxicity (onset, mo) | Outcome (mo) |
|---|---|---|---|---|---|---|---|
| 29/F | T3 | 100% | Dysphagia only | 59.4 | CR | Stenosis (20) | NED, alive (152) |
| 70/M | T3 | 100% | Total obst/none | 59.4 | PR | Stenosis (5) | DOOC (12) |
| 64/M | T4a | 100% | Dysphagia only | 63.0 | PR | Stenosis (1) | DM (5), DOD (7) |
| 68/F | T3 | 100% | Dysphagia only | 63.0 | CR | Stenosis (1) | NED, alive (21) |
| 75/M | T3 | 100% | Total obst/none | 63.0 | PR | Stenosis (2) | DOOC (22) |
| 60/F | T4b | 100% | Total obst/stent | 70.0 | CR | Stenosis (4) | NED, alive (23) |
| 68/M | T3 | 100% | Dysphagia only | 70.2 | SD | Stenosis (6) | InF (8), DOD (14) |
| 73/M | T4b | 75% | Total obst/stent | 90.0[1] | PR | Stenosis (11) | DM (13), DOD (17) |
| 64/M | T3 | 100% | Dysphagia only | 50.4 | PR | Stenosis[2] (9) | InF (17), DOD (20) |
| 69/M | T4b | 100% | Total obst/stent | 50.4 | SD | Stenosis[2] (2) | DOOC (5) |
| 64/M | T4a | 100% | Dysphagia only | 59.4 | PR | Stenosis[2] (7) | DM (3)/InF (9), DOD (11) |
| 68/M | T3 | 100% | Total obst/none | 63.0 | PR | Stenosis[2] (2) | DM (3), DOD (5) |
| 73/M | T3 | 100% | Total obst/PEG | 63.0 | PR | Stenosis[2] (22) | InF (16), DOD (31) |
| 75/M | T3 | 40% | Dysphagia only | 57.6 | CR | Stenosis[2] (14) | InF (7), DOD (31) |
| 74/M | T3 | 50% | Dysphagia only | 81.0[1] | CR | Stenosis[2] (9) | InF (9), DOD (16) |
| 57/M | T3 | 100% | Dysphagia only | 63.0 | PR | TEF (3) | OutF (8), DOD (9) |
| 57/M | T3 | 100% | Total obst/stent | 60.0 | CR | Stenosis (1)/TEF[2] (6) | InF (8), DOD (14) |
| 72/M | T3 | 100% | Total obst/stent | 63.0 | PR | TEF[2] (2) | DOOC (5) |
| 51/M | T3 | 40% | Dysphagia only | 63.0 | PR | TEF[2] (2) | RF (4), DOD (6) |

[1]Boost RT (18-27 Gy) was delivered to residual tumor 1-2 mo after 63 Gy. [2]Malignant complications. Involve circumf: Percent of esophageal circumference involved by tumor; RT: Radiotherapy; obst: Obstruction; PEG: Percutaneous endoscopic gastrostomy; CR: Complete response; PR: Partial response; SD: Stable disease; InF: Infield failure; OutF: Outfield failure; RF: Regional failure; DM: Distant metastasis; DOD: Died of disease; DOOC: Died of other cause; NED: No evidence of disease; TEF: Tracheoesophageal fistula.

or TEF showed a trend towards poor LFFS in multivariate analysis ($P$ = 0.066) (Supplementary Table 3 and Figure 1A). Factors showing significant correlations with OS were 100% circumference involvement ($P$ = 0.023), stenosis at diagnosis ($P$ < 0.0001), and occurrence of radiation induced stenosis or TEF ($P$ < 0.001) in univariate analysis. Both stenosis at diagnosis ($P$ = 0.004) and occurrence of RT stenosis or TEF ($P$ = 0.023) were significantly associated with OS in multivariate analysis (Supplementary Table 4 and Figure 1B).

## DISCUSSION

The most common radiation-induced late esophageal

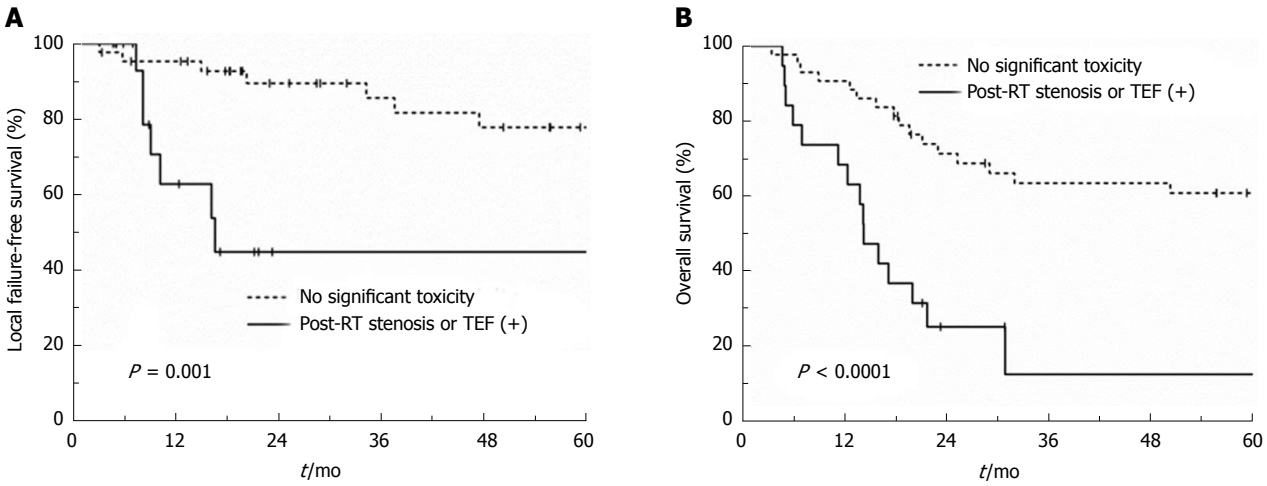


**Figure 1 Comparison of local failure-free survival (A) and overall survival (B) between patients who experienced post-radiotherapy stenosis or tracheoesophageal fistula and those who did not.** TEF: Tracheoesophageal fistula.

toxicity is dysphagia due to dysmotility and esophageal stricture[14], and these complications can result from muscular damage, submucosal fibrosis, and possibly nerve damage[15]. Unlike the lower esophagus, the proximal esophagus is composed predominantly of striated muscles, and conscious, voluntary swallowing is the key function in this part of the organ. Thus, stricture after RT rather than impaired peristalsis and involuntary swallowing may be the main cause of dysphagia in the cervical esophagus.

Toxicity evaluation of higher-than-standard-dose RT for CEC was necessary, and the primary objective of the current study was to determine clinical factors associated with the development of post-RT stenosis and TEF. Although most of the patients (96.8%) were treated with standard cisplatin and 5-FU-based CRT, the radiation dose used for the current study, at a median of 63 (range, 45-90) Gy, was significantly higher than the standard dose of 50 Gy. In the current study, preservation of the esophageal passage, either pre-RT (at diagnosis) stenosis ($P$ = 0.004) or post-RT stenosis/TEF ($P$ = 0.023), was an independent prognostic factor associated with OS, suggesting that resolution of the initial stenosis and prevention of post-treatment stenosis are indeed important in prolonging patients' survival.

The esophagus is a hollow viscous organ with a tubular structure and it functions in series, such that destruction of the complete circumference of a small volume of esophagus could result in dysfunction of the entire organ. Unlike treating head and neck or lung cancers, full circumferential treatment of the esophagus cannot be avoided when treating tumors originating in the esophagus. Maguire *et al*[16] observed that patients who received > 80 Gy to any portion of the entire organ circumference had an increased risk of late toxicity in multivariate analysis. Although a higher dose to the esophagus increases the risk of severe complications, the application of more than 50 Gy may improve local control. In the current study, the highest dose we prescribed was 63 Gy except for the 2 patients who received a boost dose of 18 Gy and 27 Gy to the residual tumor. Although this is not a dose-escalation study, 63 Gy may be safely delivered to the cervical esophagus without causing severe toxicities.

It should be noted that, while 16 patients (25.8%) developed post-RT stenosis requiring dilation and 4 patients (6.5%) developed TEF, 7 (44%) and 3 (75%) patients were because of persistent or recurrent malignancy, respectively. Clinically diagnosed post-RT stricture may grossly overestimate the risk of radiation induced stenosis and may be an early sign of tumor recurrence[17]. In fact, only complete circumferential tumor involvement was an independent predictor of post-RT stenosis, while T stage, stenosis at diagnosis, and a higher dose (⩾ 60 Gy) were not (Table 3). When both post-RT stenosis and TEF were considered, complete circumference tumor involvement and endoscopic CR were both independent predictors (Supplementary Table 1). Considering that 75% of TEF cases were malignant and occurred within the first 6 mo after completion of RT and after achieving a CR or PR, a rapid response to CRT, rather than a higher radiation dose, may be a contributing factor to the development of post-RT TEF.

A study by Atsumi *et al*[18] suggested that esophageal stenosis is associated with tumor regression after RT. In this study, 109 patients who achieved a CR after definitive CRT were evaluated with esophagography within 3 mo after completion of RT; and T stage, extent of involved circumference, and wall thickness of the tumor region were significantly correlated with esophageal stenosis in multivariate analysis[18]. Luminal narrowing of the esophagus after RT is largely due to fibrosis and inflammation of the submucosal and muscular layers[19,20]. These processes accompany infiltration of inflammatory cells[21] and probably include accumulation of macrophages with increased local levels

of proinflammatory cytokines induced by radiation[22,23]; this, in turn, produces edema and fibrosis in the submucosal and underlying muscular layers. These processes may be much more pronounced in and around the shrinking tumors that respond well to RT[18], which may explain the significant correlation between complete circumferential involvement and post-RT stenosis in our study.

Our study showed that, although pre- and post-RT stenosis was a prognostic factor for patients' survival, complete circumference involvement rather than a higher radiation dose was the key contributing factor. In clinical practice, physicians are often tempted to prescribe a higher-than-standard dose of 50 Gy for esophageal cancer, especially when it is expected that the patient is unable to undergo surgical resection because of tumor location, poor generalized condition, or patient's refusal for surgery. Our data suggests that patients with cervical esophageal cancer may undergo radiotherapy of up to 63 Gy without increasing the risk of radiation-induced toxicities. Since prospective data is lacking, our study warrants a prospective trial to investigate toxicity and efficacy of high-dose radiotherapy for cervical esophageal cancer.

In conclusion, CRC for CEC was well tolerated, and a higher dose was not associated with post-RT stenosis. Patients with complete circumferential tumor involvement at diagnosis require close follow-up.

## ARTICLE HIGHLIGHTS

### *Research background*

The surgical procedure for cervical esophageal cancer (CEC) is extensive, and concurrent chemoradiotherapy (CRT) is the preferred treatment modality. Although a higher-than-standard dose of 50 Gy is suggested for CEC, the increased dose may lead to a higher incidence of severe toxicities, such as ulcer, perforation and stenosis.

### *Research motivation*

Clinical data on radiotherapy with increased dose for CEC are scarce, and a toxicity evaluation is required before the administration of dose-escalated protocols.

### *Research objectives*

To evaluate toxicity and treatment outcome of high dose radiotherapy for CEC, and to determine the factors associated with post-treatment esophageal stenosis.

### *Research methods*

In this study, the authors reviewed 62 consecutive patients who received definitive RT for stage Ⅰ to Ⅲ cervical esophageal cancer between 2001 and 2015. Patients (received < 45 Gy) treated for lesions below sternal notch, treated with palliative aim and subsequent surgical resection, or diagnosed with synchronous hypopharyngeal cancer were excluded. Treatment failures were divided into local, outfield-esophageal, and regional failures. The factors predictive of esophageal stenosis requiring endoscopic dilation were analyzed.

### *Research results*

With a median follow-up of 24.3 (range, 3.4-152) mo, the 2-year local control, outfield esophageal control, progression-free survival, and overall survival (OS) rates were 78.9%, 90.2%, 49.6%, and 57.3%, respectively. Grade 1, 2, and 3 esophagitis occurred in 19 (30.6%), 39 (62.9%), and 4 patients (6.5%), respectively, without grade ⩾ 4 toxicities. Sixteen patients developed post-RT stenosis, of which 7 cases were malignant. Four patients developed tracheoesophageal fistula (TEF), of which 3 cases were malignant. Factors significantly correlated with OS were complete circumference involvement, stenosis at diagnosis, and occurrence of post-RT stenosis or TEF in univariate analysis, while stenosis at diagnosis and occurrence of post-RT stenosis or TEF were significant in multivariate analysis. Factors significantly correlated with post-RT stenosis were stage T3/4, complete circumference involvement, stenosis at diagnosis, and endoscopic complete response in univariate analysis, while complete circumference involvement was significant in multivariate analysis. A higher dose (⩾ 60 Gy) was not associated with the occurrence of post-RT stenosis or TEF.

### *Research conclusions*

This study showed that, although pre- and post-RT stenosis was a prognostic factor for patients' survival, complete circumference involvement rather than a higher radiation dose was the key contributing factor, and suggesting that CEC can be treated with higher than the current standard dose of 50 Gy. CRT for CEC was well tolerated, and patients with complete circumferential involvement require close follow-up.

### *Research perspectives*

The data suggests that patients with CEC may undergo radiotherapy of up to 63 Gy without increasing the risk of radiation-induced toxicities. Since prospective data is lacking, our study warrants a prospective trial to investigate toxicity and efficacy of high-dose radiotherapy for CEC.

## ACKNOWLEDGMENTS

This study was selected for a poster presentation at the 59th Annual Meeting of the American Society for Radiation Oncology (ASTRO), San Diego, CA, United States September 2017.

## REFERENCES

1 **Lee DJ**, Harris A, Gillette A, Munoz L, Kashima H. Carcinoma of the cervical esophagus: diagnosis, management, and results. *South Med J* 1984; **77**: 1365-1367 [PMID: 6494955]
2 **Torre LA**, Bray F, Siegel RL, Ferlay J, Lortet-Tieulent J, Jemal A. Global cancer statistics, 2012. *CA Cancer J Clin* 2015; **65**: 87-108 [PMID: 25651787 DOI: 10.3322/caac.21262]
3 **Grass GD**, Cooper SL, Armeson K, Garrett-Mayer E, Sharma A. Cervical esophageal cancer: a population-based study. *Head Neck* 2015; **37**: 808-814 [PMID: 24616217 DOI: 10.1002/hed.23678]
4 **Archibald S**, Young JE, Thoma A. Pharyngo-cervical esophageal reconstruction. *Clin Plast Surg* 2005; **32**: 339-346, vi [PMID: 15979473 DOI: 10.1016/j.cps.2005.01.002]
5 Esophageal and esophagogastric junction cancers. NCCN guidelines Version 3.2017: 2017: September 28, 2017. Available from: URL: https://www.nccn.org/professionals/physician_gls/pdf/esophageal.pdf
6 **Hoeben A**, Polak J, Van De Voorde L, Hoebers F, Grabsch HI, de Vos-Geelen J. Cervical esophageal cancer: a gap in cancer knowledge. *Ann Oncol* 2016; **27**: 1664-1674 [PMID: 27117535 DOI: 10.1093/annonc/mdw183]
7 **Gkika E**, Gauler T, Eberhardt W, Stahl M, Stuschke M, Pöttgen C. Long-term results of definitive radiochemotherapy in locally advanced cancers of the cervical esophagus. *Dis Esophagus* 2014; **27**: 678-684 [PMID: 24147973 DOI: 10.1111/dote.12146]
8 **Wang SL**, Liao Z, Liu H, Ajani J, Swisher S, Cox JD, Komaki R. Intensity-modulated radiation therapy with concurrent chemotherapy for locally advanced cervical and upper thoracic esophageal cancer. *World J Gastroenterol* 2006; **12**: 5501-5508 [PMID: 17006988 DOI: 10.3748/wjg.v12.i34.5501]
9 Head and Neck Cancers. NCCN guidelines Version 2.2017, 2017:

September 28, 2017. Available from: URL: https://www.nccn.org/professionals/physician_gls/pdf/head-and-neck.pdf
10 **Minsky BD**, Pajak TF, Ginsberg RJ, Pisansky TM, Martenson J, Komaki R, Okawara G, Rosenthal SA, Kelsen DP. INT 0123 (Radiation Therapy Oncology Group 94-05) phase III trial of combined-modality therapy for esophageal cancer: high-dose versus standard-dose radiation therapy. *J Clin Oncol* 2002; **20**: 1167-1174 [PMID: 11870157 DOI: 10.1200/JCO.2002.20.5.1167]
11 **Emami B**, Lyman J, Brown A, Coia L, Goitein M, Munzenrider JE, Shank B, Solin LJ, Wesson M. Tolerance of normal tissue to therapeutic irradiation. *Int J Radiat Oncol Biol Phys* 1991; **21**: 109-122 [PMID: 2032882]
12 **Chen AM**, Li BQ, Jennelle RL, Lau DH, Yang CC, Courquin J, Vijayakumar S, Purdy JA. Late esophageal toxicity after radiation therapy for head and neck cancer. *Head Neck* 2010; **32**: 178-183 [PMID: 19536858 DOI: 10.1002/hed.21164]
13 **Kim HW**, Kim JH, Lee IJ, Kim JW, Lee YC, Lee CG, Park JJ, Youn YH, Park H. Local control may be the key in improving treatment outcomes of esophageal squamous cell carcinoma undergoing concurrent chemoradiation. *Digestion* 2014; **90**: 254-260 [PMID: 25531173 DOI: 10.1159/000368983]
14 **Werner-Wasik M**. Treatment-related esophagitis. *Semin Oncol* 2005; **32**: S60-S66 [PMID: 16015537]
15 **Vanagunas A**, Jacob P, Olinger E. Radiation-induced esophageal injury: a spectrum from esophagitis to cancer. *Am J Gastroenterol* 1990; **85**: 808-812 [PMID: 2371980]
16 **Maguire PD**, Sibley GS, Zhou SM, Jamieson TA, Light KL, Antoine PA, Herndon JE 2nd, Anscher MS, Marks LB. Clinical and dosimetric predictors of radiation-induced esophageal toxicity. *Int J Radiat Oncol Biol Phys* 1999; **45**: 97-103 [PMID: 10477012]
17 **Hazard L,** Minsky B. Esophagus In: Shrieve D, Loeffler J. Human Radiation Injury. 1st ed. Philadelphia, PA: Lippincott Williams Wilkins, 2011: 403-420
18 **Atsumi K**, Shioyama Y, Arimura H, Terashima K, Matsuki T, Ohga S, Yoshitake T, Nonoshita T, Tsurumaru D, Ohnishi K, Asai K, Matsumoto K, Nakamura K, Honda H. Esophageal stenosis associated with tumor regression in radiotherapy for esophageal cancer: frequency and prediction. *Int J Radiat Oncol Biol Phys* 2012; **82**: 1973-1980 [PMID: 21477944 DOI: 10.1016/j.ijrobp.2011.01.047]
19 **Seaman WB**, Ackerman LV. The effect of radiation on the esophagus; a clinical and histologic study of the effects produced by the betatron. *Radiology* 1957; **68**: 534-541 [PMID: 13432180 DOI: 10.1148/68.4.534]
20 **Berthrong M**, Fajardo LF. Radiation injury in surgical pathology. Part II. Alimentary tract. *Am J Surg Pathol* 1981; **5**: 153-178 [PMID: 7013506]
21 **Papazian A**, Capron JP, Ducroix JP, Dupas JL, Quenum C, Besson P. Mucosal bridges of the upper esophagus after radiotherapy for Hodgkin's disease. *Gastroenterology* 1983; **84**: 1028-1031 [PMID: 6832554]
22 **Handschel J**, Sunderkötter C, Prott FJ, Meyer U, Kruse-Lösler B, Joos U. Increase of RM3/1-positive macrophages in radiation-induced oral mucositis. *J Pathol* 2001; **193**: 242-247 [PMID: 11180172 DOI: 10.1002/1096-9896(2000)9999:9999<::AID-PATH754>3.0.CO;2-P]
23 **Sonis ST**, Peterson RL, Edwards LJ, Lucey CA, Wang L, Mason L, Login G, Ymamkawa M, Moses G, Bouchard P, Hayes LL, Bedrosian C, Dorner AJ. Defining mechanisms of action of interleukin-11 on the progression of radiation-induced oral mucositis in hamsters. *Oral Oncol* 2000; **36**: 373-381 [PMID: 10899677]

**P- Reviewer**: Arigami T, Kato H, Ono T **S- Editor**: Wang JL
**L- Editor**: A **E- Editor**: Huang Y

World Journal of Gastroenterology

Submit a Manuscript: http://www.f6publishing.com

*World J Gastroenterol* 2018 February 21; 24(7): 870-875

DOI: 10.3748/wjg.v24.i7.870

ISSN 1007-9327 (print) ISSN 2219-2840 (online)

CASE REPORT

# Esophageal metastasis of stem cell-subtype hepatocholangio carcinoma: Rare presentation of a rare tumor

Maëva Salimon, Nicolas Chapelle, Tamara Matysiak-Budnik, Jean-François Mosnier, Eric Frampas, Yann Touchefeu

Maëva Salimon, Nicolas Chapelle, Tamara Matysiak-Budnik, Yann Touchefeu, Institut des Maladies de l'Appareil Digestif, Nantes University Hospital, Nantes 44000, France

Jean-François Mosnier, Department of Pathology, Nantes University Hospital, Nantes 44000, France

Eric Frampas, Department of Radiology, Nantes University Hospital, Nantes 44000, France

ORCID number: Maëva Salimon (0000-0001-9155-0128); Nicolas Chapelle (0000-0003-4834-9693); Tamara Matysiak-Budnik (0000-0003-0780-6261); Jean-François Mosnier (0000-0003-2637-3641); Eric Frampas (0000-0002-8414-6626); Yann Touchefeu (0000-0001-8421-3182).

Author contributions: Salimon M and Touchefeu Y designed the research; Salimon M, Chapelle N, Mosnier JF and Frampas E performed the research; Salimon M, Matysiak-Budnik T and Touchefeu Y wrote the paper.

Informed consent statement: This is a non-interventional report; the patient died before the writing of the report. The report is in accordance of the Declaration of Helsinki and its latter amendments.

Conflict-of-interest statement: The authors have no conflicts of interest to declare.

CARE Checklist (2013) statement: The authors have read the CARE Checklist (2013), and the manuscript was prepared and revised according to the CARE Checklist (2013).



Manuscript source: Unsolicited manuscript

Correspondence to: Yann Touchefeu, MD, PhD, Doctor, Institut des Maladies de l'Appareil Digestif, Nantes University Hospital, 1 Place Alexis Ricordeau, Nantes 44000, France. yann.touchefeu@chu-nantes.fr
Telephone: +33-240-083152
Fax: +33-240-083154

Received: December 12, 2017
Peer-review started: December 12, 2017
First decision: December 27, 2017
Revised: January 2, 2018
Accepted: January 16, 2018
Article in press: January 16, 2018
Published online: February 21, 2018

## Abstract

Hepatocholangiocarcinoma (cHCC-ICC) is a rare primary hepatic tumor defined by the presence of histological features of both hepatocellular carcinoma (HCC) and intrahepatic cholangiocarcinoma (ICC). Its prevalence ranges from 1%-5% of all primary liver cancers. We report the case of a 55-year-old cirrhotic male patient admitted to our university hospital for dysphagia, revealing a 10 cm lower-third esophageal metastasis of an unresectable cHCC-ICC with stem-cell features. Computed tomography and abdominal magnetic resonance imaging scans revealed multiple hepatic lesions combining features of both HCC and ICC, associated with synchronous bone metastasis. Histological and immunohistochemical analyses of biopsies from the esophageal lesion and the hepatic tumor confirmed the diagnosis of cHCC-ICC with a stem cell-subtype, according to the World Health

Organization classification. After a multidisciplinary meeting, the patient was treated with chemotherapy. He received two cycles of a gemcitabine plus cisplatin regimen before bone progression, and he died 3 mo after the initial diagnosis.

**Key words:** Hepatocholangiocarcinoma; Stem cell-subtype; Esophageal metastasis; Chemotherapy; Gemcitabine plus platinum-based chemotherapy



**Core tip:** Hepatocholangiocarcinoma (cHCC-ICC) represents less than 5% of all hepatic tumors and remains an uncommon cancer, with no guidelines concerning its management. Esophageal metastasis is a rare presentation of hepatic tumors. To our knowledge, this case report is the first to describe an esophageal lesion revealing a metastatic stem cell-subtype cHCC-ICC.

Salimon M, Chapelle N, Matysiak-Budnik T, Mosnier JF, Frampas E, Touchefeu Y. Esophageal metastasis of stem cell-subtype hepatocholangiocarcinoma: Rare presentation of a rare tumor. *World J Gastroenterol* 2018; 24(7): 870-875 Available from: URL: http://www.wjgnet.com/1007-9327/full/v24/i7/870.htm DOI: http://dx.doi.org/10.3748/wjg.v24.i7.870

## INTRODUCTION

Primary liver cancer is the sixth most common cancer worldwide[1]. The majority of intrahepatic cancers are hepatocellular carcinomas (HCCs) or intrahepatic cholangiocarcinomas (ICCs). The prevalence of hepatocholangiocarcinoma (cHCC-ICC), combining histological features of HCC and ICC, ranges from 1% to 5% of primary hepatic cancers[2]. In 1949, Allen and Lisa[3] were the first to describe and classify cHCC-ICC into three subtypes (A, B and C). The classification subsequently evolved until the latest World Health Organization classification, proposed in 2010 (Table 1)[4].

Here we report the case of a patient diagnosed with a cHCC-ICC of stem cell-subtype, presenting with dysphagia and revealing an esophageal metastasis.

## CASE REPORT

A 55-year-old male was admitted to the University Hospital of Nantes, France, in January 2017 for investigation of a recent and elective dysphagia to solids associated with an alteration in general status (ECOG score 2) and weight loss of 14 kg.

The patient had a medical history of schizophrenia, alcoholic cirrhosis with Child-Pugh score A and a daily alcohol intake of 30 g, Barrett's esophagus C1M6, and heavy cigarette smoking.


**Figure 1 Endoscopic appearance of the elevated lesion in the esophagus.** Upper digestive endoscopy showed a 10-cm polypoid tumor at 30 cm from incisors.

The first biological analyses showed isolated thrombocytopenia of 107 G/L, and normal renal and hepatic functions. The C-reactive protein level was 9.9 mg/L.

Esophageal endoscopy (Figure 1) revealed a significant, quasiobstructive lesion of the lower third of the esophagus. Histological analysis confirmed an esophageal localization of an undifferentiated carcinoma, with immunohistochemical analysis indicating HCC with positive hepatocyte antigen.

Thoraco-abdomino-pelvic computed tomography (CT) and abdominal magnetic resonance imaging (MRI) scans were performed. CT scans were performed before and after injection of contrast media, including arterial, portal and delayed phase at 5 min. MRI scan included T1-weighted sequence with fat suppression before and after injection of gadolinium chelates at the same phases. CT and MRI scan analyses (Figure 2) revealed the esophageal lesion and multiple hepatic nodules, mainly located in the right liver. Hepatic tumors exhibited atypical imaging features for classic HCC but showed combined imaging features of both HCC with peripheral arterial enhancement and delayed wash out, and ICC with delayed central fibrous enhancement. The tumors more closely resembled ICC. Metastases were present in adrenal glands (33 mm on the right adrenal gland and 17 mm on the left adrenal gland) and lymph nodes of the celiac region, associated with a bony lesion of the right iliac branch invading the pubic symphysis.

All tumor markers were normal: alpha fetoprotein ($\alpha$FP): 1.8 ng/mL (normal range: 0.8-8.8 ng/mL); carbohydrate antigen 19-9 (CA19-9): 4.5 U/mL (normal range: < 37 U/mL); and, carcinoembryonic antigen: 2.4 $\mu$g/L (normal range: < 5 $\mu$g/L).

A liver biopsy was performed. Histological and immunohistochemical analyses showed cHCC-ICC with stem cell features (small cells) and an intermediate cell subtype, as described in Table 1. The tumor consisted

**Table 1 World Health Organization 2010 classification of combined hepatocholangiocarcinoma**

| World Health Organization 2010[4] |
|---|
| cHCC-ICC classical: Typical HCC and typical ICC |
| cHCC-ICC-SC |
| cHCC-ICC-SC-typical: Nests of mature-looking hepatocytes with peripheral clusters of small cells that have a high nucleus:cytoplasm ratio and hyperchromatic nuclei. |
| cHCC-ICC SC-int: Tumor cells show features intermediate between hepatocytes and cholangiocytes. These tumor cells show strands, solid nests and/or trabeculae of small, uniform cells with scant cytoplasm and hyperchromatic nuclei. |
| cHCC-ICC-SC-CLC: Admixtures of small monotonous glands, antler-like anastomosing patterns. Each tumor cell is cuboidal, smaller in size than normal hepatocytes, with a high nucleus: cytoplasm ratio, and distinct nucleoli. |

cHCC-ICC: Combined hepatocholangiocarcinoma; cHCC-ICC-SC-typical: Combined hepatocholangiocarcinoma, stem cell features, typical subtype; cHCC-ICC-SC-int: Combined hepatocholangiocarcinoma, stem cell features, intermediate cell-subtype; cHCC-ICC-SC-CLC: Combined hepatocholangiocarcinoma, stem cell features, cholangiolocellular subtype; HCC: Hepatocellular carcinoma; ICC: Intrahepatic cholangiocarcinoma; SC: Stem cell.

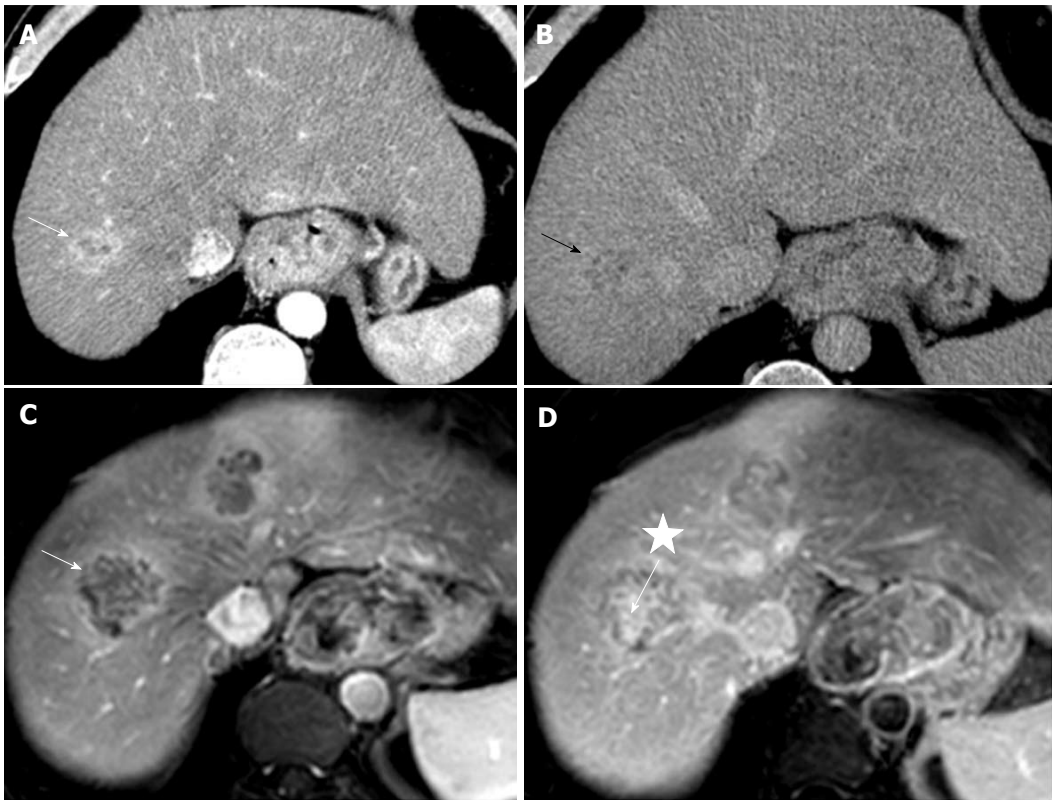


**Figure 2 Computed tomography scan and magnetic resonance imaging scan imaging.** Axial-enhanced computed tomography scans with arterial (A) and 5-min delayed times (B). Corresponding axial enhanced MRI in T1-weighted sequence with fat suppression (C and D). Tumor of the junction of the segments Ⅷ-Ⅶ combined the double imaging features with peripheral arterial contrast enhancement (white arrow) and secondary wash out (black arrow) (HCC part) and a late fibrous contrast enhancement of the central part (white asterisk) (ICC part). MRI was performed at 2-mo intervals and demonstrated a second tumor with comparable behavior in segment Ⅳ. CT: Computed tomography; MRI: Magnetic resonance imaging.

of small cuboidal cells arranged in a ductal pattern at the borders of nodules, in continuity with a trabecular pattern at the center. Tumor cells concomitantly expressed hepatocyte antigen HepPar1 and cytokeratin 19, normally expressed by biliary cells (Figure 3). The tumor cells appeared to be growing within and replacing regenerative nodules of cirrhosis.

The patient was treated with systemic intravenous gemcitabine and cisplatin combined chemotherapy (gemcitabine 1000 mg/m$^2$ and cisplatin 25 mg/m$^2$ every week for 2 wk, with 1 wk of rest before a new cycle). He received two cycles of chemotherapy. During the follow-up, the patient showed a progressive alteration in general condition, with an ECOG score of 3, associated with the appearance of diffuse bone pain. A bone scintigraphy was performed 2 mo after the beginning of chemotherapy, and revealed a multifocal metastatic spread over the entire axial and peripheral skeleton with right ilio-pubic and voluminous right humeral lesions. The patient was then managed with

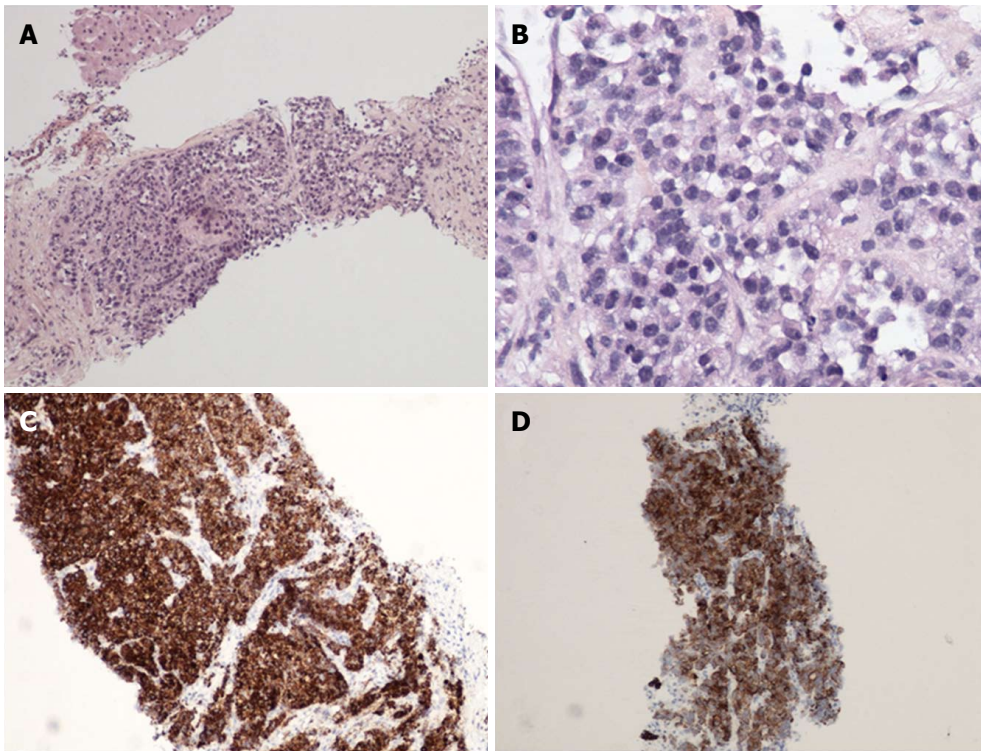


**Figure 3 Histological and immunohistochemical appearance of hepatic lesions.** A: Combined hepatocellular cholangiocarcinoma, stem cell features, intermediate cell-subtype with underlying cirrhosis; B: The tumor is composed of small tumor cells arranged in bays, with some ill-defined glands; C: Cells express both markers of hepatocyte cells (Her Par1); D: Markers of biliary cells (cytokeratin 19).

best supportive care and died 87 d after the beginning of treatment.

## DISCUSSION

To our knowledge, this is the first report of an esophageal metastasis of a cHCC-ICC. Esophageal metastases are uncommon. In HCC, the incidence of metastatic esophageal tumors is low, accounting for less than 0.4%[5]. Few case reports have described the presence of esophageal metastases from HCC or ICC[6-14]. These metastases could develop by the spread of tumor cells infiltrating the portal system[15]. The dissemination by hepatofugal portal flow to the esophagus seems to be one possible route for esophageal metastasis[8].

There are no current guidelines for the treatment of unresectable, locally advanced or metastatic cHCC-ICC. We recently described the first series of patients with unresectable cHCC-ICC treated with gemcitabine plus platinum-based chemotherapy. In that retrospective study, including 30 patients, according to RECIST criteria, the partial response rate was 28.6%, stable disease rate 50% and progressive disease rate 21.4%. Median progression-free survival and overall survival were 9.0 mo and 16.2 mo, respectively[16].

The diagnosis of cHCC-ICC is challenging. The radiological diagnosis is difficult due to the high frequency of cHCC-ICC mimicking HCC, from 30% to 50% when considering the major features of HCC (arterial phase hyperenhancement, wash out and capsule appearance)[17,18]. However, the addition of non-HCC features in the radiologic assessment could improve the diagnostic accuracy[18]. Histological diagnosis is the gold standard, but is difficult to obtain in the absence of surgical specimens. The conduct of liver biopsies to sample both components of cHCC-ICC is infrequent. In a series of 23 resected cHCC-ICC, all of the tumors were misdiagnosed at preoperative histology, with 20 considered to be HCC and three classed as ICC[19].

As in the case presented here, criteria for identifying cHCC-ICC have been proposed previously[20]. The combination of elevated serum tumor markers and enhancement patterns on imaging should strongly suggest the diagnosis of cHCC-ICC in the following circumstances: imaging features of both ICC and HCC, regardless of marker levels; elevation of both αFP and CA19-9, regardless of imaging appearance; or discordance between imaging and tumor marker elevation (typical HCC enhancement pattern with elevated CA19-9 or typical ICC enhancement pattern with elevated αFP)[20].

The combination of histological, radiological and biological criteria is important to identify cHCC-ICC patients. Even in patients with cirrhosis and liver tumor with typical enhancement patterns of HCC, biopsies should be advocated in the presence of biological or imaging features suggesting a cHCC-ICC, as the

prognosis and the management of these tumors could be different[21].

## ARTICLE HIGHLIGHTS

### Case characteristics
A 55-year-old cirrhotic male patient was admitted for dysphagia.

### Clinical diagnosis
Elective dysphagia for solids associated with an alteration in general status and a weight loss of 14 kg.

### Differential diagnosis
Primary esophageal cancer.

### Laboratory diagnosis
Normal renal and hepatic functions. Normal carbohydrate antigen 19-9, carcinoembryonic antigen and alpha fetoprotein.

### Imaging diagnosis
Thoraco-abdomino-pelvic computed tomography and abdominal magnetic resonance imaging scans were performed and revealed hepatic lesions combining imaging features of both hepatocellular carcinoma, and intrahepatic cholangiocarcinoma.

### Pathological diagnosis
Stem cell-subtype hepatocholangiocarcinoma.

### Treatment
Chemotherapy: gemcitabine - cisplatin.

### Term explanation
Hepatocholangiocarcinoma is a primary hepatic tumor representing less than 5% of all hepatic tumors. This is the first report of an esophageal metastasis of a hepatocholangiocarcinoma.

### Experiences and lessons
The diagnosis of hepatocholangiocarcinoma is challenging. The addition of non-HCC features in the radiologic assessment could improve the diagnostic accuracy.

## REFERENCES


1 **Ferlay J**, Soerjomataram I, Dikshit R, Eser S, Mathers C, Rebelo M, Parkin DM, Forman D, Bray F. Cancer incidence and mortality worldwide: sources, methods and major patterns in GLOBOCAN 2012. *Int J Cancer* 2015; **136**: E359-E386 [PMID: 25220842 DOI: 10.1002/ijc.29210]

2 **Bergquist JR**, Groeschl RT, Ivanics T, Shubert CR, Habermann EB, Kendrick ML, Farnell MB, Nagorney DM, Truty MJ, Smoot RL. Mixed hepatocellular and cholangiocarcinoma: a rare tumor with a mix of parent phenotypic characteristics. *HPB* (Oxford) 2016; **18**: 886-892 [PMID: 27546172 DOI: 10.1016/j.hpb.2016.07.006]

3 **Allen RA**, Lisa JR. Combined liver cell and bile duct carcinoma. *Am J Pathol* 1949; **25**: 647-655 [PMID: 18152860]

4 **Theise ND,** Nakashima O, Park YN. Combined hepatocellular-cholangiocarcinoma. In: Bosman FT, Carneiro F, Hruban RH, Theise ND, (Eds), WHO classification of tumors of the digestive system. Lyon: IARC 2010: 225-227

5 **Liver Cancer Study Group of Japan**. Primary liver cancer in Japan. Clinicopathologic features and results of surgical treatment. *Ann Surg* 1990; **211**: 277-287 [PMID: 2155591]

6 **Sohara N**, Takagi H, Yamada T, Ichikawa T, Abe T, Itoh H, Mori M. Esophageal metastasis of hepatocellular carcinoma. *Gastrointest Endosc* 2000; **51**: 739-741 [PMID: 10840317]

7 **Kume K**, Murata I, Yoshikawa I, Kanagawa K, Otsuki M. Polypoid metastatic hepatocellular carcinoma of the esophagus occurring after endoscopic variceal band ligation. *Endoscopy* 2000; **32**: 419-421 [PMID: 10817184 DOI: 10.1055/s-2000-13269]

8 **Cho A**, Ryu M, Yoshinaga Y, Ishikawa Y, Miyazawa Y, Okazumi S, Ochiai T. Hepatocellular carcinoma with unusual metastasis to the esophagus. *Hepatogastroenterology* 2003; **50**: 1143-1145 [PMID: 12846000]

9 **Tsubouchi E**, Hirasaki S, Kataoka J, Hidaka S, Kajiwara T, Yamauchi Y, Masumoto T, Hyodo I. Unusual metastasis of hepatocellular carcinoma to the esophagus. *Intern Med* 2005; **44**: 444-447 [PMID: 15942091]

10 **Yan SL**, Hung YH, Yang TH. Metastatic hepatocellular carcinoma of the esophagus: an unusual cause of upper gastrointestinal bleeding. *Endoscopy* 2007; **39** Suppl 1: E257-E258 [PMID: 17957604 DOI: 10.1055/s-2007-966480]

11 **Choi CS**, Kim HC, Kim TH, Seo GS, Kim KH, Cho EY, Seo SO, Oh HJ, Choi SC. Does the endoscopic finding of esophageal metastatic hepatocellular carcinoma progress from submucosal mass to polypoid shape? *Gastrointest Endosc* 2008; **68**: 155-159 [PMID: 18513720 DOI: 10.1016/j.gie.2008.02.043]

12 **Xie LY**, Fan M, Fan J, Wang J, Xu XL, Jiang GL. Metastatic hepatocellular carcinoma in the esophagus following liver transplantation. *Liver Transpl* 2008; **14**: 1680-1682 [PMID: 18975278 DOI: 10.1002/lt.21546]

13 **Sato T**, Krier M, Kaltenbach T, Soetikno R. Cholangiocarcinoma metastasis to the esophagus. *Endoscopy* 2010; **42** Suppl 2: E250 [PMID: 20931466 DOI: 10.1055/s-0030-1255641]

14 **Boonnuch W**, Akaraviputh T, Nino C, Yiengpruksawan A, Christiano AA. Successful treatment of esophageal metastasis from hepatocellular carcinoma using the da Vinci robotic surgical system. *World J Gastrointest Surg* 2011; **3**: 82-85 [PMID: 21765971 DOI: 10.4240/wjgs.v3.i6.82]

15 **Arakawa M**, Kage M, Matsumoto S, Akagi Y, Noda T, Fukuda K, Nakashima T, Okuda K. Frequency and significance of tumor thrombi in esophageal varices in hepatocellular carcinoma associated with cirrhosis. *Hepatology* 1986; **6**: 419-422 [PMID: 3011630]

16 **Salimon M,** Prieux-Klotz C, Tougeron D, Hautefeuille V, Caulet M, Gournay J, Matysiak-Budnik T, Bennouna J, Tiako Meyo M, Lecomte T, Zaanan A, Touchefeu Y Gemcitabine plus platinum-based chemotherapy for first-line treatment of hepatocholangiocarcinoma: an AGEO French multicentre retrospective study. Br J Cancer 2017 [PMID: 29169182 DOI: 10.1038/bjc.2017.413]

17 **Fowler KJ**, Sheybani A, Parker RA 3rd, Doherty S, M Brunt E, Chapman WC, Menias CO. Combined hepatocellular and cholangiocarcinoma (biphenotypic) tumors: imaging features and diagnostic accuracy of contrast-enhanced CT and MRI. *AJR Am J Roentgenol* 2013; **201**: 332-339 [PMID: 23883213 DOI: 10.2214/AJR.12.9488]

18 **Potretzke TA**, Tan BR, Doyle MB, Brunt EM, Heiken JP, Fowler KJ. Imaging Features of Biphenotypic Primary Liver Carcinoma (Hepatocholangiocarcinoma) and the Potential to Mimic Hepatocellular Carcinoma: LI-RADS Analysis of CT and MRI Features in 61 Cases. *AJR Am J Roentgenol* 2016; **207**: 25-31 [PMID: 26866746 DOI: 10.2214/AJR.15.14997]

19 **Taguchi J**, Nakashima O, Tanaka M, Hisaka T, Takazawa T, Kojiro M. A clinicopathological study on combined hepatocellular and cholangiocarcinoma. *J Gastroenterol Hepatol* 1996; **11**: 758-764 [PMID: 8872774]

20 **Maximin S**, Ganeshan DM, Shanbhogue AK, Dighe MK, Yeh MM, Kolokythas O, Bhargava P, Lalwani N. Current update on combined hepatocellular-cholangiocarcinoma. *Eur J Radiol Open* 2014; **1**: 40-48 [PMID: 26937426 DOI: 10.1016/j.ejro.2014.07.001]

21 **Serra V**, Tarantino G, Guidetti C, Aldrovandi S, Cuoghi M, Olivieri T, Assirati G, De Ruvo N, Magistri P, Ballarin R, Di Benedetto F. Incidental Intra-Hepatic Cholangiocarcinoma and Hepatocholangiocarcinoma in Liver Transplantation: A Single-Center Experience. *Transplant Proc* 2016; **48**: 366-369 [PMID: 27109957 DOI: 10.1016/j.transproceed.2015.12.044]

**P- Reviewer**: Goral V, Lee CL, Tarnawski AS **S- Editor**: Wang JL
**L- Editor**: Filipodia **E- Editor**: Huang Y

World Journal of Gastroenterology

Submit a Manuscript: http://www.f6publishing.com

*World J Gastroenterol* 2018 February 21; 24(7): 876-876

DOI: 10.3748/wjg.v24.i7.876

ISSN 1007-9327 (print) ISSN 2219-2840 (online)

CORRECTION

# Correction for "Evaluation of a multiplex PCR assay for detection of cytomegalovirus in stool samples from patients with ulcerative colitis" (*World J Gastroenterol* 2015; 21: 12667-12675)

Akira Hokama

Akira Hokama, Department of Endoscopy, University of the Ryukyus Hospital, Nishihara, Okinawa 903-0215, Japan

ORCID number: Akira Hokama (0000-0002-8310-9989).

Author contributions: Hokama A wrote the correction.

Conflict-of-interest statement: No potential conflicts of interest relevant to this article were reported.



Manuscript source: Unsolicited manuscript

Correspondence to: Akira Hokama, MD, PhD, Professor, Department of Endoscopy, University of the Ryukyus Hospital, 207 Uehara Nishihara, Okinawa 903-0215, Japan. hokama-a@med.u-ryukyu.ac.jp
Telephone: +81-98-8951144
Fax: +81-98-8951414

Received: November 7, 2017
Peer-review started: November 7, 2017
First decision: December 20, 2017
Revised: December 21, 2017
Accepted: December 26, 2017
Article in press: December 26, 2017
Published online: February 21, 2018



Hokama A. Correction for "Evaluation of a multiplex PCR assay for detection of cytomegalovirus in stool samples from patients with ulcerative colitis" (*World J Gastroenterol* 2015; 21: 12667-12675). *World J Gastroenterol* 2018; 24(7): 876-876 Available from: URL: http://www.wjgnet.com/1007-9327/full/v24/i7/876.htm DOI: http://dx.doi.org/10.3748/wjg.v24.i7.876

## CORRECTION

Correction to: Nahar S *et al*. Evaluation of a multiplex PCR assay for detection of cytomegalovirus in stool samples from patients with ulcerative colitis. *World J Gastroenterol* 2015; 21: 12667-12675 PMID: 26640344 DOI: 10.3748/wjg.v21.i44.12667. A part of authors' affiliation is missing. In the left side column of page 12667[1], "Department of Infectious, Respiratory, and Digestive Medicine, University of the Ryukyus, Okinawa 903-0215, Japan" should be "Department of Infectious, Respiratory, and Digestive Medicine, Graduate School of Medicine, University of the Ryukyus, Okinawa 903-0215, Japan".

## REFERENCES

1 **Nahar S**, Iraha A, Hokama A, Uehara A, Parrott G, Ohira T, Kaida M, Kinjo T, Kinjo T, Hirata T, Kinjo N, Fujita J. Evaluation of a multiplex PCR assay for detection of cytomegalovirus in stool samples from patients with ulcerative colitis. *World J Gastroenterol* 2015; **21**: 12667-12675 [PMID: 26640344 DOI: 10.3748/wjg.v21.i44.12667]

**S- Editor**: Gong ZM **L- Editor**: A **E- Editor**: Huang Y

Published by **Baishideng Publishing Group Inc**
7901 Stoneridge Drive, Suite 501, Pleasanton, CA 94588, USA
Telephone: +1-925-223-8242
Fax: +1-925-223-8243
E-mail: bpgoffice@wjgnet.com
Help Desk: http://www.f6publishing.com/helpdesk
http://www.wjgnet.com

ISSN 1007-9327